PROCEEDINGS

PROCEEDINGS
of the 2nd International Conference on Advanced Production and Processing
May, 2023.

Title:
Proceedings of the 2nd International Conference on Advanced Production and Processing publishes abstracts from the following fields: Innovative Food Science and Bioprocesses, Nutraceuticals and Pharmaceuticals, Sustainable Development, Chemical and Environmental Engineering, Materials Design and Applications.

Publisher:
University of Novi Sad, Faculty of Technology Novi Sad,
Bulevar cara Lazara 1, 21000 Novi Sad, Serbia

For publisher:
prof. Biljana Pajin, PhD, Dean

Design and Printing Layout:
Saša Vulić

CIP - Каталогизација у публикацији
Библиотеке Матице српске, Нови Сад

658.5(082)

INTERNATIONAL Conference on Advanced Production and Processing (2 ; 2023 ; Novi Sad)
Proceedings of the 2nd International Conference on Advanced Production and Processing ICAPP 2022, Novi Sad [Elektronski izvor] / [editor-in-chief Zita Šereš]. - Novi Sad : Faculty of Technology, 2023

Način pristupa (URL): https://www.tf.uns.ac.rs/download/icapp-2022/icapp-proceedings.pdf. - Opis zasnovan na stanju na dan 1.6.2023. - Nasl. s naslovnog ekrana. - Bibliografija uz svaki rad.

ISBN 978-86-6253-167-4

a) Технологија -- Производња -- Зборници

COBISS.SR-ID 117323785

PROCEEDINGS
of the 2nd International Conference on Advanced Production and Processing

Innovative Food Science and Bioprocesses

TEXTURAL AND RHEOLOGICAL PROPERTIES OF COOKIE DOUGH WITH ADDITION OF CHESTNUT FLOUR

Ljubica Dokić*, Ivana Nikolić, Dragana Šoronja Simović, Biljna Pajin, Zita Šereš

University of Novi Sad, Faculty of Technology, Bul cara Lazara 1, Novi Sad, Serbia

**ldokic@uns.ac.rs*

Abstract

Functional food products usually contain some component, in the aim to realize some health benefits and to improve diet quality. Application of chestnut flour is one of the ways to achieve functional properties of cookies, as one of the widely used bakery product. Due to nutritional quality and potential beneficial health effects, chestnut flour is suitable for formulation of functional cookies. But, that means significant changes of textural and rheological properties of dough, which must be adapted to easy manipulation during processing. In that aim, the influence of applied chestnut flour, as an ingredient, on textural and rheological properties of obtained dough was observed. Dough with 100 % of wheat flour and moisture content of 20, 22 and 24 % were control samples. Other dough formulations were prepared with the addition of chestnut flour (20, 40 and 60 %), as the partial replacement of wheat flour, calculated on the flour weight. Increase in amount of chestnut flour for 20 % caused an increase in the dough hardness and the decrease in dough extensibility and resistance to extension. Also, high amount of chestnut flour caused low flexibility and brittle consistency of dough structure with domination of linkages with hard, elastic nature. Increase in dough moisture for 2 % caused softer dough consistency, higher dough extensibility and more flexible dough structure with pronounced ability to recover. Optimal textural and rheological properties, which provide flexible manipulation with dough during processing, can be achieved with dough formulation with 20 and 40 % of chestnut flour and 24 % of dough moisture.

Keywords: Functional food, cookies, chestnut flour, rheology, texture

1. Introduction

The chestnut (*Castanea sativa*) is a deciduous tree that belongs to *Fagaceae* family (1) and it is widely present in the Mediterranean countries. The application of chestnut fruit, as high

nutritive ingredient, became popular in last few years with increasing demand for functional food products.

The chemical composition of chestnut fruit includes high level of polymeric carbohydrates (starch), significant content of vitamins (B1, B2, B3, C, E), fibers, acceptable lipids content and adequate micro and macro minerals (2,3). Chestnut fruit also contains protein–derived components and amino acids, as well as simple phenolic component and more complex tannins (4). Chestnut is also characteristic by high content of antioxidants, low content of fat and absence of cholesterol, which also contributes to the high nutritional value and provides positive influence on human health. Due to the presence of non–digestible components, chestnut fruit belongs to functional food and can achieve prebiotic role. The chestnut fruit can be consumed as roasted, cooked and even raw, but according to content of carbohydrates that is approximately the same as in wheat and rice kernels, the chestnut fruit is a good source of starch with a large potential of commercial application in food industry (5). The production of food products with chestnut flour is subject of interest, because of possibility of partial replacement of wheat, rice or corn flours by chestnut flour (CF) in bakery products (1). In the bakery industry chestnut flour is mostly used for production of special bakery products based on flour. Chestnut flour can be used as a functional component because it improves nutritive properties of by increasing the content of dietary fibers, essential amino acids, complex of vitamin B and vitamin E (6,7). A significant characteristic of chestnut flour is the absence of gluten, so it could be used for gluten–free products aimed for patients with celiac disease. Considering that most gluten–free raw materials do not contain sufficient amount of B vitamins, iron, folic acid and dietary fibers, the application of chestnut flour in gluten–free products improves their nutritional value (8).

Cookies are widely accepted bakery/confectionery products, which are traditionally made of wheat flour. It is possible to add other cereal or non–cereal flours, like chestnut flour, to provide special flavors or improve nutritional quality of cookies. Several studies reported the application of chestnut flour in bread formulations (7,8), but a lack of information about addition of chestnut flour in cookies and its impact on rheological properties of the dough is available. Unlike bread dough, cookies dough has low water content. In such a dough small alteration in flour formulation influence rheological properties of dough and quality of cookies. This study focuses on the application of chestnut flour, as partial supplement for wheat flour, in production of cookies. The objective of this work was to determine the textural and rheological properties of the dough for cookies with different amount of chestnut flour.

2. Materials and Methods

In the experimental work cookies were produced from following: tailormade flour T-500 (WF) for bakery products, chestnut flour (CF) (Castellino, Italy), powdered sugar ("Centroproizvod", Serbia), vegetable fat "Vitalina" („Dijamant", Serbia), chemicals NaCl, NH_4HCO_3 and $NaHCO_3$ ("Centrohem", Serbia), NaCl ("Centrohem", Serbia) and distilled water.

2.1. Experimental design

Experiment was planned according to factorial plan 3^2, where variation of two independent variables (amount of CF and dough moisture content) are on three levels (-1, 0, +1). Independent variable–amount of chestnut flour [%] (calculated on wheat flour basis) was changed in levels 20, 40 and 60 %. Independent variable–dough moisture content was in levels 20, 22 and 24 %. Dough formulations with 100 % of WF and dough moisture content 20, 22 and 24% were control samples. Other dough formulations were prepared with the addition of CF as partial replacement of WF, calculated on the flour weight used in the control sample. Thus, total number of observed dough samples was twelve.

2.2. Dough preparation

The dough for cookies was prepared as follow: the amount of dough of 350 g was obtained by mixing 199.4 g of flour (WF or WF/CF blends), 69.8 g of powdered sugar, 41.9 g of vegetable fat, 1.1 g of NaCl, 0.6 g of $NaHCO_3$ and 0.4 g of NH_4HCO_3. The amount of distilled water was added in quantity to ensure the adequate dough moisture (20, 22 and 24%) according to experimental design. Dough was prepared according to laboratory procedure explained in (9).

2.3. Dough textural analysis

Hardness of the dough was determined by Texture Analyser TA.HD Plus (Stable Micro Systems, Surrey, UK) using the penetration test and adequate measuring accessories, P/6 cylinder (6 mm in diameter) and heavy duty platform (HDP/90). After a trigger force of 5 g is attained, the cylinder proceeds to penetrate into the dough to a depth of 20 mm and the force registered at maximum depth is "hardness of the dough". Measurements were performed in five replicates at 20°C using load cells of 5 kg and measuring parameters: pre–test speed 1 mm/s; test speed 2 mm/s and post–test speed 10 mm/s.

Extensibility and resistance to extension of dough were determined by Kieffer extensibility micro–method, also using the Texture Analyser TA.HD Plus and Kieffer Dough & Gluten

Quality Extensibility Rig, using load cell of 5 kg and measuring parameters: pre–test speed 2.0 mm/s; test speed 3.3 mm/s; post–test speed:10.0 mm/s (TA.HD 2004).

2.4. Rheological determination of dough

Rheological properties of dough were determined by Haake Rheo Stress 600 (Karlsruhe, Germany) using plate–plate sensor geometry (60 mm in diameter with 1 mm gap) at 20°C. After closing gap of sensor geometry, the dough pieces were allowed to rest/recover for 5 min and a solvent trap was used around the sensor plate in the aim to prevent dough dehydration.

Dynamic Oscillatory Test included previous determination of linear viscoelastic (LVE) regime. Amplitude sweep was performed on frequency of 1 Hz, modulating in order to determine LVE regime. Dynamic oscillatory parameters, storage modulus (G') and loss modulus (G") were observed modulating the frequency (1–10 Hz) in a constant value of shear stress (30 Pa). Also, the parameter of viscoelastic behavior tan δ, which represent the ratio between G" and G' was calculated.

2.5. Statistical analysis

Statistical analyses of the data were performed by statistical software Statistica 12.0 (Stat Soft Inc., USA). Analysis of variance (ANOVA) and Duncan's multiple range tests were used to determine differences between means of least three measurement results at the significance level $p = 0.05$.

3. Results and Discussion

3.1. Textural characteristics of the dough

The results for hardness of dough, for dough extensibility and for resistance to extension, obtained by textural measurements, are presented in Table 1.

The increase in moisture content caused an expected reduction of dough hardness. The hardness of control sample with 20 % of moisture was twice higher than for control dough with 24 % of moisture.

The application of chestnut flour reduced the hardness of the dough compared to control samples, thus the values for dough hardness of control samples were higher than values for samples with chestnut flour and same moisture content (Table 1). The increase in moisture content of the dough downgraded this effect, due to interaction between observed factors. Also, the trend of increase in dough hardness with increase in content of chestnut flour for samples with 20 % of dough moisture was noticed. The hardness of these samples increased for 4.36–

24.52 % with increase in content of chestnut flour for 20 %. For samples with 24 % of dough moisture, the pronounced narrow interval of these values with increase in amount of chestnut flour was characteristic (from 294.7 to 331.0 g). That pointed the interaction between moisture content and amount of chestnut flour.

Table 1 Textural parameters for the dough

Ingredients		**Resistance to extension±SD (g)**	**Extensibility±SD (mm)**	**Hardness±SD (g)**
Dough moisture (%)	Amount of flour (%)			
20	Control (100% WF)	10.1±1.6^{f}	3.6±1.5^{f}	760.6±5.3^{k}
	20% CF	8.7±0.8^{e}	3.0±1.0^{e}	407.9±7.8^{g}
	40% CF	7.2±0.8^{b}	2.4±0.9^{c}	425.7±9.8^{h}
	60% CF	7.0±0.6^{ab}	1.8±0.7^{b}	530.1±7.4^{j}
22	Control (100% WF)	13.7±1.2^{g}	7.6±0.7^{h}	451.0±9.7^{i}
	20% CF	7.7±0.7^{c}	2.9±0.7^{d}	406.6±4.3^{g}
	40% CF	7.6±0.9^{c}	2.8±0.4^{d}	369.8±6.3^{f}
	60% CF	6.8±0.8^{a}	1.9±0.2^{b}	269.7±15.0^{a}
24	Control (100% WF)	8.1±0.3^{d}	5.4±1.4^{g}	351.8±5.0^{e}
	20% CF	7.7±0.5^{c}	3.1±1.1^{e}	306.0±8.3^{c}
	40% CF	8.5±0.7^{e}	3.2±0.9^{e}	331.0±6.7^{d}
	60% CF	6.8±0.3^{a}	1.5±0.6^{a}	294.7±16.2^{b}

$^{a\text{-}k}$The mean values are significantly different ($p< 0.05$) if they are followed by different letters in the superscript

The application and amount of chestnut flour had statistically significant ($p< 0.05$) influence on other textural properties of dough, such as extensibility and resistance to extension. Obtained results for these physical properties during extension pointed the significant reduction of dough extensibility and resistance to extension for samples with chestnut flour, in a wide range for 2.7–61.84 %. The samples with maximum amount of chestnut flour (60 %) and moisture content of 22 and 24 % had about four times less values of extensibility than control samples with same moisture content. This was consequence of lower content of gluten, due to replacement of wheat flour with chestnut flour, thus the compactness of dough and coherence of the dough components in samples with chestnut flour was reduced. The chestnut flour exhibits higher water absorption ability than wheat flour. The reduction of dough extensibility

and dough stability may be attributed to pronounced water absorption ability of chestnut flour and partially to low protein and lipid fraction in chestnut flour.

3.2. Rheological properties of the dough

Generally, dough is a complex viscoelastic rheological system. The importance of rheological characteristics of dough for cookies is confirmed by literature data that highlight their influence on the behavior of dough during processing and on the quality of final product (10).

Viscoelastic properties of the dough for cookies are defined by changes of storage (G') and loss (G") modulus with increase in frequency. The changes of these viscoelastic parameters were observed for dough with different moisture and different amount of chestnut flour. Domination of storage modulus over loss modulus was noticed for all samples (Fig. 1), which is characteristic for viscoelastic systems, such as dough.

Fig. 1a) illustrate that gradual substitution of wheat flour with chestnut flour in the dough with 20 % of moisture caused slight increase in the value of the storage modulus. The values of loss modulus for samples with chestnut flour were lower than for control sample. Same trend was noticed for dough samples with 22 % of moisture (Fig. 1b)).

Fig. 1c) presents the changes of modulus for samples with 24 % of moisture with different amount of chestnut flour. The difference between the storage and loss modulus for these samples is low, which indicated to lower firmness of the dough compared to samples with 20 and 22 % of moisture. For samples with the same amount of chestnut flour it can be observed that the increase in dough moisture resulted in lower values of storage modulus and increase in loss modulus. Also, it is evident that storage modulus of samples with high moisture content (22 % and 24 %) and with high amount of chestnut flour (40 and 60 %) are different compared to the control sample and compared to the sample with the lowest amount of chestnut flour.

The slight increase of the storage and loss modulus with increase in frequency from 1 to 10 Hz was characteristics for all dough samples, regardless to the moisture content. That indicated the formation of the gel structure and it was associated to reduced amount of building proteins in the dough with chestnut flour.

The obtained results pointed that the increase in moisture content in control dough increased the exhibition of viscous properties. Also, an increase in the moisture content of the dough samples with an equal amount of chestnut flour reduced the difference between the values of loss and storage modulus.

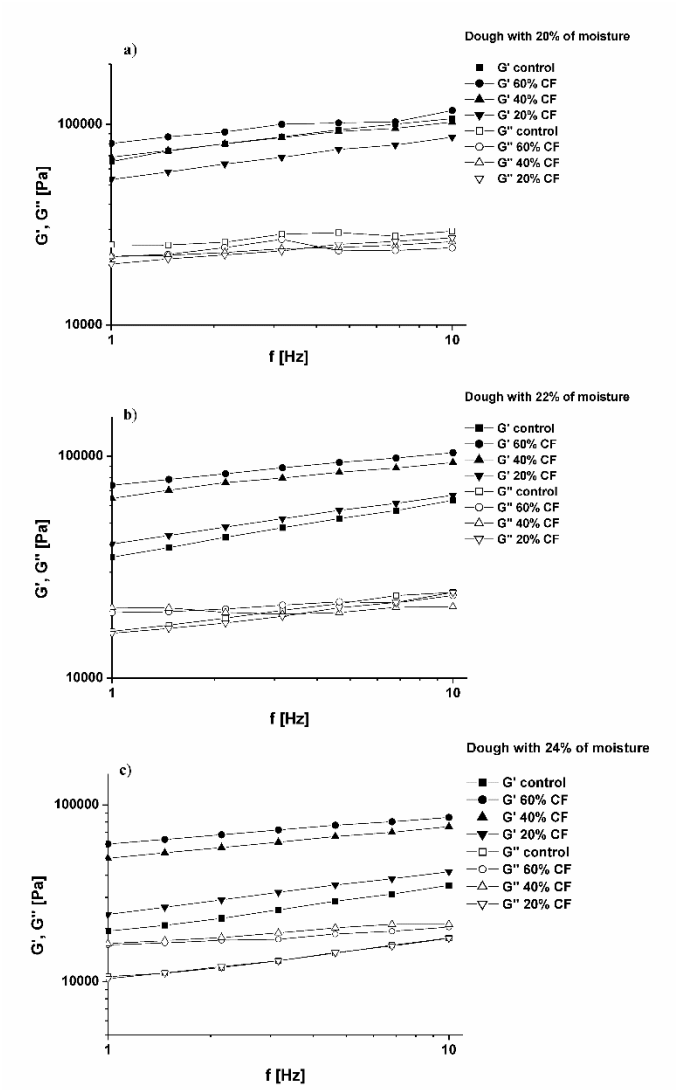

Figure 1. Viscoelastic modulus for dough samples with different dough moisture and different amount of chestnut flour

Presented observations are additionally confirmed by the fact that the lowest value of tan δ (0.233) was observed in dough with 20 % of moisture and 60 % of chestnut flour, and the highest value of tan δ was for sample with maximum moisture content of 24 % and 20 % of chestnut flour (0.419) (Table 2).

Viscoelastic parameter, tan δ, indicated the contribution of elastic and viscous components of the dough and it was less than 1 for all samples. That was confirmation that the dough samples were viscoelastic systems with dominant elastic component. Increase in the amount of chestnut flour reduced the values of tan δ (Table 3), which pointed to higher domination of storage modulus over loss modulus and to harder dough consistency. Also, increase in moisture content of dough increased the values of tan δ, so the dough consistency was softer and more flexible.

Table 2 The values of tan δ for observed dough samples

Ingredients		
Dough moisture (%)	Amount of flour (%)	**tan δ=G"/G'**
20	Control (100% WF)	0.319[f]
	20% CF	0.346[h]
	40% CF	0.281[d]
	60% CF	0.233[a]
22	Control (100% WF)	0.425[k]
	20% CF	0.371[i]
	40% CF	0.322[g]
	60% CF	0.242[b]
24	Control (100% WF)	0.522[l]
	20% CF	0.419[j]
	40% CF	0.311[e]
	60% CF	0.248[c]

[a-l]The mean values are significantly different ($p < 0.05$) if they are followed by different letters in the superscript

4. Conclusion

The application of chestnut flour changed the textural and rheological properties of the dough compared to dough with wheat flour. Increase in amount of chestnut flour for 20 % caused an increase in the dough hardness and simultaneously the decrease in dough extensibility and resistance to extension. Also, high amount of chestnut flour caused low flexibility and brittle consistency of dough structure, expressed as low compliance of the dough samples. On the other hand, the moisture of the dough significantly contributed to the textural and rheological properties of the dough and reduced the negative influence of the chestnut flour. Increase in dough moisture for 2 % caused softer dough consistency, higher dough extensibility and more flexible dough structure with pronounced ability to recover.

Based on observed dough properties, the formulation of the dough for cookies with 20 and 40 % of chestnut flour and 24 % of moisture expressed the optimal textural and rheological properties that provide flexible manipulation with dough during processing.

5. Acknowledgement

Research was done within National program no. 451-03-68/2022-14/200134

6. References

1. Moreira, R., Chenlo, F., Torres, M.D. and Prieto D.M. Influence of the particle size on the rheological behavior of chestnut flour dough. *J. Food Eng*. **2010,** *100*, 270–277.
2. Borges, O., Goncalves, B., Soeiro de Carvalho, J.L., Correia, P. and Silva, A.P. Nutritional quality of chestnut (Castanea sativa Mill) cultivars from Portugal. *Food Chem.* **2008,** *106*, 976–984.
3. De La Montana Miguelez, J., Miguez Bernandez, M. and Garcia Queijeiro, J.M. Composition of varieties of chestnuts from Galicia (Spain). *Food Chem.* **2004** *84*, 401–404.
4. De Vasconcelos, M., Bennet, R.N., Rosa, E. and Ferreira–Cardoso, J. Composition of European chestnut (Castanea sativa Mill.) and association with health effects: fresh and processed products. *J. Sci. Food and Agricul.* **2010,** *90, 10*, 1578–1589.
5. Blaiotta, G., La Gatta, B., Di Capua, M., Di Luccia, A., Coppola, R. and Liu, C., Wang, S., Chang, X., and Wang, S. Structural and functional properties of starches from Chinese chestnuts. Food Hydrocolloid **2015,** *43*, 568–576.
6. Aponte, M., Boscaino, F., Sorrentino, A., Coppola, R., Masi, P. and Romano, A. Effects of fermentation and rye flour on microstructure and volatile compounds of chestnut flour based sourdoughs. *LWT – Food Sci. Techn.* **2014,** *58*, 387–395
7. Dall'asta, C., Cirlini, M., Morini, E., Rinaldi, M., Ganino, T. and Chiavaro, E. Effect of chestnut flour supplementation on physic–chemical properties and volatiles in bread making. *LWT – Food Sci. Tech.* **2013,** *53*, 233–239.
8. Demirkesen, I., Mert, B., Sumnu, G. and Sahin, S. Utilization of chestnut flour in gluten–free bread formulations. *J. Food Eng.* **2010,** *101*, 329–336.
9. Milašinović–Šeremešić, M., Dokić, Lj., Nikolić, I., Radosavljević, M., and Šoronja Simović, D. 2013. Rheological and textural properties of short (cookie) dough made with two types of resistant starch. *J. Texture Studies*. **2014,** *44*, 115–123.
10. Berland, S. and Launay, B. Rheological properties of wheat flour dough in steady and dynamic shear: effect of water content and some additives. *Cereal Chem.* **1995** *7*, 48–52.

THE INFLUENCE OF TECHNOLOGICAL PROCESS PARAMETERS ON THE OXIDATIVE STABILITY OF BLACK CUMIN OIL (*Nigella sativa* L.)

Amela Kusur*, Ramzija Cvrk, Husejin Keran, Tijana Brčina, Halid Junuzović

Faculty of Technology, University of Tuzla, Urfeta Vejzagića 8, 75000 Tuzla, Bosnia and Herzegovina

**amela.kusur@untz.ba*

Abstract

The influence of technological process parameters on utilization and oxidative stability black cumin oil (*Nigella sativa* L.) has investigated in this study. Screw press was used for cold pressing of black cumin seeds. Three products were obtained by pressing: crude oil, oil sludge and oil cake. The process parameters were changing during the pressing: the temperature of the press head (60, 75 and 81°C), frequency of the electric motor (15, 18 and 22 Hz) and the size of the outlet for oil cake (5, 6 and 8 mm). Crude oil was naturally precipitated for 7 days at room temperature in a dark place and after that filtered. In the produced oil were determined the following quality parameters using standard methods: peroxide value, content of free fatty acids, unsaponifiable matter and moisture content. In oil cake as a by-product of oil producing, the content of oil and moisture was determined. The same was determined in black cumin seeds. Based on these parameters, the degree of pressing efficiency was calculated. Increasing temperature of the press head, decreasing the size of the outlet for oil cake and frequency of the electric motor, higher production of black cumin oil was achieved. Furthermore, the oxidative parameters i.e. peroxide value and free fatty acids content were best in this case. Based on the research results, we can conclude that the process parameters are a key factor in the technological process of pressing black cumin seeds and greatly affect oil yield and quality.

Keywords: Black cumin oil, cold pressing, process parameters, oxidative stability

1. Introduction

Nigella sativa L. is an annual herbaceous plant belonging to the Ranunculaceae family, growing in countries bordering the Mediterranean Sea, commonly known as black seed or black cumin (1). Black cumin seeds are gaining popularity precisely because of the production

of black cumin oil, which has many benefits and positive effects on human health and the prevention of various diseases (2).

Pressing is one of the oldest methods for extracting oil and it is a technological process during which oil is extracted from oilseeds by mechanical extraction and application of pressure. Screw or hydraulic presses are used for pressing (3). The process of cold pressing of seeds, pits or kernels produces crude oil that goes to purification (sedimentation, filtration, centrifugation) in order to obtain the final product of cold pressed oil. As a by-product of the oilseed pressing process, an oil cake is obtained, in which a certain amount of oil, important proteins, minerals, fibers and other ingredients remain (4).

Continuous screw presses used for pressing are basically screw conveyors with a variable volume for the material, which can change the working pressure along the press and compensate for the loss of pressure due to the outflow of the pressed oil. The main elements of these presses are the horizontal screw, the basket located around the screw, the device for filling and dosing the material, the device for regulating the thickness of the cake, the gear transmission and the press housing. The screw pushes the material from a larger to a smaller closed space, which causes the material to be compressed, and at the same time, there is an increase in pressure and oil draining. The regulation of the thickness of the cake in the press is achieved by the appropriate construction of the output cone, and the working pressure in the press is regulated through the different thickness of the cake (5).

Friction in the material and the press is high, so temperature rise is inevitable. High friction can lead to an increase in the temperature of the material up to 170 °C. In the production of cold-pressed oils, the temperature of the raw oil leaving the press is very important, as it should not be higher than 50 °C. In order to achieve this, presses of special construction are needed, or the pressing must be carried out under milder conditions, i.e. at lower pressure. In this case, the content of residual oil in the cake is usually higher, that is, the yield of oil is lower (6).

When determining the quality of cold-pressed oils, it is very important to determine the oxidation stability or durability in order to assess their susceptibility to oxidation deterioration. Fat spoilage is mostly based on oxidation processes. Lipid autoxidation occurs due to the action of oxygen from the air on the unsaturated bonds of fatty acids. Factors that accelerate the autooxidation process are: elevated temperature, light, heavy metals, etc. During the oxidation process, primary products are formed: hydroxyperoxide and peroxide. Decomposition of hydroxyperoxide creates secondary oxidation products: aldehydes, ketones, alcohols, free fatty acids, etc., which are the cause of the unpleasant smell and taste of oxidized fats. Insight into

the degree of oxidation of oils and fats, that is, the share of primary oxidation products, is obtained by determining the peroxide value (3).

The aim of this work was to examine the influence of the parameters of technological process of cold pressing of black cumin seeds (*Nigella sativa* L.) on the utilization and oxidative stability of the oil. During the pressing process, the process parameters were changed: the temperature of the press head, the frequency of the electric motor and the size of the outlet for the oil cake.

2. Experimental

2.1. Materials

In this study was used black cumin seeds that is bred in Syria. From these unground seeds was produced oil by the cold pressing process.

2.2. Oil production

For oil producing was used continuous low-capacity screw press manufactured by ElektroMotor-Simon, Serbia. Three products were obtained by cold-pressing: crude oil, oil sludge and oil cake. The process parameters were changing during the pressing: the temperature of the press head (60, 75 and 81°C), frequency of the electric motor (15, 18 and 22 Hz) and the size of the outlet for oil cake (5, 6 and 8 mm). The mass of raw materials was 1.8 kg. After pressing, crude oil was naturally precipitated for 7 days at room temperature in a dark place and after that filtered.

2.3. Methods

Determination of peroxide value

The peroxide value represents the primary oxidation degree of fats and oils at which peroxides are formed, as the primary products of oil oxidation. The oil sample was treated with a mixture of glacial acetic acid and chloroform with the addition of potassium iodide. The released iodine was titrated with a standard solution of sodium thiosulfate, with vigorous shaking to release all the iodine from chloroform. A blind test was performed under the same conditions. The peroxide value is expressed in millimol of active oxygen per kg of oil (mmol (7)O_2/kg oil). The analysis procedure and results calculation were performed in accordance to the Standard IUPAC method (2.501).

Determination of free fatty acid content

The acid value is a measure of the oil hydrolysis degree, and is defined as the value of milligrams of KOH required to neutralize free fatty acids in 1 g of oil. The oil sample was titrated with ethyl ether-ethanol mixture (1:1), previously neutralized with NaOH, with phenolphthaleine as indicator, according to the Standard IUPAC method (2.201). The acid value is expressed as the percentage of free fatty acids (oleic).

Determination of the unsaponifiable matter

Unsaponifiable matter is defined as the substances soluble in the oil, which after saponification are insoluble in water but soluble in the solvent used for the determination. The analysis procedure and results calculation were performed in accordance with the Standard IUPAC method (2.401).

Determination of moisture content

Moisture content was determined using standard drying method. 5 g of sample was weighted into dried and weighed vessels and dried at 105 °C to constant weight. Moisture content was calculated according to the expression:

$$Moisture\ content\ (\%) = \frac{m_1 - m_2}{m_1 - m_0} \times 100$$

where is:

m_0 – mass of empty vessel, g

m_1 – mass of vessel and sample before drying, g

m_2 – mass of vessel and sample after drying, g

Determination of oil content

Oil content in oil cake and in black cumin seeds was measured using standard Soxhlet method. The principle of Soxhlet method is extraction of oil from samples using some organic solvent. We have used n-hexane. The oil content was determined using modern Soxhlet apparatus, automatic extractor (Velp Scientifica – SER 148). 5 g of sample was weighted into a cellulose sleeve and connected to the apparatus. 150 mL of n-hexane are poured into dried and weighed extraction vessels. After extraction (about 4 hours) after the solvent was distilled off. Extraction vessels were dried at 105 °C to constant weight. Oil content was calculated according to the expression:

$$Oil\ content\ (\%) = \frac{a - b}{c} \times 100$$

where is:

a – mass of vessel with oil, g

b – mass of empty vessel, g

c – mass of sample, g

3. Result and Discussion

For the production of quality oil, it is important to have quality raw materials. In this research, the content of moisture and oil in seeds and oil cake was determined. Based on the content of oil and dry matter in the raw material and the obtained cake, the yield of pressed oil, i.e. the degree of pressing efficiency, was calculated. The degree of pressing efficiency (P) is calculated according to the expression $P\ (\%)=(U/U_0)\times 100$, where U is the amount of pressed oil and calculated according to the expression $U(\%)=U_0-U_p\times(a/b)$, U_0 is the proportion of oil in the raw material, U_p the proportion of oil in the cake, a is the dry matter in the raw material (%), b is the dry matter in the cake (%).

Before the pressing process, the moisture and oil content of black cumin seeds was determined. Black cumin seeds (raw material) have an oil content of 33.40% and a moisture content of 5.27%.

Table 1 shows the volume of crude oil and the volume of oil after precipitation and filtration, the mass of the oil cake, the content of oil and moisture in the cake, as well as the degree of pressing efficiency. The results differ depending on different process parameters. Size of the outlet for oil cake affects the oil utilization during cold pressing. By applying a 5 mm cake output extension, the largest volume of crude oil and final cold-pressed black cumin oil was obtained compared to the application of 6 and 8 mm extensions. When the size of the outlet for oil cake is smaller, the process pressure during pressing is higher, so a larger amount of oil is produced. It was expected that the largest amount of oil would be produced by applying the lowest frequency of the electric motor, because the material remains in the press system longer and this affects the squeezing efficiency. Also, as the temperature of the press head increases, the process pressure increases and the viscosity of the oil decreases, which results in greater squeezing and therefore utilization during pressing (7). However, based on the obtained results, it is noted that the process parameters N=6 mm, F=18 Hz and T=75 °C, which are between the

highest and the lowest values of the process parameters, are optimal for the black cumin oil production from the point of view of oil utilization.

Maslovac et al. (7) also examined the influence of process parameters on oil utilization by changing one of the parameters and keeping the other two constant. The conclusion of that research is that the best oil utilization is by using the smallest size for the cake outlet, the highest temperature of the press head, and using the lowest frequency.

Table 1. Influence of process parameters on the degree of pressing efficiency

SAMPLE	Process parameters	Mass of raw material (kg)	Volume of crude oil (mL)	Volume of oil 7 days after precipitation and vacuum filtration (mL)	Mass of oil cake (g)	Oil content in oil cake (%)	Moisture content in oil cake (%)	The degree of pressing efficiency (%)
1.	N=5 mm F=22Hz T=60 °C	1.8	546	343	557.75	24.64	6.50	26.55
2.	N=6 mm F=18 Hz T=75 °C	1.8	525	319	539.20	23.40	6.86	30.51
3.	N=8 mm F=15 Hz T=81 °C	1.8	481	271	572.34	24.30	6.59	27.63

N- size of the outlet for oil cake (mm)
F- frequency of the electric motor (Hz)
T- temperature of the press head (°C)

Table 2 shows the basic qualitative parameters of the obtained oil. The obtained values of the basic parameters of oil quality are not in accordance with the values of the Rulebook on edible vegetable oils, edible vegetable fats and mayonnaise ("Sl. gl. BiH", number 21/11) (8). Higher values of peroxide number and acidity may be the result of inadequate seeds storage. There are differences in quality parameters depending on the process parameters.

Table 2. Quality parameters of produced black cumin oil depending on different process parameters

SAMPLE	Process parameters	Peroxide value (mmol O_2/kg)	Free fatty acids (% oleic acid)	Moisture content in oil (%)	Unsaponifiable matter (%)
1.	N=5 mm F=22Hz T=60 °C	17.85	6.19	0.5	1.19
2.	N=6 mm F=18 Hz	17.04	5.71	0.58	1.19

	T=75 °C				
3.	N=8 mm F=15 Hz T=81 °C	19.44	6.10	0.54	1.87

The highest value of the peroxide number is for sample 3, where the pressing temperature was the highest (81 °C), and temperature is one of the factors that lead to the formation of primary oxidation products. There are no significant differences in the content of free fatty acids, and the lowest is in sample number 2. The moisture content also does not differ significantly, and the content of unsaponifiable matter is the highest in sample number 3.

Table 3 shows the presentation and comparison of the obtained quality parameters with the same parameters from different studies. Literature data also show higher values of peroxide number and free fatty acid content.

Table 3. Quality parameters of the obtained oil compared to the same parameters in different studies

SAMPLE	Process parameters	Peroxide value (mmol O_2/kg)	Literature data for peroxide value	Free fatty acids (% oleic acid)	Literature data for free fatty acids
1.	N=5 mm F=22Hz T=60 °C	17.85	25.9[1] 12.7[2] 13.5[3] 9.78[4] 28.5[5]	6.19	2.86[1] 12.01[2] 11.00[3] 9.29[4] 10.18[5]
2.	N=6 mm F=18 Hz T=75 °C	17.04		5.71	
3.	N=8 mm F=15 Hz T=81 °C	19.44		6.10	

[1] Argon, Zeliha Ustun and Ali Gökyer: Determination of Physicochemical Properties of Nigella sativa Seed Oil from Balıkesir Region, Turkey. *Chemical and Process Engineering Research.* **2016,** 41, 43-46.

[2] Ali, M Abbas; Sayeed, M.; Alam, M.; Yeasmin, Sarmina; Khan, Astaq and Muhamad, Ida: Characteristics of oils and nutrient contents of *Nigella sativa* Linn. and *Trigonella foenum-graecum* seeds. *Bulletin of the Chemical Society of Ethiopia* **2012**, 26 (1), 55-64.

[3] Bassim Atta, Mohamed: Some characteristics of nigella (*Nigella sativa* L.) seed cultivated in Egypt and its lipid profile. *Food Chemistry.* **2003**, 83 (1), 63-68.

[4] Khoddami, Ali; Mohd Ghazali, Hasanah; Yassoralipour, Ali; Ramakrishnan, Yogeshini and Ganjloo, Ali: Physicochemical Characteristics of Nigella Seed (Nigella sativa L.) Oil as Affected by Different Extraction Methods. *Journal of the American Oil Chemists' Society.* **2011**, 88, 533-540.

[5] Maslovac Tihomir; Jokić Stela; Jozinović Antun; Lončarević Ante and Bagarić Eva: Influence of black cumin seed pressing on the production and quality of cold pressed oil. *Glasnik zaštite bilja*. **2022**, 26-36.

4. Conclusion

Process parameters represent a key factor for the efficiency of the technological process of black cumin oil production. Also, the process parameters have a great influence on the quality of the obtained oil.

Based on this research it can be concluded that at the process parameters N=6 mm, F=18 Hz and T=75 °C, the highest pressing efficiency was achieved. Although the quality parameters are not in accordance with the prescribed values, the oil produced at these parameters has better values than the other two. It can be concluded that these parameters are optimal for the quality black cumin oil production.

5. References

1. Erener, G., Altop, A., Ocak, N., Aksoy, HM., Cankaya, S., Ozturk, E. Influence of black cumin seed (Nigella sativa L.) and seed extract on broilers performance and total coliform bacteria count. *Asian Journal of Animal and Veterinary Advances.* **2010**, *5(2)*, 128-135.
2. Yimer, M. E., Tuem K. B., Karim, A., Ur-Rehman, N., Anwar, F. Nigella sativa L. (Black Cumin): A Promising Natural Remedy for Wide Range of Illnesses. *Evid Based Complement Alternat Med.* **2019.**
3. Dimić, E. Hladno ceđena ulja. Tehnološki fakultet, Novi Sad, **2005**.
4. Zubr, J. Oil-Seed Crop: Camelina sativa. *Industrial Crops and Products*. **1997**, *6(2)*, 113-119.
5. Rac, M. Ulja i masti. Poslovno udruženje proizvođača biljnih ulja, Beograd, **1964**.
6. Bockisch, M. Fats and oils handbook. Academic Press and AOCS Press, Ilions, **1998**.
7. Maslovac, T., Jokić, S., Jozinović, A., Lončarević, A., Bagarić, E. Influence of black cumin seed pressing on the production and quality of cold pressed oil. *Glasnik zaštite bilja*. **2022**, 26-36.
8. Pravilnik o jestivim biljnim uljima, jestivim biljnim mastima i majonezama, Službeni glasnik BiH br. 21/11.

THE IMPACT OF COMBINED EMULSIFIER ON CRYSTALLIZATION PROPERTIES OF TRANS FREE FAT INTENDED FOR FAT FILLING PRODUCTION

Ivana Lončarević[1*], Biljana Pajin[1], Jovana Petrović[1], Ivana Nikolić[1], Branislav Šojić[1], Danica Zarić[2], Jelena Jurić[1,3]

[1] University of Novi Sad, Faculty of Technology Novi Sad, Bulevar cara Lazara 1, 21000 Novi Sad, Serbia,

[2]Innovation Centre of the Faculty of Technology and Metallurgy ltd., University of Belgrade, Karnegijeva 4, 11120 Belgrade, Serbia,

[3]Chocolate factory „Barry Callebaut“, Veliki rit, Novi Sad, Serbia

**ivana.loncarevic@uns.ac.rs*

Abstract

This paper investigated the influence of two separate emulsifiers (E1 and E2) and emulsifier 2 in 1 (E2in1) on crystallization characteristics of fat with no trans fatty acids intended for production of confectionary fat fillings. The emulsifiers were added to fat in amounts 0.3, 0.45 and 0.75 wt%.

The crystallization properties of fat samples were determined by rheometer, measuring the viscosity during cooling process. Also, NMR technique was used for measuring the solid fat content (SFC) at different temperatures, as well as for measuring the change of SFC in a function of time at 20 ºC. The results showed that all amounts of both types of emulsifiers affect the acceleration of crystallization in accordance with the added amounts during the crystallization of molten fats from 50 to 10 ºC, where the same amount of E2in1 has significantly ($p<0.05$) higher impact on viscosity increasing. Also, the fat samples with E2in1 have significantly ($p<0.05$) higher values of SFC at temperatures 20, 25, 30, and 35 ºC in comparison to fats with the same amount of two separate emulsifiers E1 and E2. However, observing the crystallization kinetics, it is shown that emulsifier E2in1 causes higher crystallization rates compared to control fat sample and samples with E1 and E2 and lower amount of crystals formed. The least amount of formed crystals is present in the fat sample with the addition of 0.75% of E2in1 which may negatively or positively affect the hardness of fat filling during cookie production, as future research will show.

Keywords: Trans free fat, emulsifiers, solid fat content, viscosity, crystallization kinetics

1. Introduction

Nowadays, much attention has been paid to consumer demand for ready to-eat foods with long shelf live, including filled cookies (1). Fat fillings basically consist of sugar and fat, where also other ingredients are included in the recipe. Powdered sucrose is the most used ingredient and acts both as sweetener and as bulking agent and also affects sensory properties such as sweetness, hardness and dryness of the final product (2). Fat content in fat fillings reaches over 40%. Such a high fat content, which presents a continuous filling phase, completely determines the consistency of the fat filling. When consuming the cookie with fat filling, the filling can melt faster or slower, depending on the type of fat and particle size distribution of solid particles (3).

Fat fillings contain emulsifiers that reduce the interfacial tension between fat and water by adsorbing on the surface of the hydrophilic particles. The polar lipid molecules of emulsifier adsorb on the sugar crystals surfaces by their polar heads, where the free hydrophobic tails are immersed in the fat phase. Emulsifiers allow solid particles to remain suspended in the fat phase, without fat migration, and therefore facilitate production and ensure finished products with a uniform quality and long shelf-life (4).

In fat-based products, emulsifiers can be also used to control fat crystallization properties. Some emulsifiers are added as modifiers of crystal structure and polymorphic retardant agents, since they can crystallise together with triacylglycerols and therefore prevent or retard the polymorphic transformations. Moreover, emulsifiers can also act as seeds for crystallisation by crystallizing before the triacylgycerols and thereby accelerating the nucleation rate (5). For that reason, it is of great importance to be also focused on fat crystallization kinetics (6).

This research examined the influence of combination of two kind of emulsifiers and combined emulsifier 2 in 1 on crystallization properties of edible fat without *trans*-fat acids, intended for production of fat fillings for filled cookies. Combined emulsifier 2 in 1 could serve as an alternative instead of combination of two different type of emulsifiers.

2. Experimental

2.1. Starting materials

Edible fat used in the experiments was DELIAIR^{TM}04 (AarhusKarlshamn, Sweden). According to specification, it is a non-temper filling fat with low content of lauric fatty acids and *trans*-fatty acids, with extremely good aerating properties.

The emulsifiers added to fat were:

GRINDSTED ® PGPR 90 (Danisco, Malaysia), in following text E1, was polyglycerol ester of polycondensed fatty acids from castor oil, with antioxidants added: alpha-tocopherol (max 200 ppm) and citric acid (max 200 ppm) dissolved in propylene glycol.

GRINDSTED ® CITREM LR 10 EXTRA KOSHER (Danisco, Germany), in following text E2, was citric acid ester of mono-diglyceride made from edible refined sunflower oil, with antioxidants added: alpha-tocopherol (max 200 ppm) and citric acid (max 200 ppm) dissolved in citric acid ester.

GRINDSTED ® CITREM 2 IN 1 KOSHER (Danisco, Germany), in following text E2in1, was citric acid ester of mono-diglyceride made from edible refined sunflower oil with antioxidants added: alpha-tocopherol (max 200 ppm), ascorbyl palmitate (max 200 ppm), and citric acid (max 50 ppm) dissolved in propylene glycol.

2.2. Plan of experiments

The emulsifiers E1 and E2 were dosed together in fat filling production in industrial conditions, in relation 1:2. In this experimental work, these two emulsifiers were replaced with a combined emulsifier E2in1, where the sum of E1 and E2 was equal to the percentage of E2in1. In this way, the possibility of replacing these two emulsifiers with a combined emulsifier 2 in 1 was investigated.

The emulsifiers were added in different amounts to pure fat in order to examine their influence on its crystallization characteristics (Table 1).

Sample	E1 (%)	E2 (%)	E2in1 (%)
F control	/	/	/
F 0.3 E1+E2	0.1	0.2	/
F 0.45 E1+E2	0.15	0.3	/
F 0.75 E1+E2	0.25	0.5	/
F 0.3 E2in1	/	/	0.3
F 0.45 E2in1	/	/	0.45
F 0.75 E2in1	/	/	0.75

2.3. Preparation of fat samples

The F control and the mixture of fat and emulsifiers were homogenized for 5 minutes at room temperature using homogenizer Ultraturrax T-25, Janke Kunkel, with a rotation speed of 6000 rpm.

2.4. Fatty acid composition

The fatty acid composition of examined fat was determined by gas chomatography, according to the method ISO 5508:1990 (7).

2.5. Solid fat content (SFC)

The SFC at temperatures 20, 25, 30, 35 and 40ºC was determined using Bruker minispec mq20 NMR Analyzer pulse device, according to the method ISO 8292:1991 (8).

2.6. Rheological examination of crystallization properties

The crystallization properties of fat samples were first determined by rotational rheometer Rheo Stress 600 (Haake, Karslruhe, Germany) using a concentric cylinder system (sensor Z20 DIN). The samples were dosed in cylinder and melted at 50 °C for 30 minutes. Then, the cooling was programmed from 50 °C to 10 °C in a period of 60 minutes.

2.7. Crystallization rate

The crystallization rate of examined fat was followed by measuring the change of SFC as a function of time by Bruker minispec mq 20 NMR Analyzer pulse device. The prepared fat samples were first placed into the glass NMR tubes and melted for 30 minutes at 50 ºC. Then, the samples were placed directly in a water bath at a crystallization temperature of 20 ºC. SFC content was measured every minute in a period of 60 minutes.

Crystallization kinetics was then described by Gompertz mathematical model (9, 10). On the basic of obtained experimental data od SFC in the function of time at 20 ºC, by means of nonlinear regression, Gompertz's mathematical model gives the dependence of the solid phase during crystallization of time under isothermal conditions:

$$S(t) = a \cdot \exp\left(-\exp\left[\frac{\mu \cdot e}{a}(\lambda - t) + 1 \right] \right) \quad (1)$$

where *S* was the SFC (%) at time t (min), *a* was the value for *S* when *t* was approaching infinity (%), μ was the maximum crystallization rate (%/min), and λ was a parameter proportional to inductive time (min).

2.8. Statistical analysis

Three replications were performed for each analysis, except for fatty acid composition, where one measurement was performed. The obtained results were statistically tested using analysis of variance (ANOVA) and the means were compared by one-factor ANOVA with subsequent

comparisons by Duncan's test at a significance level at 0.05 using Statistica 13.2 software (StatSoft, USA).

3. Results and discussion

3.1. Fatty acid composition of fat samples

The fatty acid composition of DELIAIRTM04 edible fat is given in Table 1.

Table 1. Fatty acid composition of trans free fat

Fatty acid	%
12:0	0.6
14:0	1.0
16:0	26.5
18:0	18.8
18:1	31.9
18:2	7.1
20:0	2.6
22:0	11.5
Trans-fatty acids	n.d.

* n.d. – not detected

The fat contained the highest proportion of saturated fatty acids (SAFA) - 61.0%, where palmitic fatty acid was most present (26.5%). The content of monounsaturated oleic fatty acid was 31.9%, while the content of polyunsaturated linoleic fatty acid was 7.1%. No undesirable trans-fatty acids were detected in DELIAIRTM04 fat, intended for the production of fat fillings.

3.2. SFC in fat samples

Fig. 1 shows the SFC of examined fat samples with 0.3%, 0.45%, and 0.75% of emulsifiers at the different selected temperatures. The fat samples with emulsifier E2in1 had significantly ($p<0.05$) higher values of SFC at all selected temperatures compared to F control.

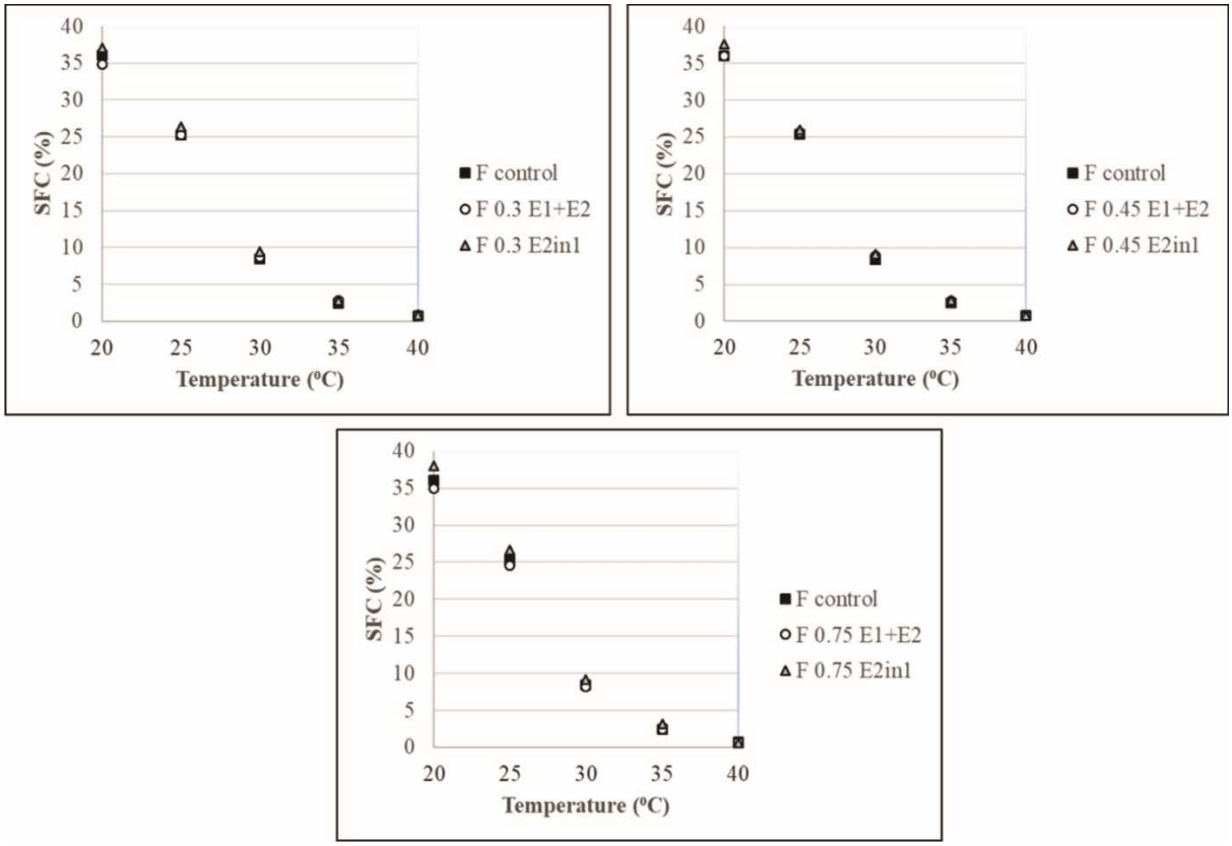

Figure 1. SFC of fats with 0.3%, 0.45%, and 0.75% of emulsifiers at 20, 25, 30, 35, and 40ºC

Also, the fat samples with certain amount of emulsifier E2in1 had significantly ($p<0.05$) higher values of SFC at temperatures 20, 25, 30, and 35 ºC in comparison to fat samples with the same concentration of two separate emulsifiers E1 and E2. At 40 ºC, there was no significant difference between SFC in samples with the same amount of E1+E2 and E2in1.

3.3. Rheological examination of crystallization properties of fat samples

The viscosity of fats during the cooling from 40 to 10 ºC in a period of 60 minutes is presented in Fig. 2, while the values of viscosity at selected temperatures are presented in Table 2. It can be seen from the Fig. 2 that the crystallization of molten fat samples begins at room temperature (25 ºC). It can also be seen that the addition of all amounts of emulsifier and E2in1 and the combination of E1 and E2 affect the acceleration of fat crystallization during cooling from 40 to 10 ºC, according to the adding amount. Moreover, it is obvious that the same amounts of emulsifier E2in1 had a greater impact on accelerating the crystallization of fat compared to the same amounts of added combinations of E1 and E2.

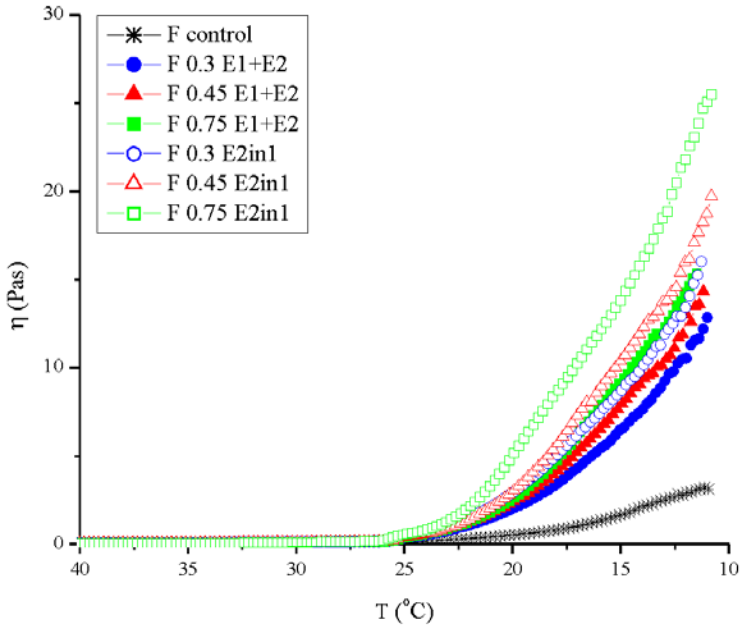

Figure 2. The viscosity of fat samples during the cooling from 40 to 10 ºC in a period of 60 minutes

All fat samples with emulsifiers added had significantly ($p<0.05$) higher values of mean viscosity at all selected temperatures (25, 20, 15, and 10 ºC) compared to F control (Table 2).

Table 2. Mean values of viscosity at different temperatures during fat cooling from 50 to 10ºC

Sample	Mean value of viscosity (Pa·s)			
	25ºC	20 ºC	15ºC	10 ºC
F control	0.07 ± 0.02^{a}	0.49 ± 0.02^{a}	1.57 ± 0.08^{a}	10.82 ± 0.28^{a}
F 0.3 E1+E2	0.23 ± 0.06^{b}	1.71 ± 0.12^{b}	6.18 ± 0.28^{b}	12.82 ± 0.20^{b}
F 0.45 E1+E2	0.26 ± 0.07^{b}	1.98 ± 0.14^{bc}	7.36 ± 0.31^{c}	14.67 ± 0.58^{c}
F 0.75 E1+E2	0.24 ± 0.05^{b}	2.13 ± 0.16^{c}	8.82 ± 0.30^{e}	15.35 ± 0.57^{c}
F 0.3 E2in1	0.25 ± 0.06^{b}	2.60 ± 0.21^{d}	8.20 ± 0.26^{d}	16.11 ± 0.35^{d}
F 0.45 E2in1	0.39 ± 0.05^{c}	2.65 ± 0.12^{d}	10.03 ± 0.35^{f}	19.79 ± 0.18^{e}
F 0.75 E2in1	0.42 ± 0.04^{c}	4.01 ± 0.37^{e}	13.41 ± 0.41^{g}	25.43 ± 0.39^{f}

Values followed by different lower-case letters in the same column are significantly different from each other ($p<0.05$).

At 25 ºC, the addition of E2in1 in the amount of 0.45 and 0.75% statistically significantly ($p<0.05$) accelerated crystallization and increased the viscosity of fat, compared to F control and other fat samples. At 20ºC the differences in viscosity were much more pronounced, where the fat samples with E2in1 had significantly ($p<0.05$) higher values of viscosity compared to samples with the same amount of combination of E1 and E2 and the fat sample with 0.75% of E2in1 had significantly ($p<0.05$) highest value of mean viscosity compared to all fat samples. Also, at 15 ºC and 20 ºC increasing the amount of combination of emulsifiers E1 and E2 and

E2in1 affected the increase in fat viscosity, where the addition of emulsifier E2in1 significantly ($p<0.05$) increased mean viscosity with increasing the amount of E2in1 and significantly ($p<0.05$) increased mean viscosity compared to the same amounts of combination of emulsifiers E1 and E2.

3.4. Crystallization kinetics

Fig. 3 shows the the fat crystallization at the crystallization temperature of 20ºC.

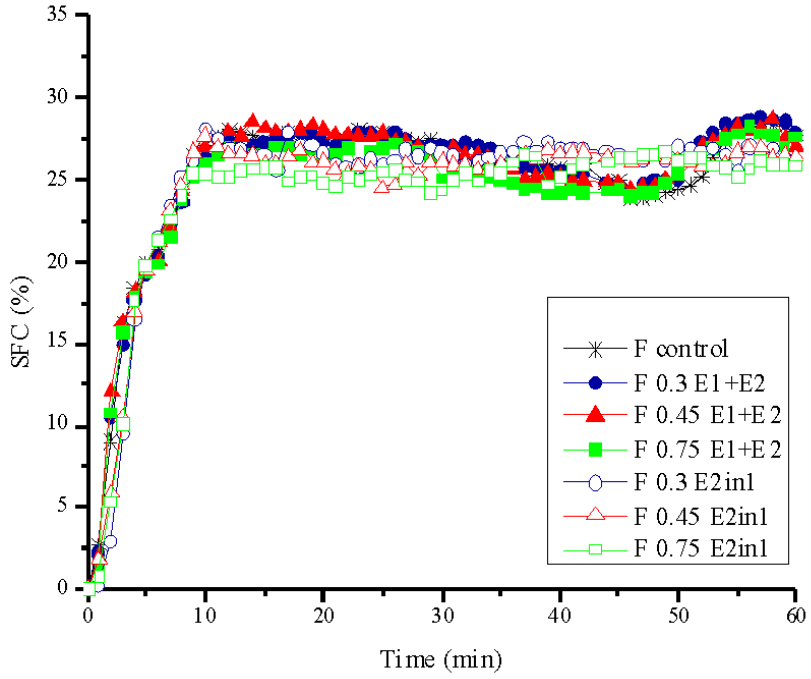

Figure 3. Crystallization rate of the fat samples at the crystallization temperature of 20ºC

Generally, it can be seen from Fig. 3 that all fat samples begin to crystallize at aproximatelly 10 ºC during the cooling of melted fat samples at 20 ºC. The parameters of Gompertz mathematical method are presented in Table 3.

Table 3. Parameters of Gompertz's mathematical model

Sample	Solid fat a (%)	Crystallization rate μ (%/min)	Induction period λ (min)	R^2
F control	26.52 ± 0.21^{cd}	4.91 ± 0.20^{a}	1.18 ± 0.15^{a}	0.94
F 0.3 E1+E2	26.80 ± 0.11^{d}	4.50 ± 0.47^{a}	1.10 ± 0.09^{a}	0.95
F 0.45 E1+E2	26.75 ± 0.15^{d}	4.57 ± 0.11^{a}	1.06 ± 0.05^{a}	0.93
F 0.75 E1+E2	25.98 ± 0.46^{b}	4.67 ± 0.15^{a}	1.13 ± 0.13^{a}	0.94
F 0.3 E2in1	26.61 ± 0.11^{d}	6.17 ± 0.13^{c}	2.47 ± 0.24^{c}	0.99
F 0.45 E2in1	26.21 ± 0.10^{bc}	5.43 ± 0.27^{b}	1.97 ± 0.13^{b}	0.98
F 0.75 E2in1	25.54 ± 0.11^{a}	5.72 ± 0.18^{b}	2.13 ± 0.13^{b}	0.99

Values followed by different lower-case letters in the same column are significantly different from each other ($p<0.05$).

Contrary to expectations, the addition of the emulsifier E2in1 affected the formation of the smallest amount of solid phase during the crystallization of melted fat samples at 20 ºC. The addition of 0.75% E2in1 affects the formation of the lowest amount ($p<0.05$) of solid phase compared to all fat samples. The combination of emulsifiers E1 and E2 did not have significant impact on crystallization rate and induction period of fat samples. On the other hand, the fat samples with emulsifier E2in1 had significantly ($p<0.05$) higher crystallization rates and induction periods compared to F control and fat samples with combination of emulsifiers E1 and E2. The high values of the coefficient of determination (R2) (0.93-0.99) indicated that the application of the Gompertz's mathematical model for describing experimental data by a theoretical curve is justified.

4. Conclusions

E2in1 may be used in confectionery industry instead of combination of two different type of emulsifiers, which are usually combined in order to give the necessary technological characteristics of cookies filled with fat fillings. Emulsifier accelerates the crystallization of fat without trans fatty acids, which is increasingly used in the production of fatty fillings. On the other hand, the addition of 0.75% of emulsifier E2in1 causes the lowest amount of crystals formed during the crystallization at isothermal conditions at 20 ºC. The future investigations will include the influence of examined emulsifiers on the physical and sensory characteristics of fat fillings intended for filled cookies production.

5. Acknowledgments

This work was supported by the Ministry of Education, Science and Technological Development, Republic of Serbia program (451-03-68/2022-14/200134).

6. References

1. Battaiotto, L. L., Lupano, C. E., Bevilacqua, A. E. Optimization of basic ingredient combination for sandwich cookie filling using response surface methodology. *Food Bioprocess Technol.* **2013**, *6(7)*, 1847-1855.
3. Mielea, N. A., Di Monaco, R., Masia, P., Cavellaa, S. Reduced-calorie filling cream: Formula optimization and mechanical characterization. *Chem. Eng. Trans.* **2015**, *43*, 67-72.

3. Lončarević, I., Fišteš, A., Rakić, D., Pajin, B., Petrović, J., Torbica, A., Zarić, D. Optimization of the ball mill processing parameters in the fat filling production. *Chem. Ind. Chem. Eng.* **2017**, *23(2)*, 197-206.
4. Delbaere, C., Van de Walle, D., Depypere, F., Gellynck, X., Dewettinck, K. Relationship between chocolate microstructure, oil migration, and fat bloom in filled chocolates. *Eur. J. Lipid Sci. Technol.,* **2016**, *118(12)*, 1800-1826.
5. Lončarević, I., Pajin, B., Omorjan, R., Torbica, A., Zarić, D., Maksimović, J., Švarc Gajić, J. The influence of lecithin from different sources on crystallization and physical properties of nontrans fat. *J. Texture Stud.,* **2013**, *44(6)*, 450-458.
6. Foubert, I., Vanrolleghem, P.A., Vanhoutte, B., Dewettinck, K. Dynamic mathematical model of the crystallization kinetics of fats. *Food Res. Int.,* **2002**, *35*, 945-956.
7. ISO 5508:1990 Animal and vegetable fats and oils - Analysis by gas chromatography of methyl esters of fatty acids.
8. ISO 8292:1991 Animal and vegetable fats and oils - Determination of solid fat content - Pulsed nuclear magnetic resonance method.
9. Foubert, I., Dewettinck, K., Vanrolleghem, P. A. Modelling of the crystallization kinetics of fats. *Trends Food Sci. Technol.,* **2003**, *14*, 79-92.
10. Foubert, I., Dewettinck, K., Janssen, G., Vanrolleghem, P.A. Modelling two-step isothermal fat crystallization. *J. Food Eng.*, **2006**, *75*, 551-559.

NUTRITIONAL MARKETING AND CONSUMER BEHAVIOR

Sasko Martinovski*, Tatjana Kalevska, Valentina Pavlova, Daniela Nikolovska Nedelkoska

Faculty of Technology and Technical Sciences Veles, "Dimitar Vlahov" bb, 1400Veles, R. N. Macedonia

**sasko.martinovski@uklo.edu.mk*

Abstract

Detecting the behavior of consumers of food products, but also the behavior of people in general is one of the most complex issues in the marketing of companies and therefore requires extensive research. This is so because of the individuality and complexity of people. Knowing all the impact factors grouped into determinants and discovering the links between them will lead to obtaining a wealth of information on the impacts and behaviors of food consumers. The research subject of this paper is the theoretical development of a new methodology of the so-called Nutrition marketing based on several principles (5N), aimed at the importance of nutritional determinants, but also other important determinants that influence consumer behavior when choosing food products. Including and highlighting the nutritional properties and quality and safety of food products as benefits to human health and well-being are part of the principles of Nutrition Marketing. As one of the concepts of Nutritional marketing, a survey was conducted in R.N. Macedonia on the impact of nutritional determinants on consumers. The analysis of the survey was done by creating multiple models. In the paper, the results of statistical methods for associativity and clustering model are presented. The principles of nutrition marketing and the developed methodology will enable companies to create a successful marketing strategy for food products. The benefit can be threefold: a benefit for companies through greater profits, a benefit for citizens through the consumption of healthy, quality and safe food products, and finally, a benefit for the state.

Keywords: Nutrition marketing, food, nutrition determinant, consumer behavior, nutritional quality

1. Introduction

Consumer behavior as one of the European perspectives (1), is explored through various marketing concepts, in order for companies to obtain information on how to meet consumer needs and directly influence the success of the company's operations. Consumer behavior

research is complex, because there is no ready-made formula for consumer behavior of human beings and the decisions are often hidden deep in the consumer's mind. Human consumer behavior, despite its complexity, can be presented as a business model through dynamic modelling and model creation. As a result, human behavior during purchasing can be explored by analyzing all dynamic behaviors in a series of assumptions and conditions.

When detecting consumer behavior, it is necessary to include scientific methods by using modern information technology. This includes: database management system (DBMS) needed for consumer database analysis; geographic information system (GIS), (2), (3), (4), for creating thematic consumer maps and business areas and for analysis of the current and future situation. It is also important to use it advanced analysis of databases using data mining methods, such as: association, classification, cluster analysis and etc., (5), (6), (7), methods that will enable detecting purchasing rules and obtaining clustered customer profiles.

In recent years, disease prevention has been an important part of social living and is increasingly moving in the direction of consuming healthy, safe and quality food. The importance of research on healthy food and nutrition for people is one of the goals of companies and societies (8), (9). The pandemic caused by the coronavirus, has changed the way consumers react to food. Their behavior when choosing food has changed and how they perceive food regarding searching for quality and functional food stuffs rich with nutrients. Our research shows that the number of consumers of food products, for whom the nutritional properties of food products, are one of the significant determinants of influence (10), (11), (12) has increased. Because of all that, it is important to create a new marketing strategy. One of the new aspects detected in our research is the creation of the so-called Nutritional marketing, which will determine: a) the degree of influence of the determinant - nutritional properties of food products (vitamins, minerals and other elements important for the human body), b) nutritional quality by emphasizing nutritional benefits, and c) creating nutritional awareness and attitudes.

2. Nutrition Marketing

Nutritionism is a multidisciplinary, scientific and applied field based on food science and nutrition. Nutrition marketing is an innovation based on a number of our studies. This concept is very important in the planning process of companies and in their marketing concepts. The aim is to achieve success in the development of new food products or to add additional

nutritional value to existing ones, by informing consumers and promoting all the benefits obtained by the consumption of nutritional quality and safe food products.

The modern marketing mix is based on several principles, for example the 4P principle (1. Product, 2. Place, 3. Price, 4. Promotion), (13) and nutrition marketing is based on five principles or the so-called 5N:

1N - Nutrition related consumer behavior. Includes advanced analysis of consumer databases and databases from marketing research such as surveys and other, by using advanced information technology and scientific methods. The results obtained from those analyses will contribute to the detection of nutritional factors influencing consumer behavior.

2N - Nutritional properties. Defining the nutritional properties of food products and their selection. The main purpose of this principle is **to define the nutritional determinant**. This includes selecting nutritional properties from the nutritional determinant that are significant in food products, i.e. which make them stand out. **Nutrition determinant:**

- Proteins: Quantity and origin: vegetable or animal
- Vitamins and minerals: Content and quantity
- Amino acids: Content and quantity of: lysine, histidine, arginine, aspartic acid, threonine, serine, glutamic acid, proline, glycine, cystine, valine, methionine, isoleucine, leucine, tyrosine, phenylalanine, tryptophan
- Enzymes: Content and quantity of: invertase, diastase (amylase), catalase, acid phosphatase, glucose-octase, polyphenoloxidase, peroxidase, esterase and proteolytic enzymes
- Fibers: Content and quantity
- Carbohydrates and energy value: Content and quantity in the form of: monosaccharides (glucose, fructose, sucrose), disaccharides, oligosaccharides, etc.
- Organic acids: Content and quantity of: ormic, oxalic, citric, tartaric, lactic, malic, pyroglutamin, glucose, valerian, benzoic and other higher fatty acids
- Salts: Content and quantity of: phosphates, chlorides, sulfates
- Lipids: Content and quantity of: triglycerides, sterols, phospholipids, free fatty acids, fatty acid esters
- Nutritional heath claims: Certificates
- Sensory characteristics: Color, taste, smell, hardness
- Product safety: Security standards
- Certification: Organic food, for quality

3N - Nutritional quality. This principle defines the ways of emphasizing the nutritional quality of food products and informing consumers. The first aim is adding value to food products by increasing and maintaining the nutrition quality by using creative and innovative solutions. The second aim includes ways the nutritional quality and safety can be emphasized as one of the key elements that can influence consumer behavior, i.e. its perception of quality and safe food and decision to buy.

4N-Nutritional benefits. This principle is aimed at informing consumers about: nutritional benefits; improving health through the diet; and the nutritional needs of human beings. Packaging design is very important, but even more important is for the nutritional properties to be clearly stated in the declaration, which would influence consumers in buying the product. There are several ways of communicating nutritional benefits to consumers: mass media using mass media techniques such as advertising and propaganda; another way is through educational programs of educational institutions; a third way is social media that has a huge impact with a huge number of users (Statista, 2022,https://www.statista.com/) and is used as marketing tools (Facebook, Instagram, blogs, forums, gastrogloblogs and influencers as channels used in marketing), and information about nutrition, the way of eating, gastronomy and food habits are distributed through them.

5N - Nutritional awareness. This involves creating awareness and attitudes about the nutritional value of food products. Marketing concepts should be applied here to develop awareness and create attitudes as much as the product can offer. This principle should enable the creation of awareness and the formation of attitudes through:

- Continuous introduction of consumers to healthy food and nutrition.
- Educational programs that will include a comparative analysis between healthy and unhealthy food.
- Continuous conveying of messages to consumers about the benefits of using food products that have nutritional quality and all the health benefits they offer.

3. Survey research into the influence of nutritional properties on consumer behavior

For the last few years, our marketing surveys have been aimed at surveys to detect key influencing factors of consumer behaviors (14), (15) related to the nutritional characteristics of food products. A database is formed from the conducted research, and the conducted advanced analyzes result in concluding observations. In the analysis of the data obtained, moreover, more methods have been used apart from the data aggregation: a ranking-based method; hypothesis

tests Chi-Square and Cramér's V to determine the relationship between two variables (answers to two questions); and the clustering method, to obtain consumer clusters. This paper shows only a small part of the analyses and the results obtained.All analyzes are performed in R-version 4.0.5, a software for statistical and other types of analysis.

The ranking-based method was used in a survey conducted in the Republic of North Macedonia of 300 respondents to determine the factors influencing the selection of honey (from 1-lowest, 5th - highest). Table 1 shows a result obtained by the ranking-based method when selecting honey. It can be concluded that all five factors have an impact of about 20%, but the influence value of the nutritional properties of 20% should still be noted, a value that is significant and equated with the other influence factors.

Table 1: Results obtained by a ranking-based method when selecting honey

Rank	**Packaging** ***Σ (f*Rank)***	**Color of honey** ***Σ (f*Rank)***	**Taste of honey** ***Σ (f*Rank)***	**Price of honey** ***Σ (f*Rank)***	**Nutritional properties of honey** ***Σ (f*Rank)***	**Total**
1 and 2	158	150	89	147	139	
3	141	159	171	237	153	
4 and 5	622	720	863	502	686	
SUM	921	1029	1123	886	978	4937
Influence	**19%**	**21%**	**23%**	**18%**	**20%**	**100%**

where: Σ: SUM; f: frequency; Rank: from 1-lowest 5th – highest; Influence = SUM / Total
The Chi-Square and Cramér's V hypothesis tests were used to determine the association (association) of the answers to two core questions in a survey (table 1) conducted on 450 respondents in the Republic of North Macedonia. Table 2 shows the frequency of answers to questions 1 and 2 in pairs, which are classified into two nominal variables (question 1 and 2) and the result of the Chi-Square and Cramer's V tests.

Explanation: $p<\alpha$ which means that **there is a statistical dependence** between the nominal variables, i.e. the answers to both questions are **statistically dependent**, and the value of Cramer's V is 0.3629 and it shows that this dependence is moderate. This means that the price is not the only factor in the decision making during the purchase, but the nutritional properties that are placed on the declaration also have an impact.

Table 2. Frequency of answers to questions 1 and 2 in pairs, which are classified into two nominal variables and the result of the Chi-Square and Cramer's V tests.

	2. I rate the value of the product not only according to the price, but also according to the nutritional quality.			
1. Irrespective of the nice shape and packaging, it is essential for me to have a list of the nutritional properties in the product declaration.	Yes	Partially	No	SUM
Yes	200	50	9	259
Partially	44	120	9	173
No	8	8	2	18
Total				450

Chi-Square				Cramer's V
118.51	df	α	p	0.3629
	4	0.05	<0.0001	

In the same survey on the impact of nutritional properties of food products on consumer purchasing decisions, using the Partitioning Clustering Method, a cluster was obtained (Figure 1) of respondents who answered yes simultaneously to three questions (with answers yes, no or partially):

Q1. Irrespective of the nice shape and packaging, it is essential for me to have a list of the nutritional properties in the product declaration.
Q2. I rate the value of the product not only according to the price, but also according to the nutritional quality.
Q3. Declarations with nutritional properties help me determine nutritionally healthy foods.

Of the total number of respondents (450), 50,5% answered these questions simultaneously with "yes" as set pattern 1. Q1 (yes) - Q2 (yes) - Q3 (yes).

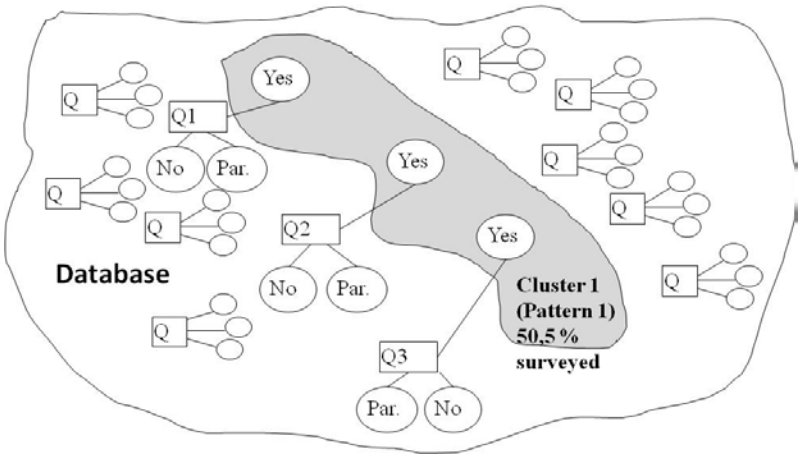

Figure 1. Cluster of respondents who answered "yes" simultaneously to questions 1, 2 and 3.

The information obtained from the clustering is that there is a cluster of 50.5% of respondents (out of a total of 450) who consider that the price is not the only factor in their decision making when buying, but the nutritional properties that are placed on the declaration also have an influence helps them in determining healthy nutritious food.

4. Conclusion

A novelty in the paper is the so-called Nutrition marketing based on five principles (5N). Nutrition marketing is a concept to determine the impact on consumer behavior of foods with improved nutritional quality, by emphasizing the components that affect human well-being and health. This concept provides guidelines for highlighting the nutritional properties of products in order to choose higher quality and healthier nutritional products, and thus, improve human health.

The analysis and results of the survey research shown in the paper are only a small part in using this concept, but it shows the use of advanced analysis that is important for obtaining a picture of how much the consumer is familiar with the benefits of the nutritional properties of food products and their impact. The fact that new food regulations have been adopted in the Republic of North Macedonia and the large number of regulations in the EU, declarations of food products should be marked clearly and concisely especially regarding the significance of nutritional values that are important for consumers, which means that companies and individuals who produce food products should include Nutritional Marketing to create a successful marketing strategy.

The research done in the paper is relevant for: large and small food companies; consumer organizations; and the Food and Veterinary Agencies. They will be able to find out how to

determine how consumers informed about the declaration of food products, with their quality and nutritional properties, and how much all of this affects the purchase decision. These insights will enable food industry companies to plan a successful Nutritional Marketing Strategy.

The further development of the research can continue by including new determinants which can significantly influence consumer behavior and establishing new principles in marketing strategies.

5. References

1. Solomon, M. "Consumer Behavior: A European Perspective". *3rd ed. Harlow: Prentice Hall*, **2006**, 1-200.
2. James B. Pick James B. Pick, University of Redlands, USA, "Geographic Information Systems in Business", *Published in the United States of America by Idea Group Publishing*, **2005**, 1-80.
3. Martinovski, S. "Gis modelling for strategic planning of the urban environment". Book, *LAP LAMBERT Academic Publishing*, **2017**, 1-208.
4. Martinovski, S. Gis modelling for the strategic urban development planning, Doctoral Dissertation, *University "St. Kliment Ohridski" – Bitola*, **2013**, 1-249.
5. Perner, P. "Advances in Data Mining, Applications in Medicine, Web Mining, Marketing, Image and Signal Mining". *6th Industrial Conference on Data Mining, ICDM Leipzig, Germany*, **2006**, 10- 47.
6. Jannach, D., Zanker, M., Felfernig, A., Friedrich, G.," Recommender Systems An Introduction". *Cambridge University Press*, **2011**, 1-49.
7. Han, J., Kamber, M., Pei, J. "Data mining: Methods and Models", *Third Edition Morgan, Kaufmann is an imprint of Elsevier*,**2012**, 1-86.
8. Lori, A. Smolin, D., Mary B. Grosvenor, M.S., R.D., "Healthy eating: a guide to nutrition". *Chelsea House*, **2011**, 29-166.
9. Steve, L. Taylor, "Advances In Food And Nutrition Research", *Copyright _ 2007. Elsevier Inc.*, **2007**, 37-51.
10. Martinovski, S. "Self-Explanatory Nutrition Business Models of Consumer Behavior"/ *International Journal of Business and Management Invention*,**2016**, URL:http://www.ijbmi.org/papers/ Vol(5)9/F05903240.pdf
11. Nikolovska Nedelkoska. D., Martinovski S., Nikolovska A.," Development of a food frequency questionnaire to assess the dietary intake of a phytate in the urban

Macedonian population". *Journal of Hygienic Engineering and Design*, Original scientific paper, **2016**, *19*, 11-14.

12. Martinovski S., Gulevska F. "Nutritive Marketing with a Special Review on Honey". *International Journal of Business and Management Invention*, **2017**, *6 (7)*, 5-11.
13. Kotler, P., Amstrong, G. "Principles of marketing", *12th ed., Pearson education, Inc, translation: Academski Pecat, R.N. Macedonia*, **2008**, 34-55.
14. Martinovski, S., Gulevska, F. "Nutritive Marketing with a Special Review on Honey". *International Journal of Business and Management Invention*, **2017**, *6 (7)*, 5-11.
15. Martinovski, S., Gulevska, F. "Nutritive marketing and analysis ofconsumption behaviour for honey". *Nutricom Congress Skopje*, **2017**.

STABILIZATION OF SUNFLOWER OIL BY ADDING GARDEN SAVORY (*SATUREJA HORTENSIS*)

Gorica Pavlovska[1*], Violeta Ognenoska[2], Vezirka Jankuloska[1], Anka Trajkovska Petkoska[1]

[1]St. Kliment Ohridski University Bitola, Faculty of Technology and Technical Sciences, Dimitar Vlahov bb. 1400 Veles, R. N. Macedonia,

[2]Ministry of Defense of Republic of North Macedonia, Orce Nikolov 16, 1000 Skopje, R. N. Macedonia

[*]gorica.pavlovska@uklo.edu.mk

Abstract

Sunflower oil is one of the most widely used oils in the food industry and it is categorized into two groups: cold pressed and refined sunflower oil. Cold pressed sunflower oil has better nutritional properties than refined one, but it oxidizes more easily which decreases its stability. In this study, refined sunflower oil (brand „Briliant“) and cold pressed sunflower oil (brand „Fila“) were analyzed. Bottles with volume of 1L were used for storing the examined oils; however, part of the oil was removed in order to investigate oil volume of ¼, ½ and ¾ of the total bottle volume. Dry garden savory (*Satureja hortensis*) was added to one part of the oils in order to examine their stability.

The oil samples were stored for a period of 4 weeks, after which period the peroxide values of each sample were determined/peroxide values a measure of the oil oxidation. The highest peroxide values observed in the oil sample with a volume of ¼; namely, for refined oil this value is 5.88 mmol O_2/kg, while for cold pressed oil is 11.76 mmol O_2/kg. The oils with the same volume ratio that contain savory had significantly lower peroxide values.

In general, the addition of garden savory reduced the oil oxidation, especially in cold pressed sunflower oil, resulting in more stable oils.

Keywords: Sunflower oil, garden savory, peroxide number, stabilizing, oxidation

1. Introduction

Sunflower oil is derived from sunflower seeds. This plant is mostly grown in Russia, Ukraine, European Union countries, Turkey, Argentina, China and North Africa (1). In Macedonia it is the main oil-yielding crop, while worldwide it is among the four most important raw materials

for oil production (1). Depending on its processing, it can be manufactured as cold pressed and refined oil.

The oil obtained by mechanical extraction, i.e. pressing, is called cold pressed, and the oil obtained by chemical extraction using a solvent is called refined. Refined and cold-pressed oil, in addition to the method of production, also differ in: organoleptic properties (color, smell, taste), chemical composition, nutritional properties and stability. Cold-pressed oils are nutritionally more important, but are chemically more unstable and oxidize easily (2,3).

Oil oxidation occurs during prolonged storage, at higher temperatures and during frying. During storage, oils react with oxygen from the air and auto oxidation occurs (4,5). In general, oxidation of oils is much higher at high temperature as well as during frying (5-7).

Oxidation products are toxic and harmful to human health and therefore it is necessary to monitor their concentration (8). The main oxidation products in oils are peroxides and hydroperoxides which are determined by the peroxide value (9).

Antioxidants are widely used to reduce oxidation and they can be natural or synthetic. Today, the main focus is given to the natural antioxidants that are mostly found in many essential oils. Moreover, the antioxidants present in garlic, rosemary and parsley have been shown to be good stabilizers of oils as well (10,11). In addition, *Satureja hortensis* contains many chemical components that have high antioxidant potential (12,13).

The purpose of this paper is to evaluate the effect of the garden savory on stability of sunflower oils.

2. Experimental

Two types of sunflower oils, refined and cold pressed, were analyzed. The refined oil from brand "Brilliant" is a product of "Vitaminka" Prilep, and the cold-pressed oil "Fila" is a product of "Agrofila" Shtip, Republic of N. Macedonia. The examined oils were purchased from the market in Skopje and have a volume of 1L. A certain volume of oil was taken from all the bottles and the oil left in the bottles for analysis is 1/4, 1/2 and 3/4 of the total volume of the bottle i.e. there is left volume of 250 mL, 500 mL and 750 mL of oil in the bottles. In half of the bottles for analysis (refined and cold pressed with 1/4, 1/2 and 3/4 of the total volume) was added 20 g of dry garden savory.

The oils with and without garden savory are stored for 4 weeks at room temperature, in dark, dry place. After this period, the peroxide value of all oils is determined according to a standardized procedure, in order to examine the oxidation rate in each of the tested oils (9).

3. Results and discussion

The comparison of peroxide values of the refined and cold-pressed oils with different stored volumes without garden savory is presented in Figure 1. It can be seen that by reducing the volume of oils in the bottle, the peroxide value of both types of oil increases. This happens because of the higher amount of oxygen presented in the bottles with a lower oil volume. The oxygen cause oxidation of the oil and leads to increased peroxide value. In general, cold-pressed oils had a higher peroxide value compared to refined oils for an equal oil volume.

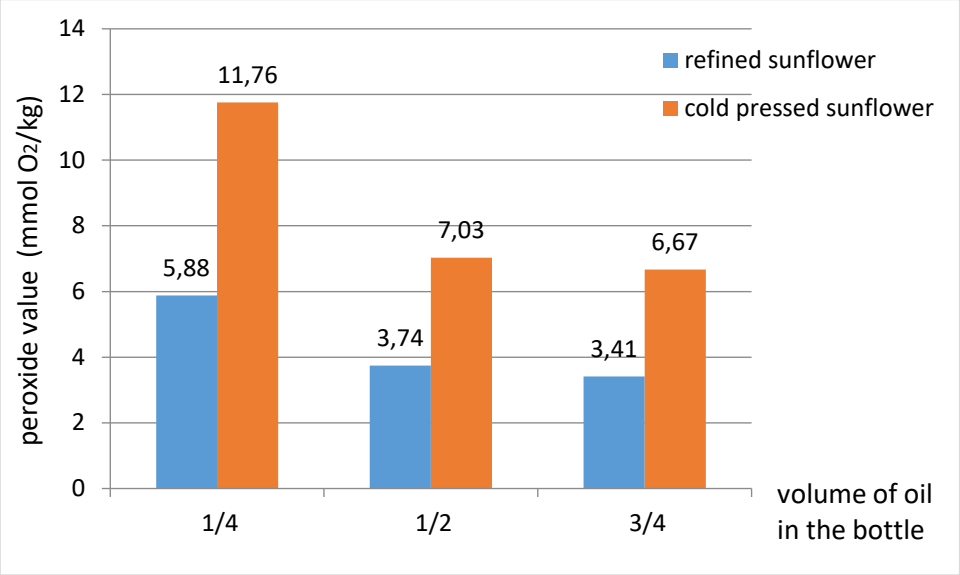

Figure 1. Peroxide value of refined and cold-pressed sunflower oil without garden savory after 4 weeks storage in dark place, at room temperature

Oils with 1/4th of the volume of the bottle have a peroxide value above the maximum allowed concentration (MAC) i.e. it is higher in both cases, refined and cold pressed oils. MAC is defined by the Rulebook for oils and the quality of fats and edible oils (MAC for refined oil is 5.0 mmol O_2/kg, while for cold-pressed oil is 7.5 mmol O_2/kg) and therefore these oils are not edible (14).

Whit addition of the garden savory in refined oil, the peroxide value decreased compared to refined oil with the same volume without savory addition (Fig. 2). The reduction in peroxide value or oils containing 3/4 oil and 1/2 oil of the total volume of the bottle is insignificant. The presence of savory in the bottle with the lower oil volume leads to a greater reduction of the peroxide value compared to the oil of the same volume (1/4 of the total volume of the bottle) without savory. All examined refined oils of varying volumes with added savory are safe for consumption.

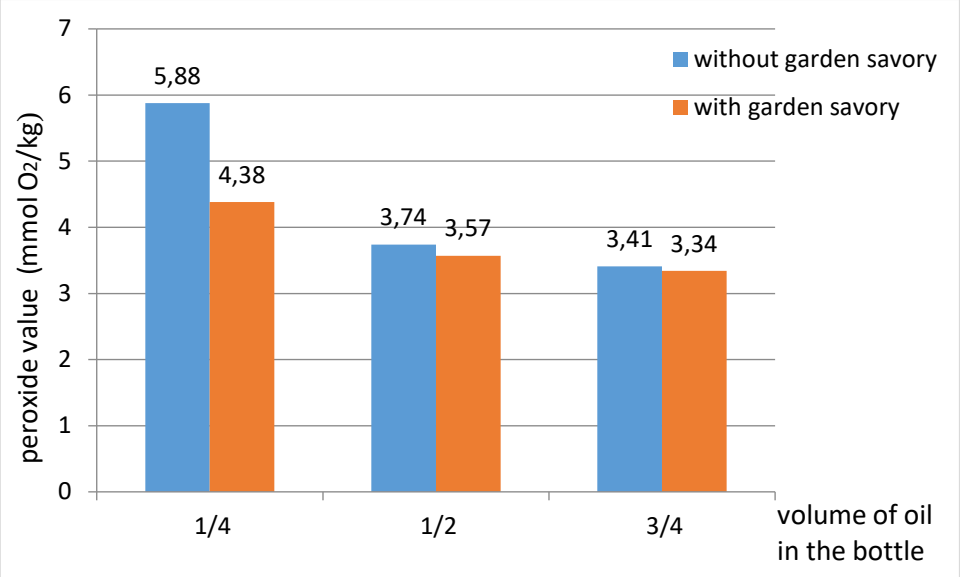

Figure 2. Peroxide value of refined sunflower oil „Briliant“ with and without garden savory after 4 weeks storage in dark place, at room temperature

The oxidation of cold-pressed sunflower oil is significantly reduced with the addition of garden savory to the oil (Fig. 3). A significant reduction in the peroxide value of the oils with savory compared to the oils without savory is found in the oils containing 3/4 oil and 1/2 oil of the total volume of the bottle, but it is highest in the oil with 1/4 of the total volume of the bottle i.e. in the bottle with the smallest volume of oil. Adding garden savory to cold-pressed oil stabilizes all oils of varying volume and makes them safe for consumption.

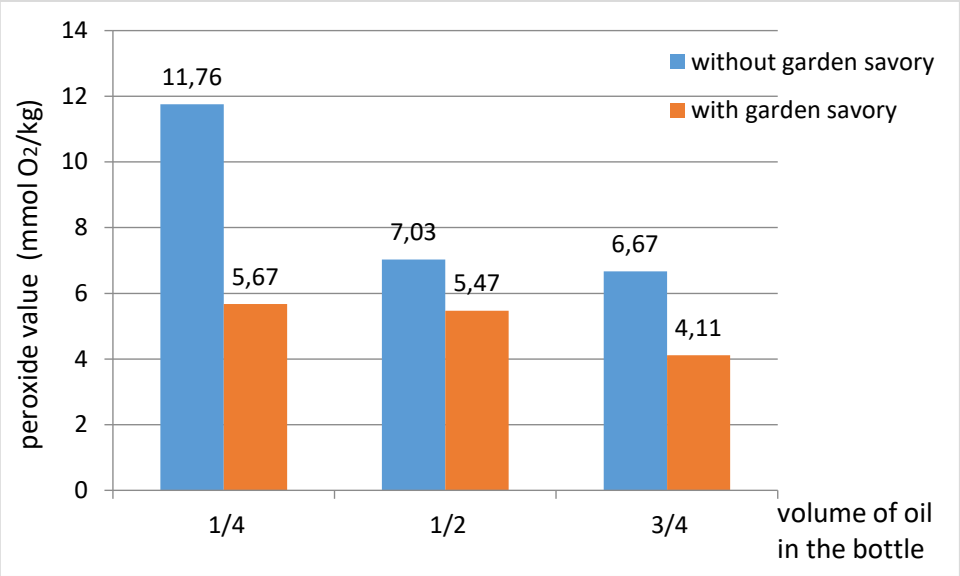

Figure 3. Peroxide value of cold pressed sunflower oil "Fila" with and without garden savory after 4 weeks storage in dark place, at room temperature

4. Conclusion

The peroxide values of two types of sunflower oil, refined sunflower oil ("Brilliant" brand) and cold-pressed sunflower oil ("Fila" brand) were determined. The volume of the oil in the bottles is different (1/4, 1/2 and 3/4 of the total volume of the bottle), in half of the analyzed oils, garden savory is added and the oils are stored for 4 weeks in dark place, at room temperature. By reducing the volume of oil in the bottle for both types of oil, refined and cold pressed, the peroxide value increases and the stability decreases during the storage period. Oils with the lowest volume, i.e. 1/4 of the total volume of the bottle, without garden savory, are not safe for consumption since peroxide value in these oils were higher than the allowed amount. Adding savory to the oils reduces the peroxide value which increases their stability and making them safe for consumption. An increase in stability is found in both types of oil (refined and cold-pressed oil) and in oils with different volumes after adding the dry garden savory.

The most significant stability increase is found in cold-pressed oils and in oils with the lowest volume, i.e. $1/4^{th}$ of the total volume of the bottle. Garden savory increases the stability of refined and cold-pressed sunflower oil and they are safe for consumption even after 4 weeks of storage when the bottle contains only 1/4 of the total volume of oil. Such stabilization of oils can be done at home for daily use.

5. References

1. Gunstone, F. D. Vegetable Oils in Food Technology: Composition, Properties and Uses. Blackweel Publishing Ltd, CRC Press, **2011**.
2. Dimic, E. Cold pressed oils. Faculty of Technology, Novi Sad, **2005**.
3. Pavlovska, G., Jankuloska, V., Antoska-Knighs, V., Stojanova, E. Differences in chemical parameters of cold pressed oil and refined cooking oil. *Maced. J. Anim. Sci.* **2016**, *6(1)*, 47-50.
4. Crapiste, G., Brevedan, M., Carelli, A. Oxidation of sunflower oil during storage. *J. Am. Oil Chem. Soc.* **1999**, *76*, 1437-1443.
5. Pavlovska, G., Shurkova, N., Jankuloska, V. Oxidative stability of refined sunflower oil at room temperature and during conventional frying. *Food and environment safety.* **2017**, *16(1)*, 29-33.
6. Sadoudi, R., Ammouche, A., Ali, Ahmed, D. Thermal oxidative alteration of sunflower oil. *AJFS*. **2014**, *8(3)*, 116-121.

7. Farhoosh, R., Hoseini-Yazdi, S. Z. Shelf-Life Prediction of Olive Oils Using Empirical Models Developed at Low and High Temperatures. *Food Chem.* **2013,** *141(1),* 557-565.
8. Di Nikolantonio, J., O'Keefe, J. Omega-6 vegetable oils as a driver of coronary heart disease: the oxidized linoleic acid hypothesis. *Open heart.* **2018**, *5(2)*, 1-6.
9. AOCS Cd 8-53, Official methods and recommended practices of the American oil chemists' society, Method Cd 8-53, **1996**.
10. Eftinzjioska, H., Pavlovska, G. Stability of oil from oil seed rape with garlic under various conditions. *JAPS*. **2019**, *17 (1)*, 51-56.
11. Temelkovska, K., Pavlovska, G. Reducing the oxidation of cold pressed sunflower oil by adding rosemary or parsley. *International Journal of Food Science and Nutrition*. **2021**, *6(5),* 65-69.
12. Kemertelidze, É. P., Sagareishvili, T. G., Syrov, V. N., Khushbaktova Z. A. Chemical Composition and Pharmacological Activity of Garden Savory (Satureja hortensis L.) Occurring in Georgia. *Pharm. Chem. J*. **2004**, *38(6),* 319–322.
13. Pländer, S., Gontaru, L., Blazics, B., Veres, K., Kery, A., Kareth, S., Simandi, B. Major antioxidant constituents from Satureja hortensis L. extractsobtained with different solvents. *Eur. J. Lipid Sci. Technol.* **2012**, *114(7)*, 772–779.
14. Official Journal of R. Macedonia: Rulebook on requirements regarding the quality of vegetable oils and vegetable fats, margarine, mayonnaise and related products. R Macedonia. **2012,** No.127.

THE PRESENCE OF NITRITE IN MEAT PRODUCTS FROM THE MARKET OF REPUBLIC OF SRPSKA

Biljana Pecanac*, Željko Slodojević

PI Veterinary Institute of the Republic of Srpska „Dr Vaso Butozan“ Banja Luka, Branka Radičevića 18, 78000 Banja Luka, Republic of Srpska, BiH

**biljana.pecanac@virs-vb.com*

Abstract

Nitrites are preservatives that are added to meat products to improve the quality, durability and safety of products. Due to carcinogenic nitrosamines in meat products, there is a potential danger to human health.

The aim of the research is to determine the content of residual nitrites in 576 meat products from the market of Republika Srpska, to identify products that contain higher and which contain lower amounts, and to look back to the requirements of the Ordinance on Food Additives (SG RS, number 96/20), which defines the amount of nitrites which is allowed to add in meat products. In the period May 2015 - May 2022, 576 meat products were tested using the *BAS ISO 2918* method.

Nitrites were not quantified in 20% of products (< LOQ). The highest average value of nitrite is in heat-treated meat sausages in pieces (45.73 ± 15.854 mg/kg), finely chopped (42.84 ± 15.245 mg/kg) and coarsely chopped boiled sausages (37.40 ± 21.396 mg/kg). In durable dry meat products, the lowest average amounts of nitrite are 6.17 ± 2.229 mg/kg, and higher in semi-durable cured meat 36.30 ± 17.331 mg/kg. In cans, the average value of nitrite is 13.29 ± 10.288 mg/kg, and in pate 15.71 ± 10.473 mg/kg.

Based on the obtained results, the amount of residual nitrite below the amount of nitrite allowed to be added to meat products by the Rulebook that can be added to meat products was determined. Larger amounts of nitrites were recorded in heat-treated products, and less in non-heat-treated permanent products. From the point of view of the potential danger of nitrites for human health, and thus the safety of meat products, the most acceptable are permanent meat products.

Keywords: Meat product, nitrites, carcinogenic

1. Introduction

"Food additive" is any substance that, regardless of its nutritional value, is not used as food by itself, nor is it a characteristic ingredient of food, but is added to food for technological reasons during production, processing, preparation, processing, packaging, transportation or storage that directly or indirectly via its intermediate products becomes or can become a food ingredient.

One of the functional classes of food additives are preservatives that extend the shelf life of food by protecting it from spoilage caused by microorganisms and/or protecting it from the development of pathogenic microorganisms. Nitrates and nitrites are listed in the list of additives approved for use in food. Nitrites are preservatives that are added to meat products to improve the quality, durability and safety of the product. They affect the change in color, smell, taste and texture of meat products, and thanks to their antioxidant effect, they contribute to the prevention of rancidity and inhibit the growth and development of the pathogenic bacterium *Clostridium botulinum*, which can lead to botulism (1, 2). Nitrite intake is normally low and is not an acutely toxic dose, but it is believed that nitrite in food primarily causes health problems because its presence in food and in the body can lead to the formation of carcinogenic nitrosamines (3, 4). It is important to emphasize that the nitrite level is monitored during all processing steps up to the end consumers (5). In the meat industry, sodium nitrite (E250) and potassium nitrite (E249), i.e. sodium nitrate (E251) and potassium nitrate (E252) are most often used as a component of brine (Toldrá, 2010) In the meat industry, as a component of brine, sodium nitrite (E250) and potassium nitrite (E249), or sodium nitrate (E251) and potassium nitrate (E252) are most often used (6). For nitrites used as food additives, experts estimated exposure to be within safe levels for all population groups, except for highly exposed children, who might slightly exceed the ADI. Exposure from all dietary sources may exceed the ADI for infants, toddlers, and children with medium exposure, and for highly exposed individuals of all age groups (7). Numerous studies have shown that nitrite can react with various meat components such as proteins, lipids, pigments and other meat components, and it is bound nitrite, and the part that remains without entering into a chemical reaction remains in free form (as NO2 and HNO2) and is called free or residual nitrite. Analytical methods can only detect amount of free (residual) nitrite. It is a well-known fact that the loss of nitrite in meat products depends on a number of factors, including the thermal process used, pH, storage conditions and the addition of ascorbic acid or other reducing agents, but analyzing the data obtained, we can say that the rate of nitrite loss also depends on the type of packaging, and all other factors

remain the same. In vacuum-packed sausages, it falls more slowly after the modified atmosphere of packaged sausages, while as it was expected for the fresh unpackaged sausages the decline was sharper (5). During storage it comes to the reduction of the concentration of nitrites, and thus the meat products on the market they contain on average 5-30 mg/kg of free nitrites (8, 9). Meat products can be contaminated with carcinogenic N-nitrosamines, which is ascribed to the reaction between a nitrosating agent, originating from nitrite or smoke, and a secondary amine, derived from protein and lipid degradation. Although in model systems it is demonstrated that many amine containing compounds can be converted to N-nitrosamines, the yield is dependent of reaction conditions (e.g., low pH and high temperature) (10). Regarding food borne intoxications, the accumulation of biogenic amines must be avoided in all kinds of food products. Moreover, biogenic amines can function as precursors for the formation of carcinogenic N-nitrosamines when nitrite is present. To estimate the food safety of the dry fermented sausages available on the Belgian market, a screening of the residual sodium nitrite and nitrate contents, biogenic amines and volatile N-nitrosamine concentrations was performed on 101 samples. The median concentrations of residual NaNO2 and NaNO3 were each individually lower than 20 mg/kg. In general, the biogenic amine accumulation remained low at the end of shelf life. Concerning the occurrence of N-nitrosamines, only N-nitrosopiperidine and N-nitrosomorpholine were detected in a high number of samples (resp. 22% and 28%). No correlation between the presence of N-nitrosamines and the biogenic amines content was observed (11). It is very important to point out that several works indicate that the majority of the nitrates intake is attributed to plant foods. Approximately 98% of the nitrates intake from food is attributed to fruits and vegetables, while only the remaining 2% to cured meat products (12).

The aim of the research is to determine the content of nitrites in meat products from the market of Republic of Srpska, to determine compliance with the requirements of the regulation (13) and to show nitrites by type.

2. Experimental

The experimental work was based on analysis of the nitrite content in different meat products, which according to systematization belonged to different groups and subgroups meat products. In the period from May 2015 to May 2022, 576 different meat products originating from the market of Republic of Srpska were examined. The samples, according to the systematization prescribed by the regulation (14) belong to four categories: sausages (permanent dry sausages

(n = 70), thermally processed sausages (n=187) and fresh (n=5)), dried meat products (permanent products (n=19) and semi-permanent products (n=27)), canned goods (canned minced meat, breakfast cuts (n=126) and pates (n = 111)) and bacon (permanent (n = 16) and semi-permanent (n = 15)).

The analytical method used to determine the nitrite content in all samples was according to the BAS ISO 2918 method using an "Agilent Technologies" Cary 60 UV-VIS spectrophotometer at 540 nm.

3. Results and discussion

Nitrites are preservatives that are added to meat products to improve the quality, durability and safety of products. Due to carcinogenic nitrosamines in meat products, there is a potential danger to human health. In the period May 2015 - May 2022, 576 meat products were tested using the BAS ISO 2918 method.

Table 1. Results of testing Na-nitrite (mg/kg) in meat products from the market of Republic of Srpska presented by groups in the period May 2015 - May 2022

Group og Meat Products	N	n< LOQ	Mean ±SD mg/kg	Min mg/kg	Max mg/ kg
Finely chopped sausages	74	-	42.84±15.245	10	88
Coarsely chopped sausages	98	-	37,40±21,396	6	106
Dry fermented sausages	70	47	9,04±5.776	< LOQ	19
Canned meat - meat breakfast	126	11	13,29±10,288	< LOQ	63
Pate	111	44	15,71±10,473	< LOQ	53
Semi-permanent dried meat products	27	4	36,30±17,331	9	84
Permanent dried meat products	19	-	6,17±2,229	< LOQ	19
Heat-treated meat sausages in pieces	15	-	45,73±15,854	14	75
Permanent bacon	16	-	9,41± 4,358	< LOQ	17
Semi-permanent bacon	15	4	29,00± 10,567	17	49
Fresh grilled sausage	5	5	< LOQ	< LOQ	<2
Total	576	115			

N−total number of analysed samples; n− the number of samples in which no nitrites were detected LOQ -limit of quantification =2 mg/kg

Table 1 shows the results of testing Na-nitrite (mg/kg) in meat products presented by groups according to the current regulation (14). Nitrites were not quantified in 20% (115 samples) of products (Figure 1). Heat-treated meat sausages in pieces have the highest average value of nitrites (45.73 ± 15.854 mg/kg), and the lowest value was found in permanent dried meat products (6,17± 15.854 mg/kg). Based on the obtained results, the amount of residual nitrite below the amount of nitrite allowed to be added to meat products by the Rulebook that can be added to meat products was determined.

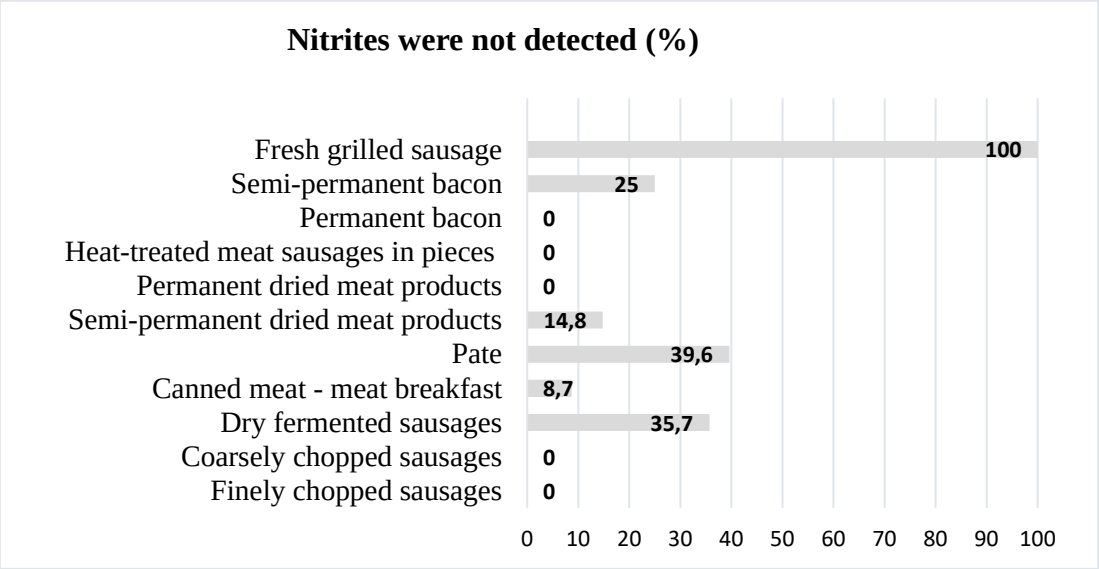

Figure 1. Representation of meat products in which nitrites were not detected (%)

The highest values of sodium nitrite were recorded in the group of heat-treated sausages, especially in coarsely chopped sausages with a determined maximum amount of 106 mg/kg, while in finely chopped sausages the maximum amount of 88 mg/kg was recorded, which is in agreement with the results of (15) who determined a maximum of 82 mg/kg. The average nitrite content in permanent sausages (9.04±5.776 mg/kg) is slightly higher than the test results of studies (6) (mean value = 7 mg/kg). Comparing our results obtained in semi-permanent cured meat products (36.30±17.331 mg/kg) with the results of research (6), lower values of nitrite content were obtained (mean value = 24 mg/kg), while in permanent cured meat products much higher results (mean = 37 mg/kg) compared to our results (6.17±2.229 mg/kg). The determined amounts of Na-nitrite in thermally processed sausages (42.84±15.245 mg kg1) agree with the results of research (6) (mean value = 42 mg kg1) for finely chopped thermally processed sausages, while for coarsely chopped salami our results are somewhat lower (mean value and standard deviation 37.40 ± 21.396 mg/kg). The average nitrite content in permanent sausages

(9.04±5.776 mg/kg) is slightly higher than the test results (6) (mean value = 7 mg/kg). In one group of thermally processed sausages (16), the nitrite content in roughly chopped sausages was determined in the range of 11.29 mg/kg to 96.33 mg/kg, and in finely chopped sausages in the range of 2.30 mg/kg. up to 78.35 mg/kg. In our research for the mentioned types of sausages, the results were very close to the results of the mentioned authors (106 mg/kg and 88 mg/kg). In homemade smoked bacon, the same authors obtained 4.5-17.79 mg/kg of nitrite, while in our research in dry bacon the average value with standard deviation was 9.41±4.358 mg/kg, and in semi-dried bacon 29.00 ± 10,567 mg/kg. In canned meat in pieces (16), a maximum of 73.47 mg/kg was determined, which is higher than our results (63 mg/kg). In fresh sausages, nitrites were not quantified, which is not accordance to the results of studies of (16) who obtained an average of 38.87 mg/kg nitrite. Many papers report the results of the analysis of the content of nitrite in different types of meat products, demonstrating a great variability in their concentrations (17). For all mentioned types of meat products from the market of Republic of Srpska, large deviations from the average value of the amount of nitrites were found between products of different, but also of the same groups (Figure 2- 4). The lowest deviations of the average value of nitrites were determined for dry cured meat products (2.229 mg/kg), dry bacon (4.358 mg/kg) and dry sausages (5.776 mg/kg), while the highest were determined for heat-treated coarsely chopped sausages (21.396 mg/ kg) and semi-permanent dried meat products (17,331 mg/kg) and finely chopped sausages (15,245 mg/ kg). According to the results of the research (19), the average values of residual nitrite in the amount of 36.9 mg/kg (36.5-37.2 mg/kg) and 37.43 mg/kg (36.7-38.4 mg/kg) were determined in two groups of tested pate samples (liver).

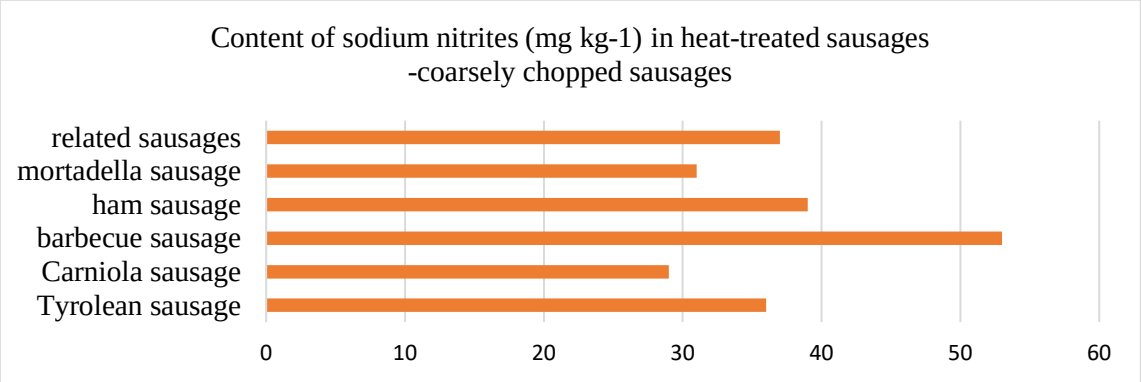

Figure 2. Deviations in sodium nitrite content (mg/kg) in different types of products from the group coarsely chopped sausages (98 samples)

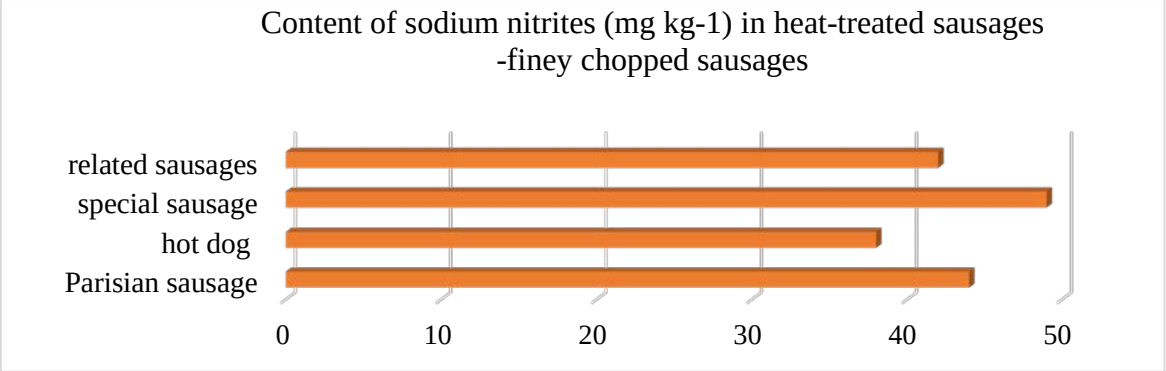

Figure 3. Deviations in sodium nitrite content (mg/kg) in different types of products from the group finey chopped sausages (74 samples)

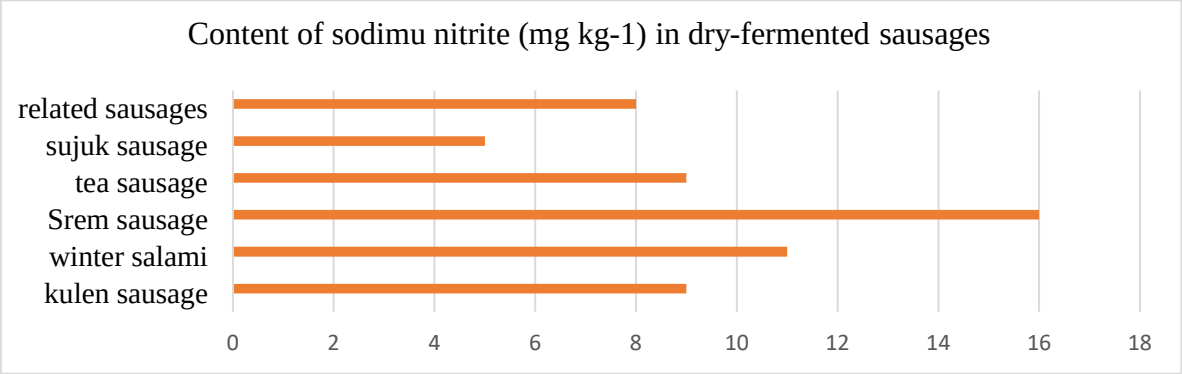

Figure 4. Deviations in sodium nitrite content (mg/kg) in different types of products from the group dry-fermented sausages (70 samples)

According to the results of the research (18), lower amounts of nitrite were found in coarsely ground sausages (32.85 ± 23.25 mg/kg) than we determined, but a greater agreement was recorded in finely ground sausages, where the mentioned authors obtained a mean value with a deviation of 40, 25 ± 20.37 mg/kg, and our laboratory 42.84 ± 15.245 mg/kg. In canned meat, our laboratory found a lower level of nitrite expressed as NaNO2 (13.29 ± 22.12 mg/kg) than the results of research by other authors (18) (34.95 ± 22.12 mg/kg). In our research of nitrites in pâtés that were declared as preserves of finely chopped meat, an average value with a deviation of 15.71±10.473 mg/kg was determined, which does not agree with the results of the mentioned author.In Greece, 30 samples of pastirma (a traditional cured meat product) were examined with the concentrations ranging from 0.85 to 189.65 mg/kg for nitrites (20). The authors (21) conducted a study of residual nitrites in various food products. In samples of dried meat and fresh meat, the nitrite content ranged from 3.7 to 86.7 mg/kg. Higher average nitrite levels expressed as NaNO2 according to research results (22) were found in cooked sausages (40.35 mg/kg in finely ground and 33.75 mg/kg in coarse ground) compared to fermented

sausages, which agrees with our test results for cooked sausages compared to fermented sausages, which agrees with the results of our tests for cooked sausages. However, the same authors obtained a lower average amount of nitrite in permanent sausages (1.86 mg/kg) than amount obtained in our study (9.04 mg/kg). The average values of nitrite content, according to the results of research conducted in Serbia in the period of 2016-2018 (23), ranged from 0.65 mg/kg in dry fermented sausages to 36.60 mg/kg in cooked sausages, while in our research in heat- treated meat sausages in pieces determined maximum average amount of nitrite 45.73±15.854. According to research results (24), the amount of nitrite determined in permanent sausages ranged from 4.51±4.91 mg/kg in tea sausage to 7.56±3.58 mg/kg in other products from that raw sausage, while in our research, the average value for this group of products was 9.04±5.776 mg/kg. Some researchers have focused on the possibility of substituting sodium nitrite with various plant extracts, bacteriocins, selected bacterial strains and high hydrostatic pressure (HHP), in addition to elimination/reduction of nitrite (25, 26)

4. Conclusion

Nitrites were not quantified in 20% of the products (< LOQ). The largest number of samples in which the amount of nitrite is below the LOQ was found in dry fermented sausages. Heat-treated meat sausages in a piece (45.73 ± 15.854 mg/kg), finely chopped (42.84 ± 15.245 mg/kg) and coarsely chopped sausages (37.40 ± 21.396 mg/kg) have the highest average nitrite value.

The highest amount of nitrites was recorded in sausages from the group of coarsely chopped sausages. In permanent dried meat products, the lowest average amounts of nitrite are 6.17 ± 2.229 mg/kg, and higher in semi-permanent dried meat products, 36.30 ± 17.331 mg/kg. In preserves, the average value of nitrite is 13.29 ± 10.288 mg/kg, and in pâté 5.71 ± 10.473 mg/kg. The determined amounts of residual nitrite are below the amount of nitrite that can be added to meat products according to the Ordinance.

5. References

1. Marco, A.; Navarro, L.; Flores, M. The Influence of Nitrite and Nitrate on Microbial, Chemical and Sensory Parameters of Slow Dry Fermented Sausage. *Meat Science.* **2006,** *73,* 660-673.
2. Sebranek, J. G.; Bacus, J. N. Cured meat products without direct addition of nitrate or nitrite: what are the issues? *Meat science.* **2007,** *77,* (1), 136–147.

3. JECFA 1996 WHO Food Additives Series: https://apps.who.int/iris/handle/10665/41742.
4. Cintya, H; Silalahi, J; Putra, E.L; Siburian, R. Analysis of Nitrosamines in Processed Meat Products in Medan City by Liquid Chromatography-Mass Spectrometry. Open Access *Maced J Med Sci*. **2019,** *16, 7(8),* 1382-1387.
5. Boci, I.; Ziu, E.; Bardhi, G. Role of Nitrite in Processed Meat Products and its Degradation during their Storage. *Albanian Journal of Agricultural Sciences.* **2014**, 1-5.
6. Kovačević, D., Mastanjević, K. Ćosić, K., Pleadin, J. Količina nitrita i nitrata u mesnim proizvodima s hrvatskog tržišta, *MESO*. **2016,** *2*, 40-46.
7. EFSA. https://www.efsa.europa.eu/en/press/news/170615 (accessed June 15, 2017).
8. Sharat, D., Gangolli, I. Nitrate, nitrite and Nitroso compounds. *Developments in Food Science*. **1995**, *37*, 385-704.
9. Pegg, R. B., Shahidi, F. Nitrite curing of Meat: The N-Nitrosamine Problem and Nitrite Alternatives. *Food & Nutrition.* **2004**.
10. De Mey, E., De Maere, H., Paelinck, H., Fraeye, I. Volatile N-nitrosamines in meat products: Potential precursors, influence of processing, and mitigation strategies. Crit Rev *Food Sci Nutr*. **2017**, *2*, 57(13), 2909-2923.
11. De Mey, E., De Klerck, K., De Maere, H., Dewulf, L., Derdelinckx, G., Peeters, M. C., Fraeye, I., Heyden, Y. V., Paelinck H. The occurrence of N-nitrosamines, residual nitrite and biogenic amines in commercial dry fermented sausages and evaluation of their occasional relation. *Meat Science*. **2014**, *96*, 2, 821-828.
12. Larsson, K, Darnerud, P.O., Ilbäck N.G., Merino, L. Estimated dietary intake of nitrite and nitrate in Swedish children. *Food Addit Contam Part A*. **2011**, *28* (5), 659-666.
13. Ordinance on food additives (SG RS, no. 96/20).
14. Ordinance on minced meat, semi-finished products and meat products (SG RS, no. 46/15).
15. Domik, F. Determination of nitrites and nitrates in meat and meat products (Diploma thesis). Retrieved from https://urn.nsk.hr/urn:nbn:hr:193: 740927 or Domika, Filip. "Determination of nitrites and nitrates in meat and meat products." Diploma thesis, University of Rijeka. **2017,** https://urn.nsk.hr/urn:nbn:hr:193:740927.
16. Prica, N., Živkov–Baloš, M., Mihaljev Ž., Jakšić, S., Kapetanov, M. Total nitrite and phosporus content in meat products on Novi Sad market. *Arhiv veterinarske medicine*. **2012**, *5*, 1, 69-75.

17. Hill, M. Nitrates and nitrites in food and water. Cambridge: Woodhead publishing, **1996**, 208.
18. Milešević, J., Vranić, D., Gurinović, M., Koricanac, V., Borović, B., Zeković, M., Šarac, I., Milićević, D. R., Glibetić, M. The Intake of Phosphorus and Nitrites through Meat Products: A Health Risk Assessment of Children Aged 1 to 9 Years Old in Serbia. *Nutrients*. **2022,** *14* (2), 242.
19. Pavlinić Prokurica, I., Bevardi, M., Marušić, N., Vidaček, S., Kolarić Kravar, S., Medić, H. Nitriti i nitrati kao prekursori N-nitrozamina u paštetama u konzervi. *Meso*. **2010,** *6,* 7.
20. Tyrpenou, A., Thanassios Gouta, E.H, Tsigouri, A.D., Vlasiotis, C.h.N. Nitrate and nitrite residues in Greek pastirma (In Greek). *Journal of the Hellenic Veterinary Medical Society,* **2000**, *51,* 302-307.
21. Hsu, J., Arcot, J., Alice Lee, N. Nitrate and nitrite quantification from cured meat and vegetables and their estimated dietary intake in Australians. *Food Chem*. **2009**, *115* (1), 334-339.
22. Vranic, D., Koricanac, V., Milicevic, D., Djinovic-Stojanovic, J., Geric, T., Lilic, S., Petrovic, Z. Nitrite content in meat products from the Serbian market and estimated intake. *OP Conf. Ser.: Earth Environ. Sci.* **2021,** *854*, 012106.
23. Bajcic, A., Petronijevic, R., Katanic, N., Trbovic, D., Betic, N., Nikolic, A. and Milojevic, L. 2018. Evaluation of the content and safety of nitrite utilisation in meat products in Serbia in the period 2016-2018. *Scientific journal "Meat Technology&quot.* **2018,** *2*, 102-109.
24. Pleadin, J., Perši, N., Vulić A., Đugum, J. Kakvoća trajnih, polutrajnih i obarenih kobasica na hrvatskom tržištu. *Hrvatski časopis za prehrambenu tehnologiju, biotehnologiju i nutricionizam.* **2009,** *4* (3-4), 104-108.
25. Munekata, P.E.S., Rocchetti, G., Pateiro, M., Lucini L., Domínguez, R., Lorenzo, J.M. Addition of plant extracts to meat and meat products to extend shelf-life and health-promoting attributes: An overview. *Curr. Opin. Food Sci.* **2020**, *31*.81–87.
26. Alahakoon, A.U., Jayasena, D.D., Ramachandra, S., Jo C. Alternatives to nitrite in processed meat: Up to date. *Trends Food Sci. Technol*. **2015**, *45,* 37–49.

PROBIOTIC ALMOND-BASED BEVERAGE: PROMISING STEP TOWARDS A CIRCULAR BIOECONOMY

Marica Rakin[1*], Maja Bulatović[1], Sara Živanović[1], Milica Milutinović[1], Duška Rakin[3], Danica Zarić[2], Maja Vukašinović-Sekulić[1]

[1]Faculty of Technology and Metallurgy, University of Belgrade, Karnegijeva 4, 11000 Belgrade, Serbia,

[2]Innovation Centre of the Faculty of Technology and Metallurgy, University of Belgrade, Karnegijeva 4, 11000 Belgrade, Serbia

[3]Faculty of Economics, University of Belgrade, Kamenička 6, 11000 Belgrade, Serbia

**marica@tmf.bg.ac.rs*

Abstract

The search for waste minimization possibilities and the valorization of by-products are key to good management and improved sustainability in the food industry. Although dairy products still remain at the forefront of probiotic food development, in recent years non-dairy food products have increased in popularity owing to their unique characteristics and advantages. Due to its beneficial properties, caused by the presence of various bioactive compounds, the almond parts that remain after almond milk production can be considered promising sources of ingredients for the development of non-dairy food products.

The aim of this study was to examine the potential and possibility of using a surplus product that remains after almond milk production. The antioxidant properties of the remained surplus product were characterized based on the polyphenol, flavonoid, and anthocyanin content as well as FRAP, DPPH, and ABTS antioxidant activity. The fermented beverage that combines the properties of almonds and probiotic bacteria, formulated using inulin, lyophilized fruit and aroma, was evaluated for physicochemical, microbiological, and sensory properties during cold storage (4 °C, 21 day).

The surplus product that remains after the almond milk production contains 61.4 mg GAE/100g DW, 16.11 mg QE/100g DW, and 0.993 mg CYE/100g DW of polyphenols, flavonoids, and anthocyanins (respectively), and expresses DPPH, FRAP and ABTS antioxidant activity of 71.56 mg DW/mL, 50.47 mg DW/mL and 53.11 mg DW/mL (respectively).

The fermentation of surplus product that remains after almond milk production leads to the production of the beverage with satisfactory values of quality parameters as follows: pH value

of 4,75, titratable acidity 28,8 °SH, syneresis 7,5%, viable cell count of 7.77 log (CFU mL^{-1}), and sensory characteristics value of 10, that is stable during 21 day of cold storage.
A new probiotic almond-based beverage that combines the properties of both almonds and probiotics can be considered as promising step toward the circular bioeconomy.

Keywords: *Almond, beverage, probiotics, circular bioeconomy, antioxidants*

1. Introduction

Almonds (*Prunus dulcis* (Mill.) D.A. Webb) are among the most popular nuts, commonly used as snacks or as ingredients in various types of processed foods, especially in bakery and confectionery products (1). Likewise, plant-based beverages are becoming increasingly popular due to the rise of vegetarianism and consumer awareness of their health effects. Depending on the method of extracting the almond pulp after the production of almond milk, about 15-20% oil, about 35-40% protein, but also numerous other valuable substances remain in it (2). The fact is that today this residue is almost unused, and actually has excellent potential for wide application in the food industry. Although dairy products, like yogurt and cheese as the most commonly used carriers for delivering probiotics to the human digestive tract, remain at the forefront of probiotic food development, non-dairy food products are becoming increasingly popular due to their unique characteristics and advantages, such as meeting the needs of vegetarians, and providing lactose-free or low-cholesterol nutritional value products. In recent years, nuts have been increasingly used to produce new nutritious alternatives to cow's milk. The most common substitutes for dairy products are drinks based on soy, almonds, and rice. In this group of products, the "milk" obtained from almonds is the most interesting for its health effects, including antioxidant effects as well as immunological and cardioprotective properties (3). On the other hand, almond pulp as a by-product that remains after the production of almond milk, represents a reservoir of very valuable substances, due to which it can be considered a surplus product worthy of exploitation. In order to exploit and increase its value, and ensure economic and ecological sustainability, it is necessary to examine the possibility of using almond pulp for the design of innovative added-value products. The aim of this study was to examine the possibility of using almond pulp, as a raw material for the production of a functional fermented almond-based beverage. As part of the study, the antioxidant activity of almond pulp was examined, in order to gain insight into the content and potential of valuable bioactive compounds whose main role is the neutralization of free radicals, and thus the quality

of the starting raw material. After an insight into the quality of the raw material, the possibility of its application in the production of a functional fermented almond-based beverage was examined.

2. Experimental

2.1. Preparation of extracts

Fresh almond pulp sample (1g) was mixed with 70.0 % ethanol (10 mL) and vortexed for approximately 5 min. The extraction was performed at 50°C for 4 h with an orbital shaker under constant rotatory agitation at 200 rpm. The mixture was centrifuged for 5 min at 6000 rpm and the resultant supernatant was separately kept at 4 °C for subsequent assays.

2.2. DPPH radical scavenging activity

Procedure described by Brand-Williams et al. (4) , with slight modification, was employed for DPPH assay. An appropriate amount of extract was mixed with a 0.2 mM solution of DPPH in ethanol, after which the samples were left for 60 min in the dark for the reaction to take place. Absorbance (A) was measured at 517nm. The DPPH antioxidant activity was calculated according to the equation:

Inhibition percentage (%) = (Acontrol – Asample) / Acontrol x 100 (1)

The results are expressed as IC_{50} (mg DW/mL), the concentration of dry matter of the sample necessary to achieve 50% inhibition of DPPH radicals.

2.3. ABTS radical scavenging activity

Procedure described by Re et al. (5) was employed for ABTS assay. Briefly, the ABTS solution was prepared by mixing 7 mM ABTS salt equal proportion with 2.45 mM potassium per sulphate and the same mixture was then put in the dark for minimum 16 h. The solution absorbance was noted at 734 nm and before mixing with extracts, it was adjusted to 0.7. The mixture was put again in the dark for 15 minutes at room temperature. An apropriate amount of extract was mixed with ABTS reagent. The mixture was homogenized and incubated for 15 min in the dark. The absorbance was measured at 734 nm. The ABTS antioxidant activity was calculated according to the equation:

Inhibition percentage (%) = (Acontrol – Asample) / Acontrol x 100 (2)

The results are expressed as IC_{50} (mg DW/mL), the concentration of dry matter of the sample necessary to achieve 50% inhibition of ABTS radicals.

2.4. Ferric ion reducing antioxidant power (FRAP)

Procedure described by Benzie and Strain (6) was employed for FRAP assay. The FRAP working solution was made by mixing 300 mM acetate buffer pH 3.6, 10 mM TPTZ in 40 mM HCl, and 20 mM FeCl3·6H2O with ratio 10:1:1. An apropriate amount of extract was mixed with FRAP reagent. The mixture was homogenized and incubated for 30 minutes in the dark. The absorbance was measured at 593 nm. Total reducing capacity of FRAP was determined using the following equation:

Inhibition percentage (%) = (Asample – Acontrol) / Asample x 100 (3)

The results are expressed as IC_{50} (mg DW/mL), the concentration of dry matter of the sample necessary to achieve 50% inhibition of FRAP radicals.

2.5. Determination of total phenolics

Total phenolics content in the sample was determined using Folin-Ciacolteu method as described by Kruawan and Kangsadalampai (7). An appropriate amount of extract was mixed with distilled water, Folin-Ciocalteu reagent and 7.5% Na_2CO_3. The mixture was homogenized and incubated for 120 minutes in the dark. The absorbance was measured at 750 nm. Total phenolics content was calculated based on the gallic acid calibration curve. The results were expressed as mg GAE/100 g DW of the sample based on standard curve equations prepared immediately before sample analysis.

2.6. Determination of total flavonoids

The aluminum chloride colorimetric method was used to determine the total flavonoids content following the procedure employed by Lee et al. (8). An appropriate amount extract was mixed with 96% ethanol, 10% aluminium chloride ($AlCl_3 \cdot 6H_2O$), and sodium acetate ($NaC_2H_3O_2 \cdot 3H_2O$) (1M). Then the mixture was homogenized and incubated for about 45 min. The absorbance of the solution was measured at a wavelength of 430 nm. Total flavonoids content was calculated based on the quercetin calibration curve. The results were expressed as mg QE/100g DW of the sample based on standard curve equations prepared immediately before sample analysis.

2.7. Determination of total anthocyanin

Total anthocyanin was quantified using a pH differential method with a two-buffer system described by Lako et al. (9). Monomeric anthocyanin pigments change color reversibly with a change in pH. The difference in absorbance of the pigments at 510 nm is proportional to the concentration of the pigment. The appropriate amount of sample was mixed with KCl buffer

pH=1 and $CH_3CO_2Na \cdot 3H_2O$ buffer pH=4.5. The absorbance of the solution was measured at wavelengths of 510 and 700 nm, in relation to the corresponding buffer as a blank, within 50 min of preparation. The results are expressed as cyanidin-3-glucoside equivalent, ie mg CYE/100g DW.

2.8. Preparation of fermentation suspension

The fermentation suspension of almond pulp, with the appropriate content of dry matter (5, 10 and 15%), was pasteurized for 60 minutes at a temperature of 60ºC. After the heat treatment the prepared suspension was cooled to the fermentation temperature (42 °C).

2.9. Fermentation

The fermentation suspension was inoculated with 0.06% (*m/v*) ABT-10 culture (Chr. Hansen A/S, Hørsholm, Denmark), composed of *Streptococcus thermophilus*, *Lactobacillus acidophilus* La-5 and *Bifidobacterium animalis* subsp. *lactis* Bb-12, transferred to a water bath where fermentation was performed at a temperature of 42°C until the pH ≈4.5 was reached (150 min), after which the fermentation was stopped by quick cooling of the samples. After cooling, the samples was enriched with lyophilized fruit (strawberry, blackberry, blueberry, raspberry) (Drenovac d.o.o., Arilje, Serbia) in the amount of 5% (*m/v*), 1.7% (*m/v*) of inulin and 0.1% (*v/v*) vanilla flavor. After the initial tests (0 day), the samples were stored for 21 days at a temperature of 4°C, during which they were analyzed for the following parameters in equal time intervals of 7 days.

2.10. Chemical analysis

The titratable acidity was determined by the Soxhlet-Henkel method (10), and the pH value was measured using a pH meter (Inolab, WTW 82362, Wellheim, Germany).

2.11. Microbiological analysis

Microbiological analysis of fermented samples was conducted according to the method described by Bulatović et al. (11), using MRS agar and anaerobic incubation at 37 °C for 48 h for the enumeration of viable cell count of probiotic bacteria.

2.12. Syneresis

Syneresis of fermented samples was determined according to the method described by Bulatović et al. (11). The fermented samples (20.0 mL) were centrifuged at 1000 rpm for 10 min. Collected supernatant was drained, weighed and the following equation was used for syneresis calculation:

$$\text{Syneresis}\,(\%) = \frac{\text{Weight of supernatant (g)}}{\text{Weight of fermented sample (g)}} \times 100\% \qquad (4)$$

2.13. Sensory analysis

Sensory analysis of fermented samples was conducted according to the method described by Bulatović et al. (11), with slight modification, using a 10-point hybrid hedonic scale (12) where 1 - disliked extremely; 5 - neither liked nor disliked and 10 – liked extremely.

2.14. Statistical analysis

The experiments were performed in triplicate. All values are expressed as mean ± standard deviation. Mean values were analyzed using one-way ANOVA (Origin Pro 8 (1991–2007), Origin Lab Co., Northampton, USA). Differences were considered significant at $p < 0.05$.

3. Results and discussion

3.1. Antioxidant activity and polyphenol composition of almond pulp

Almond pulp in its composition contains the most of nutrients present in almond seeds and skin. Several investigations on almond seeds and skin extracts revealed the presence of various phenolic compounds, well known to possess excellent antioxidant potential. Antioxidant activity and polyphenol composition of almond pulp are presented in Tables 1 and 2.

Table 1. Antioxidant activity of almond pulp expressed as the minimum inhibitory concentration of antioxidant substances (IC_{50}) necessary to neutralize 50% of free radicals

Sample	Antioxidant activity, IC_{50}		
	DPPH, mg DW/mL	ABTS, mg DW/mL	FRAP, mg DW/mL
Almond pulp	71.56 ± 1.140	53.11 ± 0.245	50.47 ± 0.472

As ABTS and DPPH measure the scavenging capacity of reactive oxygen species, and FRAP determines the metal chelating capacity (14), a combination of assays is recommended for the antioxidant activity analysis. Based on the literature data (14), the almond seeds extract is rich in vanillic acid, caffeic acid, p-coumaric acid, ferulic acid, quercetin, kaempferol, isorhamnetin, delphinidin, and procyanidins B2 and B3. On the other hand, as reported by Monagas et al. (15) almond skin contains a total of 33 compounds corresponding to flavanols, flavonols, dihydroflavonols and flavanones, and other non-flavonoid compounds.

Table 2. Polyphenol composition of almond pulp expressed per 100g of dry weight

Sample	Polyphenol composition in 100g DW		
	Total polyphenols, mg GAE/100g DW	Flavonoids, mg QE/100g DW	Anthocyanins, mg CYE/100g DW
Almond pulp	61.4 ± 1.261	16.11 ± 1.186	0.993 ± 0.045

The results presented in Tables 1 and 2 revealed that there is a strong correlation between total phenolic compounds and the antioxidant capacity of almond pulp. The presented results suggest that total polyphenols are the main compounds responsible for the antioxidant capacity of almond pulp. On the other hand, slightly lower results for the content of flavonoids and anthocyanins are consistent with the literature data (16) that amount of almond skin makes up only about 4% of the almond pulp. Therefore, it can be concluded that most of the antioxidant activity of almond pulp comes from almond seeds, which, as the dominant fraction of almond pulp, represents a reservoir of great potential.

3.2. Optimization of the production process of almond-based beverage

As part of the analysis of the possibility of applying almond pulp in the production of a fermented almond-based beverage, the amount of almond pulp necessary to achieve a maximal viable cell count of probiotic bacteria was optimized. The results are shown in Figure 1.

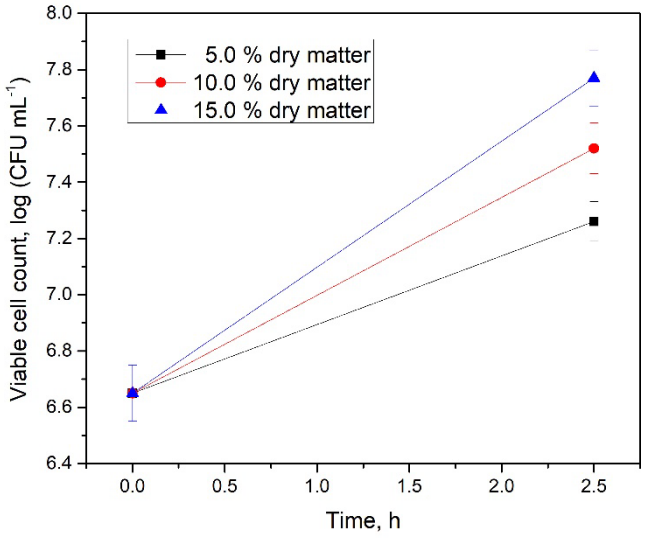

Figure 1. The effect of the amount of almond pulp on the viable cell count of probiotic bacteria in fermented almond-based beverage

As shown in Figure 1, the maximal viable cell count of probiotic bacteria, of 7.7 log (CFU mL^{-1}) was achieved at the almond pulp content of 15% (m/v). The obtained results are in accordance with the fact that by using a larger amount of almond pulp in the fermentation process, a larger amount of carbohydrates dominantly present in the almond pulp, such as

glucose, fructose, sucrose, and raffinose (17), are available to probiotic bacteria. On the other hand, a larger amount of almond pulp implies a larger amount of prebiotics (18) that significantly affect the growth of probiotic bacteria.

3.3. Optimization of the sensory characteristics of almond-based beverage

The changes in acceptability values of fermented almond-based beverages enriched with lyophilized fruits are presented in Figure 2.

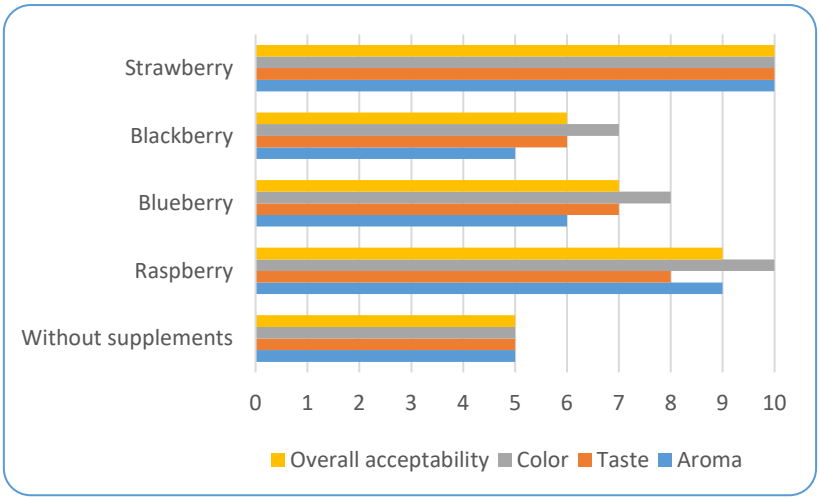

Figure 2. Influence of lyophilized fruits addition on aroma, taste, color and overall acceptability of fermented almond-based beverage

The results presented in Figure 2 indicated that the supplementation by 5% (m/v) of lyophilized fruits significantly ($p < 0.05$) improves the sensory profile of almond-based beverages. The samples enriched with strawberry and raspberry showed high acceptability values of 9 and 10, respectively. The results also show that supplementation with raspberry has a favorable effect exclusively on the color of the drink, while the other ratings are significantly ($p < 0.05$) lower than when using a strawberry. Based on all of the above, it can be concluded that strawberry enrichment is the best way to improve the sensory characteristics of the beverage and thus gain the attention of consumers.

3.4. Stability of the almond-based beverage

Storage stability is the crucial parameter related to the maintaining the quality of product.

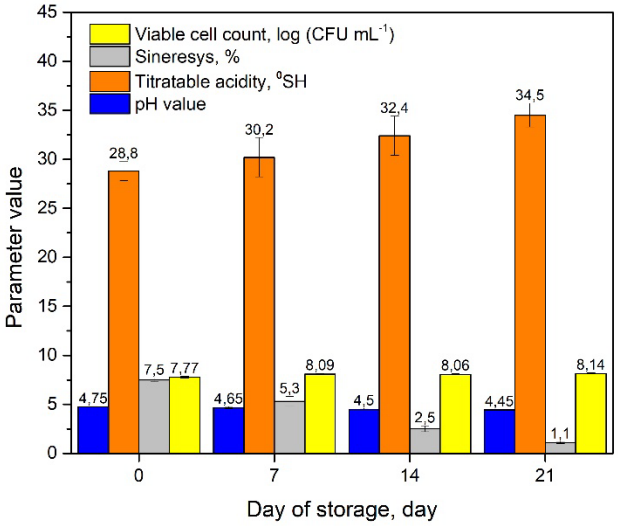

Figure 3. The influence of the storage process on the stability of the almond-based beverage

Based on the results presented in Figure 3, significant ($p < 0.05$) changes in titratable acidity and sineresys were observed between 0 and 21 days of storage. At the end of the storage period, titratable acidity was 34.5 °SH, which is in the range for fermented products (11), while syneresis was at the level of 1.1%, which can be explained by the swelling of the prebiotic fibers present and significant water absorption. On the other hand, the pH value and viable cell count of probiotic bacteria remained stable during the whole storage period which is significantly better than data reported in the literature (19). At the end of the storage period, the fermented almond-based beverage is characterized by a viable cell count of 8.14 log (CFU mL^{-1}) that satisfies the minimum recommended count of viable probiotic bacteria at the time of consumption (20).

4. Conclusion

The main conclusion of the conducted study is that almond pulp, with its excellent content of bioactive substances, represents an excellent substrate for the production of novel almond-based beverage. By fermenting almond pulp, it is possible to produce a sensory acceptable beverage, which contains over 10^8 probiotic bacteria and has a shelf life of at least 21 days.

5. Acknowledgement:

This work was supported by the Ministry of Education, Science and Technological Development of the Republic of Serbia (Contract No. 451-03-68/2022-14/200287).

6. References

1. Esfahlan, A.J., Jamei, R. Properties of Biological Activity of Ten Wild Almond (Prunus Amygdalus L.) Species. *Turkish Journal of Biology*. **2012**, 36.
2. Souza, T.S.P., Dias, F.F.G., Koblitz, M.G.B., M.L.N. de M. Bell, J. Aqueous and Enzymatic Extraction of Oil and Protein from Almond Cake: A Comparative Study. *Processes.* **2019,** 7, 472.
3. Muncey, L., Hekmat, S. Development of Probiotic Almond Beverage Using Lacticaseibacillus Rhamnosus GR-1 Fortified with Short-Chain and Long-Chain Inulin Fibre. *Fermentation*. **2021,** 7, 90.
4. Brand-Williams, W., Cuvelier, M.E., Berset, C. Use of a Free Radical Method to Evaluate Antioxidant Activity. *LWT - Food Science and Technology*, **1995**, 28, 25–30.
5. Re, R., Pellegrini, N., Proteggente, A., Pannala, A., Yang, M., Rice-Evans, C. Antioxidant Activity Applying an Improved ABTS Radical Cation Decolorization Assay. *Free Radical Biology and Medicine*, **1999,** 26, 1231–1237.
6. Benzie, I., Strain, J. The Ferric Reducing Ability of Plasma (FRAP) as a Measure of "Antioxidant Power": The FRAP Assay. *Analitical Biochemistry*, **1996,** 239, 70–76.
7. Kruawan, K., Kangsadalampai, K. Antioxidant Activity, Phenolic Compound Contents and Antimutagenic Activity of Some Water Extract of Herbs. *Thai Journal of Pharmaceutical Sciences*, **2006,** 30, 28–35.
8. Lee, S.H., Sancheti, S.A., Bafna, M.R., Sancheti, S.S., Seo, S.Y. Acetylcholineterase Inhibitory and Antioxidant Properties of Rhododendron Yedoense Var. Poukhanense Bark. *Journal of Medicinal Plants Research*, **2011,** 5, 248–254.
9. Lako, J., Trenerry, V., Wahlqvist, M., Wattanapenpaiboon, N., Sotheeswaran, S., Premier, R. Phytochemical Flavonols, Carotenoids and the Antioxidant Properties of a Wide Selection of Fijian Fruit, Vegetables and Other Readily Available Foods. *Food Chemistry*, **2007,** 101, 1727–1741.
10. Varga, L. Effect of Acacia (Robinia Pseudo-Acacia L.) Honey on the Characteristic Microflora of Yogurt during Refrigerated Storage. International *Journal of Food Microbiology*, **2006**, 108, 272–275.
11. Bulatović, M.Lj., Krunić, T.Ž., Vukašinović-Sekulić, M.S., Zarić, D.B., Rakin, M.B. Quality Attributes of a Fermented Whey-Based Beverage Enriched with Milk and a Probiotic Strain. *RSC Advances*, **2014,** 4, 55503–55510.
12. Sosa, M., Martínez, C., Marquez, F., Hough, G. Location and scale influence on sensory acceptability measurements among low-income consumers. *Journal of Sensory Studies.* **2008,** 23, 707 - 719.
13. Huang, D., Ou, B., Prior, R.L. The Chemistry behind Antioxidant Capacity Assays. *Journal of agricultural and food chemistry*. **2005,** 53, 1841–1856.

14. Amarowicz, R., Troszynska, A., Shahidi, F. Antioxidant activity of almond seed extract and its fractions. *Journal of Food Lipids,* **2005,** 12, 344–358.
15. Monagas, M., Garrido, I., Lebrón-Aguilar, R., Bartolome, B., Gómez-Cordovés, C. Almond (Prunus Dulcis (Mill.) D.A. Webb) Skins as a Potential Source of Bioactive Polyphenols. *Journal of Agricultural and Food Chemistry*, **2007,** 55, 8498–8507.
16. Milbury, P.E., Chen, C.Y., Dolnikowski, G.G., Blumberg, J.B. Determination of Flavonoids and Phenolics and Their Distribution in Almonds. *Journal of Agricultural and Food Chemistry.* **2006,** 54, 5027–5033.
17. Barreira, J.C.M., Pereira, J.A., Oliveira, M.B.P.P., Ferreira, I.C.F.R. Sugars Profiles of Different Chestnut (Castanea Sativa Mill.) and Almond (Prunus Dulcis) Cultivars by HPLC-RI. *Plant Foods for Human Nutrition.* **2009,** 65, 38–43.
18. Bernat, N., Cháfer, M., Chiralt, A., González-Martínez, C. Development of a Non-Dairy Probiotic Fermented Product Based on Almondmilkand Inulin. *Food Science and Technology International*. **2014,** 21, 440–453.
19. Bernata, N., Cháfera, M., Chiralt, A., Gonzalez-Martinez, C. Probiotic Fermented Almond "Milk" as an Alternative to Cow-Milk Yoghurt. *International Journal of Food Studies.* **2015**, 4, 201–211.
20. Sanz Y., Dalmau J. Los probioticos en el marco de la nueva normativa europea que regula los alimentos funcionales. *Acta Pediatrica Espanola*. **2008,** 66, 27–31.

ENERGY VALUE AND MYCOLOGICAL QUALITY TESTING CONTROL OF DOMESTIC JAMS

Dobrila Ranđelović*, Svetlana Bogdanović, Zvonko Zlatanović

Academy of Professional Studies South Serbia, Department of Agricultural and Technological Studies, Ćirila i Metodija 1, Prokuplje, Serbia

**dobrilarandjelovic74@gmail.com*

Abstract

Fruit is a rich source of bioactive compounds. In order to remain available out of season, while retaining bioactive compounds, the fruit is processed into a stable product, such as jam. Traditional jam preparation involves heat treatments, which can lead to changes in nutritional properties. The aim of this scientific work is to examine the energy values of jams in various domestic fruit species. Energy values of jams were calculated from the content of carbohydrates, proteins and fats made in accordance with the Regulation concerning the quality of fruit jams, jellies, marmelades, fruit spreads and sweetened chestnut paste (Official Gazette of the Republic of Serbia, No. 101/2015). The results of these tests indicated that fruit jams are low in fat but a good source of energy and carbohydrates. In order to test the frequency of yeasts and molds, microbiological methods were performed in accordance with SRPS EN ISO 21527-2: 2011 standard. The results showed a complete absence of yeast and mold.

Key words: Jam, energy values, yeasts, molds

1. Introduction

The variety of nutrients that can be found in different types of fruit is the reason why great importance is given to fruit and fruit products in a healthy diet. There are different methods of fruit processing that allow the nutritional and biological value of the fruit to be preserved. Some of the methods are drying, compote, making jams and juices (1). Jams are one of the most popular food products due to their reasonable price but availability throughout the year. Traditionally, jams were originally produced to preserve fruit out of season. According to the Regulation, jam is a product with a suitable gelatin consistency, produced from sugar, fruit pulp and/or fruit pulp/puree obtained from one or more types of fruit and water (2). The amount

of fruit pulp and/or fruit pulp/puree used to produce 1,000 g of the final product cannot be less than 350 g for all types of fruit, except for:

1) red currant, partridge (*Sorbus aucuparia*), dog thistle (*Hippophae rhamnoides*), black currant, rosehip and quince, 250 g;
2) ginger, 150 g;
3) cashew nut or cashew apple (*Anacardium occidentale*) 160 g;
4) passion fruit (*Passiflora edulis*), 60 g. (3)

Fresh fruit, which is used for the production of jam, must be of uniform technological maturity, with developed varietal characteristics, healthy, well washed and sorted. Jam produced from fresh fruit does not contain traces of preservatives and has a better color and aroma. (4). In the production of jams, fruit and sugar are mixed in a certain proportion. The mixed product is then cooked to produce a tasty product with long shelf life.

The work is based on the examination of energy values and microbiological parameters of plum, peach and apricot made in domestic production.

2. Experimental

The jam samples were made according to the traditional recipe in the domestic production of the Radovanović family farm in Mala Plana.

The jams were cooked according to the traditional recipe given in table 1. Sample 1 is made from plum, sample 2 is from apricot, sample 3 is from peach. The fruits are well washed and pitted. The pitted, unpeeled fruit was cooked in a stainless steel container at 80°C without sugar to a certain content of dry matter, after which sucrose was added and cooking was continued, with constant stirring, until the recommended dry matter. Hot jam was poured into sterilized hot jars that were hermetically sealed (5).

Table 1. Traditional recipes according to which jams were prepared

Serial number	***Jam type***	***Fruit (g/kg)***	***Sugar (g/kg)***
1.	Plum (pitted)	356	644
2.	Apricot (pitted)	400	610
3.	Peach (pitted)	550	600

Carbohydrate content, protein content and fat content were analyzed according to standard methods (5), on the basis of which the energy values of the jams were calculated.

Proving the presence of bacteria *L. monocytogens*, *Salmonella sp***.** and Enterobacteriaceae is conducted according to international standard methods, ISO 11290-1:2017 (6); ISO 6579-1:2017 (7) and ISO 21528-2:2017 (8).

3. Results and discussion

In this scientific work, the goal was to determine certain parameters in the composition of jams such as: the content of carbohydrates, proteins and fats, but also the determination of microbiological quality control.

As the basic raw material, the examined fruit met the conditions of all technological criteria, including chemical properties, because the quality of the fruit used greatly affects the quality of the final product (5). According to Voicu et al. (2008) (9) fruit that is intended for processing should have a high content of soluble dry matter, pectin matter and retain color and taste during processing into compotes, jellies, jams, juices. The results of the chemical analysis of domestic made plum, apricot and peach jams are presented in Table 2. The results indicate that the raw material used was of satisfactory quality and that the jams were cooked according to a traditional recipe that gives a finished product in accordance with the current regulations. The content of carbohydrates (presented in g/100g) is the highest in plum jam, while it is the lowest in apricot jam. The results obtained for apricot jam are lower compared to the results of the research in Malaysia (10).

The high carbohydrate content of jams in Malaysia can be explained by the high concentration of sugar used in the preparation of the jam (10). The protein content (presented in g/100g) is the highest in plum jam, while the same value was found in apricot and peach jams. All analyzed jams have a low fat content (0.1g/100g), which is in accordance with literature data (10).

Table 2. The results of the chemical analysis of jams

Serial number	***Jam type***	Carbohydrates (g/100 g)	Proteins (g/100 g)	Fats (g/100 g)
1.	Plum (pitted)	11,5	0,4	0,1
2.	Apricot (pitted)	8,5	0,1	0,1
3.	Peach(pitted)	9,0	0,1	0,1

The results of the chemical analysis of jams made in the traditional way are in accordance with the valid Regulation. A microbiological test performed according to ISO standards, which is used to detect food spoilage agents and potential opportunistic pathogens in humans, showed the absence of *Salmonella spp. and L. monocytogenes*. Representatives of the Enterobacteriaceae family were found in numbers less than 10 cfu/g (Table 3).

Table 3. The results of microbiological quality control of the analyzed jams

Microorganisms	**Limit values**(cfu/g)		**Method label**	**Confirmation of value**
	m	M		
Salmonella spp.	it must not be in 25g		SRPS EN ISO 6579-1:2017	presence has not been established
Enterobacteriaceae	10		SRPS EN ISO 21528-2:2017	< 10 cfu/g
L. monocytogenes	it must not be in 25g		SRPS EN ISO 11290-1:2017	presence has not been established

4. Conclusion

The chemical and microbiological correctness of home-made jams was tested. This research showed that the analyzed fruit jams are a good source of carbohydrates with a very low level of fat. All the examined jams were microbiologically correct. It is expected that the obtained results will find application and be helpful to primary producers, processors, as well as direct consumers.

5. References

1. Stamatovska V., KarakashovaLj., Babanovska – Milenkovska F., Delchev N., Nakov G., Necinova Lj.: The quality characteristics of plum jams made with different sweeteners, *Food science engineering and technology*. **2013**, *60*, 689-693.
2. Pravilnik o kvalitetu voćnih džemova, želea, marmelade, pekmeza i zaslađenog kesten pirea, Službeni glasnik RS, broj 101/2015.

3. Nowicka, P., Wojdylo, A., Laskowski, P.: Principal component analysis (PCA) of physicochemical compounds' content in different cultivars of peach fruits, including qualification and quantification of sugars and organic acids by HPLC, *European Food Research and Technology*. **2019**, *245*, 929 – 938.
4. Ranđelović, D., Bogdanović, S., Kostić, N.: Hemijsko i mikrobiološko ispitivanje kvaliteta džemova proizvedenih u domaćoj radinosti, *Šesti naučno – stručni skup Politehnika*. **2021**, 830 – 833.
5. Vračar, Lj: Priručnik za kontrolu kvaliteta svežeg i prerađenog voća, povrća i pečurki i osvežavajućih bezalkoholnih pića. **2001**, Tehnološki fakultet, Novi Sad
6. International Organization for Standardization (SRPS EN ISO 11290-2.) Microbiology of the food chain – Horizontal method for the detection and enumeration of Listeria monocytogenes and of Listeria spp. **2017.**
7. International Organization for Standardization (SRPS EN ISO 6579-1) Microbiology of the food chain – Horizontal method for the detection, enumeration and serotyping of Salmonella - Part 1: Detection of Salmonella spp, **2017.**
8. International Organization for Standardization (SRPS EN ISO 21528-2.) Microbiology of the food chain – Horizontal method for the detection and enumeration of Enterobacteriaceae - Part 2: Colonycount technique, **2017,** 14.
9. Voicu, A., Campenau, G.H., Bibicu, M., Mohora, A., Negoita, M., Catana, L., Catana, M.: Research regarding the setting up of the Processing Directions of Peach New Cultivars and Hybrids, *Roumanian Biotechnological Letters.* **2008**, *13*, 3955 – 3961.
10. Mohd Naeem, M.N., Mohd Fajrulnizal, M.N., Norhayati, M.K., Zaiton, A., Norliza, A.H., Wan Syuriahti, W.Z., Mohd Ayerulazree J., Aswir, A.R., Rusidah, S.: The nutritional composition of fruit jams in the Malaysian market, *Jornal of the Saudi Society of Agricultural Sciences*. **2017**, *16*, 89 - 96.

INFLUENCE OF DIFFERENT SWEETENERS ON SENSORY ATTRIBUTES OF RASPBERRY JAMS

Viktorija Stamatovska[1*], Ljubica Karakasova[2], Vezirka Jankuloska[1], Tatjana Blazhevska[1], Namik Durmishi[3]

[1]Faculty of Technology and Technical Sciences, University St. Kliment Ohridski-Bitola, Dimitar Vlahov bb, 1400, Veles, Republic of North Macedonia,

[2]Faculty for Agricultural Sciences and Food, St. Cyril and Methodius University, Edvard Kardelj bb, 1000,Skopje, Republic of North Macedonia,

[3] Faculty of Food Technology and Nutrition, University of Tetovo, Ilinden nn. 1200, Tetovo, Republic of North Macedonia

**viktorija.stamatovska@uklo.edu.mk*

Abstract

Jams are an alternative for fruit preservation, and usually, they are prepared with a high amount of sugars, mainly sucrose. There is great interest in jam production with a lower amount of sucrose or with another type of sweetener replacement because modern consumers are concerned about the nutritional and caloric value of food they consume. They are interested in healthier food with the sensory characteristics of the sucrose-based product.

Thus, this study investigates the influence of different sweeteners on the sensory attributes of raspberry jams (Willamette raspberry jams and Wild raspberry jams). The jams were prepared with different sweeteners (fructose, sorbitol, agave syrup, and a low amount of sucrose). The sensory analysis was performed by scoring method for jelly products assessment. The sensory attributes were assessed by 10 highly experienced testers, using a different number of points: color 0-4, smell 0-2, taste 0-8, and consistency 0-6.

The results of sensory analysis of processed raspberry jams showed good acceptability. However, both types of raspberry jams with sorbitol, assessed with the highest average total grade have better sensory attributes as compared with jams prepared with other sweeteners. The Willamette raspberry jams and Wild raspberry jams prepared with agave syrup had the lowest average grade for all sensory attributes.

Our results suggest that sorbitol used as a sweetener in both types of jams was the best option for sucrose replacement.

Keywords: Sensory attributes, raspberry jams, sweeteners

1. Introduction

Fruits, especially berries, abound in vitamins, minerals, antioxidants, and substances that help in the body's maintenance and development. During fruit bearing season, the fruits are in abundance and due to their low level of stability, they sometimes get spoilt and rot before they are consumed. To extend the shelf life, such fruits can be used to produce jam, making them available for consumption throughout the year (1,2).

Jams are produced mainly from fruits and sweetener with or without addition of pectin. To make jams, fruits have to be cut, and/or crushed until they reach required consistency. Jam making includes the following major steps: thermal processing (cooking crushed or cut fruits and sweetener), adding pectin and, acid, mix formation, and packaging (3,4). Sucrose derived from sugar beets or sugar cane is the main sweetener used in jam preparation. Sucrose is added to jams to enhance taste, improve the texture, and inhibit microbial growth by binding the water resulting in longer shelf life. However, a high sucrose intake is associated with high energy intake, which can increase the risks for obesity, cardiovascular disease, diabetes, and hypertension (5–7).

With increasing consumer interest in reducing sucrose intake, its replacement by alternative sweeteners is an attractive solution (8). Substitution of sucrose in jam's preparation is associated with significant changes in texture, color, flavor, and shelf life (9). These sweeteners must be safe, must be compatible with the food, and present the similarity to the characteristic flavour of the sucrose-based product (10, 11).

Determining the best sweetener for a product requires sensory evaluation. Sensory evaluation evaluates the various food properties by humans involving their own perception based on 5 senses such as sight, smell, touch, taste, and sound. In food product development, sensory evaluation provides a clear understanding of consumer acceptability (3, 12).

Therefore, given the growing consumer demand for healthier products with good sensory attributes, the aim of this study was to evaluate the impact of different sweeteners on the sensory attributes of raspberry jams.

2. Experimental

Willamette raspberry jams (WillRJ) and Wild raspberry jams (WildRJ) were used as a material for sensory testing. Jams were prepared with different sweeteners: sucrose (reduced

amount), fructose, sorbitol, and agave syrup. Jam processing was conducted following the procedure described in our previous study (13).

The sensory analysis of jams was performed by a scoring method for jelly product assessment (14). The sensory attributes (smell, taste, color, and consistency) were assessed by 10 highly experienced testers, using a different number of points: for color 0-4, for smell 0-2, for taste 0-8, and consistency 0-6. The total assessment (overall acceptability) of jams was obtained by adding the individual points for each sensory attribute with a possibility of maximum total point score of 20 points. Evaluations were performed in the laboratory for fruit and vegetable processing at the Faculty of Agricultural Sciences and Food in Skopje (Fig. 1). The tests were repeated three times over a three-year period.

The results of the research were presented, analyzed, and statistically processed by using Microsoft Excel and statistical package SPSS Statistics Version 19.

Fig. 1. Sensory evaluation

3. Results and Discussion

Sensory evaluation is carried out by the senses of sight, taste, smell, touch, and hearing when food is eaten. The complex sensation that results from the interaction of the senses is used to measure the food quality in programs for quality control and new product development (15).

The results of the sensory evaluation for the different attributes of Willamette raspberry jams (WillRJ) and Wild raspberry jams (WildRJ) produced in three different years can be observed in Table 1, Table 2, and Table 3. The samples were scored for their attributes such as colour, smell, taste, consistency/texture, and overall acceptability, and their mean value was calculated. The differences between the jams with different sweeteners in each of the productive years were statistically processed and their significance was determined.

The Willamette raspberry jams prepared with sorbitol (WillRJsorb) in three different years of testing, had the highest sensory scores for colour (3.97, 4.00, and 3.80 points, respectively), smell (1.94, 2.00, and 1.90 points, respectively), and overall acceptability (19.50, 19.71, and 19.00 points, respectively) compared with the other Willamette raspberry jams (Table 1). Also, the WillRJsorb had the highest sensory scores for taste in the first and the third year of testing (7.70, and 7.70 points, respectively). In the second year, Wild raspberry jams prepared with sucrose (WillRJsucr) had the highest sensory scores for taste (7.85).

Table 1. The results obtained by sensory analysis of the Willamette raspberry jam with different sweeteners for each year

Year	WillRJ	Colour (0-4)	Smell (0-2)	Taste (0-8)	Consistency /texture (0-6)	Overall Acceptability (0-20)
I	sucr	3.88±0,21a	1,91±0,17a	7,50±0,52a	5,73±0,36ab	19,02±0,96a
	fruc	3.87±0.23a	1.93±0.15a	7.51±0.47a	5.94±0.16a	19.25±0.71a
	sorb	3.97±0.07a	1.94±0.16a	7.70±0.42ab	5.89±0.19a	19.50±0.73a
	agave	3.50±0.50a	1.85±0.32a	6.96±0.75b	5.34±0.94b	17.65±1.24a
II	sucr	3.85±0.24a	1.95±0.16a	7.85±0.24a	5.83±0.33ab	19.48±0.73a
	fruc	3.65±0.41a	1.95±0.16a	7.60±0.66a	5.68±0.41ab	18.88±1.32a
	sorb	4.00±0.00a	2.00±0.00a	7.73±0.25a	5.98±0.06a	19.71±0.25a
	agave	3.59±0.40a	1.99±0.03a	6.91±0.71a	5.50±0.67b	17.99±1.28a
III	sucr	3.50±0.53a	1.80±0.42a	7.20±0.92a	5.60±0.70a	18.10±0.99ab
	fruc	3.30±0.67ab	1.60±0.52a	7.10±0.88a	5.60±0.52a	17.60±1.07a
	sorb	3.80±0.42b	1.90±0.32a	7.70±0.48a	5.60±0.52a	19.00±0.67b
	agave	2.70±0.67ab	1.70±0.48a	5.90±1.20a	5.00±0.82a	15.30±2.00ab

* Mean ±SD values in the same column with different letters are significantly different ($p < 0.05$); WillRJ-Willamette raspberry jams; sucr-sucrose, fruc-fructose, sorb-sorbitol, agave-agave syrup

As regards the consistency/texture analysis, different results were obtained when Willamette raspberry jams made with the above mentioned sweeteners were analyzed. In the first year Willamette raspberry jams prepared with fructose (WillRJfruc) had the highest number of points (5.94 points), in the second year the WillRJsorb were assessed with maximum points (5.98 points), and the third year the Willamette raspberry jams prepared with sucrose, fructose and sorbitol had the same number of points (5.60 points). The lowest values for all sensory attributes was detected in Willamette raspberry jams prepared with agave syrup (WillRJagave) in each of the productive years.

The data obtained in Table 1 indicated that in the first and second year, no significant difference ($p>0.05$) was found in colour scores between prepared Willamette raspberry jams, but in the third year, there was a significant difference ($p<0.05$) between WillRJsucr and

WillRJsorb. There was no significant difference ($p>0.05$) in three different years between the mean values of the smell of all prepared WillRJ. The score for the taste of WillRJagave (6.96 points) was not significantly ($p>0.05$) different from that of WillRJsorb (7.70 points), but differed significantly ($p<0.05$) from that of WRJsucr (7.50 points) and of WillRJfruc (7.51 points).

The results of the sensory evaluation for the different attributes of Wild raspberry jams (WildRJ) produced in three different years can be observed in Table 2.

Table 2. The results obtained by sensory analysis of the Wild raspberry jam with different sweeteners for each year

Year	WildRJ	Colour (0-4)	Smell (0-2)	Taste (0-8)	Consistency /texture (0-6)	Overall Acceptability (0-20)
I	sucr	3.73±0.42a	1.96±0.10a	7.17±0.94a	5.76±0.41a	18.62±1.07a
	fruc	3.63±0.42a	1.89±0.24a	7.04±0.99a	5.73±0.37a	18.29±1.14a
	sorb	3.73±0.37a	1.80±0.35a	7.17±1.12a	5.83±0.24ab	18.53±1.64a
	agave	2.92±0.88a	1.74±0.43a	5.88±1.31b	5.10±0.96b	15.64±3.06a
II	sucr	3.75±0.35a	2.00±0.00a	7.35±0.58a	5,80±0.35a	18.90±0.91a
	fruc	3.80±0.42a	1.90±0.32ab	7.20±1.01a	5,35±0.94a	18.25±2.08a
	sorb	3.95±0.16a	1.5±0.16ab	7.25±0.79a	5,40±0.74a	18.55±1.30a
	agave	2.45±1.01a	1.73±0.42b	5.23±1.62a	5,15±0.75a	14.56±2.86a
III	sucr	3.50±0.53a	1.90±0.32ab	6.70±0.82a	5.20±0.42ab	17.30±1.16a
	fruc	3.10±0.74a	1.80±0.42a	6.70±0.95a	5.40±0.70ab	17.00±1.49a
	sorb	3.60±0.52a	1.80±0.42a	7.00±0.82ab	5.70±0.48a	18.10±1.20a
	agave	2.60±0.84a	1.30±0.48b	5.70±1.25b	5.00±0.67b	14.60±1.65a

* Mean ±SD values in the same column with different letters are significantly different ($p < 0.05$); WildRJ- Wild raspberry jams; sucr-sucrose, fruc-fructose, sorb-sorbitol, agave-agave syrup

In the first year, Wild raspberry jams prepared with sucrose (WildRJsucr) had the highest sensory scores for smell (1.96) and overall acceptability (18.62), and the WildRJsucr and Wild raspberry jams prepared with sorbitol (WildRJsorb) had the same number of points for colour (3.73), and taste (7.17). The highest consistency/texture values in the first year were observed in WildRJsorb (5.83). In the second year, WildRJsucr had the highest sensory scores for smell (2.00), taste (7.35), consistency/texture (5.80), and overall acceptability (18.90) compared with the other WildRJ. In the third year, WildRJsorb had the highest sensory scores for colour (3.60), taste (7.00), consistency/texture (5.70), and overall acceptability (18.10) compared with the other WildRJ. In the same year, WRJsucr had the highest sensory scores for smell (1.90). The lowest values for all sensory attributes was

detected for Wild raspberry jams prepared with agave syrup (WildRagave) in each of the productive years.

From the data presented in Table 2, it was concluded that no significant difference ($p>0.05$) in all three different years between the mean values obtained for colour, and overall acceptability for all prepared Wild raspberry jams. As regards the smell analysis, a significant difference between WildRagave and WRJsucr was detected ($p<0.05$) in the second year, and in the third, there was a significant difference between WildRagave and Wild raspberry jams prepared with fructose and sorbitol. No significant differences were found in the first year ($p>0.05$).

The score for the taste of WRJagave was significantly ($p<0.05$) different from that of WRJsuc, WRJsorb, and Wild raspberry jams prepared with fructose (WRJfruc) in the first year, while no significant differences were found in the second year, ($p>0.05$). In the third year, a significant difference ($p<0.05$) between WildRagave and Wild raspberry jams prepared with sucrose and fructose was determined. Also, a significant difference ($p<0.05$) between WildRagave and Wild raspberry jams prepared with sucrose and fructose in context of consistency/texture was determined in the first year. No significant differences were found in the second year ($p>0.05$), but in the third year, there was a significant difference between WildRagave and WRJsorb

The average grade results obtained by sensory analysis of the Willamette raspberry jams and Wild raspberry jams with different sweeteners for the whole three-year period can be observed in Table 3.

The results suggested that the WillRJsorb were assessed with the highest average grade for the whole three-year period for colour (3.92), smell (1.95), taste (7.71), consistency/texture (5.82), and overall acceptability (19.41). The highest average grade for colour (3.76), taste (7.14), consistency /texture (5.64), and overall acceptability (18.39) for the entire three-year period was obtained when WildRJsorb were also analyzed. The three-year average for smell shows the highest value (1.95) in WildRJfruc. The Willamette raspberry jams and Wild raspberry jams prepared with agave syrup had the lowest average grade for all sensory attributes, which is probably due to the properties of the agave syrup (16) and the possibility of creating new compounds during the heat treatment. The creation of new compounds during heat treatment can affect the sensory attributes of jams (13).

The food product incorporating alternative sweetener should have textural and rheological characteristics and taste similar to that of the traditional product (17). The above results obtained, suggest that in general, sorbitol had the least effect on the colour of jams and during

the heat treatment had the low possibility of creating new compounds that would cause discoloration. Our results indicated that the sorbitol with its mild sweetness gives the product the taste typical for the fruit from which it originates and confirmed the fact that sorbitol provided the required product texture without the product being too sweet (18, 19). Sorbitol is considered as GRAS (Generally Regarded As Safe) and should be used at levels that do not exceed GMPs (Good Manufacturing Practice) (17).

Table 3. The average grade results obtained by sensory analysis of Willamette raspberry jams and Wild raspberry jams with different sweeteners for the whole three-year period

Year		Colour (0-4) $\bar{x}$± SD	Smell (0-2) $\bar{x}$± SD	Taste (0-8) $\bar{x}$± SD	Consistency /texture (0-6) $\bar{x}$± SD	Overall Acceptability (0-20) $\bar{x}$± SD
WillRJ	sucr	3.74±0.21	1.89±0,08	7.52±0.33	5.72±0.12	18.87±0.70
	fruc	3.61±0.29	1.83±0,20	7.40±0.27	5.74±0.18	18.58±0.87
	sorb	3.92±0.11	1.95±0,05	7.71±0.02	5.82±0.20	19.41±0.37
	agave	3.26±0.49	1.85±0,15	6.59±0.06	5.28±0.26	16.98±1.46
WildRJ	sucr	3.66± 0.14	1.95± 0.05	7.07± 0.34	5,59± 0.34	18,27± 0.85
	fruc	3,.51± 0.37	1.86±0.06	6.98±0.26	5,49±0.21	17,85±0.73
	sorb	3.76± 0.18	1.85± 0.09	7.14± 0.13	5,64± 0.22	18,39± 0.25
	agave	2.66± 0.24	1.59±0.25	5.60±0.34	5,08±0.08	14,93±0.61

* $\bar{x}$- average value; SD - standard deviation; WillRJ-Willamette raspberry jams; WillRJ-Willamette raspberry jams; sucr-sucrose, fruc-fructose, sorb-sorbitol, agave-agave syrup

These results are compatible with the findings of other authors (17, 20–22). Also, our previous study showed that plum and peach jams with sorbitol had the highest total average score and better sensory attributes compared to peach and plum jams prepared with fructose, agave syrup, and a low amount of sucrose (13).

4. Conclusion

Based on sensory scores of raspberry jams (Willamette raspberry jams and Wild raspberry jams) with different sweeteners (fructose, sorbitol, agave syrup, and a low amount of sucrose) was found that both types of raspberry jams with sorbitol have better sensory attributes as compared with jams prepared with other sweeteners. However, there is a need to continue this research. Future studies should consider the effect of storage on the sensory attributes of raspberry jams (Willamette raspberry jams and Wild raspberry jams) with different sweeteners (fructose, sorbitol, agave syrup, and a low amount of sucrose).

5. References

1. Darkwa, I.; Boakye, A. B. N. The Preparation of Jam: Using Star Fruit. *Global Journal of Educational Studies*, **2016**, *2*(2), 36-56.
2. Korus, A.; Banaś, A.; Korus J. Effects of plant ingredients with pro-health properties and storage conditions on texture, color and sensory attributes of strawberry (*Fragaria* × *ananassa* Duch.) jam. *Emirates Journal of Food and Agriculture*, **2017**, *29*(8), 610-619.
3. Haq, R.; Darakshan, M. Quality and Storage Stability of Developed Dried Apricot-Date Jam. *Journal of Food Product Development and Packaging*, **2014**, *1*, 37-41.
4. Ogori A.F.; Amove, J.; Evi-Parker, P.; Sardo G.; Okpala, C.O.R.; Bono, G.; Korzeniowska, M. Functional and sensory properties of jam with different proportions of pineapple, cucumber, and *Jatropha* leaf. *Foods and Raw Materials*, **2021**, *9*(1), 192–200.
5. Vilela, A.; Matos, S.; Abraão, S. A.; Lemos, M.A.; Nunes, M.F. Sucrose Replacement by Sweeteners in Strawberry, Raspberry, and Cherry Jams: Effect on the Textural Characteristics and Sensorial Profile -A Chemometric Approach, *Journal of Food Processing*, **2015**, ID 749740, 14.
6. Rippe, J.M.; Angelopoulos, T.J. Relationship between Added Sugars Consumption and Chronic Disease Risk Factors: Current Understanding. *Nutrients*, **2016**, *8*(11):697.
7. Alsuhaibani, M. A. A.; Al-Kuraieef, N.A. Effect of Low-Calorie Pumpkin Jams Fortified with Soybean on Diabetic Rats: Study of Chemical and Sensory Properties. *Journal of Food Quality*, **2018**, ID 9408715, 7.
8. Abolila, R.M.; Barakat, H.; El-Tanahy, H.A.; El-Mansy, H.A. Chemical, Nutritional and Organoleptical Characteristics of Orange-Based Formulated Low-Calorie Jams. *Food and Nutrition Sciences*, **2015**, *6*, 1229-1244.
9. Curi, P. N.; Carvalho, C. dos S.,; Salgado, D. L.; Pio, R.; Pasqual, M.; de Souza, F. B. M.; de Souza, V. R. Influence of different types of sugars in physalis jellies. *Food Science and Technology*, 2017, *37*(3), 349-355.
10. De Souza V. R.; Pereira, P. A. P.; Pinheiro, A. C. M.; Bolini, H. M. A.; Borges, S. V.; Queiroz, F. Analysis of various sweeteners in low-sugar mixed fruit jam: equivalent sweetness, time-intensity analysis and acceptance test. *International Journal of Food Science & Technology*, **2013,** *48*(7), 1541–1548.
11. Belkacem, A.; Ellouze, I.; Debbabi, H. Partial substitution of sucrose by non-nutritive sweeteners in sour orange marmalades: effects on quality characteristics and acute

postprandial glycemic response in healthy volunteers. *The North African Journal of Food and Nutrition Research*, **2021,** *5*(11), 10-14.

12. Rana, M.S.; Yeasmin, F.; Khan, M.J.; Riad, M.H. Evaluation of quality characteristics and storage stability of mixed fruit jam. *Food Research*, **2020,** *5*(1), 225-231.
13. Stamatovska, V.; Karakasova, Lj.; Uzunoska, Z.; Kalevska, T.; Pavlova, V.; Nakov, Gj.; Saveski, A. Sensory characteristics of peach and plum jams with different sweeteners. *Food and Environment Safety - Journal of Faculty of Food Engineering*, **2017,** *16*(1), 13-20.
14. Vračar, O.LJ. *Priručnik za kontrolu kvaliteta svežeg i prerađenog voća, povrća i pečurki i osvežavajućih bezalkoholnih pića*, Tehnološki fakultet, Novi Sad, 2001.
15. Gesmalla, A.; Siddeeg, A.; Mekki, M.H.; Abdelatief, I.A.; Ali, A.O.; Eljack, A.E.; AL-Farga, A. Chemical and Sensory Properties of Jam and Nectar Processed from Guava Fruit Fly Resistant Genotypes. *Journal of Academia and Industrial Research (JAIR)*, **2016**, *5*(3), 50-53.
16. Saraiva, A.; Carrascosa, C.; Ramos, F.; Raheem, D.; Raposo, A. Agave Syrup: Chemical Analysis and Nutritional Profile, Applications in the Food Industry and Health Impacts. *International Journal of Environmental Research and Public Health*, **2022**, *19*, 7022.
17. Basu, S.; Shivhare, U.; Singh, T.; Beniwal, V. Rheological, Textural and Spectral Characteristics of Sorbitol Substituted Mango Jam. *Journal of Food Engineering*, **2011**, *105*, 503-512.
18. Бимилер, Н.Ц. *Хемија на јаглехидратите за научниците на храната*; Orginal: BeMiller, N.J. *Carbohydrate chemistry for food scientists*. AACC International,Inc. 2007, Translation: Арс Ламина ДОО, Скопје, **2011**.
19. Малчев, Е.: Моллов, П. *Технология на консервирането на плодове и зеленчуци - концентрати и плодово-захарни продукти*, Второ издание, “Контраст”, Стара Загора. **2008.**
20. Kerdsup, P.; Naknean, P. Effect of sorbitol substitution on physical, chemical and sensory properties of low-sugar mango jam. *Proceeding - Science and Engineering*, **2013,** 12-18.

FATTY ACIDS PROFILE OF FUNCTIONAL OHRID TROUT PÂTÉ

Tanja Stojanovska*, Tatjana Kalevska, Daniela Nikolovska Nedelkoska, Gorica Pavlovska

Faculty of Technology and Technical Sciences, University St. Kliment Ohridski

DimitarVlahov bb 1400 Veles, R.N.Macedonia

**tanja.b.stojanovska@uklo.edu.mk*

Abstract

Fish pâté is a functional product because of its nutritive qualities. In this study, three formulations of fish pâté with different amounts of meat (60%, 50%, and 40%) of the endemic specie Ohrid trout (*Salmo letnica)* and extra virgin olive oil as a fat substitute, were made. The content of unsaturated fatty acids, as well as the ingredients like extra virgin olive oil and vegetable fibers make the functionality of the obtained products. The fatty acids profile of the three different formulations of Ohrid trout pâté were determined. The olive oil as ingredient in the pâté formulations affects their fatty acids profiles and increases the content of monounsaturated fatty acids. The presence of docosahexaenoic acid in all three types of pâté is related with the quantity of meat in the pâté and varies from 0.91% to 1.16%.

Keywords: Functional pâté, ohrid trout, fat substitute, fatty acids profile

1. Introduction

Fish is important functional food with potentially positive effects for the human health (1). Human organisms cannot synthesize certain essential fatty acids, so they have to be taken in through certain types of food. Fish is a significant source of monounsaturated (MUFA) and polyunsaturated (PUFA), n-3 and n-6 fatty acids in human consumption (2). Regular or increased consumption of fish contributes to normal development and function of the organism and decreases the occurrence of cardiovascular diseases, atherosclerosis, hypertension and similar (2-3). PUFA can be used for prevention and control of chronic diseases like cancer, diabetes, inflammatory and autoimmune diseases, atopic excema, Alzheimer's disease, depression, schizophrenia, multiple sclerosis, and it also has a positive effect on the cognitive development and learning at children (4-5). A balanced intake of n-6/n-3 fatty acids ratio is necessary for good health condition. The healthy nutrition needs to include a combination of n-3 and n-6 fatty acids in an approximate ratio of one to four times more n-6 compared to n-3

fatty acids intake (5). Fish pâtés distinguish themselves from other meat products with their better nutritive characteristics, presence of n-3 fatty acids, eicosapentanoic and doxohexaenoic acid, and their low level of cholesterol (6). The functionality of the pâtés increases with the usage of olive oil and other types of vegetable oils which decreases the content of saturated fats, and on the other side improves the fatty acid profile of the product (7-11). The substitution of fats with olive oil in the production process results with a pâté that has a high level of oleic acid and monounsaturated fatty acids (MUFA), without a significant influence on the physico-chemical and technological characteristics (12-13).

2. Material and methods

The research material was a fish pâté made of the endemic specie Ohrid trout (Salmo letnica), formulated and produced in laboratory conditions. The Ohrid trout fish meat was taken from fish cultivated in the aquaculture fish pond “Tabana” in village Belica, Porechie region, R. N. Macedonia. In the process of production, commercially produced cold pressed extra virgin olive oil “Santorina” was used as an added fatty component. Isolated pea proteins and dietary fibers produced by “Cosucra”, Belgium, were used to stabilize the emulsion. White pepper and black pepper extract produced by “Akras”, Austria, were used as spices. The vegetable components included were carrots and caramelized onion produced by “Raps”, Germany, to enrich the taste. Rosemary extract by “Fratelli Pagani”, Italy, was used as a natural antioxidant. Three different types of functional pâté s were formulated, each with different Ohrid trout meat quantity content: Pâté A with 600g meat/kg, Pâté B with 500g meat/kg and Pâté C with 400g meat/kg. Other variable materials added in the pâté s were bouillon, dietary fibers and pea proteins in the following quantities: 138.3g bouillon/kg, 225.3g bouillon/kg and 291.8g bouillon/kg for Pâté A, Pâté B and Pâté C, respectively. The pea fibers were used in the following quantities: 15 g/kg, 23 g/kg and 43 g/kg for pâtés A, B and C respectively and pea proteins were included with 8 g/kg, 13 g/kg and 26.5 g/kg in pâté s A, B and C. The other components were included in the same quantities in all three formulations: olive oil with 130 g/kg pâté, carrot 70 g/kg, caramelized onion 15 g/kg, salt 17 g/kg, white pepper 2 g/kg, black pepper extract 0.5 g/kg, rosemary 0.2 g/kg, rosemary extract 0. 02g/kg and lemon juice 4 g/kg pâté .

The production of the pâtés was done in laboratory conditions and included several steps. First, the fish is cleaned and deboned and the vegetables and other ingredients are measured. Then, the fish meat, carrot and caramelized onion are separately thermally processed. After that, the

fish meat was blended together for five minutes with the oil, salt, bouillon and pea proteins added. Next, carrot and onion were added, blended for 2 more minutes and the other ingredients were added. The mixture w transferred into glass containers that are thermally processed. After that, the containers are cooled down and stored at temperature of 4°C.

The determination of the fatty acids profile of the three formulated pâté s was made at the Food Institute at the Faculty for Veterinary Medicine in Skopje, following the accredited method AOAC 996.06 with gas chromatography in a mass detector produced by Agilent.

3. Results and discussion

The total content of fatty acids in the three different types of Ohrid trout pâtés are shown in Table 1.

Table 1. Content of saturated, monounsaturated and polyunsaturated fatty acids in the three types of pâté A, B and C (%)

Fatty acids	Pâté A	Pâté B	Pâté C
SFA%	15.33	15.69	15.49
MUFA%	69.86	69.1	70.03
PUFA %	14.81	15.21	14.48

From the results shown in Table 2 we can conclude that the content of SFA is in the range from 15.69 % for pâté B, to 15.49% and 15.33% for pâté s C and A respectively. The pâté B contains the largest quantity of PUFA of 15.21% , while in pâté C, the quantity of PUFA is 14.48% and in pâté A, it is 14.81%. In all three pâté formulations (A, B and C) the quantity of MUFA is significantly higher compared to the quantities of SFA and PUFA and it goes in the range from 70.03% to 69.86% and 69.1% in pâté s C, A and B, respectively. The fatty acids contained in the final product reflect the fatty acids content in the oils that are used in the emulsions (14). MUFA dominate in the olive oil (15), and in the Ohrid trout fish meat, the author obtained the following results: SFA 25.335%, MUFA 39.462% and PUFA 35.204% (16). The domination of MUFA was expected in all three types of fish pâté.

The influence of fats used in the pâté production on the fatty acids profile of the products, was also confirmed in studies made by other authors. Pâté s that include olive oil in their content compared to ones with pork fat tissue, have lower content of SFA, highest content of MUFA of 67.6±4.1% and the lowest values for PUFA 9±0.28% (10). In the analysis of three pâté s

from different types of fish made with addition of 20% butter, the obtained values for SFA were higher (from 60.42% to 55.56%), the obtained values for MUFA were lower and they were variable depending on the type of fish used (from 25.27% to 26.16%). The obtained results for PUFA were similar and they went in the range from 11.66% to 13.03% (6). The replacement of pork fat with olive oil (13) led to the following results: in the control pork pâté SFA were 33.05%, and with the replacement of 50% of the fats they decreased to 29.74%, with 100% replacement of the fats SFA decreased to 25.43%, while the content of MUFA increased from 49.84% to 55.28 and 63.21%, and PUFA content decreased from 17.12% to 14.97% and in the pâté with complete fats replacement to 11.36%.

The results obtained from the fatty acids profile analysis in the Ohrid trout pâté s are shown in Table 2, while Pictures 1, 2, and 3 show the chromatograms of the fatty acids profiles of pâté s A, B and C, respectively.

Table 2. Fatty acids content(%) in the three types of pâtés A, B and C.

Structure	Name	Pâté A	Pâté B	Pâté C
C14:0	Tetradecane (Myristic)	**0.28**	**0.32**	**0.30**
C16:0	Hexadecane (Palmitic)	**11.71**	**12.01**	**11.93**
C18:0	Octadecane (Stearic)	**2.73**	**2.68**	**2.68**
C20:0	Eicosanova (Peanut)	**0.61**	**0.68**	**0.58**
C16:1	Hexadecene (Palmitoleic)	**1.33**	**1.50**	**1.45**
C18:1n9c	cis-Octadecene (Oleic)	**68.53**	**67.60**	**68.58**
C18:2n6c	cis-Octadecadiene (Linolenic)	**13.09**	**13.51**	**13.03**
C18:3n6	y-Octadecatriene (y-Linolenic)(n-6 GLA)	**0.56**	**0.57**	**0.54**
C22:6n3	cis-Docosahexaenoic (n-3 DHA)	**1.16**	**1.13**	**0.91**

From the obtained results (Table 2), a conclusion can be drawn that SFA (C16:0) dominates in Pâté B with 12.1%. The MUFA detected in the pâté s were presented with: (C18:1n9c) and (C16:1) acids. The PUFA were presented with (C18:2n6c), which had its highest percentage of 13.51% in pâté B, and 13.09% and 13.03% in pâté s A and C, respectively, then DHA (C22:6n3) and GLA (C18:3n6).

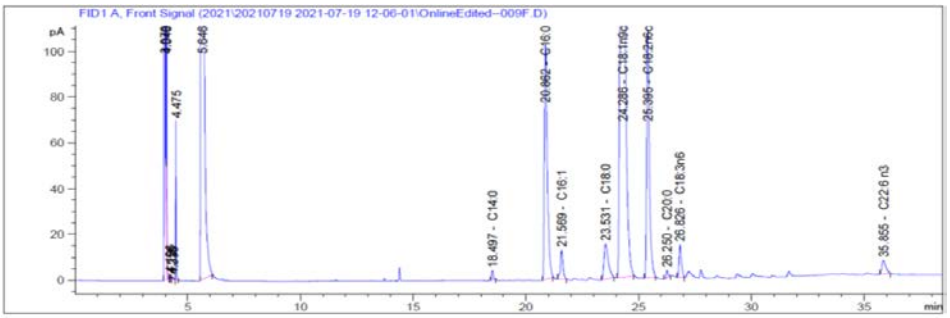

Picture 1. Chromatograme of fatty acid profile for pâté A.

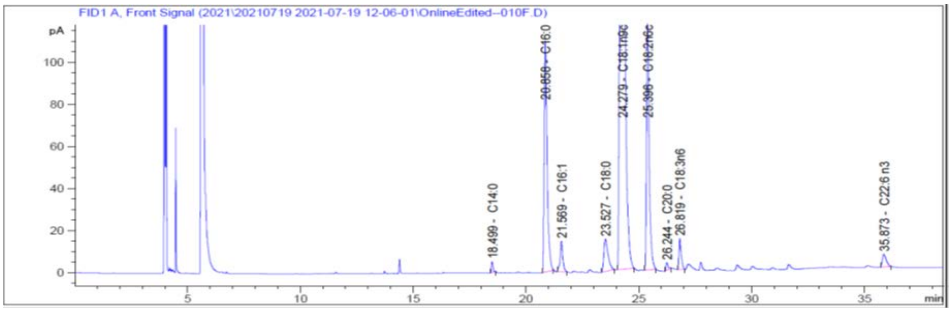

Picture 2. Chromatograme of fatty acid profile for pâté B.

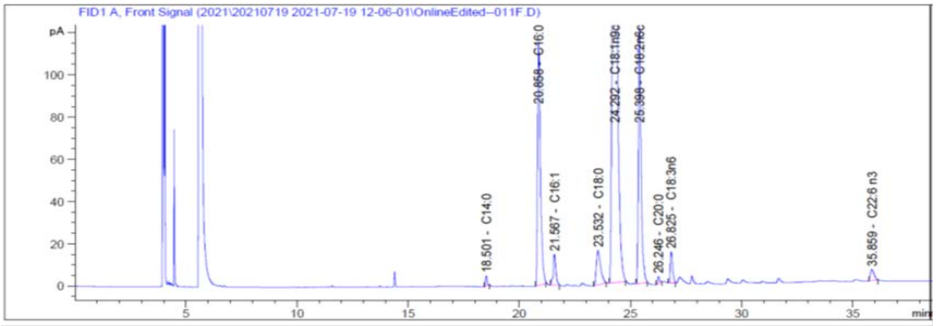

Picture 3. Chromatograme of fatty acid profile for pâté C.

Same quantity of oil (13%), but different percentage of fish meat was used for the production of the three different types of pâté. Hence, the obtained differences in the results for the fatty acids content (especially for PUFA) vary depending on the percentage of fish meat in the pâté. In the PUFA profile n-6 acids dominate over n-3. The influence of the type and the quantity of fish meat added in the final percentual representation of PUFA and the n-6/n-3 ratio is also confirmed by other authors. For example, in the research conducted by (17) the addition of fish roe and fish meat in the pork pâté changed the n-6/n-3 ratio i.e it decreased, while DHA

increased from 0.03% in the control pâté to 0.21% with addition of fish meat, and 0.73% with addition of fish roe. Compared to these results, the DHA content in all the three fish pâté formulations in our study is higher. Actually, the DHA in the Ohrid trout meat is present with 5.320±0.25% (16) while the DHA content in all the three pâté formulations is lower: 1.16% in pâté A, 1.13% in pâté B and the lowest result of 0.91% is obtained in Pâté C. As for the fatty acid C18:3n6, its content in the Ohrid trout is 3.424±0.07%, but in the pâté formulations it goes in the range from 0.57% to 0.54%. Compared to the pâté s formulated in our study that have typical PUFA profile shown in Table 3, the Ohrid trout meat (16), also reports the presence of eicosatrienoic (C20:3n6) и eicosapentaenoic acid (C20:5n3). The lower presence or even complete absence of certain PUFA in the pâté s is due to the added fish meat quantity and also to the thermal treatment of the fish before and after the process of grounding. The type of thermal processing and the temperature of the process affect the decrease of the content of PUFA and their n-3/n-6 ratio (18).

4. Conclusion

Three types of Ohrid trout pâté were formulated with different content of fish meat, bouillon, pea fibers and pea proteins. In all three formulations equal quantities of extra virgin olive oil, caramelized onion and other spices with organic origin were added. Analysis of the fatty acids profile was made and it led to the conclusion that the extra virgin olive oil used in the production of the Ohrid trout (*Salmo letnica*) functional pâté s, influences their fatty acids profile increasing the quantity of monounsaturated fatty acids and significantly decreasing the quantity of saturated and polyunsaturated fatty acids.

The analysis of the fatty acids profile of the produced pâté s showed that the content of docosahexaenoic acid in the three pâté formulations variably depends on the quantity of fish meat added in the pâté. The fatty acids profile of the produced pâté s contributes to the functional characteristics of the products. The commercialization of the production process for these pâté s would offer a new functional product on the market containing the meat of an endemic fish species – Ohrid trout (*Salmo letnica*).

5. References:

1. Kalevska, T.; Nikolovska Nedelkoska, D.; Stamatovska, V.; Jankulovska, V., Nakov, Gj. Functional characteristics of food of animal origin. *Proceedings of university of Ruse,* **2020,** *59(10),*74-79.

2. Kris-Etheron, P.M.; Harris, S.W.; Appel, J.L. Fish consumption, fish oil, omega-3 fatty acids, and cardiovascular disease. *Circulation*, **2002,** *106(21)*, 2747-2757.
3. Maynesris-Perhachs, J,; Bondia-Pons I., Serra-Majem, L,; Castellote, A.L. Long-chain n-3 fatty acids and classical cardiovascular disease risk factors among the Catalan population. *Food Chemistry*, **2010**, *119(1)*, 54-61.
4. Zamaria, N. Alteration of polyunsaturated fatty acid status and metabolism in health and disease. *Reproduction Nutrition Development*, **2004,** *44(3)*, 273-282.
5. Fontani, G.; Corradeschi, F,; Felici, A,; Alfatti, F.; Migliorini, S,; Lodi, L. Cognitive and physiological effects of Omega-3 polyunsaturated fatty acid supplementation in healthy subjects. *European Journal of Clinical Investigation*, **2005,** *35(11)*, 691–699.
6. Ünlusayin, M.; Bilgin, S.; İzci, L.; Gunlu, A. Chemical and sensory assessment of hot-smoket fish pâté . *Journal of Fisheries Sciences*, **2007**, *1(1)*, 20-25.
7. Agregan, R.; Dominguez, R.; Munekata, P.E.; Goncalves, A.; Borrajo, P.; Lorenzo, J.M. Effect of olive oil amount on physic-chemical properties of pâté from celta pig breed. In: 61st International Congress of Meat Science and Technology, August 23-28th 2015. Clermont-Ferrand, France, **2015,** 180-184.
8. Reddy, J.K.; Jayathilakan, K.; Pandey, M.C. Olive oil as functional component in meat and meat products. *Journal of Food Science and Technology*, **2015**, *52(11).*
9. Branciari, R.; Roila, R.; Valiani, A.; Ranucci, D.; Ortenzi,R.; Miraglia, D.; Bailetti, L.; Franceschini, R. Nutritional quality, safety and sensory properties of smoked tench *(Tinca tinca)* pâté from Trasimeno Lake, Italy. *Italian Journal of Food Safety*, **2019** *8(3), 8130.*
10. Teixeira, A.; Almeida, S.; Periera, E.; Mangachaia, F.; Rodrigues, S. Physicochemical characteristics of sheep and goat pâtés. differences between fat sources and proportions. *Heliyon*, **2019** *5(7), 02119.*
11. Martins, A.J.; Lorenzo, J.M.; Franco, D.; Pateiro, M.; Domínguez, R.; Munekata, P.E.S.; Pastrana, L.M.; Vicente, A.A.; Cunha, R.L.; Cerqueira, M.A. Characterization of Enriched Meat-Based Pâté Manufactured with Oleogels as Fat Substitutes. *Gels.* **2020**, *6(2), 17.*
12. Delgado-Pando, G.; Cofrades, S.; Rodríguez-Salas, L.; Jiménez-Colmenero, F. A healthier oil combination and konjac gel as functional ingredients in low-fat pork liver pâté. *Meat Sci*, **2011** *88(2)*, 241-248.

13. Dominguez, R.; Agregan, R.; Goncalves, A.; Lorenzo, J.M. Effect of fat replacement by olive oil on physico-chemical properties, fatty acids, cholesterol and tocopherol content of pâté. *GrasasAceites,* **2016,** *67 (2),* 133.
14. Vargas-Ramella, M.; Munekata, E.S.P.; Gagoua, M.; Franco, D.; Campagnol, C.B.R.; Pateiro, M.; Carla de Silva Barretto, A.; Dominguez, R.; Lorenzo, M.J. Inclusion of Healthy Oils for Improving the Nutritional Characteristics of Dry-Fermented Deer Sausage. *Foods,* **2020,** *9(10),* 1487.
15. Hannacni, H.; Nasri, N.; Elfalleh, W.; Tlili, N.; Ferchichi, A.; Msallem, M. Fatty acids, sterols, polyphenols, and chlorophylls of olive oils obtained from Tunisian wild olive trees *(Oleaeuropaea L. Var. Sylvestris). International Journal of Food Properties,* **2013**, *16(6),* 1271–1283.
16. Saveski, A.; Kalevska, T.; Stamatovska, V.; Uzunoska, Z.; Josevska, E. Comparative analysis of fatty acids in the meat of the Macedonian and ohrid trout from aquaculture production. *In. Proceedings of the 11th International Symposium Modern Trends in Livestock Production* October 11-13, **2017,** 685-695.
17. Skałecki, P.; Kaliniak-Dziura, A.; Domaradzki, P.; Florek, M.; Poleszak, E.; Dmoch, M. Effect of Pork Meat Replacement by Fish Products on Fatty Acid Content, Physicochemical, and Sensory Properties of Pork Pâtés. *Appl. Sci.* **2021,** *11*, 188.
18. Schneedorferová, I.; Tomčala, A.; Valterová, I. Effect of heat treatment on the n-3/n-6 ratio and content of polyunsaturated fatty acids in fish tissues. *Food Chemistry*, **2015** *176*, 205-211.

TESTING OF VITAMIN C CONTENT AND MICROBIOLOGICAL QUALITY CONTROL IN FRESH AND DRIED ROSE HIP (*Rosa canina* L.) FRUIT

Svetlana Bogdanović[1]*, Dobrila Randjelović[1], Zvonko Zlatanović[1], Violeta Rakić[1], Dragana Stanisavljević[1]

Toplica Academy of Applied Studies, Department of Agricultural and Technological Studies Prokuplje, Ćirila i Metodija 1, 18400 Prokuplje, Serbia

**celebogdanovic@gmail.com*

Abstract

Rose hip (*Rosa canina* L.), wild rose or dog rose is widespread in almost all of Europe, Africa, western and northern Asia. Rose hip fruit is a rich source of vitamin C and contains a large number of different chemical compounds including pectins, tannins, organic acids. The fruit is usually used to make jam, syrup or dried. The aim of this scientific work is to examine the activity of water (a_w), pH value, acid content, vitamin C content and microbiological quality control in fresh and dried rose hips. Water activity was measured with an a_w-meter (Pawkit Decagon, Germany). pH value was measured with a pH meter (InoLab WTW, Germany). The acid content was determined by volumetric method, titration with NaOH. Vitamin C content was determined spectrophotometrically (Jenwey spectrophotometer 6305, United Kingdom). Microbiological quality control included food spoilage bacteria *Salmonella* spp. ISO 6579-1:2017, *Listeria monocytogenes* ISO 11290-1:2017, *E. coli* ISO 16649-1:2018 and *Enterobacteriaceae* ISO 21528-2:2017. The results of these tests indicated that both fresh and dried rose hips are a good source of vitamin C. The results of microbiological analysis showed the absence of *Salmonella* spp., *L. monocytogenes* and *E. coli*. The presence of *Enterobacteriaceae* was less than 10 cfu / ml.

Keywords: Vitamin C, rose hip fruit, quality control

1. Introduction

The genus *Rosa* (roses) contains from 120 to 6000 plant species that are spread over almost all of Europe, Africa, Western and Northern Asia. The most famous species of this genus is *Rosa canina* L. dog rose or wild rose. Rosehip fruit has antioxidant and antimicrobial activity, affects the regulation of digestion and body weight. Rosehip fruit contains a high content of vitamins

C and E, carotenoids, phenols, pectins, terpenes, as well as fatty acids. A small part of this fruit is consumed fresh, because it has a pleasant taste in a short period of time, while most of it undergoes drying or is used to prepare jam, syrup, marmalade, jelly, while in the last few years, pomegranate is also used as an ingredient in probiotic drinks, yogurt, soup, as well as dietary supplements (1), (2), (3). In ethnomedicine,it is used as a preventive measure against a large number of diseases such as vitamin C deficiency, diseases of the gastrointestinal and urogenital tract, arthritis, diabetes, etc. (4). Rosehip of the species *Rosa canina* has also found its application in the food industry. It is most often used as an additive for fruit juices with low vitamin C content, as well as in the control of "enzymatic browning" of fruit products (5), (6), Ganhão et al. (2010) (7) describes it as an agent for the inhibition of lipid oxidation in fresh raw pork hamburger. Wild roses are attracting more and more attention from agricultural producers due to their high yield and resistance to various diseases and pests (8), (9).

2. Experimental

Fresh rose hips were collected in the Toplička district and dried in a laboratory dryer (manufactured by Gorenje) at a temperature of 70°C. The content of water activity (a_w), *pH* values, acid content, vitamin C content and microbiological quality control of fresh and dried rose hips were analyzed. From a chopped sample of fresh and dried rose hip, the water activity was measured with an a_w meter (Pawkit Water Activity Meter).

The *pH* value is determined from the stock solution, which was prepared from a previously homogenized 10 g sample of fresh and dried rose hips, which was poured with 250 cm^3 of hot distilled water and filtered after cooling. The stock solution is also used to determine the acid content by acid titration with a standard sodium hydroxide solution in the presence of the phenolphthalein indicator (10).

The content of vitamin C was determined by the spectrophotometric method according to Tilmans, which is based on the reduction of vitamin C with 2,6-dichlorophenol-indophenol (10).

Microbiological quality control included food spoilage bacteria Salmonella spp., *Listeria monocytogenes*, *Enteriobacteriaceae*. All methods were performed on the basis of ISO standards, namely *Salmonella* spp. ISO 6579-1:2017 (11), *Listeria monocytogenes* ISO 11290-1:2017 (12), *Enterobacteriaceae* ISO 21528-2:2017 (13).

3. Results and discussion

Various studies indicate the use of plants of the genus *Rosa* in ethnomedicine in Europe as early as around 500 BC. Species of the genus *Rosa* are among the twenty most commonly used plants (14). Plants of the genus *Rosa* occupy an important place in the treatment of medieval Serbs, where *R. canina* is the most famous plant of this genus, described as the second most commonly used plant (15).

The results of the chemical analysis of fresh and dried rosehip fruit are presented in Table 1. The results of the determination of water activity clearly indicate a higher value in the fresh fruit compared to the dried fruit. The value of water activity in the fresh fruit was 0.98, while it was 0.8 in the dried fruit. The pH value is 3.4 in fresh and 3.3 in dried fruit. In contrast to the water activity values, drying the fruit does not affect the pH values. The acid content was 1.9% in fresh fruit and 1.7% in dried fruit. Also, the vitamin C content (expressed in g/kg) was 2.21 g in fresh fruit, while it was 1.56 g in dried fruit.

Table 1. Results of the chemical analysis of fresh and dried rose hips

	Water Activity (a_w)	**pH**	**Acid content (such as citric) %**	**The content vitamin C g/kg**
Fresh rosehip	0,98	3,4	1,9	2,21
Dried rosehip	0,80	3,3	1,7	1,56

Widely known and scientifically proven biological activity of vitamin C of *Rosa* species could be one of the parameters that would indicate the potential of rosehip products as functional food. *Rosa canina* rosehips contain six times more vitamin C than oranges (16). Literature data indicate that *R. canina* species contain the most vitamin C.

The obtained results are in accordance with the results of Barros et al. (2011) (17) and Demir et al. (2014) (3). It is important to note that the amount of vitamin C remained preserved even after drying the fruit. These results prove the justification of the use of dried fruit.

A microbiological test performed according to ISO standards, which is used to detect food spoilage agents and potential opportunistic pathogens in humans, showed the absence of *Salmonella* spp. and *L. monocytogenes*. Representatives of the *Enterobacteriaceae* family were found in numbers less than 10 cfu/g. The results of microbiological quality control of fresh and dried rosehip fruit are presented in Table 2.

Table 2. Results of microbiological quality control of fresh and dried rosehip fruit

Microorganisms	Limit values (cfu/g)		Method label	Established value
	m	M		
Salmonella spp.	it must not be in 25g		SRPS EN ISO 6579-1:2017	no presence was established
Enterobacteriaceae	10		SRPS EN ISO 21528-2:2017	< 10 cfu/g
L. monocytogenes	it must not be in 25g		SRPS EN ISO 11290-1:2017	no presence was established

The results indicate the presence of *Enterobacteriaceae* in a value less than 10 cfu/g, as well as the absence of *Salmonella* spp. and *L. monocytogenes* species, which represent possible human pathogens.

4. Conclusion

Every day we encounter people's mistrust in the healing and microbiological correctness of dried rose hips. The results of this scientific work show us that the concentration of vitamin C in fresh and dried fruit is at a satisfactory and expected level. Microbiological quality control performed according to ISO standards does not indicate the presence of *Salmonella* spp. and *L. monocytogens, Enterobacteriaceae* are present less than 10 cfu/ml. The obtained values of the chemical analysis, including the vitamin C content, indicate the justification of the use of rose hips in ethnomedicine. The performed microbiological quality control indicates the safe use of rose hips.

5. References

1. Grlić,Lj.: *Enciklopedija samoniklog jestivog bilja.* August Cesarec. **1990**, Zagreb,SFR Jugoslavija
2. Patel,S.: Rose hips as complementary and alternative medicine :overview of the present status and prospects. *Mediterranean Journal of Nutrition and Metabolism,* **2013**, *6*, 89–97.
3. Demir, N., Yildiz, O., Alpaslan, M., Hayaloglu, A. A.: Evaluation ofvolatiles, phenolic compounds and antioxidant activities of rose hip (Rosa L.) fruitsin Turkey. *LWT - Food Science and Technology*, **2014**, *57*, 126-133.

4. Chrubasik, C., Wiesner, L., Black, A., Chrubasik, S.: A one-year surveyon the use of a powder from Rosa canina lito in acute exacerbations of chronic pain. *Phytotherapy Research*, **2008**, *22*, 1141–1148.
5. Şakiroğlu, H., Küfrevioğlu, Ö. I., Kocaçalişkan, I., Oktay, M., Onganer, Y.: Purification and characterization of Dog-rose (Rosa dumalis Rechst.) polyphenol oxidase. *Journal of Agricultural and Food Chemistry,* **1996**, *44*, 2982-2986.
6. Zocca, F., Lomolino, G., Lante, A.: Dog rose and pomegranate extractsas agents to control enzymatic browning. *Food Research International*. **2011**, *44*, 957–963.
7. Ganhão, R., Estévez, M., Kylli, P., Heinonen, M., Morcuende,D.: Characterization of selected wild Mediterranean fruits and comparative efficacy as inhibitors of oxidative reactions in emulsified raw pork burger patties. *Journal of Agricultural and Food Chemistry*. **2010**, *58*, 8854–8861.
8. Uggla, M., Martinsson, M.: Cultivate the wild roses-Experience from rosehip production in Sweden. *Acta Horticulturae,* **2005**, *690*, 83-93
9. Ercisli, S.: Chemical composition of fruits in some rose (Rosa spp.) species. *Food Chemistry*. **2007**, *104*, 1379-1384.
10. Vračar Lj.: Priručnik za kontrolu kvaliteta svežeg i prerađenog voća, povrća i pečurki i osvežavajućih bezalkoholnih pića. **2001**, Tehnološki fakultet, Novi Sad
11. International Organization for Standardization (SRPS EN ISO 6579-1) Microbiology of the food chain – Horizontal method for the detection, enumeration and serotyping of Salmonella - Part 1: Detection of Salmonella spp. **2017**.
12. International Organization for Standardization (SRPS EN ISO 11290-2.) Microbiology of the food chain – Horizontal method for the detection and enumeration of Listeria monocytogenes and of Listeria spp. **2017**.
13. International Organization for Standardization (SRPS EN ISO 21528-2.) Microbiology of the food chain – Horizontal method for the detection and enumeration of Enterobacteriaceae - Part 2: Colonycount technique. **2017**.
14. De Vos, P.: European materia medica in historical texts: Longevity of atradition and implications for future use. *Journal of Ethnopharmacology,* **2010**, *132*, 28–47.
15. Jarić,S., Mitrović,M., Đurđević,L., Kostić,O., Gajić,G., Pavlović,D., Pavlović,P.: Phytotherapy in medieval Serbian medicine according to the pharmacological manuscripts of the Chilandar Medical Codex (15–16thcenturies). Journal of Ethnopharmacology, **2011**, *137,* 601-619.

16. Nojavan, S., Khalilian, F., Kiaie, F. M., Rahimi, A., Arabanian,A., Chalavi, S. Extraction and quantitative determination of ascorbic acid during different maturity stages of Rosa canina L. fruit. *Journal of Food Composition and Analysis*, **2008**, *21*, 300-305.
17. Barros,L., Carvalho,A., Ferreira,I. Exotic fruit sasa source of important phytochemicals: Improving the traditional use of Rosa canina fruits in Portugal. *Food Research International*, **2010**, *44*, 2233-2236.

ANTIBACTERIAL ACTIVITY OF MANUKA HONEYS WITH DIFFERENT UMF VALUES

Vesna Kalaba*, Tanja Ilic, Dragana Kalaba

PI Veterinary Institute of Republika Srpska "Dr Vaso Butozan" Branka Radičevića 18, Banja Luka, Republic of Srpska, Bosnia and Herzegovina

**vesna.kalaba@virs-vb.com*

Abstract

Manuka honey is a dark monofloral honey, rich in phenol compounds and attracts a lot of attention because of its antimicrobial action. The antibacterial power of Manuka honey is linked with the Unique Manuka Factor (UMF) which correlates with the contents of methylglyoxal and total phenols. Different types of Manuka honey have different effects on bacteria, so gram-negative bacteria are more resistant than gram-positive bacteria.

The aim of this research was to compare the effects of Manuka honey UMF 15+, Manuka honey UMF 5+ and their growth inhibition of five different species of bacteria: Streptococcus group D, β-hemolytic streptococcus, *Pasteurella multocida*, *Streptococcus uberis* and *Truepqera pyogenes* from the collection isolate of the Laboratory of clinical microbiology.

Two samples of Manuka honey of different UMF were used in the experiment. Honey was used in undiluted and diluted state (honey: distilled water 50:50% and 75:25% (v/v)). Disc diffusion method was used to evalaute antibacterial activity.

Manuka honey UMF 5+ had an inhibitory effect on all tested strains in all combinations with a range of action from 10.67 (Streptococcus D group) to 43.33 mm (*Trueperella pyogenes*), except for *Trueperella pyogenes* in combination with honey: distilled water 75:25% (v / c) (0.00 mm).

Manuka honey UMF15 + in all combinations had an inhibitory effect on the tested bacteria with a range of action from 12.33 mm to 42.00 mm.

Keywords: Manuka Honey, UMF 5 +, UMF15 +, inhibition, antibacterial effects

1. Introduction

Honey has been used as a natural medicine for more than 2000 years, mainly for healing wounds. Healing properties of honey has derived from nectar. Antimicrobial properties of

honey's have ability to inhibit bacterial growth which has been documented in numerous studies focused on alternative approaches to treating bacterial infections (1). It has been confirmed that honey can be used as an alternative medicine in the healing of wounds caused by microorganisms including *S. aureus*, *S. pyogenes*, *P. aeruginosa* and *E. coli* (1) but also as an anti-cancer agent (Saeed et al. 2018). It is important to underline that so far not a single case of honey resistance has been recorded (2,3). Bacterial resistance to antimicrobial drugs is a major public health problem and a small number of new antibacterial drugs are being developed. Honey has been used since ancient times to treat wounds and as a drug for gastrointestinal problems, also it acts on a wide range of pathogens and on bacteria involved in food spoilage. Many studies have confirmed that honey is potent "in vitro" for bacteria resistant to antimicrobial drugs and that it is successfully applied in the treatment of chronic wound infections where antibacterial therapy does not achieve good, satisfactory results. All these reasons have increased the interest of modern medicine in Manuka honey as an antimicrobial medicine.

Manuka honey is a monofloral honey produced by *Apis mellifera* honeybees from the nectar of the flowers of the Manuka tree (*Leptospermum scoparium*) a plant that grows as a shrub or tree in New Zealand and Eastern Australia (4). The quality of Manuka honey is evaluated using a classification system known as the unique Manuka factor (UMF) which reflects the equivalent concentration of phenols (%, v/v) required to produce the same antibacterial activity as honey. It is the first registered "medicinal honey" and one of the most researched types of honey. The UMF values guarantees that the honey has been laboratory tested, its originality and origin. Also, the UMF values guarantees the presence of non-peroxide activity that is not found in any other type of honey (5).

Manuka honey was approved as an alternative and natural wound healing material by the US Federal Drug Administration in 2007. Manuka honey has various biological effects and is widely used in complementary and conventional medicine. Manuka honey among other types of honey has the ability to release hydrogen peroxide which is an important factor for reducing and eliminating bacterial activity (6).

Manuka honey consists of carbohydrates, minerals, proteins, fatty acids, phenolic and flavonoid compounds. Manuka honey is a unique honey due to its extremely high level of methylglyoxal (MGO) formed from dihydroxyacetone (DHA) which correlates with the honey's antibacterial activity (7,8).

Numerous studies have confirmed the therapeutic effect of Manuka honey in the treatment of various infections (9,10) and proven to be an excellent choice when it comes to infections

caused by strains resistant to antibacterial drugs, such as MRSA (*Methicillin-resistant Staphylococcus aureus*) (6). Thanks to the rich composition of phytochemical compounds that act as active bio-compounds Manuka honey shows antioxidant and anticancer, anti-inflammatory and immunostimulating properties (11,12,13). Recent research has confirmed the good potential of Manuka honey in the treatment of viral infections and influenza (14). The MGO values of Manuka honey have been found to be up to 100 times higher than other non-Manuka honeys (15). Manuka honey has a positive effect on the nervous system, is good for cardiovascular diseases and complications of diabetes, as well as for maintaining oral health.

Various studies have shown that Manuka honey of different unique Manuka factor (UMF) exhibits selective activity against different bacteria. The UMF value refers to the content of methylglyoxal (MGO) in honey and it is assumed that the content of MGO and hydrogen peroxide is responsible for a large part of the antibacterial properties of honey (16,17). Other factors such as osmotic pressure, pH, low protein content, bee defensin-1, hyper-osmolality effect, different levels of flavonoids and phenolic complexes, as well as carbon and nitrogen, also contribute to its activity (18). The presence of MGO and hydrogen peroxide contributes to the inhibition of bacterial growth (19,20), but there are other components that help and enhance the effects of MGO and hydrogen toxicity (21). Also, antimicrobial activity depends on a number of factors such as: source of nectar, geographical location of flowers and weather conditions, as well as storage period and storage conditions (4).

The aim of this research is to compare the effects of Manuka honey UMF 15+ and UMF 5+ in inhibiting the growth of five different types of bacteria: group D streptococcus, β-hemolytic streptococcus, *Pasteurella multocida*, *Streptococcus uberis* and *Truepqera pyogenes* from the collection of laboratory isolates from clinical microbiology.

2. Material and methods

Two samples of Manuka honey were used as material in this research: Manuka honey UMF 15+ (Somvita Ltd. Te Puke. New Zealand) and Manuka honey 5+ (GO healthy New Zealand) originating from New Zealand.

2.1. Test microorganisms

Bacterial cultures used in this research are: group D streptococci, β-hemolytic streptococci, *Pasteurella multocida*, *Streptococcus uberis* and *Truepqera pyogenes* from the collection of isolates of the Laboratory for clinical bacteriology (PI Veterinary Institute RS" Dr. Vaso Butozan" Banja Luka).

Cultures were seeded in nutrient broth and incubated at 37°C/18h. 100 µl of a bacterial suspension with a concentration of 10^5 CFU/ml was seeded on the surface of a Petri plate with a suitable substrate (Müeller - Hinton agar).

2.2. Test method

The antibacterial sensitivity of the tested clinical isolates to the effects of Manuka honey was determined using the disk diffusion method. Discs with a diameter of 9 mm were placed on a solid sterile substrate (Müeller-Hinton-agar). 50 µl of honey was dripped into the discs with a micropipette: undiluted honey and diluted samples in the proportion of honey:water 50:50% and 75:25% (v/v). Honey samples were diluted with sterile deionized water. As a control, 50 µl of sterile deionized water which was used to dilute the honey samples, was dripped onto the discs.

After that the plates were left in the refrigerator for 30 minutes to allow the sample to diffuse into the substrate and then incubated for 24 hours at 37°C.

Three repetitions were made for each sample and after incubation for 18-24 hours and the results were read by measuring the diameter of the zone of inhibition and the mean value was calculated for each sample.

2.3. Type of action

In order to see if the honey had a bactericidal or bacteriostatic effect a small piece of agar was taken from the zone of inhibition and added to the nutrient broth. Incubation was done at 37ºC for 24 hours. If the broth becomes cloudy after incubation, it is considered that the effect of honey is bacteriostatic or if the broth remains clear, the effect of honey is bactericidal.

3. Results

The antibacterial activity of Manuka honey with two different UMFs values (UMF 5+ and UMF 15 +) was tested against five bacterial strains (group D streptococcus, β-hemolytic streptococcus, *Pasteurella multocida*, *Streptococcus uberis* and *Truepqera pyogenes*) from the collection of isolates of the Laboratory of clinical bacteriology (PI Veterinary Institute of RS " Dr. Vaso Butozan" Banja Luka).

The results are shown in graphs 1 and 2 (Graph 1 and Graph 2).

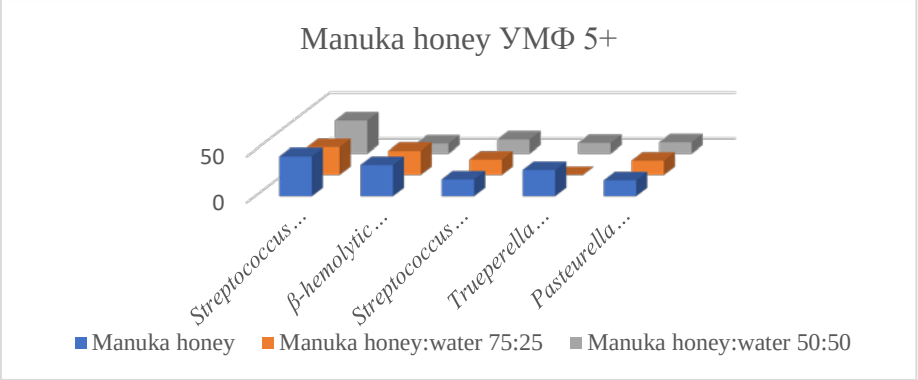

Graph 1. Antibacterial activity of Manuka honey UMF 5+

Manuka honey UMF 5+ had an inhibitory effect on all tested strains in all combinations with a range of action from 10.67 mm (Streptococcus group D) to 43.33 mm (*Trueperella pyogenes*), except for *Trueperella pyogenes* in the combination honey:water 75:25 (0.00 mm). Undiluted Manuka honey UMF 5+ had an inhibitory effect on all tested strains with a range of effect from 17.33 mm to 43.33 mm.

Diluted Manuka honey in a ratio of honey:water 75:25 had no inhibitory effect on *Trueperella pyogenes*, while it had an inhibitory effect on the other tested pathogens in the range from 15.67 mm to 30.00 mm.

Diluted honey in the ratio of honey:water 50:50 acted on all tested strains with a lower intensity of inhibition, and the range of inhibition ranged from 10.67 mm to 35.67 mm.

Graph 2 shows the antibacterial activity of Manuka honey UMF15+ and we can see that in all combinations the honey had an inhibitory effect and the range of action was from 12.33 mm to 42.00 mm. Undiluted Manuka honey had an inhibitory effect on all tested strains with a range from 18.00 mm to 42.00 mm. Diluted manuka honey in the ratio honey:water 50:50% (v/v) was effective in the range from 12.66 mm to 16.67 mm, while in the ratio honey:water 75:25% (v/v) the range of inhibition was from 12.33 mm to 19.00 mm. Unlike Manuka honey UMF 5+, Manuka honey UMF 15+ was inhibitory in all combinations on *Trueperella pyogenes* with a range of 15.67 mm to 19.67 mm. If we compare the effectiveness of honey diluted with water in the proportion of 50:50% (v/v) and 75:25% (v/v), we observe that the higher efficiency in inhibiting the growth of the tested bacterial strains is in the combination of honey:water 75:25% (v/v), but still weaker compared to undiluted honey.

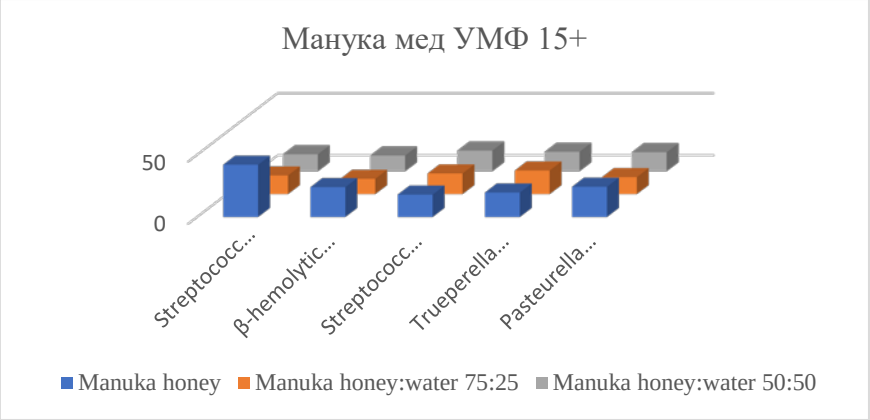

Graph 2. Antibacterial activity of Manuka honey UMF 15+

Honey has the ability to act bactericidally or bacteriostatically, that is to prevent the growth and reproduction of certain bacteria or to destroy them which has been confirmed by numerous studies (22,23).

The results of testing the effects of undiluted and diluted Manuka honey with different UMF are shown in graphs (Graph 1).

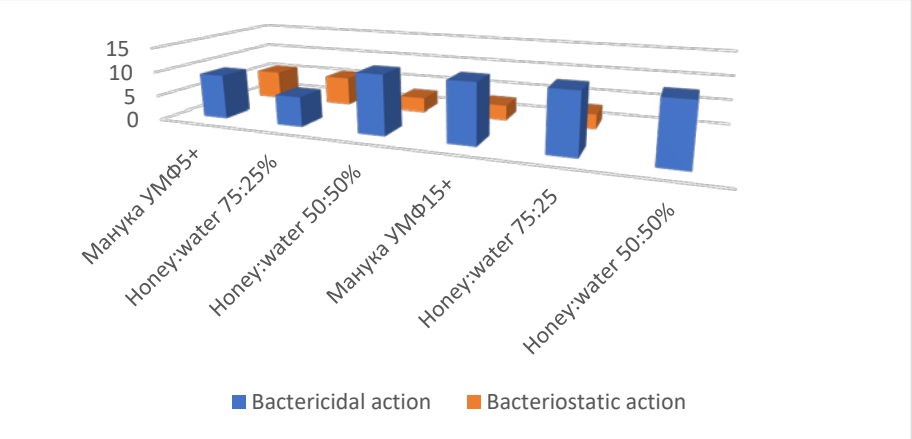

Graph 3. Bactericidal and bacteriostatic activity of honey Manuka UMF 5+ and UMF15+

As can be seen from the displayed graph Manuka honey UMF15+ is partially more bactericidal in all combinations in contrast to Manuka honey UMF 5+, which was slightly less bactericidal in relation to the combination and type of pathogen.

Due to the influence of various factors on the antibacterial activity of honey it is not possible to accurately predict how much antibacterial activity a certain honey will possess. The antibacterial activity of honey can vary significantly among different bacterial species even among related bacteria, as in this case (24).

Some types of honey have the same antibacterial effect as sugar, while others can be diluted a hundredfold and still inhibit the growth of bacteria. The effectiveness of Manuka honey is not

the same due to different resistance mechanisms. Gram-negative bacteria are more resistant than Gram-positive bacteria (25). The explanation may be in the fact that Gram-negative bacteria have a three-layer cell envelope which consists of a thin peptidoglycan layer located between the outer membrane and the inner bi-lipid membrane. An asymmetric outer membrane with a lipopolysaccharide-rich layer facing outwards offers additional protection against lysosomes and other agents.

The difference in antimicrobial potency can be a hundredfold. The mechanism of antibacterial activity of Manuka honey can be divided into two groups of mechanisms by which antibacterial activity is achieved. The mechanism of antimicrobial activity is based on physico-chemical properties (osmolarity - high concentration of carbohydrates eliminates microorganisms; rN value - is 3.57 to 4.21 and is low enough for inhibitory activity on a large number of bacteria (26,27); Defensin-1- a peptide secreted by honey bees by hypopharyngeal glands and showing activity against Gram-positive bacteria (it is also found in royal jelly and is assumed to be important for larval health) (25). The universal elements of honey are a high proportion of carbohydrates and a low rN value, while a large difference in the amount of defensin-1 peptides was observed in different types of honey.; hydrogen peroxide (peroxide activity) is produced in honey as a by-product by the bee enzyme glucose oxidase; oxidoreductase that catalyzes the oxidation of glucose to gluconic acid. Glucose oxidase protects honey during ripening from pathogenic microorganisms and is present in mature honey, but is inactive because honey is sufficiently protected by high osmotic pressure and low rN. By diluting honey, it is reactivated and the resulting H_2O_2 has significant antibacterial activity, but the enzyme catalase present in body fluids dilutes and inactivates it and glucose oxidase is rapidly degraded under the influence of heat and light. Methylglyoxam, MGO (non-peroxide activity-NPA)-1,2-dicarbonyl compound present in high concentration is a key element of Manuka honey that is not broken down by catalase from body fluids and serum. The non-peroxide activity depends on the type of manuka plant from which the honey was made and on the proportion of manuka nectar in the honey. Other phytochemicals, especially phenols, are important for the antibacterial effect of Manuka honey (28). The obtained results are difficult to compare with the results of other researchers because there is no officially standardized method for determining the antibacterial activity of honey. The disk diffusion method is most often used to assess the antibacterial activity of honey. A limiting factor is that different types of bacteria are differently sensitive to different types of honey. The activity of honey using the agar-diffusion method is estimated according to the size of the zone of growth inhibition which depends on the antibacterial activity, but also of the speed of diffusion of antibacterial

components through the agar. A limiting factor in migration through agar may be compounds of relatively high molecular mass so that the antibacterial activity of honey can be mistakenly estimated as low. Since the antibacterial activity of honey is influenced by other factors (temperature and incubation time, thickness and type of substrate, rN of the substrate, age of the tested material, etc.) it is necessary to perform the procedure in accordance with the principles that standardize the methodology. Different national standards are used in European countries so that the interpretation of the test results depends on both the performance of the standardized method and the applied standards and protocols (29).

Undiluted Manuka honey was effective for all tested isolates, but with different intensity of inhibition depending on the type of isolate. The results of the research are in agreement with the research of other actors (20, 30).

4. Conclusion

Manuka honey UMF 5+ had an inhibitory effect on all tested strains in all combinations with a range of action from 10.67 (Streptococcus β hemolyticus) to 43.33 mm (Streptococcus D group), except for the bacterium *Trueperella pyogenes* in the combination honey: water 75% (v/v) (0.00 mm);

Manuka honey UMF15+ in all combinations had an inhibitory effect on the tested bacteria with a range of action from 12.33 mm (Streptococcus β hemolyticus) to 42.00 mm (Streptococcus D group).

In almost all combinations, both Manuka honeys were more bactericidal

A lack of understanding of how honey destroy bacteria and promotes healing limits its acceptance by conventional medicine, but Manuka honey is available as a therapeutic agent and functional food and most consumers accept it as a mysterious, hedonistic product.

6. References

1. Saeed S, Farkhondeh T, Fariborz S. (2018): Honey and health: A review of recent clinical research. Pharmacogn Res. ;9:121–127.
2. Blair S., Cokcetin N., Harry E., Carter D. (2009): The unusual antibacterial activity of medical-grade *Leptospermum* honey: antibacterial spectrum, resistance and transcriptome analysis. *Eur. J. Clin. Microbiol. Infect. Dis.* 28 1199–1208. 10.1007/s10096-009-0763-z

3. Cooper R., Jenkins L., Henriques A., Duggan R., Burton N. (2010): Absence of bacterial resistance to medical-grade manuka honey. *Eur. J. Clin. Microbiol. Infect. Dis.* 29 1237–1241. 10.1007/s10096-010-0992-1
4. Alvarez-Suarez J, Gasparrini M, Forbes-Hernández T, L. Mazzoni, F. Giampieri (2014): The composition and biological activity of honey: a focus on Manuka honey. Foods.:420–432.
5. Atrott J. (2013): Methylglyoxal in Manuka-Honig (Leptospermum scoparium): Bildung, Wirkung, Konsequenzen. Dissertation. Dresden
6. Otto M. (2009): *Staphylococcus epidermidis*—the 'accidental' pathogen. Nat Rev Microbiol. 7:555–567.
7. Kato Y , Rie Fujinaka, Akari Ishisaka, Yoko Nitta, Noritoshi Kitamoto, Yosuke Takimoto (2014): Plausible authentication of Manuka honey and related products by measuring leptosperin with methyl syringate. J Agr Food Chem. 62:6400–6407.
8. Adams CJ, Manley-Harris M, Molan PC.(2009): The origin of methylglyoxal in New Zealand Manuka (*Leptospermum scoparium*) honey. Carbohyd Res. 344:1050–1053.
9. Sojka M., Valachova I., Bucekova M., Majtan J. (2016): Antibiofilm efficacy of honey and bee-derived defensin-1 on multi-species wound biofilm. *J. Med. Microbiol.* 10.1099/jmm.0.000227 [Epub ahead of print].
10. Lee DS, Sinno S, Khachemoune A (2011): Honey and wound healing: an overview. American journal of clinical dermatology 12: 181–190.
11. Johnston Matthew, Michael McBride, Divakar Dahiya, Richard Owusu-Apenten, and Poonam Singh Nigam (2018) Antibacterial activity of Manuka honey and its components: An overviewAIMS Microbiol. 2018; 4(4): 655–664. Published online 2018 Nov 27. doi: 10.3934/microbiol.2018.4.655
12. Portokalakis I, Yusof H, Ghanotakis D, R. Owusu-Apenten (2016): Manuka honey-induced cytotoxicity against MCF7 breast cancer cells is correlated to total phenol content and antioxidant power. J Adv Biol Biotechnol. 8(2):1–10. [Google Scholar]
13. Henderson K, Aldhirgham T, Nigam P, R. Owusu-Apenten (2016): Evaluation of Manuka honey estrogen activity using the MCF-7 cell proliferation assay. J Adv Biol Biotechnol. 10 (3):1–11.
14. Shahzad A., Cohrs R. J. (2012): *In vitro* antiviral activity of honey against varicella zoster virus (VZV): a translational medicine study for potential remedy for shingles. *Transl. Biomed.* 3:2

15. Kwok T, Kirkpatrick G, Yusof H, P. Nigam R. Owusu-Apenten (2016): Rapid colorimetric determination of methylglyoxal equivalents for Manuka honey. J Adv Biol Biotechnol. 7(1):1–6

16. Saeed S, Farkhondeh T, Fariborz S. (2018): Honey and health: A review of recent clinical research. Pharmacogn Res. ;9:121–127.

17. Almasaudi SB, Al-Nahari AAM, EI Sayd M, Elie Barbour , Al Muhayawi SM, Al-Jaouni S, Azhar E., Qari M, Qari A, Harakeh S (2017): Antimicrobial effect of different types of honey on *Staphylococcus aureus*. Saudi J Biol Sci. 24:1255–1261

18. Al-Waili N, Ghamdi AA, Ansari MJ, Al-Attal, Al-Mubarak A, Salom K.(2013): Differences in composition of honey samples and their impact on the antimicrobial activities against drug multi-resistant bacteria and pathogenic fungi. Arch Med Res. 44:307–316

19. Lu J , Dee A. Carter, Lynne Turnbull, Douglas Rosendale, Duncan Hedderley, Jonathan Stephens, Swapna Gannabathula, Gregor Steinhorn, Ralf C. Schlothauer, Cynthia B. Whitchurch, Elizabeth J. Harry (2013): The effect of New Zealand Kanuka, Manuka and clover honeys on bacterial growth dynamics and cellular morphology varies according to the species. PLoS One. 8:e55898

20. Lu, J Turnbull L, Burke C M, Liu M, Carter DA., Schlothaue RC.r, Whitchurch C B. , Harry EJ (2014): Manuka-type honeys can eradicate biofilms produced by *Staphylococcus aureus* strains with different biofilm-forming abilities. Peer J. 2014;2:e326.

21. Paramasivan S, Drilling A, Jardeleza C, (2014): Methylglyoxal-augmented Manuka honey as a topical anti-*Staphylococcus aureus* biofilm agent: safety and efficacy in an *in vivo* model. Int Forum Allergy Rh. 2014;4:187–195.

22. Kalaba Vesna, Bojan Golić, Tanja Ilić (2020) Antibacterial activity of different types of honey on pathogenic bacteria IX International Symposium on Agricultural Sciences AgroReS 2020 – Proceedings, pp149-162

23. Halawani E i Shohayeb M. (2011): Survey of the antibacterial activity of Saudi and some international honeys. Journal of Microbiology and Antimicrobials, 3:94-101,.

24. Sherlock O, Dolan A, Athman R, Power A, Gethin G,Cowman S, (2010): Comparison of the antimicrobial activity of Ulmo honey from Chile and Manuka honey against methicillin-resistant Staphylococcus aureus, Escherichia coli and Pseudomonas aeruginosa. BMC Complement Altern Med 2010;10:47.

25. Mittal L, Kakkar P, Verma A, Dixit KK,Mehrotra M.(2012): Anti microbial activity of honey against various endodontic microorganisms-an in vitro study. J Int Dent Med Res 2012;1;9-13.

26. Bang LM, Buntting C, Molan P. (2003): The effect ofdilution on the rate of hydrogen peroxide production in honey and its implications for wound healing. J Altern Complement Med 2003;9:267–73

27. Taormina PJ, Niemira BA, Beuchat LR.(2001): Inhibitory activity of honey against foodborne pathogens as influenced by thepresence of hydrogen peroxide and level of antioxidant power. Int J Food Microbiol;69:217-25.

28. Szweda P.(2017): Antimicrobial activity of honey. Honey analysis. Dostupno na: http://www.intechopen.com/books/honey-analysis. 12. rujan 2017.

29. Jorgensen JH, Turnidge JD. (2008): Susceptibility test methods: dilution and disc diffusion methods. In: Murray PR, Baron E J, Jorgensen JH, Pfaller MA, Yolken RH (eds). Manual of Clinical Microbiology, 8th Edition. Washington DC: ASM Press, 2003;1119-25.

30. White R (2016): Manuka honey in wound management: greater than the sum of its parts? J Wound Care. 2016 Sep;25(9):539-43. doi: 10.12968/jowc.2016.25.9.539.

Materials Design and Applications

The surface characterization of the anodized ultrafine-grained Ti-13Nb-13Zr alloy

Dragana R. Barjaktarević[1], Marko P. Rakin[1], Bojan I. Međo[1], Zoran M. Radosavljević[2], Veljko R. Đokić[3]

[1] University of Belgrade, Faculty of Technology and Metallurgy, Karnegijeva 4, 11120 Belgrade, Serbia, dbarjaktarevic@tmf.bg.ac.rs, bmedjo@tmf.bg.ac.rs, marko@tmf.bg.ac.rs

[2]Lola Institute, Kneza Višeslava 70a, 11030 Belgrade, Serbia, z.radosavljevic@mont-r.rs

[3]Innovation Centre of the Faculty of Technology and Metallurgy, Karnegijeva 4, 11120 Belgrade, Serbia, vdjokic@tmf.bg.ac.rs

Abstract

Titanium alloys are metal materials widely used in medicine owing to their suitable characteristics such as low density, good corrosion resistance and biocompatibillity. High biocompatibility of the titanium alloy results from the creation of a spontaneous oxide layer with good adhesion and homogeneous morphology. In order to improve characteristics of the metallic materials for application in medicine, electrochemical methods that enable surface nanostructured modification are extensively used, and one of these methods is electrochemical anodization which makes it possible to obtain a nanostructured oxide layer composed of nanotubes on the surface of the metal material. The tested material was ultrafine-grained Ti-13Nb-13Zr (UFG TNZ) alloy obtained by the severe plastic deformation (SPD) processing using the high pressure torsion (HPT) process. Nanostructured oxide layer on the titanium alloy was formed by electrochemical anodization during the time period from 30 to 120 minutes. Characterization of the surface morphology obtained during different times of electrochemical anodization was done using scanning electron microscopy (SEM), while the topography and surface roughness of the titanium alloy before and after electrochemical anodization was determined using atomic force microscopy (AFM). Scratch test was used to determine the cross profile of the surface topography. Electrochemical anodization led to the formation of a nanostructured oxide layer on the surface of the titanium alloy. The obtained results indicated strong influence of the electrochemical anodization time on the oxide layer morphology - with its increase the diameter of the nanotubes increases too, while the wall thickness of nanotubes decreases. Also, electrochemical anodization led to an increase in the surface roughness.

Keywords: Titanium alloy for biomedical application, High pressure torsion process, Electrochemical anodization, Surface morphology, Surface roughness

1. Introduction

The main goal of developing materials for use in medicine is to achieve the desired material properties, primarily mechanical and physical, for which thermomechanical processing procedures and the addition of alloying elements are used. Contemporary research in the field of metallic biomaterials is focused on the possibility of converting conventional macroparticle biomaterials into submicron and nanoparticle biomaterials while achieving adequate mechanical, physical, biological and corrosion properties. Numerous researches are focused on the process of forming ultrafine-grained and nanocrystalline structures (grain size less than 100 nm), because it has been shown that such structures are characterized by higher tensile strength, better biocompatibility and corrosion stability, as well as better wear resistance [1,2]. Severe plastic deformation (SPD) uses different methods for refining material structure by reducing the grain size and for conversion of a coarse-grained structure into an ultrafine-grained structure or a nanostructure [3-5]. Several different SPD procedures are available, but one of the most effective one is the high-pressure torsion (HPT) processing, that enables small grains and high strength to be obtained, as it is shown in [6]. HPT apparatus consists of two anvils, Fig 1. A thin disc is pressed between two anvils, under high pressure, and the rotation of the one of the anvils causes large shear deformations of the material.

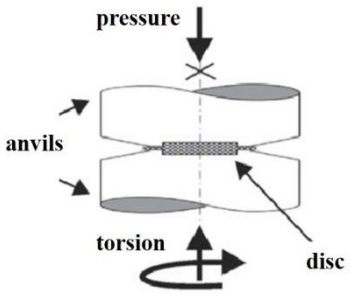

Figure 1. HPT apparatus [7]

The behavior of biomaterials in the human body depends on its biocompatibility and surface properties. For this reason, biomaterials often require surface modification in order to optimize the properties of the implants and increase their bioactivity when connecting with the natural surrounding tissue. There are various procedures that can be used to modify the surface of metal biomaterials (including bringing the material to an ultrafine-grained structure) and which lead to an improvement in their properties compared to conventionally made implants. The primary need for surface nanostructural modifications in titanium-based

materials, apart from better and faster connection with bone tissue, is also due to the improvement of the degree of osseointegration, biocompatibility, as well as resistance to corrosion and wear. Chemical methods for surface modification of materials are used in order to improve biocompatibility, corrosion resistance, wear resistance and contamination removal [8]. Some of the most commonly used chemical methods are chemical treatments, electrochemical treatments, i.e. electrochemical anodization (anodic oxidation), sol-gel process and chemical vapor deposition [9-11]. In this work, electrochemical anodization was used to modify the surface of the titanium alloy. The basic characteristics of the modified surface of the titanium alloy obtained by electrochemical anodization are shown in table 1. As a result of electrochemical anodization, a nanostructured oxide layer composed of nanotubes is obtained. The morphology and structure of the obtained nanostructured oxide layer depends on the characteristics of the substrate, the composition of the electrolyte and the parameters of the electrochemical anodization procedure [12,13].

Table 1. Main characteristics of the modified surface of the titanium alloy obtained by electrochemical anodization

Electrochemical andization (Anodic oxidation)	Formation of a nanostructured oxide layer composed of TiO_2-based nanotubes with a thickness of 10 nm to 40 μm	Formation of a specific topography of the surface, improvement of corrosion resistance, biocompatibility, bioactivity, reduction of the value of the surface modulus

The most significant advantage of the electrochemical anodization procedure is the creation of a homogeneous nanotubular oxide layer. The shape of the nanotubular oxide layer (diameter, length, and thickness of the nanotubes) can be controlled using electrochemical anodization parameters [14-16]. TiO_2 nanotubes of different diameters (from 15 nm to 300 nm) and different lengths can be formed during the process of electrochemical anodization of titanium or titanium alloys.

It has been shown that the nanostructured surface of titanium alloy can be formed by applying electrochemical anodization, but the question remains open as to the morphology of ultrafine-grained titanium alloys obtained by high pressure torsion (HPT) process.

2. Materials and methods

The tested material was ultrafine-grained Ti-13Nb-13Zr (UFG TNZ) alloy obtained by the SPD processing using the HPT process. The HPT process was done by rotating one of the anvils with speed of 0.2 rpm at a pressure of 4.1 GPa. Nanostructured oxide layer on the UFG TNZ alloy was formed by electrochemical anodization during 60 and 90 minutes. Electrochemical anodization was performed using a system of two electrodes: platinum and a sample of the UFG TNZ alloy as working electrode. It was conducted at a voltage of 25V, while 1M H_3PO_4 + 0.5 wt. % NaF was chosen as the electrolyte. The PEQLAB EV 231 device was used to supply power during the electrochemical anodization process.

The scanning electron microscopy (SEM) was used to characterize the nanostructured oxide layer morphology. The TESCAN MIRA3 XMU microscope at a voltage of 20 keV was used for SEM analysis. The topography and surface roughness of the titanium alloy before and after electrochemical anodization was determined by atomic force microscopy (AFM) with NanoScope 3D (Veeco, USA) microscope operated in tapping mode in ambient conditions.

The scratch test was performed on nanoindenter G200, Agilent Technologies, using as an indenter Berkovich-type diamond tip. Scratch length was 500 μm and applying an increasing load up to 40 mN, Fig. 2. In this study, scratch test was used to determine the cross profile of the surface topography.

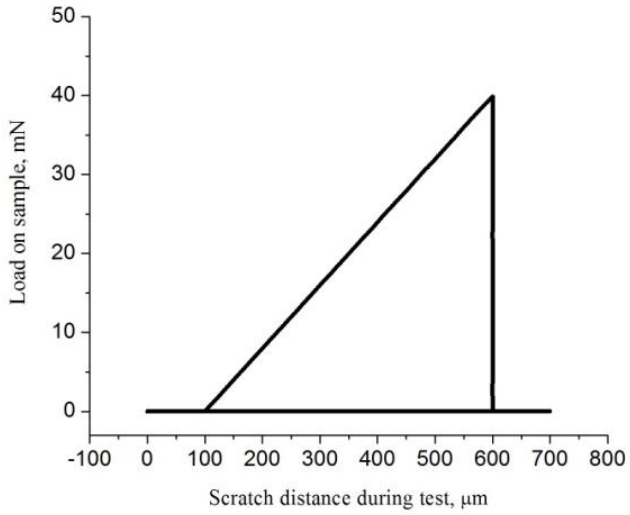

Figure 2. Applied load during scratch test

3. Results and Discussion

Fig. 3. presents morphology of the surface of the UFGG TNZ alloy after electrochemical anodization for 60 and 90 minutes. After 60 minutes of electrochemical anodization, a nanoporous oxide film was formed on the surface of the UFG TNZ alloy, Fig 3 (a). The nanotubular oxide layer was formed after a procedure lasting 90 minutes, Fig 3 (b). During the shorter process of electrochemical anodization, nanotubes were formed and connected to each other, while during the longer process, nanotubes were formed and separated from each other due to dissolution.

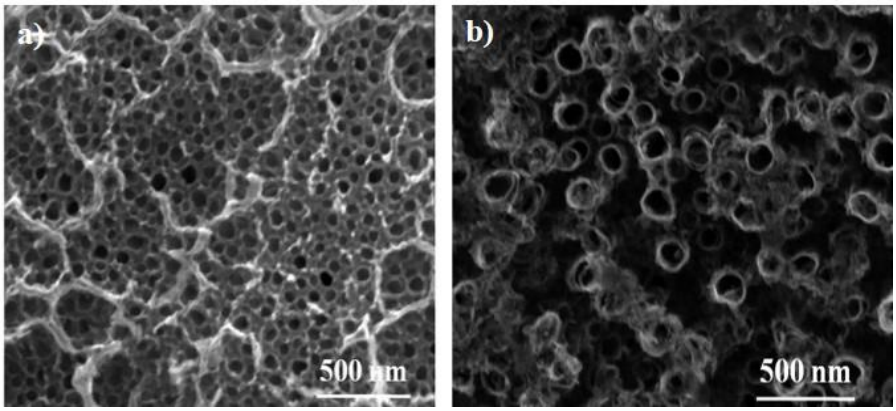

Figure 3. Morphology of the surface of the UFG TNZ alloy after electrochemical anodization for (a) 60 and (b) 90 minutes

The mean value of the nanotube diameter (obtained after 30 measurements) after 60 minutes of electrochemical anodization was 56.22 nm, while after 90 minutes of electrochemical anodization it increased to 90.17 nm. On the other hand, the mean value of the nanotube wall thickness (obtained after 30 measurements) decreased from 22.20 nm to 19.54 nm with increasing anodization time. The existence of the influence of the anodizing time on the dimensions of the nanotubes has been shown, so that with increasing time, the diameter increases too while the thickness of the nanotubes decreases. Also, increasing anodizing time led to the formation of the more homogeneous oxide layer on the surface, Fig 3 (b).

As we presented in our previous paper [17] the SEM side-view image of the oxide layer created on the UFG TNZ during 60 minutes showed that nanotubes were parallel on the surface with an average thickness of 1.63 nm, while it was theoretically known that increasing the anodizing time leads to an increase in the length of the nanotubes [18]. Further, HPT process, as the method for obtaining ultrafine-grained microstructure, leads to the formation of smooth walls.

AFM was used to characterize the surface topography of the UFG TNZ alloy before and after electrochemical anodization, and results of the analysis are presented in Fig 4.

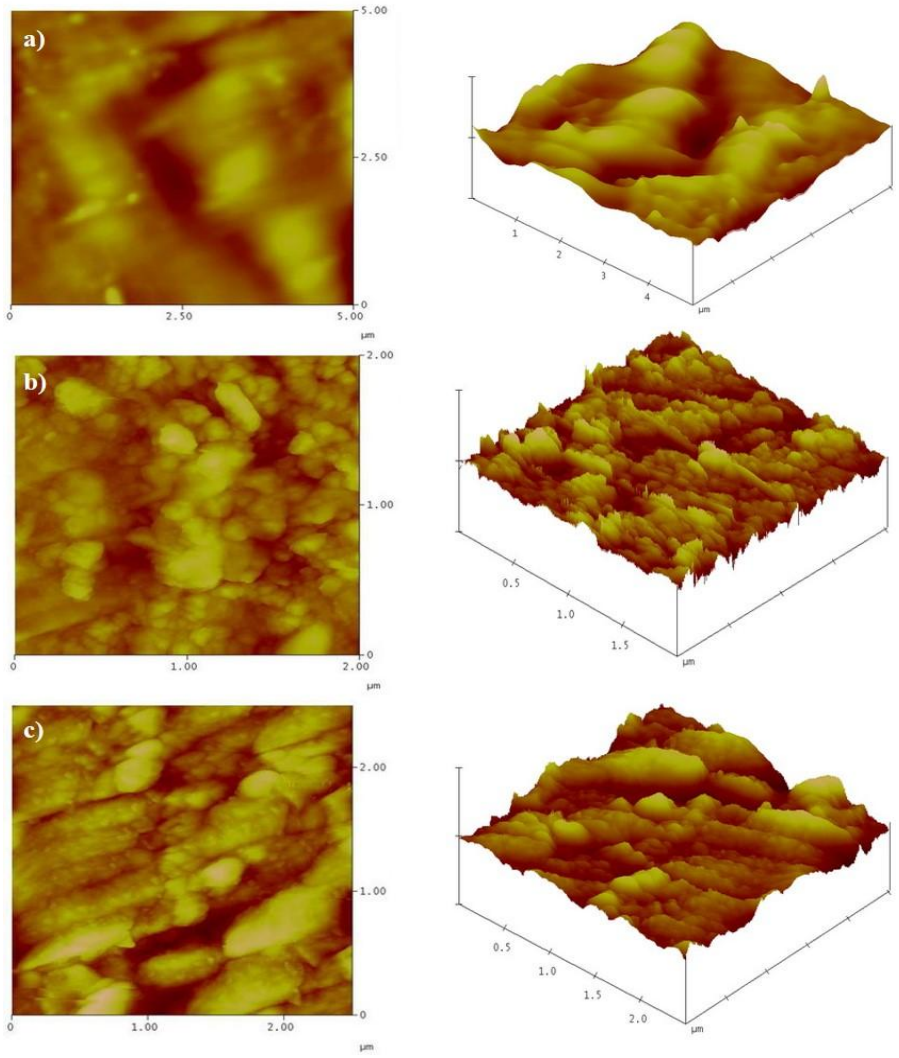

Figure 4. 2D and 3D AFM images of the UFG TNZ alloy (a) before anodization (5x5x0.1) and after anodization for (b) 60 (2.5x2.5x0.4) and (c) 90 (2.5x2.5x0.4) minutes

Table 2. presents values of the surface roughness (RMS-root mean square average of height deviations (expressed in nm)) of the UFG TNZ alloy before and after electrochemical anodization for 60 and 90 minutes.

The obtained results showed that the process of electrochemical anodization resulted in the creation of a rough topography of the surface of the UFG TNZ alloy. The UFG TNZ alloy

anodized for 60 and 90 minutes is characterized by a typical rough surface topography compared to the base alloy surface which has a wavy topography, Fig 4.

The anodized ultrafine grained alloy has an order of magnitude higher roughness value in comparison to the alloy before anodization, Table 2. The results show that increasing the time of electrochemical anodization also increases the roughness of the alloy as a result of increasing the size and number of pores [19].

Table 2. Surface roughness values before and after electrochemical anodization

Materials	Anodizing time, min	RMS, nm
UFG TNZ	/	3.61
	60	33.39
	90	34.15

Fig. 5. presents the cross profile of the surface topography of UFG TNZ alloy after electrochemical anodization for 60 and 90 minutes obtained after scratch test. The surface roughness of UFG TNZ after electrochemical anodization for 90 minutes is higher than for 60 minutes, as shown in Fig. 5, and the texture parameter is 61 μm in diameter for alloy after anodization for 90 minutes and 52.9 μm for alloy after anodization for 60 minutes.

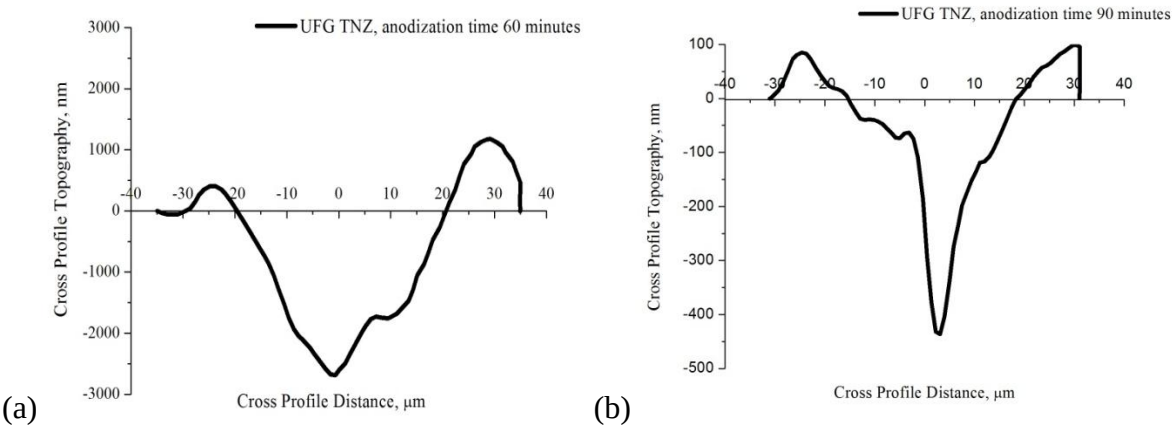

(a) (b)

Figure 5. The cross profile of the surface topography of UFG TNZ alloy after electrochemical anodization for (a) 60 and (b) 90 minutes, obtained after scratch test

4. Conclusion

It can be concluded that electrochemical anodization is a suitable method for the formation of nanostructured surface on the titanium alloy. The roughness of the nanostructured surface is greater compared to the bare surface of UFG TNZ alloy. It indicates that the UFG TNZ alloy with nanostructured surface would be more suitable for medical application, because of better contact of the modified surface with surrounding tissue and their adhesion. Also, it can be said that the anodizing time of 90 minutes is more suitable for using compared to 60 minutes, because this anodizing time leads to the formation of a homogeneous nanotubular oxide layer with larger roughness.

Increasing of anodizing time leads to the increase of the surface roughness and therefore to the increase of cell adhesion in the human body. In our previous paper [17] we showed that increasing anodizing time led to the improvement of corrosion resistance in the artificial saliva, simulating the oral environment. From everything analyzed so far, we concluded that the deterioration of the surface properties occurred during the formation of a nanostructured oxide layer at a shorter anodizing time. The previous paper also analyzed morphology of the nanostructured oxide layer and dimension of the nanotubes obtained for the anodizing time of 120 minutes, but the surface characterization after this anodizing parameter will be considered in the future.

Acknowledgements

This work was supported by the Ministry of Education, Science and Technological Development of the Republic of Serbia (Contracts No. 451-03-68/2022-14/200135). The authors gratefully acknowledge Dr. Sanja Stevanović from the Institute of Chemistry, Technology and Metallurgy, University of Belgrade, Serbia, for performing the AFM measurements and Dr Anton Hohenwarter from the Erich Schmid Institute of Material Science, Leoben, Austria, for the preparation of the UFG TNZ alloy.

References

1. Y. Estrin, A. Vinogradov, Extreme grain refinement by severe plastic deformation: A wealth of challenging science, Acta Mater, 61(2013) 780-786.

2. I. Dimić, I. Cvijović-Alagić, B. Volker, A. Hohenwarter, R. Pippan, Đ. Veljović, M. Rakin, B. Bugarski, Microstructure and metallic ion release of pure titanium and Ti-13Nb-13Zr alloy processed by high pressure torsion, Mater Des, 5 (2016) 340-347.
3. I. Turkyilmaz, Implant Dentistry - A Rapidly Evolving Practice, In Tech (2011) 57-82.
4. H. Yilmazer, M. Niinomi, M. Nakai, K. Cho, J. Hieda, Y. Todaka, T. Miyazaki, Mechanical properties of a medical β-type titanium alloy with specific microstructural evolution through high-pressure torsion, Mater Sci Eng C, 33 (2013) 2499-2507.
5. J. Wongsa-Ngam, M. Kawasaki, T. Langdon, A comparison of microstructures and mechanical properties in a Cu–Zr alloy processed using different SPD technique, J Mater Sci, 48 (2013) 4653-4660.
6. G. Crawford, N. Chawla, K. Da, S. Bose, A. Bandyopadhya, Microstructure and deformation behavior of biocompatible TiO_2 nanotubes on titanium substrate, Acta Biomater, 3 (2007) 359-367.
7. A. Hohenwarter, R. Pippan, Fracture and fracture toughness of nanopolycrystalline metals produced by severe plastic deformation, Philo Trans A, Published by Royal Society, 2014.
8. M. Kulkarni, A. Mazare, P. Schmuki, A. Iglič, Biomaterial surface modification of titanium and titanium alloys for medical applications, Nanomedicine, Publisher: One Central Press, 2014.
9. T. Kasuga, M. Hiramatsu, A. Hoson, T. Sekino, K. Niihara, Formation of titanium oxide nanotube, Lang, 14 (1998) 3160-3163.
10. C. Tsai, N. Nian, H. Teng, Mesoporous nanotube aggregates obtained from hydrothermally treating TiO_2 with NaOH, Appl Surf Sci, 253(2006) 1898-1902.
11. D. Barjaktarević, I. Cvijović-Alagić, I. Dimić, V. Đokić, M. Rakin, Anodization of Ti-based materials for biomedical applications: A review, Metall Mater Eng, 22 (2016) 129-143.
12. M. Hu, P. Lai, M. Bhuiyan, C. Tsouris, B. Gu, M. Paranthaman, J. Gabitto, L. Harrison, Synthesis and characterization of anodized titanium-oxide nanotube arrays, J Mater Sci, 44 (2009) 2820-2827.
13. H. Park, H. Kim, W. Choi, Characterizations of highly ordered TiO_2 nanotube arrays Obtained by anodic oxidation, Trans Electro Electron Mater, 11 (2010) 112-115.

14. K. Kim, N. Ramaswamy, Electrochemical surface modification of titanium in dentistry, Dent Mater J, 28 (2009) 20-36.
15. J. Hernández-López, A. Conde, J. Damborenea, M. Arenas, Electrochemical response of TiO_2 anodic layers fabricated on Ti-6Al-4V alloy with nanoporous, dual and nanotubular morphology, Corr Sci, 112 (2016) 194-203.
16. A. Tan, B. Pingguan-Murphy, R. Ahmad, S. Akbar, Review of titanium nanotubes: Fabrication and cellular response, Ceramics Inter, 38 (2012) 4421-4435.
17. D. Barjaktarevića, V. Djokića, J. Bajata, I. Dimića, I. Cvijović-Alagićb, M. Rakina, The influence of the surface nanostructured modification on the corrosion, resistance of the ultrafine-grained Ti–13Nb–13Zr alloy in artificial saliva, Theor and Appl Fract Mech 103 (2019) 102307.
18. A. Ghicov, H. Tsuchiya, J. Macak, P. Schmuki, Titanium oxide nanotubes prepared in phosphate electrolytes, Electrochem Commun, 7 (2005) 505-509.
19. M. Manjaiah, R. Laubscher, Effect of anodizing on surface integrity of grade 4 titanium for biomedical applications, Surf Coat Technol, 310 (2017) 263-272.

PRINCIPALS OF DIGITAL RESTORATION AND ITS APPLICATION IN CULTURAL HERITAGE

***Jovan Djordjevic*[1]**

Affiliation

[1]*Università Ca' Foscari, Dorsoduro, 3246, 30123 Venezia VE, Italy,*

jovandjordjevic44@gmail.com

Abstract

Even though material science and engineering constitute the core aspects of practical restoration, there are other ways to help preserve cultural heritage. One such approach is digitalization together with digital restoration and reconstruction. Although the main postulates of their application in conservation have been elaborated many times, insufficient attention has been given to their connection with practice. Hence, this paper aims to briefly present the main aspects of digital restoration/reconstruction, upon which, their application in practice will be presented. The basic idea is to show in which ways digital restoration and reconstruction can affect the material object following restoration principles. Four main application niches can be distinguished: documentation, predicatory tool, monitoring, and presentation. The last one can be further divided depending on the targeted audience. Therefore, the goal of the paper is to try and summarize the relationship between digital restoration and practice, as well as present the possible use of digital tools in modern-day conservation.

The so-called "experimental" part, i.e. the case studies will be borrowed from papers that deal with practical solutions, as well as from personal practice related to conservation issues in the basilica of Santa Maria Assunta on the island of Torcello near Venice. The church has three main conservation issues that can be partially (or completely) solved using digital tools. These are double-layered wall decoration in the main apse, dismantling of the crypt's *pergola*, and inaccessible murals in the diaconicon chapel. Since dealing with all three goes beyond the scope of this paper, I will focus on them solely as an illustration of the digital approach discussed in the first part of the paper.

Keywords: Digital Restoration, Digital Reconstruction, Cultural Heritage, Conservation, Restoration Theory.

1. Introduction

Digitalization has found a wide range of applications in the domain of cultural heritage. On one side, it can be used for documentation, as well as monitoring deterioration, on the other side, it can help create virtual models and later present them to the audience. In addition, it can also enhance the visitors' experience in a museum or at an archaeological site, with education as its final goal. This paper, however, will focus on virtual models and the problematics of their presentation.

It will briefly present the basics of digital heritage, i.e. digital objects, as well as the differences between virtual restoration and reconstruction. The second part is conceived as exemplary support to the first one.

2. Theory of Digital Heritage

Conservation of cultural heritage aims at preserving the patrimony through the safeguarding of tangible and intangible objects. Hence, before venturing into the theory of digital heritage, we should examine the tangible non-virtual objects, i.e. artworks, and their documentary role. The ideas that art holds in itself are representative of the time in which that specific object is created. Art objects are often presented in a museum, or in the case of whole structures, in an archaeological site. These have "a double role: 1) to present [the artworks] to the audience, for they [the artworks] shape its view through the emotion-stimulating experience that is being offered, and 2) to be able to carefully examine these artworks…" (1) To summarize this, the two main roles are communication through presentation and analysis. The artwork is there to cause an emotional response, to be absorbed by the viewer, while the museum gives it institutionalized support and status. (1) It preserves the emotional experiences of the artworks, allows them to communicate with the audience, and, as a consequence, it helps create a narrative.

Therefore, the aim is to extract information from the object, which will, through the presentation in a museum, transmit knowledge to the visitor. If used in an adequate and justified way, the digital media can catalyze this process because they allow "the transition of the given problem…into other possible solutions." (1) When a digital version of an object is

made, it allows for innumerable changes to be done, in contrast with the one in the material reality, that, when once altered, permanently remains as such. Their purpose is to introduce the past to the present. "The past can never be re-created as it was and thus our fascination and dedication to come as close as we can to re-presenting it to contemporary audiences via digital heritage applications." (2) With this understanding, we enter the domain of digital heritage. "Digital heritage can be considered to comprise facts and information (architectural plans, 3D scans of heritage artifacts or sites, photos of locations, etc.), fiction, interpretations, or 'best guess' (re-creations of landscapes, people, building adornments, etc.) and fantasy (highly engaging for the audience) in varying forms and degrees with interpretive narratives of the past." (2) This, so-called "electrification of imagination," allows for the viewer to come in contact with that which is otherwise impossible to see and experience. (2)

The digital object "can be a reproduction of a physical artifact, or it can be natively digital. The digital object, if limited to the reproduction of a real object, becomes a replica, if it is obtained through criteria and methodologies that guarantee fidelity and accuracy both at the topological/metric level and at the surface properties level. In this sense, the digital replica becomes a transmitter of information and allows the preservation of the knowledge of the object, even if the real original is lost." (3) This definition given by E. Pietroni and D. Ferdani encompasses all the key aspects: reproduction or natively digital (model), based on information accumulated within the object as a document, transmission of information, creating knowledge, and creating a digital testimony/patrimony.

However, the point is not just to digitize something, but to create "a parallel testimony" between the material original and the virtual copy. As nice as this might sound, there is another theoretical problem with understanding the virtual. These equivalents, i.e. digital replicas, are paradoxically unequal to the starting material object and are self-referent images, or at least tend to become. The real danger of the virtualization of an object used in a museum context (bear in mind the educational aspect) is the annihilation of the referential aspect, leading to a simulacrum. As a consequence, the parallel testimony is lost. (4) The charm of digitalization, however seductive it may be, should be resisted. The idea that digital copies and models are connected to museological purposes must always be kept in mind. What further increases this danger of creating a simulacrum, is the usual lack of the material object, or in other terms – the subject of the digital. By this, I am referring mostly to the archaeological remains that survive in often illegible fragments.

To restrict the excessive and unjustified additions, international charters had to be accepted. Just like the principles of practical restoration were laid out in Brandi's "Teoria del Restauro"[1] and the Venice Charter (1964), so too, do the digital/virtual restoration principles have their own. The two main documents are the London Charter (2006) and the Principles of Seville (2011). The London Charter emphasized the importance of documentation, not just the one used in creating a virtual model, but also in model production. "Sufficient information should be documented and disseminated to allow computer-based visualization methods and outcomes to be understood and evaluated in relation to the contexts and purposes for which they are deployed." (3) The stress is now on *paradata* that is defined as a document of the intellectual process, as opposed to *metadata* that "describes observational technicalities such as equipment settings, data ownership, hardware, and software." (5) The London Charter was followed by the Principles of Seville that "aim to build a clear and rigorous basis for presenting cultural heritage virtually." (6) The former one stresses the need to distinguish the "real, genuine, or authentic" from the additions and reconstructions. The latter addresses the same issue by pointing out the need to "gather and present transparently the entire work process." (3)

According to these internationally accepted postulates, the process consists of a survey, documentation, data processing, creation of the models, and source mapping/transparency. (3)

- **The survey** represents the gathering of information from objects using various "image-based and range-based technologies."
- **Documentation** is used for the so-called philological approach. It implies the usage of all available information, both bibliographical and visual for further study of the object.
- **Data processing** is the third phase in which the gathered information is analyzed, discussed, and then used to propose a suitable model that will be representative of the accumulated knowledge.
- **Model creation** occurs simultaneously with the previous phase since the final result should depict not just the visual aspect of the object, but also its use and purpose. Therefore, when making a model, the team must rely on all the data acquired and try to represent it. (4)

[1] For understanding the principles of practical restoration, I suggest reading: Бранди, Чезаре. *Теорија Рестаурације*, ур. и прев. Б. Шекарић, Италијанска кооперација, Београд, 2007.

- **Source mapping and transparency** are connected with the previous two points. The importance of this last step lies in the need to have a clear representation of what is original and which parts of the 3D or 2D model are invented. (3) As was stressed earlier, transparency is very important because usually, the final models are put online and, as such can be visited from any place in the world. On the other hand, "quantification and transparency ask for the order, conformity, systematic process, and repeatability, but these attributes are not often feasible or desirable within visual research practice." (5) Therefore, a compromise between the two needs to be achieved.

As for the relationship between virtual and practical restoration, they are quite compatible. In general, the former is not connected much with the latter except for the "recognition of intervention" and "minimal intervention" (that depends on the purpose of the model).2 It allows for all the possibilities that in material reality are otherwise impossible, because "all actions have no consequences for the original cultural object." (3) Hence, virtual restoration proves to be a quite potent tool for the presentation and communication of cultural heritage. "The virtual reconstruction in fact, through special presentation and simulation tools, improves cognitive processes by making it easy for anyone to understand the historical and archaeological data represented and transforming the raw data into information." (3) This is the precise goal of museology and the tool for larger accessibility to cultural heritage, resulting in its increased popularity and relevance in education through various digital models.

The logic of virtual restoration can be partially identified with the "stylistic restoration"[3] that is deemed unacceptable by today's standards. "This 'total retouch' is possible only in a virtual environment, since it only involves a digital edition of the artwork without damaging the original, especially when restoring the original in its integrity is impossible…This approach is also called 'virtual iconographic restoration', especially when applied to paintings." (3) It uses the analogy as a tool for filling in the missing parts. They are added

[2] *Recognition of intervention*: It concerns the legibility of the original parts. Integrations should be recognizable. The same applies to virtual restoration. This is emphasized both in the London Charter and the Principles of Seville and is formulated as the last part of the process of model creation – source mapping and transparency. Minimal intervention: It is necessary to repair or conserve original parts rather than replace materials to maintain the historical value. The other principles of practical restoration according to C. Brandi are: respect for aesthetic and historic value, compatibility, and reversibility.

[3] About the history of restoration and further definition of stylistic restoration, I suggest reading: Špikić, Marko. *Konzerviranje europskih spomenika od 1800. do 1850. godine*, Leykam international, d.o.o., Zagreb, 2009.

based on the evidence and suggestions that are inherent to the object itself. That is why the parts of the process that include the survey and data gathering/analysis are crucial. Otherwise, the restorer would have the full freedom to invent any shape resulting in, however paradoxical this may sound, a digital forgery of the historical authenticity. The connection with the material cultural object and its museality[4] must never be severed. That is why authenticity is one of the main issues in virtual restoration and the reason for creating the London Charter and Principles of Seville.

What happens when the missing parts are too large and the object and various sources provide no evidence about the original appearance? One option is to "borrow" the logic of current restoration practice and, in the case of paintings, use "schematic reconstruction, neutral retouching, and chromatic dampening…to visually harmonize" the remaining parts. (3) However, this is not always the case, and practice shows it. There are examples where whole structures were recreated even though it is unknown what they truly looked like in the past. Even though comparative stylistic analysis based on surviving examples has been done, there is still no guarantee that the cultural object looked like that. This is especially problematic in the case of architecture, and yet, it is in this field that the "stylistic restoration" in the digital domain found its biggest applicability. By adding missing parts, even when using comparative analysis, one still enters the domain of the subjective. Many historians and archaeologists are concerned by the subjectivity of their interpretation of a site or an object. (5) Where does the justification for such reconstruction lay then? It lies in the context. The context is what justifies the interventions, both physical and digital.

Speaking of context, two very similar yet different terms need to be defined: virtual restoration and virtual reconstruction. The first one "aims at digital preservation of the information about this [cultural] content, enhancing its legibility," while the second one "aims at 'valorization' and dissemination of the object, enhancing its meaning and function." (3) It can be stated that the virtual restoration serves as improving the documentary aspect of the object, while the virtual reconstruction puts the object in a wider context. In addition, the latter needs to satisfy three conditions: legibility, contextualization, and narration. The first condition implies the clear identification of the object. The second is the object's relation to the primary context for which it was created or in which it was used. The third condition, in a certain way, goes beyond the reconstruction. It uses it as a visual background (3), but the

[4] For further understanding of this term, I suggest reading: Maroević, Ivo. *Uvod u Muzeologiju*, Zavod za informacijske studije Odsjeka za informacijske znanosti Filozofskog fakulteta Sveučilišta u Zagrebu, Zagreb, 1993.

narrative itself belongs to the communication of knowledge, or in other words, education. Therefore, which of the two approaches will be used depends on what needs to be achieved. The goal dictates the context and the context dictates the tools.

The main difference regarding the goal is to identify who is the audience: for whom is the model being made? This determines the visual result and the overall approach. The problem that occurs with technological advancement is that the better the models look, the easier it is to believe them. "Certainly, a compelling visualization can make itself 'easy to love and difficult to doubt'." (5) The basic difference between the visualization of a model made for an expert audience and a wider one is that the former is more analytical, while the latter is usually more narrative, visually stimulating, and dynamic. Communication tools can be active and demand more participation from the spectator, such as VR or augmented reality, or passive, as is the case with a movie, a material 3D model, or a picture. Both approaches can be used for both types of audiences, even though it would be advisable to have a more interactive one for non-expert visitors.

Regarding VR aimed at professionals with an in-depth knowledge of the topic presented, it should have a visualization of various levels of information. By this, I mean a connection to the database on which the model was based, "records about construction materials or executive techniques…additional textures…or to make the inner stratigraphies visible and comparable." (3) Using this information, experts can, for example, test a hypothesis or gain ideas about possible further problems or model developments. As for the non-expert audience, the goal is to educate them by explaining the primary context of the cultural object, its origins, use, what it looked like, etc. These models are usually virtual reconstructions because they need to narrate. As a result, their creation often employs the "stylistic restoration" where lots of details have to be invented even though no precise documentation exists. There is an aspect of fantasy in these models. "That does not mean that a 'fantasy' element is a bad or negative quality. It can be much more of a dynamic catalyst that sparks audience engagement with the digital heritage representation." (2) The narrative justifies the hypothetical reconstruction as it usually needs to take into account a much wider range of objects and information that surpass the cultural object itself. Hence, artistic freedom is more justified in this case. This is further promoted by the rise of post-processualism. (7) Consequentially, it has promoted the discussion about using artistic methods in research, hypothesis testing, and presentation of knowledge. It also prompted "supporting self-reflexive phenomenological approaches and the creation of narratives as an academically viable means

of experiencing and understanding sites and landscapes," (5) as well as artistic and cultural objects.

Regarding presentation, the best, and probably the most complex digital tool that is available to us is virtual reality (VR). Since VR cannot be realized without the headset that the viewer needs to wear, the person becomes a slave to the machine. (8) Through telepresence, this dependence on the machine allows him or her to see the object, or in this case, the artworks, which are physically very distant: "The classic position of an observer directly in front of a material work of art was replaced by a participatory relationship that surmounts great distances but still appears to be immediately present in the work." (9) He or she no longer needs to go to a museum, church, or gallery but can access them from his home, provided that all of the technical requirements have been met. In it, the whole space as well as the artwork itself, are presented in predetermined circumstances. These circumstances transform the "ritual" aspect of the object[5] into a mass-accessible digital version. Three main problems resulting now are the decrease of aesthetic distance, the extrapolation of the artwork from its original context, and the inconsistency between the real and virtual experience:

1) The first problem is the so-called aesthetic distance. Increasing the level of symbiosis between the observer and the illusion decreases this distance proportionately. As a result, a feeling of real presence within the virtual is achieved, but the critical understanding of the artwork is diminished. (9)

2) Extrapolation of a work of art from its original context by the means of digitalization refers to a shift that consequentially appears in the relationship between the viewer and the object. As was mentioned above, "the classic position of an observer directly in front of a material work of art was replaced by a" feeling of being "immediately present in the work." (9) The location of the reproduction is in the domain of the digital; it is stored as digital data on a webpage that the whole world can access through the same link.

3) Lastly, the former two result in the inconsistency between the real and the virtual experience. This is obvious since the virtual version shows "an idealized" museum setting. The circumstances within the digital version are predetermined. They are also constant and unchanging and, as such, not a faithful reproduction. The person watching it from home will have a hard time enjoying it the same way in real life due to the presence of tourists or meteorological impacts.

[5] The concept of artistic aura and its ritual aspects was presented by W. Benjamin in his work titled "The Work of Art in the Age of Mechanical Reproduction." (Benjamin, Valter. "Umetničko Delo u Veku Svoje Tehničke Reprodukcije," u: *Studije Kulture*, ur. J. Đorđević, Službeni Glasnik, Beograd, 2008.)

3. Examples

A fine example of the usage of VR for educating the audience through participation is the project of the Forum of Augustus from 2019, which recreated the appearance of the 1st century AD temple with its surrounding buildings. The VR headset allows the viewer to take on the role of the forum guard and perform tasks and activities, gaining knowledge of that period in the process. (3) This immersion is achieved when the machine, that is the headset, the virtual, and the sight unite into an indistinguishable entity. As a result, the consciousness of being present in the virtual realm is turned into unconsciousness, i.e. the medium becomes temporarily invisible. (9)

The reconstruction itself is also very transparent and allows one to understand upon which sources is it based. The team that was in charge of making the model had to rely on archaeological data from the site, but also historical documents, art history, literary sources, etc. "The reconstructive model has been designed starting from the three-dimensional survey of the archaeological site and from some architectural fragments that have been relocated with a process of virtual anastylosis. The missing parts have been completed by referring to the numerous iconographic testimonies, historical archaeological documents, and stylistic comparisons." (3) All of this was needed for a more accurate reconstruction. However, missing data still needs to be implemented hypothetically, relying on subjective decisions. For example, the color of the details, or how the sculptures on the forum in front of the temple looked like. These are minor, but still, key elements, that allow for the impression of the past time to be reinvented, and through VR relived. "In a brief time, the viewer can cross centuries." (2)

Speaking of a digital object which is just a copy of the material original, a fine example is a statue of Zeus (or Poseidon) from the National Archaeological Museum in Athens. The original "is retained in the ritual space of the museum, whereas the patterns and codes of the digital Zeus do not have a materially conserved quality, are not subject to wear, and have a ubiquitous, nonexclusive quality. For example, Zeus has been put into situations not available to the 'real' in a way that photographs were previously. These are now accessed locally in the exhibition 1000 Years of the Olympic Games, and dispersed through the Web site." (10)

Digital technologies can also be used to present inaccessible objects. Two such examples can be found in the basilica of Santa Maria Assunta on the island of Torcello, located in the northern part of the Venetian lagoon. After the removal of the marble slabs

from the main apse, early 11th-century frescoes have been discovered in a deteriorated and hardly legible state. (11) In a later part of the same century, they were completely covered by mosaics, while the lower section which depicts a row of bishops, was overlaid by marble slabs. (12) If the restorers decide to return the slabs and recreate the aesthetic unity of the apse, the fresco fragments would remain inaccessible to the visitors. However, they can be conserved and scanned, and as such, virtually restored. These hypothetical restorations can then serve as a basis for a supposed reconstruction of the lower part of the apse from the early 11th century. If presented in an adjacent room, they can visually narrate the dynamics of history to contemporary visitors.

The final example comes from the same architectural object, in which, in 2020 two murals were discovered between the roof and the vault of the deaconicon chapel. (13) Due to their complete inaccessibility, even to the expert audience, it is hard to present them. However, with the use of photogrammetry, 3D virtual models can be made and later turned into material 3D objects that, when exhibited within a museum, would create a fuller picture of Torcello's artistic heritage.

4. Conclusion

To summarize, virtual restoration and virtual reconstruction are two different concepts that are applied to digital cultural objects. The former aims at preserving and emphasizing the documentary function of the object, while the latter serves to communicate knowledge to the audience, educating it. "The reproductions are the means by which cultural capital is spread, and the rules and habits of looking are developed." (10) The audience can be either an expert or a non-expert, and depending on this, different methodologies and tools can be used. In the case of the former, the model should be more analytical, while in the case of the latter, the importance shifts to the narrative and participation. The process of making a virtual model needs to be clearly documented allowing transparency. The advantage that virtual restoration has over practice, is that the "stylistic restoration" is allowed in the digital domain. However, the downside is the loss of referential connection with the original material object. If this occurs, the model becomes self-referential and, as such, no longer serves in preserving and presenting the "digital patrimony." The risk of overworking the model, or inventing the missing parts raises ethical questions of data loss, the decrease in the ability to understand the fragmented material, and the issue of authenticity.

Thus, the main conclusion regarding the relationship between the virtual restoration/reconstruction and the practical one is that they "should no longer be perceived as opposed, but as a 'continuum,' bringing values to cultural and human experience." (3)

Acknowledgments

I thank my mentor, Prof. Diego Calaon for the support and supervision of my work.

References

1. Deloš, Bernar. *Virtuelni Muzej*, prev. V. Pavlović, Clio, Beograd, 2006.
2. Thwaites, Harold. "Digital Heritage: What Happens When We Digitize Everything?" In *Visual Heritage in the Digital Age*, ed. E. Ch'ng, V. Gaffney and H. Chapman, Springer, London, 2013. pp. 327-349.
3. Pietroni, E.; Ferdani, D. Virtual Restoration and Virtual Reconstruction in Cultural Heritage: Terminology, Methodologies, Visual Representation Techniques, and Cognitive Models. *Information 2021*, 12, 167. https://doi.org/10.3390/info12040167
4. Popadić, Milan. *Diskretni šum peščanika: baština i njene nauke*, ur. Dr N. Krstović, Centar za muzeologiju iheritologiju Filozofskog fakulteta Univerziteta u Beogradu, Beograd, 2021.
5. Watterson, A. "Beyond Digital Dwelling: Re-thinking Interpretive Visualization in Archaeology", *Open Archaeology*, 2015; 1: 119-130 DOI 10.1515/opar-2015-0006
6. Silver, Minna. "Conservation Techniques in Cultural Heritage." In *3D Recording, Documentation and Management of Cultural Heritage*, ed. E. Stylianidis and F. Remondino, Whittles Publishing, Dunbeath, 2016. pp. 15-107.
7. Renfrew, Colin and Bahn, Paul. *Archaeology*, Thames&Hudson, London, 2016.
8. Manovič, Lev. *Metamediji*, Centar za savremenu umetnost, Beograd, 2001.
9. Grau, Oliver. *Virtual Art: From Illusion to Immersion*, trans. G. Custance, MIT Press, London, 2003.
10. Cameron, Fiona. Beyond the Cult of the Replicant – Museums and Historical Digital Objects: Traditional Concerns, New Discourses, in: *Theorizing Digital Cultural Heritage*, ed. F. Cameron and S. Kenderdine, MIT Press, Massachusetts, 2007. pp. 49-77.
11. Trevisan, Gianpaolo. "Il rinnovamento architettonico degli edifice religiosi a Torcello, Aq-uileia e Venezia nella prima meta del secolo XI," in: *La reliquia del Sangue di*

Cristo: Man-tova, l'Italia e l'Europa al tempo di Leone IX, Atti del Convegno internazionale (Mantova, 23-26 novembre 2011), ed. G. Cantarella and A. Calzona, Scripta, Verona, 2012. pp. 479-504.

12. Fabbri, Luca. "La cripta di Santa Maria Assunta a Torcello: il richiamo a Bisanzio all'interno della politica di legittimazione orseoliana," in: *Citazioni, modelli e tipologie nella produzione dell'opera d'arte*. Atti delle Giornate di studio. Padova 29-30 maggio 2008, 2011. pp. 3-10.
13. https://www.historywalksvenice.com/2020/07/new-frescoes-in-the-torcello-basilica/ [28.9.2022]

Suggested readings:

1. Бранди, Чезаре. *Теорија Рестаурације*, ур. и прев. Б. Шекарић, Италијанска кооперација, Београд, 2007.
2. Špikić, Marko. *Konzerviranje europskih spomenika od 1800. do 1850. godine*, Leykam international, d.o.o., Zagreb, 2009.
3. Maroević, Ivo. *Uvod u Muzeologiju*, Zavod za informacijske studije Odsjeka za informacijske znanosti Filozofskog fakulteta Sveučilišta u Zagrebu, Zagreb, 1993.
4. Benjamin, Valter. "Umetničko Delo u Veku Svoje Tehničke Reprodukcije," u: *Studije Kulture*, ur. J. Đorđević, Službeni Glasnik, Beograd, 2008.

CARBON BASED MATERIALS AS ADSORBENTS FOR WATER TREATMENT

Marijana M. Kragulj Isakovski*, Snežana P. Maletić, Tamara B. Apostolović, Irina B. Jevrosimov, Tajana M. Simetić, Aleksandra M. Tubić, Jasmina R. Agbaba

*University of Novi Sad, Faculty of Sciences, Trg Dositeja Obradovića 3, 21000 Novi Sad, R. Serbia, *Corresponding author: marijana.kragulj@dh.uns.ac.rs*

Abstract

Environmental pollution has been a recognized problem for human health and the ecosystem. Remediation is usually costly and time-consuming, so researchers' attention has been drawn to developing and using materials of the new generation. Based on the available literature, an increasing trend in carbon-based material application can be observed. Although it is a mainly new approach considered environmentally friendly, there are findings, observations, negative aspects, and conclusions that must be taken into consideration. In this paper, we discuss fundamental knowledge of different types of carbonaceous adsorbents and their possible application in water treatment. A wide range of carbonaceous low-cost and possibly more sustainable sorbents have been considered including different types of chars. Since agricultural production is an important economic sector around the world, the amount of produced waste biomass is significant. Therefore, cost-efficient production of these materials produced from residual waste biomass may simultaneously address additional environmental problems such as biomass waste management. In order to investigate the adsorption potential for removal of the most commonly employed organic UV filter (3-(4'-methylbenzylidene)-camphor), different types of biochars (originating from *Frumentum* and *Paleas*) were investigated. The obtained adsorption isotherms were well described by the Freundlich model. The nonlinearity of the isotherms was below 0.9. In general, all the investigated adsorbents demonstrated higher adsorption affinity for the investigated organic UV filter. This type of research is necessary to obtain safe adsorbents for water remediation.

Keywords: biochars, sorption, water treatment, organic compound

1. INTRODUCTION

In recent years, population growth, urbanization, industrial development and changes in people's lifestyles contributed to the release of many potentially polluting substances into the

environment. Additionally, the discharge of diverse pollutants into the water environment has threatened ecological safety and human health. Emerging contaminants or contaminants of emerging concern (ECs) represent a great risk to the quality of aquatic ecosystems, which include a wide range of structurally different pollutants of the new generation in the last two decades (1). ECs have still not been included in routine monitoring, neither at European Union level, nor at national level in the Republic of Serbia. Deeper knowledge and a thorough understanding of fate, transformation, and toxicity of these contaminants are still lacking and insufficient. The different classes of chemicals which fall under ECs are personal care products (PCPs), pharmaceuticals, surfactants, flame retardants, artificial sweeteners, industrial additives, and by-products of water treatment. The compounds from the group of UV filters belong to the group of emergent substances according to the NORMAN Network (Network of reference laboratories, research centers and related organizations for monitoring of emerging environmental substances). UV filters are synthetic compounds mainly used in personal care products and even industrial products (e.g. plastics, paints, and textiles) in order to protect from UV radiation (2). Generally, organic UV filters have low water solubility and high octanol-water partition coefficient, logK_{ow}, and are therefore expected to accumulate in sediments and biota (3). One of the most widely used compounds from the group of UV filters is 3-(4-methylbenzylidene) camphor (4-MBC), which is an organic camphor derivative (4). The presence of 4-MBC and other UV filters has been detected in rivers, lakes, sediment, groundwater and seawater, biota, and even drinking water. The concentration of 4-MBC in the environment ranges from ~ 1 μg/L in surface waters, while its concentration in wastewater and water from wastewater treatment plants ranges from 3-7 μg/L (5). To date, a wide variety of technologies for water and wastewater treatment such as coagulation/flocculation, filtration, biological digestion, adsorption, and chemical oxidation have been extensively discussed in the literature. With no need for the addition of chemicals and energy, thus avoiding the generation of possible secondary pollutants, adsorption proved to be an effective technique to remove contaminants from complex systems due to its environmental friendliness and sustainability (6). However, the economic and technical characteristics of adsorption processes depend on many factors, such as the adsorbent type, the target adsorbate, the operating conditions (including fluid properties), the possibility for adsorbent regeneration, and its final disposal. Carbon materials obtained from biomass are receiving special attention among researchers due to their abundance, availability, low cost, renewability, as well as outstanding physical-chemical properties. These characteristics are the main reason adsorption on biochar is a technique more and more frequently applied in

water remediation. Biochar (BC) is a carbon-rich material with many environmental benefits, which has been mostly attributed to its surface characteristics and special properties, such as large specific surface area, rich oxygen-containing functional groups, high cation-exchange capacity, aromatic carbon structure, and high mineral content (7). The knowledge of biochar-adsorbate interactions and their implications are also important aspects for the development of biochars as competitive adsorbents, as well as to optimize the adsorption process.

The main objective of this work was to produce carbon-based materials originating from different biomass (corn and straw), characterized and used in order to investigate the adsorption potential of biochars for the removal of the most commonly employed organic UV filter (3-(4-methylbenzylidene)-camphor from water.

2. MATERIALS AND METHODS

2.1. Adsorbate

4-MBC (*Sigma Aldrich*, CAS No. 36861-47-9) was used as adsorbate. It has low water solubility (1.3 mg/L) and high lipophilicity (logK_{ow} 4.95), which conditions its stability in the environment.

2.2. Adsorbents

Biochars used in this study are commercially available from wholesale and have a European Biochar Certificate (EBC, 2012). The materials were made in a *KonTiki* system using hard wood with charring temperatures around 680°C to 740°C.

2.3. Characterization of the adsorbents

Physico-chemical characterization of different carbon adsorbents originating from corn biomass (BC1) and straw (BC2) included the determination of the specific surface area (SSA), as well as the elemental composition of biochars and the determination of surface chemistry. Multi-point BET (*Brunauer-Emmett-Teller*) SSAs of biochars were determined by nitrogen adsorption at 77 K using an AutosorbiQ Surface Area Analyzer (*Quantochrome Instruments, USA*). Analysis of the elemental composition (C, H, N, and S) of biochars was carried out using Vario EL III CHNS Analyzer in three repetitions. The identification of functional groups present in the examined materials was conducted by Fourier transform infrared spectroscopy (FTIR) (*Thermo-Nicolet Nexus 670 FTIR spectrometer, Thermo Fisher Scientific, USA*).

2.4. Adsorption experiments

Adsorption experiments were performed in duplicates at room temperature (20±2°C) and pH 6.5. Adsorption experiments were set up as follows: a certain mass of adsorbent was measured in glass vials, and then the background solution of 0.01 M $CaCl_2$ in deionized water with 100 mg/L NaN_3 as a biocide was added. Due to the low solubility, before spiking the background solution, a stock solution of organic compound (1000 µg/mL) was prepared in methanol (*J.T. Baker*, for organic residue analysis). The volume of stock solution used for spiking was < 0.1% (v/v) and there is no measurable influence on the sorption behaviour of organic compounds (8). The adsorption kinetics was performed as follows: a certain mass of biochars was measured in a glass vial and then a certain volume of background solution spiked with a methanol stock solution of organic compounds was added. The initial concentration of 4-MBC in the background solution for each kinetic point was about 600 µg/L. The kinetics experiment was performed by shaking the samples at 180 rpm (IKA-Werke KS501 digital) over different time periods varying from 30 min to 96 h. To determine the initial concentration of 4-MBC for each kinetic point, control samples without any sorbent were prepared and treated in the same way in order to account for investigated compounds' losses other than adsorption. The recoveries for initial concentrations were in the range of recoveries for the applied analytical procedures which shows there are no significant losses other than adsorption. Adsorption isotherms were run in triplicate at room temperature (20±2°C). For the adsorption isotherms, the procedure was as follows: in the glass vials containing premeasured amounts of adsorbent (10 mg) background solution was added, and then was agitated before a certain volume of methanol stock solution of organic compounds was spiked and equilibrated at room temperature. After that, the obtained suspension of spiked background solution with the corresponding adsorbent was subjected to continuous shaking at 180 rpm (IKA-Werke KS501 digital) during equilibrium time (48 h) which was obtained from the previously conducted kinetics experiment. The concentration range of 4-MBC was 20-2000 µg/L. In order to determine the initial concentration of investigated organic compounds for each isotherm point, control samples without any sorbent were prepared and treated in the same way. The recoveries were in the range of recoveries of the applied analytical procedures.

2.5. Chemical analysis

After the precipitation of the adsorbent, liquid-liquid extraction of 30 mL of supernatant with hexane (*J.T. Baker*, for organic residue analysis) was performed. The hexane extract was

analyzed using a gas chromatograph with a quadrupole mass spectrometer (GC/MS) (7890A/5975C GS/MS system, Agilent Technologies, Santa Clara, California, USA, with a DB-5 MS capillary column, J&W Scientific, Santa Clara, California, USA). The chromatography conditions were adjusted according to the UV filter analysis method given in the literature (9).

2.6. Data analysis

The Freundlich model for the adsorption isotherm describes the heterogeneity of the adsorbent surface and the exponential distribution of the active sites and their energies. The Freundlich isotherm is represented by equation (1) (10-11):

$$q_e = K_F \cdot C_e^n \quad (1)$$

where q_e and C_e are the solid phase and aqueous phase equilibrium concentrations (in µg/g and µg/L, respectively), while K_F and the exponent n are the Freundlich sorption capacity coefficient [expressed as (µg/g)/(µg/L)^n], and the site energy heterogeneity factor indicating isotherm nonlinearity (dimensionless), respectively. K_F and n were obtained from direct nonlinear curve fitting of the adsorption data sets.

3. RESULTS AND DISCUSSION

3.1. Characterization of investigated biochars

Results of biochars characterization including BET SSA and elemental composition are shown in Table 1. The BET SSA for investigated biochars ranged from 61 to 111 m^2/g. Based on the obtained results for elemental composition, it can be observed that both investigated biochars consist mainly of carbon (67-71%), while the content of hydrogen, nitrogen and sulphur is much lower.

Table 1. *Characterization of investigated adsorbents originating from biomass of corn (BC1) and biomass of straw (BC2)*

Adsorbents	***Parameter***				
	BET (m^2g^{-1})	***Elemental analysis***			
		C (%)	**H (%)**	**N (%)**	**S (%)**
BC1	111	70.7	0.210	1.12	1.39
BC2	61.0	67.8	0.281	1.05	2.21

Based on the FTIR spectrum, characteristic bands corresponding to the structure of biochar can be observed. The broad absorption band around 3436-3444 cm^{-1} for both investigated biochars is attributed to O-H stretching vibration of phenol hydroxyl functional group, including hydrogen bonding due to adsorbed water. Two weak bands appearing in the region around 2915-2839 cm^{-1} (BC1) and 2929-2849 cm^{-1} (BC2) correspond to the C-H stretching vibration from the methyl and methylene groups (-CH_2-). The peak at 1620-1631 cm^{-1} for both biochars can be attributed to C=C stretching vibrations caused by the aromatic structure. While the peak at 1384 cm^{-1} is present only in BC1, which is due to the C-H bending in alkanes/alkyl groups. The wavenumber at 1099 cm^{-1} for BC1 and 1101 cm^{-1} for BC2 can be attributed to -C-O-C- stretching vibrations of groups in polysaccharides or from bending vibration of -C-OH groups. In BC2, there is also a peak at 469 cm^{-1}, which may be a consequence of adsorption from O-Si-O, and therefore indicates the presence of certain amounts of silica (12).

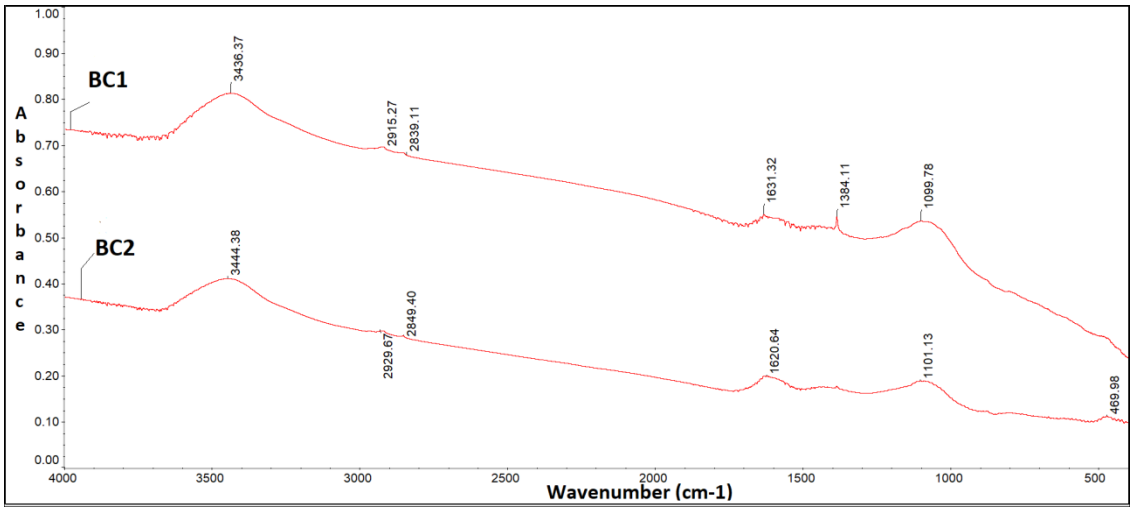

Figure 2. *FTIR spectra of the investigated biochars originating from biomass of corn (BC1) and biomass of straw (BC2)*

3.2. Adsorption kinetics

In order to determine the mechanisms of 4-MBC adsorption on biochar from corn and straw, it was necessary to conduct an investigation of adsorption kinetics, as well as to determine the time necessary to establish the adsorption-desorption equilibrium. Kinetics of 4-MBC adsorption on biochar was monitored for 96 h in order to investigate the adsorption potential of the target compound on selected adsorbents. Based on the presented results from the dependences of C_e/C_0 on time (min), it can be observed that the establishment of the adsorption-desorption equilibrium of 4-MBC for both biochar (BC1 and BC2) occurs after 48 h. The obtained results are shown in Figure 2. Additionally, the efficiency of

4-MBC removal on the investigated carbon adsorbents was calculated. The obtained results indicate that no major deviation was recorded in the efficiency of 4-MBC removal in relation to the applied adsorbents. The percentage of 4-MBC removal ranged from 62-71%.

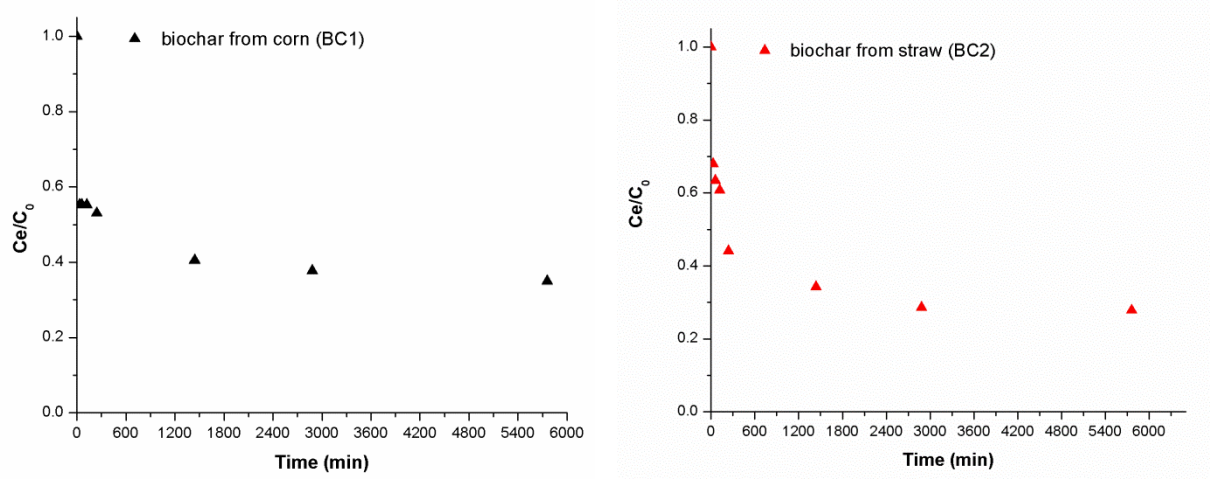

Figure 2. *Kinetics of 4-MBC adsorption on biochar from corn (BC1) and biochar from straw (BC2)*

3.3. Adsorption isotherms

Isothermal adsorption models are applied to describe the adsorption behavior between two phases, which are very important to optimize the adsorption effect. Freundlich isotherm model was applied as one of the most used adsorption isotherm model. Adsorption isotherms of 4-MBC on different types of biochars are shown in Figure 3, while adsorption parameters obtained by Freundlich model are given in Table 2.

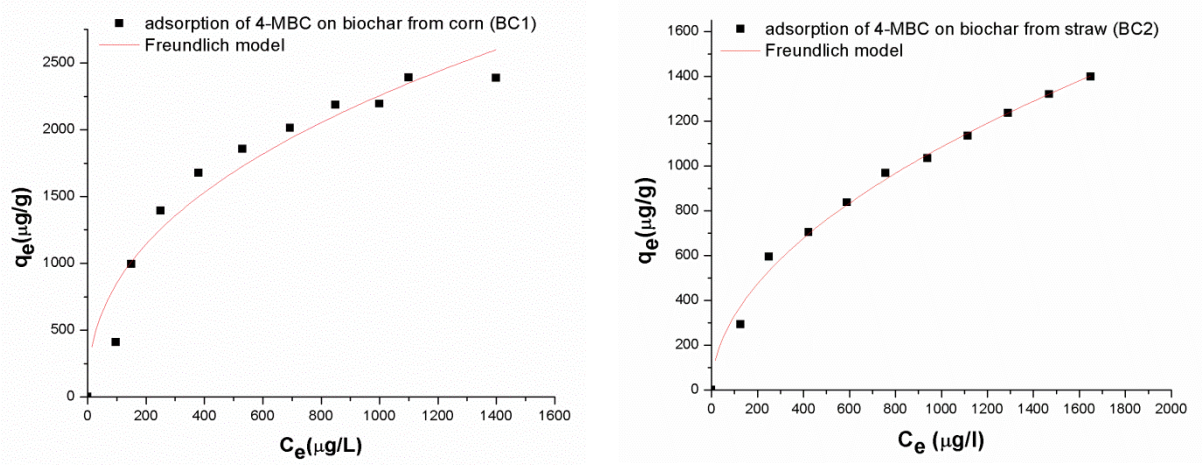

Figure 3. *Adsorption isotherms of 4-MBC on biochar from corn (BM1) and biochar from straw (BM2)*

Table 2. *Parameters of Freundlich's adsorption model for both investigated biochars*

Adsorbents	***Freundlich model***					
	R^2	**n**	K_F $(\mu g/g)/(\mu g/L)^n$	$logK_d$		
				$0.01S_w$	$0.1S_w$	$0.5\ S_w$
BC1	0.906	0.422	122.4	6.178	5.600	5.196
BC2	0.988	0.513	31.31	5.414	4.927	4.587

Adsorption of 4-MBC is well fitted by the Freundlich model with satisfactory correlation coefficients ($R^2 > 0.9$) for both biochars. Adsorption of 4-MBC on both biochars was nonlinear (n = 0.422-0.513). As it is infeasible to compare K_F values due to their units of measurement, distribution coefficients (K_d) were calculated at three selected equilibrium concentrations (C_e = 0.01; 0.1 and 0.5 solubilities in water, S_w) based on the equation for distribution coefficients and the obtained Freundlich parameters (table 2). The equilibrium concentrations were chosen to cover a wide range of concentrations, ranging from very low (1% solubility in water) to high (about 50% water solubility). Higher K_d values were obtained for BC1, which may be the result of higher SSA obtained for this material. An explanation for this could be that SSA controls the adsorption of 4-MBC on biochars thanks to the larger number of available adsorption sites. The importance of SSA for the adsorption of organic compounds is also observed by other authors, who showed that an increase in SSA of biochars increases the adsorption affinity for polycyclic aromatic hydrocarbons, phenols, organochlorine compounds, herbicides, insecticides, antibiotics, etc. (13-15). Also, the mentioned groups of authors indicate that the physicochemical properties of biochars significantly affect the adsorption mechanism of organic pollutants.

4. CONCLUSION

The application of biochar in water treatment indicates that biochar has good environmental and economic benefits compared with other adsorbents. Adsorption isotherm studies of 4-MBC on biochars were conducted and the experimental data well fitted the Freundlich model. The results illustrated that both biochars could be succesfuly applied for the removal of 4-MBC from water. More laboratory studies are required to systematically investigate the adsorption of different organic compounds on biochars. Additionally, adsorption experiments in the presence of sacrificial electron donor agents could give additional information on the surface charge of the investigated materials and the influence of electrostatic interactions in the overall adsorption mechanism.

Acknowledgments

The authors gratefully acknowledge the support of the Provincial Secretariat for Science and Technological Development, Republic of Serbia, Autonomous Province of Vojvodina (Project No. 142-451-2693/2021-01/2).

REFERENCES

1. Scaria J., Gopinath A., Ranjith N., Ravindran V., Ummar S., Nidheesh P.V., Suresh Kumar M. Carbonaceous materials as effective adsorbents and catalysts for the removal of emerging contaminants from water, J. Clean. Prod., 2022, 350, 131319.
2. Huang Y., Law J.C-F., Lam T-K., Leung K.S-Y. Risks of organic UV filters: a review of environmental and human health concern studie, *Sci. Total Environ.* **2021**, 755, 142486.
3. Campos D., Machado A.L., Cardoso D.N., Silva A.R.R., Silva P.V., Rodrigues A.C.M., Simão F.C.P., Loureiro S., Grabicová K., Nováková P., Soares A.M.V.M., Pestana J.L.T. (2020) Effects of the organic UV-filter, 3-(4-methylbenzylidene) camphor, on benthic invertebrates and ecosystem function in artificial streams, *Environ. Pollut.*, **2020**, *260*, 113981.
4. Liang M., Yan S., Chen R., Hong X., Zha J. 3-(4-Methylbenzylidene) camphor induced reproduction toxicity and antiandrogenicity in Japanese medaka (Oryzias latipes), *Chemosphere*, **2020**, *249*, 126224.
5. Quintaneiro C., Teixeira B., Benedé J.L., Chisvert A., Soares A.M.V.M., Monteiro M.S. Toxicity effects of the organic UV-filter 4-Methylbenzylidene camphor in zebrafish embryos, *Chemosphere* **2019**, *218*, 273-281.
6. Zeghioud H., Fryda L., Djelal H., Assadi A., Kane A. A comprehensive review of biochar in removal of organic pollutants from wastewater: Characterization, toxicity, activation/functionalization and influencing treatment factors, *JWPE*, 2022, 47, 102801.
7. Barquilha C.E.R., Braga M.C.B. (2021) Adsorption of organic and inorganic pollutants onto biochars: Challenges, operating conditions, and mechanisms, *Bioresour. Technol. Rep.*, **2021**, *15*, 100728.
8. Weber W.J., Huang W. A Distributed reactivity model for sorption by soils and sediments: intraparticle heterogeneity and phase-distribution relationships under nonequilibrium conditions, *Environ. Sci. Technol.* **1996**, *30*, 881-888.
9. Díaz-Cruz M.S., Llorca M., Barceló D., Barceló D. Organic UV filters and their photodegradates, metabolites and desinfection by-products in the aquatic environment, *TrAC*, **2018**, *27*, 873-887.

10. Králik M. Adsorption, chemisorption, and catalysis, *Chem. Pap.*, **2014**, 68, 1625-1638.
11. Ayawei N., Ebelegi A.N., Wankasi D. Modelling and Interpretation of Adsorption Isotherms, *J. Chem.,* **2017**, *2017*, 1-11.
12. Liu Y., Zhao X., Li J., Ma D., Han R., (2012) Characterization of bio-char from pyrolysis of wheat straw and its evaluation on methylene blue adsorption, *Desalination and Water Treatment*, 46, 115-123.
13. Tan X., Liu Y., Zeng G., Wang X., Hu X., Gu Y., Yang Z. Application of biochar for the removal of pollutants from aqueous solutions, *Chemosphere* **2015**, *125*, 70-85.
14. Zeghioud H., Fryda L., Djelal H., Assadi A., Kane A. A comprehensive review of biochar in removal of organic pollutants from wastewater: Characterization, toxicity, activation/functionalization and influencing treatment factors, *JWPE*, **2022**, 47, 102801.
15. Dai Y., Zhang N., Xing C., Cui Q., Sun Q. The adsorption, regeneration and engineering applications of biochar for removal organic pollutants: a review, *Chemosphere*, **2019**, *223*, 12-27.
16. Qiu B., Shao Q., Shi J., Yang C., Chu H. Application of biochar for the adsorption of organic pollutants from wastewater: Modification strategies, mechanisms and challenges, *Sep. Purif. Technol.,* **2022**, 300, 121925.

MAGNETIC NANOPARTICLES: NEW GENERATION ADSORBENTS FOR ARSENIC REMOVAL

Jasmina B. Nikić[1], Malcolm A. Watson[1*], Aleksandra M. Tubić[1], Marijana M. Kragulj Isakovski[1], Marko D. Šolić[1], Marija Ž. Ćurčič[1], Jasmina R. Agbaba[1]

**Corresponding author: Malcolm Watson, e-mail: malcolm.watson@dh.uns.ac.rs*

[1]University of Novi Sad, Faculty of Sciences, Trg Dositeja Obradovića 3, 21000 Novi Sad,

Abstract

Arsenic contamination of drinking water sources is a global problem and therefore many countries make a lot of effort to solve this urgent public health issue. Among the different approaches for arsenic removal, nanomaterials, especially magnetic nanoparticles (MNPs), as new generation adsorbents, received a lot of attention. In this study a one-step co precipitation method was applied to produce magnetite nanoparticles and a specially designed magnetic separation unit was used to assess their applicability as part of a real drinking water treatment plant. Batch adsorption tests were carried out to determine the adsorption capacity of the synthesized adsorbent for arsenic removal. Continuous adsorption experiments using a magnetic pilot plant were conducted with real arsenic contaminated groundwaters, whereby different doses of magnetite nanoparticles (0.5-2 g/l) and flow rates were applied (7-14 l/h). Characterization of the synthesized magnetite nanoparticles shows BET specific surface area of 40.36 m^2/g, while the XRD and FTIR analysis confirmed the formation and presence of magnetite nanoparticles. The results obtained from the dynamic experiments show that 50-70% of arsenic can be removed, depending on groundwater quality, whilst successfully recirculating the magnetite nanoparticles within the magnetic separation unit. Additional investigations are necessary to further improve the design and performance of the magnetic separation unit as a highly promising cost effective solution for small water utilities.

Keywords: magnetite nanoparticles, arsenic, adsorption, drinking water, magnetic separation

1. INTRODUCTION

The presence of arsenic in groundwater, which use for drinking water supply, affect more than 150 million peoples of 70 countries and this trend continues to escalate (1). The main concern related to arsenic in groundwater are its high toxicity, since chronic exposure of arsenic, primarily through drinking water, can cause numerous effects on the human health, including cancer as the most serious consequence (2). In order to prevent and reduce the

adverse health effects of arsenic, the World Health Organization (WHO) recommends maximum allowable concentration (MAC) of arsenic in drinking water of 10 μg/l (3). Among various technologies which have been employed for arsenic removal from groundwater, adsorption processes stand out due to their high efficiency, simple and stable operation, and generally lower operation and capital costs (4-6). Different adsorbents have been developed and applied for arsenic removal. However, in recent years, iron oxide nanoparticles (INPs) have been the most interesting novel materials, due to their unique physicochemical properties and their strong affinity for arsenic species (7). Among the iron oxide nanoparticles, magnetite (Fe_3O_4) and maghemite (γ-Fe_2O_3) nanoparticles, have sparked an immense interest in research for engineering applications with arsenic contaminated waters (8-10). They are easy to fabricate, have high adsorption capacities for arsenic and their magnetic properties allow for their easy separation from water and subsequent reuse. In order to extract real data representing an industrial set up, magnetic separation systems must operate continuously and particles must possess sufficient magnetic properties to facilitate their isolation from a flowing stream (11). Investigations relating to application of magnetic nanoparticles are mainly limited to batch operation mode. Therefore, there is an urgent need to develop a cost effective continuous magnetic separation system that can simultaneously achieve both arsenic removal and magnetic separation. This work thus employs a one-step process to synthesize the magnetic nanoparticles (MNP) and then investigates arsenic adsorption under environmentally relevant conditions in both batch and continuous flow experiments, using a magnetic separation unit whereby the effects of various process variables such as flow rate and MNP dose on arsenic removal could be investigated.

2. EXPERIMENTAL

2.1. Reagents

As(III) and As(V) stock solutions of 1 g/l were prepared by dissolving As_2O_3 and As_2O_5 (purity > 99.9, obtained from Sigma Aldrich) in deionized water. $Fe_SO_4 \cdot 7H_2O$ (p.a., POCH Poland S.A.) and $FeCl_3 \cdot 6H_2O$ (p.a., POCH Poland S.A.) were used for preparation of the magnetic nanoparticles.

2.2. Synthesis of magnetic nanoparticles

Magnetic nanoparticles (MNP) were prepared in a single step process by conventional co-precipitation method, using $Fe^{3+}$and Fe^{2+} salts at a molar ratio of 2:1. Briefly, mixture of 100 ml of 0.2 M $FeCl_3$ solution, 100 ml of 0.1 M $FeSO_4$ solution was vigorously stirred.

Afterwards 2M NaOH was added dropwise until the mixture reached pH 10 and black precipitate developed. The synthesized MNP were then separated from the suspension by external magnet and washed repeatedly with deionized water until a supernatant of neutral pH was observed. Collected Fe_3O_4 nanoparticles were dried at 105°C for 4h.

2.3. Characterization of magnetic nanoparticles

The surface morphology of the synthesized magnetic nanoparticles was analyze using scanning electron microscopy (SEM) (Hitachi TM3030, Japan). The specific surface area of nanoparticles was measured by nitrogen adsorption using the Brunauer–Emmett–Teller (BET) method with a Autosorb TMiQ surface area analyzer (Quantachrome, Boynton Beach, FL, USA). Mesopore and micropore volumes were determined using the Barett–Joyner–Halender (BJH) method using desorption isotherm, and *t*-test method, respectively. Crystal structures of magnetic nanoparticles were analyzed by X-ray powder diffraction (Philips PW automated X-ray powder diffractometer (USA)), with a focusing primary monochromator (CuKα radiation, λ = 1.5406 Å). Fourier transform infrared (FTIR) spectra of magnetic nanoparticles were recorded by infrared spectrophotometer (FTIR Nexus 670, Thermonicolet, USA). Samples for FTIR determination were ground with spectral grade KBr in an agate mortar.

2.4. Batch experiments: adsorption isotherms

Arsenic adsorption experiments were performed in 1 l glass containing 0.5 l aqueous solution and 0.25 g of magnetic nanoparticles. Adsorption isotherms were obtained by varying the initial As(III)/As(V) concentration (0.2–2 mg/l). The pH was adjusted to 7.0 ± 0.2 by adding 0.1 M HNO_3 and/or NaOH; ionic strength was adjusted to 0.01 M with $NaNO_3$. The suspensions were shaken at 120 rpm (22±1°C). Afterwards the glasses were placed on a magnet for a few seconds to separate the adsorbents from the aqueous solution. Arsenic concentrations in the supernatant were analyzed by ICP/MS.

2.5. Continuous experiments

Continuous experiments were performed in a magnetic separation plant (MSU) which consist of: 1) contactor tank - for mixing adsorbent suspension and water to be treated, 2) separator tank with electromagnetic drum, 3) collector tank with recirculation pump and 4) teflon skimmer plate for removing the adsorbent particles from the surface of the magnetic drum, (Figure 1).

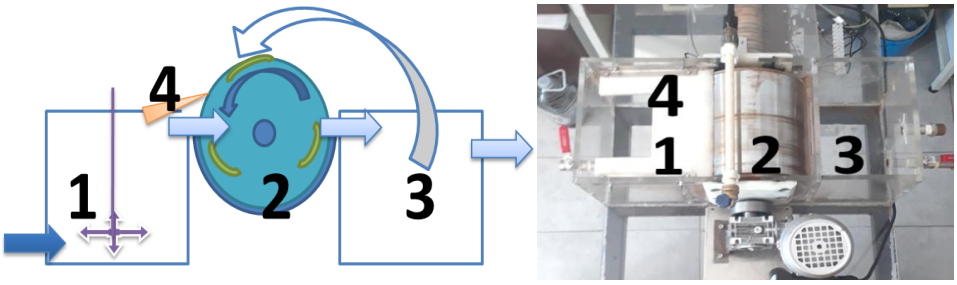

Figure 1. Diagram and photograph of the magnetic separator unit

During these experiments, the synthesized magnetic nanoparticles were added as a suspension to Tank 1, where they are stirred rapidly with the arsenic contaminated water pumped with different flow rates (7, 10 and 14 l/h). The water then overflows into the halfpipe Tank 2, where the magnetic nanoparticles are picked up by the rotating electromagnetic drum and returned to Tank 1 by the recirculation water. The treated water overflows into the collector tank (3), where samples were collected and analysed for residual As and Fe concentrations.

2.6. Analytical methods

pH measurements were carried out using an InoLab pH/ ION 735 instrument. Arsenic and iron concentrations were determined by Agilent 7700x ICP/MS, according to EPA Method 7010 (12). DOC concentrations were analyzed after filtration through a 0.45 mm membrane filter on an Elementar LiquiTOCII in accordance with the standard method (13). Conductivity, alkalinity, hardness and orthophosphates were determined by standard method (14).

3. RESULTS AND DISCUSSION

3.1. Characterization of magnetic nanoparticles

The surface morphology of synthesized magnetic nanoparticles was investigated by SEM analysis, and obtained images are present in Figure 2a. It can be seen that the surface of magnetic nanoparticles contains a large number of aggregated particles, irregular in shape and size. This observation is in agreement with other authors, who also used precipitation method for synthesis of magnetic nanoparticles (9).

Nitrogen adsorption-desorption isotherms of the magnetic nanoparticles, are present on Figure 2b. According to IUPAC classification of N_2 adsorption-desorption isotherms, the corresponding adsorption-desorption isotherms of the magnetic nanoparticles can be classified as Type IV isotherm with H1 hysteresis loops indicating that synthesized adsorbent can be classified as mesoporous material consisting of agglomerates of approximately

uniform spheres or well-defined cylindrical like pore channels (15). This was in accordance with results obtained by SEM analysis which showed the presence of agglomerated particles on surface of MNP.

The specific surface area of MNP was 42.8 m^2/g and was comparable with commercially available magnetite and maghemite nanoparticles of 40 and 39 m^2/g, respectively (7). The mesopore volume of MNP obtained by BJH method was 0.223 cm^3/g while micropore volume of this adsorbent was insignificant (0.017 $cm^{3/}g$). According to Di Iorio et al. (8) the presence of mesopores in structure of MNP could be attribute to microcavities formed by aggregation of nanoparticles visible from SEM image (Figure 2a). Additionally, the mean pore diameter of MNP obtained from BJH pore size distribution plots was 10.6 nm and confirm that MNP is mesoporous material.

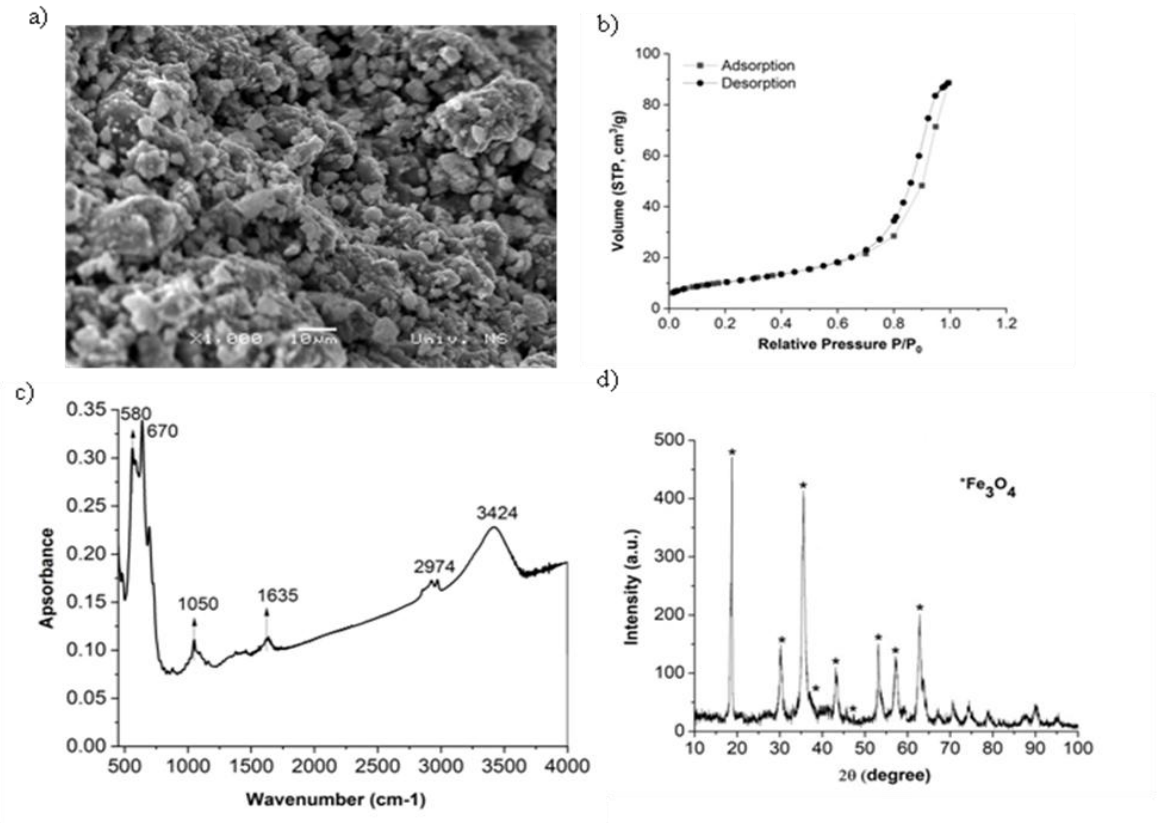

Figure 2. Characterization of MNP a) SEM images b) N_2 adsorption-desorption isotherms c) FTIR spectrum d) XRD pattern

The XRD pattern of synthesized Fe_3O_4 nanoparticles (Figure 2d) showed good agreement with the phase structure of magnetite with sharp peaks at 2θ = 30.4°, 35.6,° 37.2°, 43.4°, 47.3°, 53.2°, 57.4° and 62.5, corresponding to crystal planes of (220), (311), (222), (400), (331), (422), (511) and (440), respectively (4).

The magnetic nanoparticles were also analyzed by FTIR spectroscopy and the corresponding FTIR spectrum of MNP is present in Figure 2c. The bands at 3424 and 1635 cm^{-1} correspond to the stretching and bending vibration of hydroxyl groups of surface adsorbed water (5) while the band at 2974 cm^{-1} is attributed to the C-H stretching vibration of hydrocarbon chains. The peak at 1050 cm^{-1} corresponds to the bending vibration of the hydroxyl groups (Fe-OH) (6). Absorption peaks at 670 and 580 cm^{-1} were related to Fe–O–Fe and Fe–O stretching modes of magnetite (9,10).

3.2. Adsorption isotherms

In order to evaluate the adsorption capacities of MNP for As(III) and As(V), equilibrium data were fitted using Freundlich and Langmuir adsorption models and corresponding parameters of these models are given in Table 1. As can be seen from Table 1, the Freundlich model showed a better fit for both arsenic species, which implies an irreversible and non-ideal adsorption and the heterogeneous surface of the adsorbents (16). The Freundlich constant K_F, a measure of adsorption affinity, was twice as higher for As(V), compared to As(III). This can be explained by different interaction occurred between these arsenic species and MNP at experimental pH (pH = 7.0 ± 0.2). Namely, at this pH, As(V) exists in anionic form such as $H_2AsO_3^-$. $HAsO_3^{2-}$ while As(III) exists as a neutral species till pH < 9 (17). Taking into account that point of zero charge, pHpzc, of MNP was 6.2, positive electrostatic interaction between As(V) and MNP was promoted, resulting in its higher uptake. In contrast, at this pH, these interaction are insignificant for adsorption of neutral As(III) species on MNP.

Table 1. Isotherm parameters of Freundlich and Langmuir model for adsorption of As(III) and As(V) on MNP

Freundlich model			**Langmuir model**		
	As(III)	As(V)		As(III)	As(V)
K_F	1.01	2.24	q_{max} (mg/g)	1.15	2.86
1/n	1.10	0.53	K_L(l/g)	0,78	2.67
R^2	0.9841	0.9372	RL	0.39-0.86	0.16-0.65
			R^2	0.8865	0.8930

The Freundlich exponent 1/n is the measure of intensity of the adsorption or surface heterogeneity factor and in both of case was less than 1, suggest that the adsorption of both arsenic species on MNP was favorable (16).

3.3. Adsorption performance of magnetic separation unit

In assessing the viability of a MNP, continuous adsorption experiments were conducted with two different arsenic contaminated groundwater (GW 1 and GW 2), which is used as a

drinking water source in Serbia (Table 2). Arsenic concentration in each investigated water was about 5 and 12 times higher than the maximum allowed concentration of 10 µg/l, respectively. In addition to the high content of arsenic, groundwater GW2 is also characterized by high concentration of phosphate (1.33 mg PO_4/l), which can negatively affect the efficiency of the adsorption process (18).

Table 2. Characteristics of the real groundwater investigated

Parameter	Unit	GW1	GW2
pH		7.85	8.22
Conductivity	µS/cm	585	678
Hardness	mg $CaCO_3$/l	150	133
DOC	mg/l	0.31	2.00
Alkalinity	mmol/l	6.36	7.68
Carbonate	mg/l	388	118
Sulphate	mg SO_4/l	25.0	15.7
Phosphate	mg/l	0.124	1.33
Fe	µg/l	38.4	40.2
Mn	µg/l	48.2	31.4
As	µg/l	52.2	120

3.3.1. The effect of flow rate on the arsenic removal efficiency

Arsenic removal from groundwater and the magnetic separation of the MNP were explored in this experiment at different flow rates (7, 10 and 14 l/h). The samples were collected and analyzed at 30, 60, 90, 120 and 150 minutes and corresponding results are presented in Figure 3.

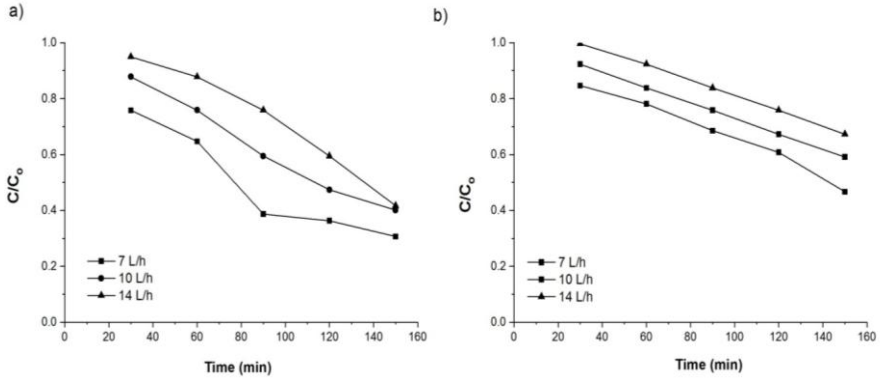

Figure 3. Effect of flow rate on arsenic removal from a) GW1 b) GW2 using MNP

It was showed that efficiency of arsenic removal from both investigated groundwaters GW1 and GW2 decreased from 69% to 50% and 53% to 24%, respectively, when flow rates were increased from 7 to 14 l/h (Figure 3a and b). These lower arsenic removal at higher flow rates can be attributed to the less contact time at higher flow rates as well higher impact of competing forces (drag force, inter-particle, centrifugal, gravitational) against magnetic force

(11). Notably, at 10 l/h the arsenic removal efficiency was 60% which was almost similar to that at 7 l/h (69%). As the flow rate increased further to 14 l/h, there was a significant drop in the capture efficiency from 69% to 49% (Figure 3a). The arsenic removal from GW2 at 7 l/h and 10 l/h was 53 and 41% but further increase in flow rate results in significant reduction of arsenic removal of 24% (Figure 3b). In addition, it was noted that arsenic removal from GW2, was lower at all applied flow rates, compared with GW1, which implies that water matrix has the significant negative impact on arsenic removal. As shown in Table 2, the phosphate concentration in GW2 is 11 times higher than the arsenic concentration, so their negative effect on arsenic removal can be attributed to competition since phosphates similar to arsenic, bind to active sites on the MNP surface (19,20). Except phosphate, other factors (such as higher content of DOC) can be also responsible for the lower arsenic removal from GW2. From techno-economically point of view, and based of the above findings, subsequent experiments were performed at 7 l/h.

3.3.2. The effect of MNP dose on arsenic removal efficiency

Effect of three different dosage of MNP (0.5 g/l, 1 g/l and 2.5 g/l) on arsenic removal was investigated and results are presented in Figure 4. Flow rate of treated water was set at 7 l/h, while the reactor continued to operate for 2 h.

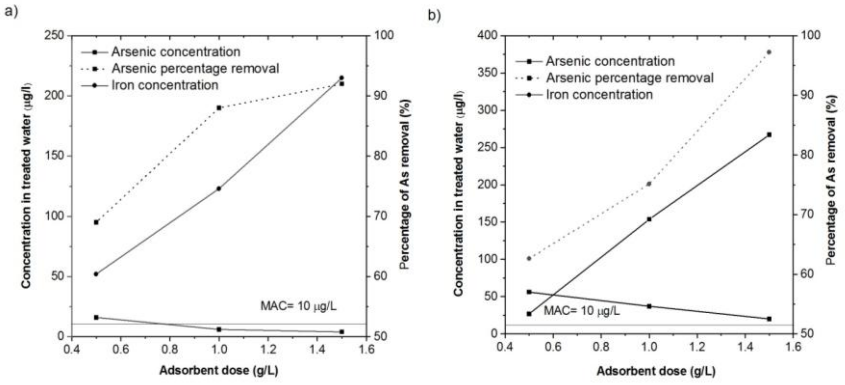

Figure 4. Effect of MNP dose on arsenic removal from a) GW1 b) GW2

As can be see form Figure 4, increased adsorbent dosage results in higher arsenic uptake, whereby the use of 2.5 g/l of MNP was enough to reduce arsenic concentration below MAC of 10 µg/l, in both investigated groundwater. This observation was attributed to an increase in the adsorptive surface area and greater accessibility of surface binding sites to the adsorbent, at the higher dosage of MNP (21). However, during these experiments, iron concentrations in the treated water increased as the MNP dose increased, suggesting incomplete separation of the MNP particles and subsequent loss of adsorbent material during the process.

4. CONCLUSION

Magnetic nanoparticles, a new generation adsorbent for arsenic removal, were successfully synthesized using simple precipitation method. SEM, FTIR and XRD analyses confirmed the production of magnetite (Fe_3O_4) nanoparticles and its mesoporous structure was confirmed by BET surface and pore analysis. In terms of adsorption capacity, synthesized magnetic nanoparticles show better performance for removal of As(V), compared to As(III). Experiments performed in continues magnetic separation system demonstrated that an increased flow rate decreased arsenic removal. In contrast, increased adsorbent dose led to higher arsenic removal. However, the higher adsorbent dose led to elevated residual Fe concentrations in the treated water, implying that the separation of MNP was incomplete. Future research will therefore focus on modification of MNP surface by different support media such as polymer to create nanocomposite material and avoid problems with agglomeration and improve separation.

Acknowledgments

The authors gratefully acknowledge the support of the Provincial Secretariat for Higher Education and Scientific Research, Autonomous Province of Vojvodina, Republic of Serbia (Grant No. 142-451-2356/2022-01/01).

References

1. Shaji, E.; Santosh, M; Sarath, K.V.; Prakash, P.; Deepchand, V.; Divya, BV. Arsenic contamination of groundwater: A global synopsis with focus on the Indian Peninsula. *Geoscience Frontiers* **2021**,*12(3)*, 101079.
2. Sodhi K.K.; Kumar, M.; Agrawal, K.P.; Singh, D.P. Perspectives on arsenic toxicity, carcinogenicity and its systemic remediation strategies. *Environ. Techn. Innov*. **2019**, *16*, 100462.
3. World Health Organisation (WHO). Guidelines Drinking-Water Quality. 4th ed. Geneva, Switzerland: WHO 2011.
4. Wojciechowska, A.; Lendzion-Bieluń, Z. Synthesis and Characterization of Magnetic Nanomaterials with Adsorptive Properties of Arsenic Ions. *Molecules*, **2020**, *25(18)*, 4117.
5. Zeng, H.; Zhai, L.; Qiao, T.; Qiao, T.; Yu, Y.; Zhang, J.; Li, D. Efficient removal of As(V) from aqueous media by magnetic nanoparticles prepared with Iron-containing water treatment residuals. *Sci. Report*, **2020**, *10*, 9335.
6. Wen, Z.; Dai, C.; Zhu, Y.; Zhang, Y. Synthesis of ordered mesoporous iron manganese bimetal oxides for arsenic removal from aqueous solutions. *RSC Advance.* **2015**, 5, 4058–4068.

7. Song, K.; Kim, W.; Suh, C.Y.; Shin, D.; Ko, K.S.; Ha, K. Magnetic iron oxide nanoparticles prepared by electrical wire explosion for arsenic removal. *Powder Technol.* **2013**, *246*, 572–574.
8. Di Iorio, E.; Colombo, C.; Cheng, Z.; et al. Characterization of magnetite nanoparticles synthetized from Fe(II)/nitrate solutions for arsenic removal from water. *J. Environ. Chem. Eng*. **2019**, *7*,1–9.
9. Rajendran, K.; Balakrishnan, G.S.; Kalirajan, J. Synthesis of Magnetite Nanoparticles for Arsenic Removal from Ground Water Pond. *Int. J. Pharmtech Res.* **2015**, *8*, 670-677.
10. Kotoulas, A.; Dendrinou-Samara, C.; Angelakeris, M., Kalogirou, O. The Effect of Polyol Composition on the Structural and Magnetic Properties of Magnetite Nanoparticles for Magnetic Particle Hyperthermia. *Materials*, **2019**, *12*, 2663.
11. Muliwa, A.M.; Leswifi, T.Y.; Onyango, M.S.; Maity, A. Magnetic adsorption separation (MAS) process: An alternative method of extracting Cr(VI) from aqueous solution using polypyrrole coated Fe_3O_4 nanocomposites. *Sep. Purif. Technol*. **2016**, *158*, 250–258.
12. USEPA, Method 200.8:1994. Determination of Trace Elements in Waters and Wastes by Inductively Coupled Plasma-Mass Spectrometry, Revision 5.4. Cincinnati, OH, (1994).
13. SRPS ISO 8245:2007. Guidelines for determination of total organic carbon (TOC) and dissolved organic carbon (DOC) in water, (2007).
14. APHA - AWWA – WPCF. Standard Methods for the Examination of Water and Wastewater; American Public Health Association; Washington, 1998.
15. Thommes, M.; Kaneko, K.; Neimark, A.V.; Olivier, J.P.; Rodriguez-Reinoso, F.; Rouquerol, J; Sing, K.S.W. Physisorption of gases, with special reference to the evaluation of surface area and pore size distribution (IUPAC Technical Report). *Pure Appl. Chem.*, **2015**, *87*, 1051-1069.
16. Al-Ghouti, M.A.; Da'ana, D.A. Guidelines for the use and interpretation of adsorption isotherm models: A review. *J. Haz. Mat*. **2020**, 393, 122383.
17. Liu, C.H.; Chuang, Y.H.; Chen, T.Y.; Tian, Y.; Li,H.; Wang, M.K.; Zhang, W. Mechanism of Arsenic Adsorption on Magnetite Nanoparticles from Water: Thermodynamic and Spectroscopic Studies. *Environ. Sci. Technol*. **2015**, *49*, 7726−7734.
18. Qin, C.; Liu, L.; Han, Y. *et al.* Mesoporous Magnetic Ferrum-Yttrium Binary Oxide: a Novel Adsorbent for Efficient Arsenic Removal from Aqueous Solution. *Water Air Soil Pollut.* **2016,** *227*, 337.
19. Tiberg, C.; Sjöstedt, C.; Eriksson, A.K.; Klysubun, W.; Gustafsson, J.P. Phosphate competition with arsenate on poorly crystalline iron and aluminum (hydr)oxide mixtures. *Chemosphere*. **2020**, *255*, 126937.
20. Nikić, J.; Tubić, A.; Agbaba, J., Watson, M.A.; Maletić, S.; Šolić, M.; Majkić, T:; Agbaba, J. Arsenic Removal from Water by Green Synthesized Magnetic Nanoparticles. *Water*. **2019**, *11*, 2520.
21. Joshi, S.; Sharma, M.; Kumari, A.; Shrestha, S.; Shrestha, B. Arsenic Removal from Water by Adsorption onto Iron Oxide/Nano-Porous Carbon Magnetic Composite. *Appl. Sci*. **2019**, 9, 3732.

INVESTIGATION OF THE INFLUENCE OF THE INITIAL CONCENTRATION OF HEAVY METALS IN BINARY SOLUTIONS ON THE EFFICIENCY OF ADSORPTION

Indira Šestan[1*], Amra Odobašić[1], Melisa Ahmetović[1], Sabina Begić[1], Halid Junuzović[1]

[1]Faculty of Technology, University of Tuzla, Urfeta Vejzagića 8, 75000 Tuzla, Bosnia and Herzegovina,

*indira.sestan@untz.ba

ABSTRACT

In recent years, new, more low-cost and more efficient materials for reducing pollutants in wastewater have been studied. At the same time, most attention is paid to natural materials, most often food waste. There are numerous literature data that testify to the strong adsorption capacity of coffee-derived materials, which are able to adsorb significant amounts of various adsorbates. In many cases, the obtained values were competitive with commercial materials of well-known physical and chemical characteristics, and therefore the approach of using this type of waste was opened, as economically justified, and satisfactory in purpose. This paper presents the results of testing the influence of the initial concentration of copper and chromium ions in binary solutions on the sorption capacity of coffee waste. The characterization of the material was performed, where physical, chemical and physicochemical properties were determined. The content of organic matter in water, cation exchange capacity, as well as the point of zero charge were determined. Different functional groups present on the surface of the adsorbents, which can participate in the binding of cations due to dissociation in the aqueous medium, were determined by the FTIR method. The effect of biosorbent concentration on the removal of Cu(II) and Cr(III) ions from aqueous solutions was investigated at initial concentrations of 10 mg/L, 50 mg/L and 100 mg/L.

Keywords: binary solution, heavy metals, adsorption, physicochemical characterization

1. INTRODUCTION

The development of human society and the introduction of new technologies, in addition to great positive effects, have also led to one of the most severe forms of pollution, which is certainly water pollution (1). All those waters that come out of industrial plants, and which contain dissolved or suspended contaminants that can contaminate surface or underground water resources, are called wastewater (2). In the process of metal processing and coating in electroplating, chemical compounds are used that have a very harmful effect on the environment, and these are mainly heavy metals, their salts, organic solvents, acids and bases, which lead to a series of physical and chemical changes of water (3). Galvanic wastewater poses a great danger to waterways due to high concentrations of heavy metals, if not purified before discharge (4). Some of the most common components of wastewater from the galvanic industry are copper and chromium. Copper is one of the necessary microelements, and is essential for the activity of various enzymes. However, in higher concentrations it is extremely toxic to living organisms (5). One of the significant pollutants present in wastewater in nature is chromium, which exists in six oxidation states. It is most stable in its elemental state, as a trivalent (Cr(III)) and hexavalent (Cr(VI)) ion. It occurs most often in the form of these two ions, with (Cr(VI)) being much more toxic. The conventional and most often implemented method for the separation of metals from waste water is alkaline precipitation in the form of insoluble hydroxides (6). In recent decades, an increasing number of new and improved technologies have been tested, including: chemical precipitation (7), classical and electrochemical coagulation and flocculation (8, 9), flotation (10), membrane filtration (11), ion exchange (12), adsorption on commercial activated carbon (13) and biosorption (14). In practice, most technological operations have significant drawbacks and limitations, requiring high investment and operational costs, generating large amounts of secondary waste. Biosorption in the broadest sense implies a change in the concentration of some of the components at the interface between the phases of a heterogeneous system (15). During the adsorption process, interactions occur between the atoms and molecules of the adsorbate with the particles of the porous material (adsorbent). On the solid surface there are sites with certain electronic and steric effects that are characteristic of the basic structure of the adsorbent, and which induce energetically heterogeneous energy levels, based on the degree of interaction with the adsorbate (16). There are numerous literature data that testify to the strong adsorption capacity of materials originating from coffee, which are able to adsorb significant amounts of several types of adsorbates. In many cases, the values obtained were

competitive with commercial materials of well-known physicochemical characteristics. With the increased level of production and industrial processing of coffee, proportionally larger amounts of by-products are created, both in producing countries and in consumer countries (17). The coffee remaining after the extraction of bioactive ingredients can be used as an adsorbent. In the past decades, the spectrum of the possibility of adsorbing various types of components on the material prepared from coffee has been intensively investigated (18,19,20,21). Before use, the coffee material is well dried and used in its native form. In the analysis of the adsorption process, in addition to the choice of adsorbent, it is important to know the influence of many important process variables, in order to achieve a high degree of effectiveness and economy. The parameters that are of particular importance are, first of all, the characteristics of the material - adsorbent, the properties of the reaction medium, as well as the type of adsorbate. Regarding the adsorbent, its surface area, functionality, porosity, irregularities, tightly bound impurities, internal surface area, particle size, ionic strength and pH are considered. Among the essential properties of the reaction medium are the type of solvent, pH, ionic strength, solution concentration and competition between dissolved substances, and interaction at the interface. In the end, the adsorbate affects the entire process through its own physical and chemical characteristics (22).

In this paper, the influence of the initial concentrations of copper and chromium in binary solutions on the efficiency of their adsorption was examined, using coffee waste as a biosorbent.

2. EXPERIMENTAL

The coffee waste used in the experiment was collected as a residue of the coffee beverage, in the form of a precipitate, after which it was dried and prepared for analysis. To adjust and measure the pH value, for hysicochemical characterization of the native biosorbent, a potentiometric method was applied using a Mettler Toledo MP 220 pH meter with a combined electrode. The volumetric method with $KMnO_4$ was used to determine organic matter in water. The content of organic matter, moisture and inorganic components in the biosorbent was determined using the gravimetric method. The total capacity of exchangeable cations was determined by the standard method of ion exchange with NH_4Cl. Functional groups on the biosorbent were characterized by the FTIR method. The pH value of the point of zero charge represents the state of the surface of the material when the sum of the negative

charges is equal to the sum of the positive charges. This value is determined based on the change in the pH solution of the corresponding electrolyte under the influence of the biosorbent (23). To determine the concentrations of copper and chromium in synthetic aqueous solutions before and after adsorption, a spectrophotometric method was applied using a Perkin Elmer ICP OPTIMA 2100 DV optical emission spectrophotometer. In all adsorption experiments, an adsorbent mass of 1 g was used. Binary solutions were tested individually, in the following order: Cu(II) + Cr(III) at initial concentrations of 10 mg/L, 50 mg/L and 100 mg/L. The initial pH value of the solution was adjusted to pH 5 using 1M NaOH and 0.1 mol/L HNO_3. The solutions were mixed on an electric mixer at 250 rpm for 1 hour. After 1 h, the solutions were filtered, the filtrates were stored in plastic vials, after which they were analyzed and the residual concentrations of the examined heavy metals were obtained, on the basis of which the efficiency of removal of Cu(II) and Cr(III) ions was calculated.

3. RESULTS AND DISCUSSION

3.1. Physicochemical characterization of biosorbent

The determined contents of ash and moisture in the biosorbent were 1.41% and 1.5%. The ash content originates from mineral substances (alkaline and alkaline earth metals). The low moisture content is favorable because the biosorbent can be stored in the open air, without particles sticking together and the consequent change in granulation. This feature is of particular importance for easy handling of the biosorbent when applied in large wastewater treatment systems.

The washing of the biosorbent with distilled water was done to determine the amount of these metals that passed into the solution and which remained in the biosorbent and to to show the amount of alkaline and alkaline earth metals leached during washing (Table 1). On the basis of the leached percentage, it can be concluded that the ions are leached in the following order: Ca(II)>K(I)> Mg(II)>Na(I). The content of total organic matter in water, expressed as the amount of oxygen required for their oxidation, was 10 mg/L.

Table 1. Leached alkali and alkaline earth metals from the biosorbent.

Leached metal ions	**Na(I)**	**K(I)**	**Mg(II)**	**Ca(II)**
Amount leached from the biosorbent (mmol/g)	0,0021	0,0167	0,0011	0,0017
Leached percantage (%)	1,87	4,3	2,8	4,6

The increase in the pH value of the aqueous solution obtained by washing the biosorbent with distilled water (Figure 1) is the result of the transfer of alkaline and alkaline earth metals from the surface of the biosorbent to the aqueous phase. Namely, it depends on the pH in which form they can be found in the aqueous solution, but also what is the surface charge of the adsorbent itself. In order to examine the charge of the biosorbent surface, the point of zero charge was determined, which was pH=5. This implies that below the stated pH value, the biosorbent will be positively charged, while above that value, its charge will be negative. Although this value is relatively high, significant sorption activity is expected even at lower pH values, where it will have a positive charge.

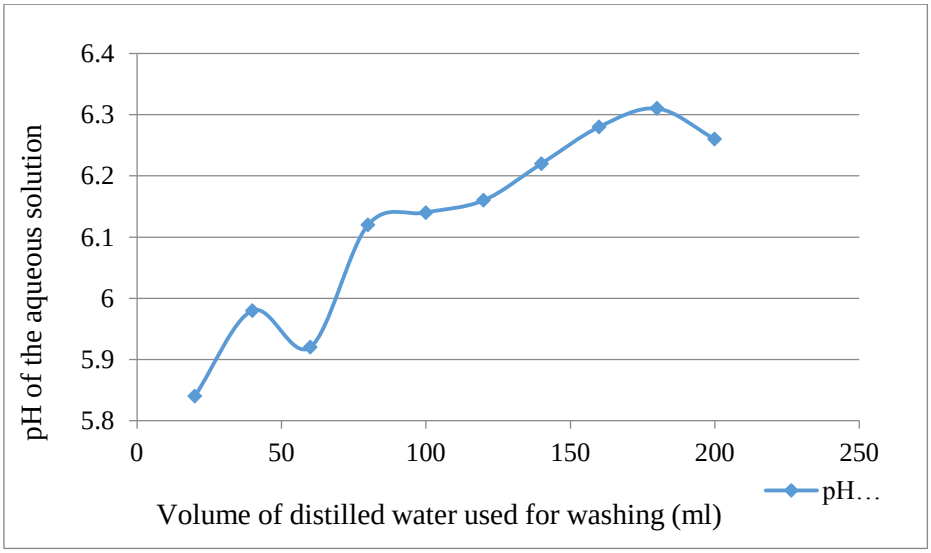

Figure 1. Changes in the pH value of the aqueous solution obtained by washing the biosorbent with distilled water

The contents of alkaline and alkaline earth metal ions in the biosorbent (mmol/g) were: calcium 0.43, potassium 0.3, magnesium 0.22 and sodium 0.11. The total exchange of all cations was 1.06 mmol Me^{z+}/g. Based on the obtained results, it can be seen that the Ca(II) ion is dominant in compared to other metals, which means that calcium ions from the

biosorbent will probably be exchanged with ions of heavy metals according to the principle of ion exchange, and that ion exchange plays a major role in the process of binding the examined ions. The FTIR method showed changes in the bands in the wave number range of 3200-3600 cm^{-1}, with a maximum at 3430.96 cm^{-1}, which is a characteristic of the valence vibrations of hydroxyl groups. Very pronounced, sharp peaks at 2924 cm^{-1} and 2850 cm^{-1} may be a consequence of the existence of asymmetric vibrations of CH_2 groups. Also observed is a peak characteristic of bonds with the C=O group, most likely in esters, while a less pronounced peak most likely corresponds to the valence vibrations of the C=C bond of the aromatic ring. Peaks in the range 1550–1750 cm^{-1} may indicate the presence of traces of xanthine derivatives, such as caffeine. The appearance of the peak at 1454 cm^{-1} verifies the assumption of the existence of C-H vibrations from CH_3 and CH_2 groups.

3.2. Adsorption experiments for the removal of Cu(II) and Cr(III) from aqueous solutions

The influence of the initial concentration was examined in the range of concentrations of 10 mg/L, 50 mg/L and 100 mg/L in binary systems Cu(II) + Cr(III). The duration of the sorption processes was 1 hour, at a mixing speed of 250 rpm. The pH value is adjusted to the pH value of zero charge of the biosorbent. As seen in Figure 2, the efficiency of removal of metal ions from aqueous solutions significantly depends on their initial concentration. As a diffusion parameter, the initial concentration of metal cations represents the driving force for the mass transport process between the liquid and solid phases, while in the reaction sense it dictates the dynamics of the chemical binding of cations to functional groups (24). Galvanic waters that are created during the production process in various industrial plants, most often contain a combination of several different metals, which can cause mutual influence and interference during their removal by the biosorption process. The present metal ions compete with each other for the binding sites for the active centers on the biosorbent. In order to examine the adsorption of heavy metal cations in complex multicomponent systems, the composition of which corresponds to real samples, experiments were conducted with a mixture of metal cations.

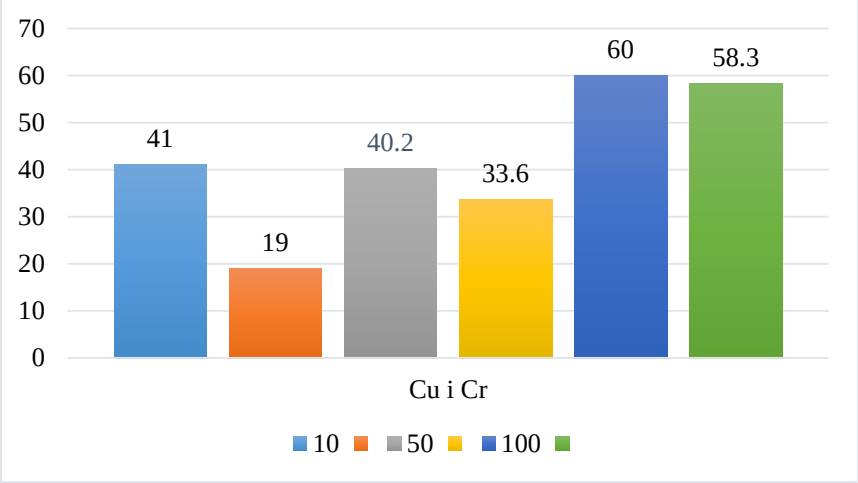

Figure 2. Efficiency of removal of metal ions (%) using coffee waste in Cu-Cr binary systems at initial metal concentrations of 10, 50 and 100 mg/L

Cu(II) had a higher adsorption value in the examined binary system, compared to Cr(III). Given that Cu(II) has an unpaired electron configuration, it can be assumed that the ion's tendency to bind to the surface of the adsorbent is the determining factor, due to the mentioned unpaired electrons. Cr(III) has a stable electronic configuration, but a smaller radius that is easier to incorporate into the surface structure of the adsorbent. In addition, this ion can be found in water solutions in several forms, depending on its concentration and pH value of the solution. Its efficiency decreases with increasing pH value, because the concentration of H(II) ions decreases, and the surface of the adsorbent becomes more negatively charged, which prevents the binding of chromium ions, because at the pH value at which the sorption procedures were performed, chromium can also be found in the form of Cr(II).

The results obtained in this way confirm the previously stated hypothesis that the affinity of the biosorbent towards a specific metal ion is correlated with the investigated physicochemical properties of that metal ion. In this regard, it can be concluded that the smaller the ionic radius of the metal and the higher the electronegativity of the metal ion, as well as the unpaired electronic configuration, the higher the degree of adsorption of the given metal ion. The removal efficiency of Cu(II) and Cr(III) increases with increasing their initial concentrations, where the highest removal efficiency of Cu(II) was 60% at an initial ion concentration of 100 mg/L, and 58% for Cr(III) at initial ion concentration of 100 mg/L.

4. CONCLUSIONS

Coffee grounds can be used as a native biosorbent for the removal of Cu(II) and Cr(III) from waste galvanic waters and is an important material for further research, with the fact that it would be necessary to modify it to increase the adsorption efficiency. The obtained values for the cation exchange capacity show that the Ca(II) is dominant during the ion exchange mechanism with Cu(II) and Cr(III). The obtained value of the point of zero charge was 5.0. At pH values below these, the surface of the biosorbent is positively charged, and at higher pH values, it is negatively charged. The assumption that there is an exchange of heavy metal ions with hydrogen ions and ions of alkaline and alkaline earth metals was also confirmed by FTIR analysis of the biosorbent.

An increase in the initial concentration of Cu(II) and Cr(III), from 10 to 100 mg/L, leads to a significant difference in the efficiency of their removal and increases with increasing concentration.

REFERENCES

1. Milan D. Gorgievski. (2015) Adsorpcija jona teških metala iz vodenih rastvora korišćenjem pšenične slame kao adsorbensa, Univerzitet u Beogradu, Tehnički fakultet u Boru, Doktorska disertacija, Bor.
2. Arsenijević, S.R. (2001). Hemija opšta i neorganska. Beograd : Partenon
3. Ahmetović M., Šestan I., Bergić S., Tučić E., Hasanbašić A. (2019). Biosorption of heavy metals from the multi-component systems of the galvanic industry using brewer's grain as adsorbents. EPH - International Journal of Applied Science ISSN: 2208-2182, Volume-5, Issue-5.
4. Šteka I. (2016) Obrada otpadnih voda nakon postupka galvanizacije metala. Master' Thesis. University of Zagreb, Faculty of Mining, Geology and Petroleum Engineering; Available at: https://repozitorij.rgn.unizg.hr/islandora/object/rgn:494/preview.
5. Tatjana D.Šoštarić. (2016). Uklanjanje teških metala iz vodenih rastvora biosorbentom na bazi koštica kajsija kao otpadne biomase, Doktorska disertacija, Univerzitet u Beogradu, Poljoprivredni fakultet.
6. V. V. Ranade, V.M. Bhandari, Industrial Wastewater Treatment, Recycling and Reuse, Elsevier Science, 2014.

7. P. Grimshaw, J.M. Calo, G. Hradil, Cyclic electrowinning/precipitation (CEP) system for the removal of heavy metal mixtures from aqueous solutions, Chem. Eng. J. 175 (2011) 103–109.
8. J. Lu, Y. Li, M. Yin, X. Ma, S. Lin, Removing heavy metal ions with continuous aluminum electrocoagulation: A study on back mixing and utilization rate of electrogenerated Al ions, Chem. Eng. J. 267 (2015) 86–92.
9. O.S. Amuda, I.A. Amoo, O.O. Ajayi, Performance optimization of coagulant/flocculant in the treatment of wastewater from a beverage industry, J. Hazard. Mater. 129 (2006) 69–72.
10. X.Z. Yuan, Y.T. Meng, G.M. Zeng, Y.Y. Fang, J.G. Shi, Evaluation of tea-derived biosurfactant on removing heavy metal ions from dilute wastewater by ion flotation, Colloids Surfaces A Physicochem. Eng. Asp. 317 (2008) 256–261.
11. R. Camarillo, Á. Pérez, P. Cañizares, A. de Lucas, Removal of heavy metal ions by polymer enhanced ultrafiltration. Batch process modeling and thermodynamics of complexation reactions, Desalination. 286 (2012) 193–199.
12. A. Oehmen, R. Viegas, S. Velizarov, M.A.M. Reis, J.G. Crespo, Removal of heavy metals from drinking water supplies through the ion exchange membrane bioreactor, Desalination. 199 (2006) 405–407.
13. L. Trakal, V. Veselská, I. Šafařík, M. Vítková, S. Číhalová, M. Komárek, Lead and cadmium sorption mechanisms on magnetically modified biochars, Bioresour. Technol. 203 (2016) 318–324.
14. A. Abdolali, W.S. Guo, H.H. Ngo, S.S. Chen, N.C. Nguyen, K.L. Tung, Typical lignocellulosic wastes and by-products for biosorption process in water and wastewater treatment: A critical review, Bioresour. Technol. 160 (2014) 57–66.
15. Đorđević., S. and Dražić, V. (2010). Fizička hemija. Beograd: TMF.
16. Indira Šestan , Melisa Ahmetović, Amra Odobašić, Amra Bratovčić , Sabina Begić. (2018). Physical and Chemical Characterization of Agricultural Waste and Testing of Sorbtion Abilities for Removal of Heavy Metals from Aqueous Solutions. International Journal for Research in Applied Sciences and Biotechnology, Volume-5, Issue-6.
17. P. Esquivel, V.M. Jiménez, Functional properties of coffee and coffee by-products, Food Research International. 2012, 46, 488-495.
18. G.Z. Kyzas, N.K. Lazaridis, A.C. Mitropoulos, Removal of dyes from aqueous solutions with untreated coffee residues as potential low-cost adsorbents: Equilibrium, reuse and thermodynamic approach, Chemical Engineering Journal. 2012, 189–190, 148-159.

19. S.L. Ching, M.S. Yusoff, H.A. Aziz, M. Umar, Influence of impregnation ratio on coffee ground activated carbon as landfill leachate adsorbent for removal of total iron and orthophosphate, Desalination. 2011, 279, 225-234.
20. A.S. Franca, L.S. Oliveira, A.A. Nunes, C.C. Alves, Microwave assisted thermal treatment of defective coffee beans press cake for the production of adsorbents, Bioresource Technology. 2010, 101, 1068-1074.
21. M. Hirata, N. Kawasaki, T. Nakamura, K. Matsumoto, M. Kabayama, T. Tamura, S. Tanada, Adsorption of Dyes onto Carbonaceous Materials Produced from Coffee Grounds by Microwave Treatment, Journal of Colloid and Interface Science. 2002, 254, 17-22.
22. A.E. Navarro, R.F. Portales, M.R. Sun-Kou, B.P. Llanos, Effect of pH on phenol biosorption by marine seaweeds, Journal of Hazardous Materials. 2008, 156, 405-411.
23. S. Smiljanić, G. Ostojić, A. Došić; Ispitivanje uticaja tretmana i mineraloškog sastava na tačku nultog naelektrisanja crvenog mulja; Naučni rad ISSN 0351-9465, E-ISSN 2466-2585 UDC:622.794.2/.3:537.242.082,72 doi: 10.5937/ZasMat1801007S Zastita Materijala 59 (1) 7 - 20 (2018)
24. J. Acharya, J.N. Sahu, C.R. Mohanty, B.C. Meikap, Removal of lead(II) from wastewater by activated carbon developed from Tamarind wood by zinc chloride activation, Chem. Eng. J. 149 (2009) 249–262.

ADDITIVE MANUFACTURING AND CHARACTERISATION USING DIGITAL IMAGE CORRELATION OF TENSILE PIPE RING SPECIMENS

Isaak D. Trajković [1], Miloš S. Milošević [1], Aleksandar S. Sedmak [2], Marko P. Rakin [3], Zoran M. Radosavljević [4], Goran M. Mladenović [2], Bojan I. Medjo [3]

[1] Innovation Center of the Faculty of Mechanical Engineering, Kraljice Marije 16, 11120, Belgrade, Serbia, trajkovicisaak@gmail.com.

[2] University of Belgrade, Faculty of Mechanical Engineering, Kraljice Marije 16, 11120, Belgrade, Serbia.

[3] University of Belgrade, Faculty of Technology and Metallurgy, Karnegijeva 4, 11120, Belgrade, Serbia.

[4] Research and Development Institute Lola, Kneza Višeslava 70A, 11030 Belgrade, Serbia.

Abstract

The examination of structures and parts of pressure equipment fabricated by additive production techniques is an insufficiently studied area. With the development of new techniques and materials, additive production is becoming increasingly important when it comes to functional replacement parts for different assemblies and devices, in addition to an already established role in rapid prototyping. In order to develop a method for testing the pressure equipment, such as pipelines, prototypes of ring-shaped test specimens with a stress concentrator (new pipe ring tensile specimens) are fabricated by different techniques and from different non-metallic and metallic materials. In this work, the focus is on polylactic acid (PLA) specimens fabricated on a Fused Deposition Modeling (FDM) printer. The rings are produced in the axial direction, in such a way that the contours of the material obtained by extrusion through the nozzle are loaded with tension during the testing. 3D-printed pipe rings are tested on an electro-mechanical universal testing machine, Shimadzu. The testing is accompanied by digital image correlation (DIC) on the specimen surface; the GOM Aramis system, consisting of two cameras, acquisition equipment, and software, is utilized. In this way, 3D displacement/strain field on the specimen surface is tracked. The obtained results indicate that repeatability of the testing process is possible, and the development of the methodology will be continued in the same direction. Further work will include a discussion on the applicability and possible limitations of the proposed testing procedure in the analysis of different stress concentrators on pipelines (including corrosion and stress corrosion defects).

Keywords: pipe ring specimens, additive manufacturing, tensile testing, digital image correlation

1. Introduction

The development of test tubes in the form of a tension ring was born as an idea for the improvement and better understanding of non-standard samples for testing of pipelines, which were described in the work of Gubeljak and Matvijenko (1,2). The mentioned authors developed a type of non-standard specimens under the acronym PRNB (Pipe Ring Notched Bending) specimens. Further work on the development of PRNB test tubes and procedures for non-standard integrity testing of pipelines under pressure was carried out by the research groups of the University of Maribor and Belgrade (5-7). These research groups continued the development of fracture analysis of PRNB samples, with the main focus being micromechanical fracture analysis. What makes the difference between PRNBtype test specimens and other developed test specimens is that in PRNB-type test specimens, the crack is located in the longitudinal direction, which is critical when the pipeline is subjected to internal pressure. (3,9)

The type of test specimens examined in this study - Pipe Ring Notched Tension, PRNT, was designed and so that compared to PRNB test specimens, it tends to change the loading case; tension is applied instead of bending. This implies a change in the stress and deformation field that is monitored in this work through the application of the Aramis GOM 2M system. This type of monitoring of deformations and displacements is based on the method of digital image correlation – DIC (10,13).

2. Experimental

2.1. Techniques of additive manufacturing

2.1.1. FDM technique

One of the additive manufacturing techniques used to make samples for the purposes of this research is the FDM (Fused Deposition Modeling) technique. This technique is characterized by the stacking of layers of melted thermoplastic material (Figure 1) as shown in the given diagram. (14).

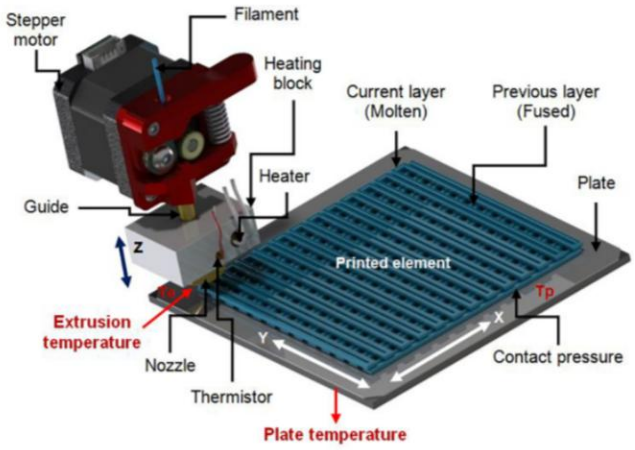

Figure 1. Schematic display of FDM 3D printer assembly and working principle (14)

The principle of operation of the FDM printer is based on passing the filament through rollers driven by stepper motors and pushing the filament through a guide that directs the filament to the heating block. Temperatures in the material heating block are defined in the gcode preparation program. Material heated to melting temperatures passes through the nozzle and stacked along paths defined by gcode.

2.1.2. SLS technique

Additive manufacturing, apart from techniques in which the objects are obtained by stacking layers of melted material, is performed through techniques in which the objects are obtained by polymerization or sintering of powdered materials. SLS (Selective Laser Sintering) additive manufacturing technique is characterized by the precise production of objects by polymerizing the powder with a laser that sinters it along the paths according to the gcode. The scheme of operation of 3D printers that work according to this principle is shown in Figure 2 (15).

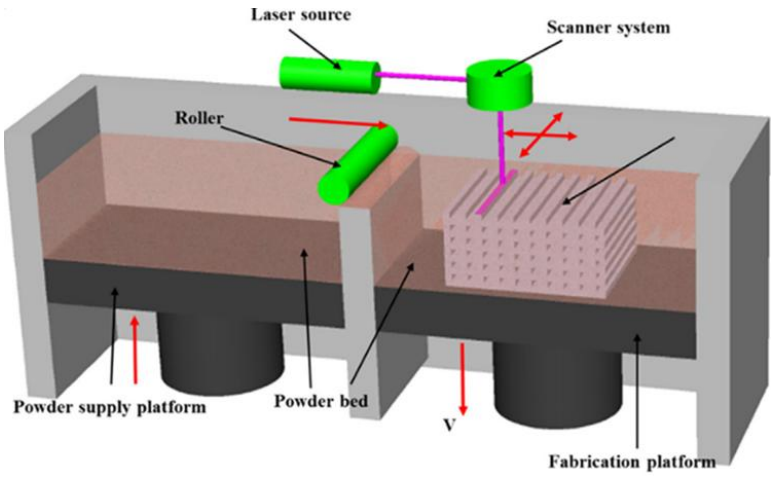

Figure 2. Schematic display of SLS 3D printer assembly and working principle (15)

3D printers for the SLS manufacturing technique have a powder supply platform that pushes the material from the powder bed up to the height of one layer, which is transferred to the fabrication platform using a roller. After coating one layer of powder, the device directs the laser along the path determined by the gcode. The powder is sintered in contact with radiation, that is, the material is polymerized layer by layer.

The described techniques are among the most used additive manufacturing techniques, and both can be considered relevant for such research. For this research, the conditions and measurements performed on the samples produced by the FDM technique will be described.

The tests were performed on ring-shaped test specimens made of PLA premium filament material from German RepRap on a 3D printer model x400 from the same manufacturer (Figure 3). The conditions for the production of the ring-shaped test tubes were constant, as were the parameters during the production of the samples according to the manufacturer's recommendation. The diameter of the filament used is 1.75 mm, while the nozzle diameter is 0.4 mm. The infill type of ring-shaped specimen is a fast honeycomb with infill material 100 %. The number of outer contours is 2.

Figure 3. Pipe Ring Notched Tensile specimens.

The rings were printed according to the specified conditions, after which a sharp notch was fabricated. Before testing, a stochastic pattern was applied to the part of the ring whose surface was recorded by the cameras of the Aramis system. This pattern represents the necessary matrix for the use of DIC methods and consists of a matte white background and finely dispersed black dots obtained using a spray.

The samples prepared in this way and ready for testing are mounted on a tool specially made and protected by the Institute for Intellectual Property (Figure 4). (16)

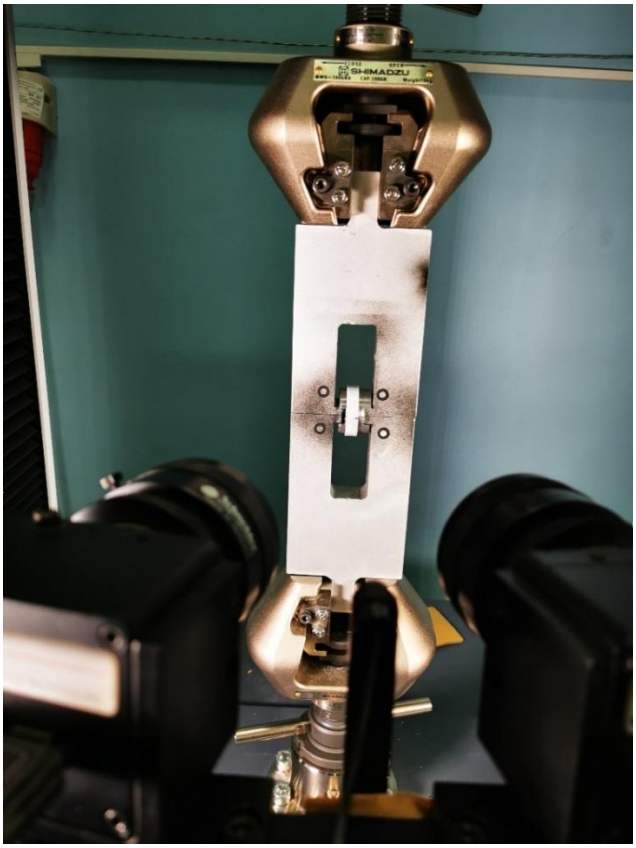

Figure 4. Test conditions.

The samples were tested on a Shimadzu AGS-X tensile testing machine with a working capacity of 100 kN. Inscribing was performed in the direction of tension at a speed of 0.5 mm/min until the material failed. During the loading of the samples, they were monitored by cameras of the Aramis GOM system. The recording speed is constant: one image every second. By using this system, data on displacements and deformations measured on the surface of the samples were obtained.

3. Results and Discussion

Figure 5 shows a tested sample after the failure of the material. This example shows the propagation of a crack that moves in the plane of the sharp notch. Crack propagation is expected and very clearly visible, regardless of the fact that the material is brittle.

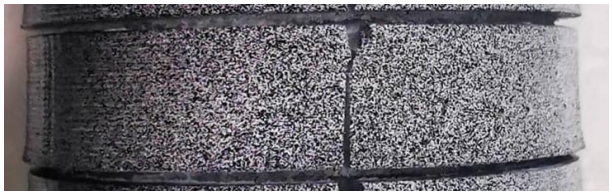

Figure 5. Photo of the tested sample after the failure.

Figure 6 shows the report from the Gom Aramis system software, with the displacement values in the direction of the Y axis. Based on the image in the upper right corner, we can register the maximum and minimum displacements, the values of which can be interpreted in the scale to the right of the image.

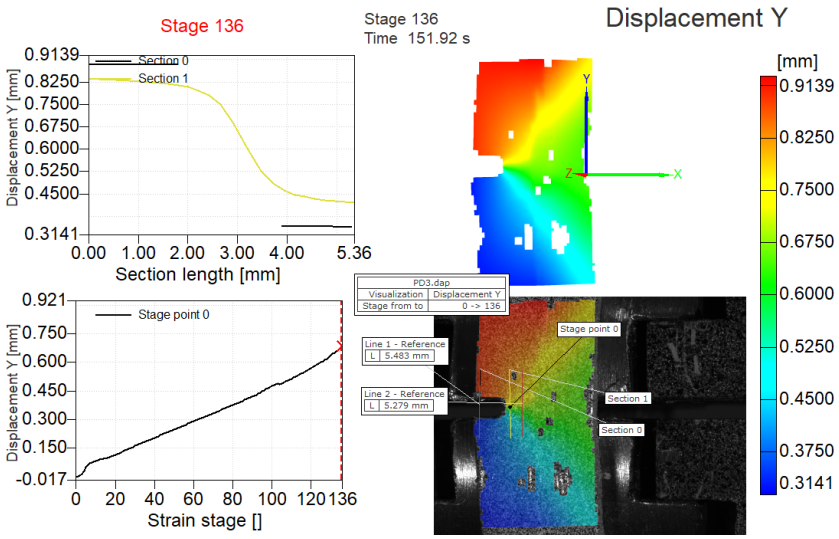

Figure 6. Report image from software of Aramis system. Field of displacement in Y direction.

4. Conclusions

In this paper, two techniques for 3D printing are briefly described - Fused Deposition Modeling FDA and Selective Laser Sintering SLS. Testing of the Pipe Ring Notched Tension – PRNT specimens, fabricated by FDM, by application of a system for monitoring the field of displacement and deformation are presented. The used additive manufacturing technique and material met the requirements regarding the structure of the manufactured samples as well as their behavior. Other available thermoplastic materials such as ABS, PET-G, PP, etc. would also be a possible choice for this type of samples.

On the basis of the displacement field obtained during this test, a gradient of displacement is clearly observed, which shows a suitable angle for crack opening and further propagation. Digital image correlation, in addition to the displacement and strain fields, allows us to monitor parameters that directly depend on displacement field, such as the Crack Opening Displacement or COD.

It should be mentioned that the examination of the 3D-printed PLA specimens presented in this work is a stage in the development of the procedure for testing the Pipe Ring Notched Tensile specimens cut from the metallic thin-walled pipes.

Acknowledgements

The Authors would like to thank the Ministry of Education, Science and Technological Development of the Republic of Serbia for providing financial support that made this work possible (by the contract: 451-03-68/2022-14/200105 and 451-03-68/2022-14/200135). The authors would also like to acknowledge the support from European Union's Horizon 2020 research and innovation program (H2020-WIDESPREAD-2018, SIRAMM) under grant agreement No 857124.

References

1. N. Gubeljak, A. Likeb, Y. Matvienko, Procedia Materials Science,3 (2014) 1934–1940.
2. Y.G. Matvienko, N. Gubeljak, Model for Determination of crack-resistance of the pipes, Patent No. RU 2564696 C, (in Russian), (2015).
3. D. Damjanović, D. Kozak, N. Gubeljak, Engineering Fracture Mechanics,205 (2019) 347–358.
4. D. Damjanovic, D. Kozak, I. Gelo, N. Gubeljak, Theoretical and Applied Fracture Mechanics, 103 (2019) 102286.
5. W. Musraty, B. Medjo, P. Štefane, Z. Radosavljević, Z. Burzić, M. Rakin, Chemical Industry,72 (2018) 39–46.
6. W. Musraty, B. Medjo, N. Gubeljak, A.Likeb, I. Cvijović-Alagić, A. Sedmak, M. Rakin, Engineering Fracture Mechanics,175 (2017) 247–261.
7. B. Medjo, M. Rakin, N. Gubeljak, Y. Matvienko, M. Arsić, Ž. Šarkoćević, A. Sedmak, Engineering Failure Analysis, 58 (2015) 429–440.
8. A. Likeb, N. Gubeljak, Y. Matvienko, Fatigue and Fracture of Engineering Materials and Structures, 37 (2014) 1319–1329.
9. B. Medjo, M. Arsić, M. Mladenović, Z. Savić, V. Grabulov, Z. Radosavljević, M. Rakin, Structural Integrity and Life, 20 (2020) 82-86.
10. M. Milošević, N. Milošević, S. Sedmak, U. Tatić, N. Mitrović, Sergej Hloch, Radomir Jovičić , Tehnicki Vjesnik, 23, no. 1 (2016) 19–24.
11. M. Milošević, N. Mitrović, R. Jovičić, A. Sedmak, T. Maneski, A. Petrović, A. Tarek, Chem. Listy, 106 (2011) 485-488.
12. M. Milošević, N. Mitrović, A. Sedmak, 15th IEEE International Conference on Intelligent Engineering Systems, (2011) 421–425.
13. N. Mitrović, M. Milošević, N. Momčilović, A. Petrović, Ž. Mišković, A. Sedmak, P. Popović, Key Engineering Materials, 586 (2014) 214-217.

14. M. Vorkapić, I. Mladenović, T. Ivanov, A. Kovačević, M.S. Hasan, A. Simonović, I. Trajković, Advances in Mechanical Engineering, 14 (2022) 1-15.
15. I. Trajković, M. Milošević, M. Travica, M. Rakin, G. Mladenović, Lj. Kudrjavceva, B. Medjo, Science of Sintering, 54 (2022) 373-386.
16. M. Travica, N. Mitrović, G. Mladenović, A. Milovanović, N. Milošević, M. Milošević, A. Petrović, "Tool for testing ring-shaped specimens," National patent No. 1629, (2019).

Nutraceuticals and Pharmaceuticals

COMPARISON OF LIQUID AND LYOPHILIZED SERPYLLI HERBA WASTE EXTRACTS PREPARED AT DIFFERENT pH VALUES

Aleksandra Jovanović[1*], Mina Volić[1], Nataša Obradović[1], Branko Bugarski[2]

[1]University of Belgrade, Innovation Centre of Faculty of Technology and Metallurgy, Karnegijeva 4, 11000 Belgrade, Serbia,

[2]University of Belgrade, Faculty of Technology and Metallurgy, Karnegijeva 4, 11000 Belgrade, Serbia

*acancarevic@tmf.bg.ac.rs

Abstract

Polyphenol recovery and physico-chemical properties of the extracts depend on the type of solvents and their pH values. Additionally, due to the presence of different biologically active compounds in plant waste, plant extracts obtained from industrial by-processing can find potential applications in various products. In the present study, Serpylli herba waste extracts were prepared using maceration (60 min), a solid-to-solvent ratio of 1:30, the particle size of plant waste 0.3 mm, and two types of the extraction medium: 50% ethanol (pH 6) and 50% ethanol with glacial acetic acid (pH 2.5). The lyophilization process was chosen as the next step (-75°C, 0.011 mbar, for 24 h). Comparison of liquid and lyophilized extracts prepared at different pH values was done *via* analyzing total polyphenol content (TPC, Folin-Ciocalteu method), total flavonoid content (TFC, colorimetric assay), antioxidant capacity (ABTS and DPPH assays), zeta potential, and conductivity (photon correlation spectroscopy). TPC of liquid extracts prepared at pH 2.5 and pH 6 amounted to 1.38 and 1.23 mg GAE/mL, respectively, while lyophilized parallels had 271.7 and 188.8 mg GAE/g, respectively. The same trend is noticed in the case of TFC: 0.368 and 0.334 mg CE/mL for liquid extracts obtained at pH 2.5 and pH 6, respectively, and 102.5 and 99.7 mg CE/mL for lyophilized parallels. ABTS radical scavenging activity of the liquid extracts at pH 2.5 and pH 6 was 0.767 and 0.750 mmol TE/L, respectively and for the lyophilized parallels was 0.136 and 0.111 mmol TE/g. IC_{50} (concentration for neutralization of 50% of DPPH free radicals) was 1.12 and 1.75 mg/mL for the liquid extracts prepared at pH 2.5 and pH 6, respectively and 0.331 and 0.391 mg/mL for the lyophilized parallels. The zeta potential of the liquid extracts at pH 2.5 and pH 6 was 1.74 and -2.56 mV, respectively, whereas the zeta potential of lyophilized parallels was -3.55 and -18.7 mV. Conductivity of the liquid extracts was 0.864

(pH 2.5) and 0.423 mS/cm (pH 6), whereas for the lyophilized extracts it was 0.199 (pH 2.5) and 0.452 mS/cm (pH 6). The presented results provide the information on physico-chemical properties of Serpylli herba waste liquid and lyophilized extracts that can add value and improve the quality of the existing food, functional food, pharmaceutical and cosmetic products, as well as for drinking water and wastewater treatment.

Keywords: lyophilization, polyphenols, Serpylli herba, waste, zeta potential

1. Introduction

The Lamiaceae family consists primarily of herbs and shrubs, with approximately 200 genera and 3200 species, and is distinguished by aromatic herbage, quadrangular stems, and verticillate inflorescences. *Thymus serpyllum* L. (creeping thyme, wild thyme, or mother of thyme) is thyme species from the Lamiaceae family, which grows in almost all the countries bordering the Mediterranean and is extensively cultivated in Central Europe, Asia, and the United States (1). According to the literature (2, 3), Serpylli herba contains a wide range of active compounds, such as essential oil (0.4-2.3%), flavonoids (luteolin-7-O-glucuronide, luteolin-7-O-glucoside, luteolin-7-O-rutinoside, apigenin, etc.), and phenolic acids (rosmarinic, syringic, vanilic, chlorogenic, p-coumaric, and caffeic acids). The all mentioned compounds could be responsible for Serpylli herba antioxidant, antimicrobial, anthelmintic, carminative, expectorant, analgesic, stimulant, diaphoretic, antispasmodic, diuretic, and anti-inflammatory properties (1, 4-6).

Plant waste, such as tea dust, banana peel, lemon skin grape, olive, apple, and carrot pomace, contains various biologically active components that can find potential applications in food, pharmaceutical, and cosmetic industries (6-9). There is the possibility to use dust particles for the isolation of active components that can be used as natural additives in food products and ingredients in pharmaceutical and cosmetic preparations (10). Tea waste of Serpylli herba contains essential oil, polyphenols, monoterpenes, polysaccharides, and proteins (5, 11, 12).

The pH of the extraction solvent is an important factor that influences the solubility of the target components. Herbal sources contain various polyphenol compounds that have different solubility at different pH values (13). The ethanolic plant extracts can be used in different industry sectors, due to their activity against different hazards and human pathogens, incorporation into different carriers, and the presence of various biologically active compounds (6, 14-16). Nevertheless, bioactive components in the liquid extracts are susceptible to chemical and physical degradation. Therefore, one of the most used drying

techniques is lyophilization which uses freezing and low pressure to obtain a dried formulation. Lyophilized samples are stable over long periods due to the prevention of hydrolytic and oxidative reactions toward the bioactive and non-active substances during storage (10, 17).

Chemical characterization of ethanol and lyophilized extracts of Serpylli herba waste included determination of total polyphenol and flavonoid contents (TPC and TFC, respectively) and radical scavenging activity (ABTS and DPPH assays), whereas analyzed physical properties were conductivity and zeta potential.

2. Experimental

2.1. Plant material and reagents

Dried and grinded Serpylli herba (particle size 0.3 mm, herbal dust or waste) was from the Institute for Medicinal Plants Research ”Dr Josif Pančić”, Pančevo, Serbia. The following reagents of the analytical purity grade were used: ethanol and sodium carbonate (Fisher Scientific, UK), Folin-Ciocalteu reagent, gallic acid and glacial acetic acid (Merck, Germany), sodium nitrite (Alkaloid, Macedonia), potassium persulfate (Centrohem, Serbia), 2,2'-azino-bis(3-ethylbenzothiazoline-6-sulphonic acid) - ABTS, 6-hydroxy-2,5,7,8-tetramethylchroman-2-carboxylic acid - Trolox, and 2,2-diphenyl-1-picrylhydrazyl - DPPH (Sigma-Aldrich, USA).

2.2. Preparation and lyophilization of the extracts

Serpylli herba waste extracts were prepared using maceration (60 min) in the shaker (KS 4000i control, IKA, Germany), a solid-to-solvent ratio of 1:30, the particle size of plant waste 0.3 mm, and two types of extraction medium: 50% ethanol (pH 6) and 50% ethanol with glacial acetic acid (pH 2.5).

Before the lyophilization, ethanol was removed from the extracts at 50 mbar and 50°C for 30 min, using Heizbad Hei-VAP rotary evaporator (Heidolph, Germany). Subsequently, the samples were lyophilized (-75˚C, 0.011 mbar, for 24 h) in Beta 2-8 LD plus lyophilizator (Christ, Germany).

2.3. Determination of total polyphenol and flavonoids content

Total polyphenol content (TPC) was determined spectrophotometrically using the modified Folin-Ciocalteu method (12), while total flavonoid content (TFC) was evaluated by a colorimetric assay described by Barros et al. (18). TPC was expressed as milligram of galic acid equivalent per milliliter of liquid extract or per gram of lyophilized extract (mg GAE/mL or mg GAE/g, respectively). TFC was expressed as milligram of catechin equivalent per milliliter of liquid extract or per gram of lyophilized extract (mg CE/mL or mg CE/g, respectively).

2.4. Determination of ABTS and DPPH radical scavenging activity

The ABTS and DPPH assays are based on the reduction of free radicals in alcohol solution by polyphenols (12). ABTS radical scavenging capacity was expressed as mmol Trolox equivalents per milliliter of liquid extract or per gram of lyophilized extract (mmol TE/mL or mmol TE/g, respectively). DPPH radical scavenging capacity was expressed as the concentration of the extract required to scavenge 50% of free radicals, IC50 (mg/mL). All absorbance readings were performed on UV spectrophotometer, UV-1800 (Shimadzu, Japan).

2.5. Determination of zeta potential and conductivity

The Zeta potential (mV) and conductivity (mS/cm) of the obtained extracts were determined by photon correlation spectroscopy (PCS) in Zetasizer Nano Series, Nano ZS (Malvern Instruments Ltd., UK). Each sample was measured three times at room temperature. Lyophilized samples were diluted before the analysis.

2.6. Statistical analysis

The analysis of variance (one-way ANOVA) followed by Duncan's post hoc test (STATISTICA 7.0) was used for the statistical analysis and the differences were considered statistically significant at $p<0.05$, $n=3$.

3. Results and Discussion

Comparison of liquid and lyophilized extracts prepared at different pH values (2.5 and 6) was performed *via* analyzing TPC, TFC, ABTS and DPPH antioxidant capacity, zeta potential, and conductivity.

3.1. Total polyphenol and flavonoid contents of the extracts

With the aim to investigate the influence of different pH values of the extraction medium on chemical composition of ethanol Serpylli herba extracts, the analyses of TPC and TFC were performed. The results are presented in Table 1.

Table 1. Total polyphenol content (TPC), total flavonoid content (TFC), ABTS and DPPH antioxidant capacity of Serpylli herba extracts (liquid and lyophilized) prepared using 50% ethanol (pH 6) and 50% ethanol with glacial acetic acid (pH 2.5).

Sample	TPC [mg GAE/mL or mg GAE/g]	TFC [mg CE/mL or mg CE/g]	ABTS [mmol TE/mL or mmol TE/g]	IC_{50} DPPH [mg/mL]
liquid pH 2.5	$1.38\pm0.01^{a*}$	0.368 ± 0.004^{b}	0.767 ± 0.027^{a}	1.12 ± 0.04^{a}
liquid pH 6	1.23 ± 0.06^{b}	0.332 ± 0.002^{a}	0.775 ± 0.035^{a}	1.75 ± 0.04^{b}
lyophilized pH 2.5	271.1 ± 17.1^{a}	102.5 ± 1.1^{a}	0.136 ± 0.001^{b}	0.331 ± 0.015^{b}
lyophilized pH 6	188.8 ± 14.2^{b}	99.7 ± 0.9^{b}	0.111 ± 0.004^{a}	0.391 ± 0.023^{a}

*Values with different letters (a-b) in each extract group showed statistically significant differences ($p<0.05$; n=3; analysis of variance, Duncan's *post-hoc* test); GAE, gallic acid equivalent; CE, catechin equivalent; TE, Trolox equivalent; IC_{50}, the concentration of the extract required to neutralize 50% of DPPH radicals.

As can be seen from Table 1, the influence of the extraction medium pH value on the TPC and TFC of the extracts was statistically significant. Namely, the TPC of the liquid extract prepared at pH 2.5 was statistically higher (1.38±0.01 mg GAE/mL) compared to the extract prepared at pH 6 (1.23±0.06 mg GAE/mL). Additionally, the lyophilized samples had TPC of 271.7±17.1 mg GAE/g (pH 2.5) and 188.8±14.2 mg GAE/g (pH 6). The same trend is noticed in the case of TFC, 0.368±0.004 and 0.334±0.002 mg CE/mL for liquid extracts obtained at pH 2.5 and pH 6, respectively, and 102.5±1.1 and 99.7±0.9 mg CE/mL for lyophilized parallels. The obtained results of TPC and TFC are in agreement with the literature data, where the concentration of polyphenols in grape extracts increased with the decrease of pH from alkaline to acidic values (19). According to Friedman and Jurgens (20), the release of polyphenols from grapes was significantly higher in extremely acidic surroundings compared to pH 6.

3.2. Antioxidant potential of the extracts

The impact of different pH values of three extraction mediums on the antioxidant capacity of ethanol Serpylli herba extracts was also examined using two antioxidant tests (ABTS and DPPH methods) and the results are presented in Table 1.

The effect of the extraction medium pH value on ABTS and DPPH radical scavenging capacity of the extracts was statistically significant, as in the case of TPC and TFC (Table 1). ABTS radical scavenging potential of the liquid extracts at pH 2.5 and pH 6 was 0.767 and 0.750 mmol TE/L, respectively. The antioxidant potential for the lyophilized parallels was 0.136 and 0.111 mmol TE/g.

In DPPH assay, IC50 was significantly lower, i.e. higher antioxidant potential, at pH 2.5 (1.12±0.04 mg/mL) in comparison to the liquid extract prepared at pH 6 (1.75±0.04 mg/mL) and 0.331±0.015 and 0.391±0.023 mg/mL for the lyophilized parallels.

The obtained results are in agreement with the literature data, where several studies have shown a positive correlation between polyphenol concentration and antioxidant capacity (21-23). Namely, polyphenols are the most important components that possess the antioxidant capacity and play an important role, as reducing agents, free radical scavengers, potential complexes of prooxidant metals, and quenchers of singlet oxygen, in protection against disorders caused by oxidant damage (21). Dastmalchi et al. (22) have reported that the fraction of the extracts from species of the Lamiaceae family, which has the highest flavonoid content, also possesses the highest antioxidant activities. According to Miraj et al. (21), the radical scavenging activities of plant extracts have arisen from the content of some representatives of polyphenol compounds, including quercetin, quercitrin, rutin, gallic, rosmarinic, and caffeic acids.

3.4. Zeta potential and conductivity of the extracts

The Zeta potential and conductivity of Serpylli herba extracts are presented in Figure 1. Zeta potential (absolute value), as a measurement of the system stability, was the highest for the lyophilized extract prepared at pH 6 (-18.7±0.7 mV), followed by lyophilized extract prepared at pH 2.5 (-3.55±0.15 mV). The zeta potential of the liquid extracts prepared at pH 2.5 and pH 6 was 1.74±0.16 and -2.56±0.21 mV, respectively (Figure 1). Determination of the extract zeta potential is important from the aspect of its future application, including potential encapsulation and use in drinking water treatment. The Zeta potential of plant

extracts depends on extraction conditions and thus of the extracted compounds, and absolute values vary from 2 mV to 15 mV (24).

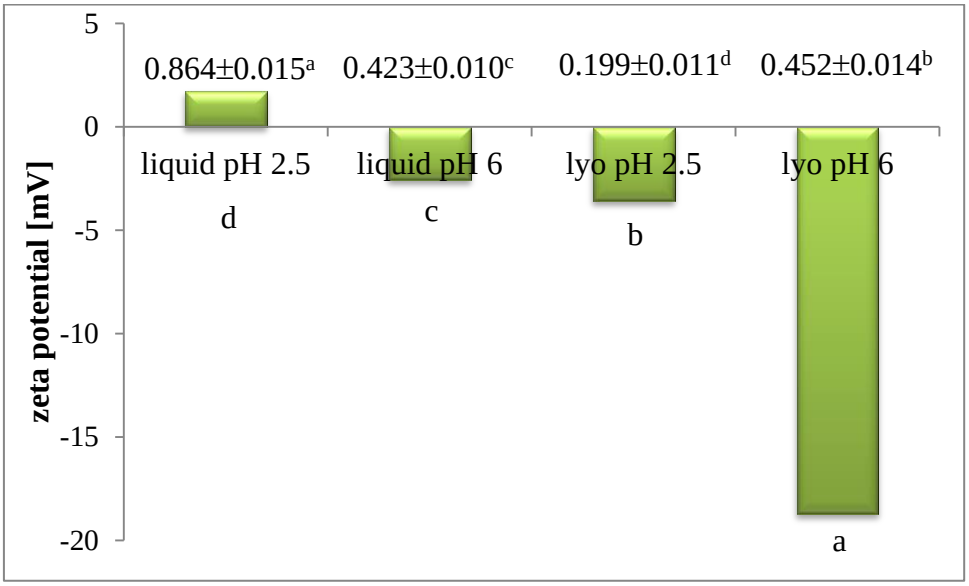

Figure 1. Zeta potential (bars) and conductivity (numbers above bars, mS/cm) of Serpylli herba extracts (liquid and lyophilized) prepared using 50% ethanol (pH 6) and 50% ethanol with glacial acetic acid (pH 2.5).

Suliman et al. (25) and Jurinjak Tušek et al. (26) have reported that the conductivity of the extracts can be used as a predictor of their antioxidant capacity and the extracts that possessed a higher antioxidant potential showed a higher value of conductivity as well. The conductivity of the liquid extracts was 0.864±0.015 and 0.423±0.010 mS/cm (for pH 2.5 and 6), whereas for the lyophilized parallels it was 0.199±0.011 and 0.452±0.014 mS/cm (Figure 1, numbers above the bars). However, the conductivity is influenced by the presence of extraneous ions, therefore analysis of the extract antioxidant activity using antioxidant assays is necessary.

4. Conclusion

In the presented research, the comparison of liquid and lyophilized Serpylli herba waste extracts prepared at different pH values was done via determination of TPC, TFC, antioxidant capacity, zeta potential, and conductivity. The liquid and lyophilized extracts prepared at pH 2.5 had statistically higher TPC and TFC in comparison to parallels prepared at pH 6. ABTS and DPPH radical scavenging potential were in a positive correlation to the polyphenol and flavonoid concentrations in the extracts. Zeta potential was the highest for the lyophilized

extract prepared at pH 6, while conductivity was the highest for the liquid extract prepared at pH 6 which was not correlated to the antioxidant capacity of the extract. Thus, the pH value of the extraction medium, as well as extract form should be chosen depending on the future application of the extract.

5. Acknowledgments

The authors acknowledge their gratitude to the Ministry of Education, Science and Technological Development of Serbia, contract numbers 451-03-68/2022-14/200003, 451-03-68/2022-14/200287, 451-03-68/2022-14/200135, and 451-03-68/2022-14/200019.

6. References

1. Khan, I., Abourashed E. Leung's encyclopedia of common natural ingredients used in food, drugs, and cosmetics. John Wiley & Sons, Inc. **2010.**
2. Monographs, Serpylli herba, Wild Thyme European Scientific Cooperative on Phytotherapy (ESCOP). Notaries House, United Kingdom. **2014.**
3. PDR for Herbal Medicines, Third ed. Thomson PDR, New Jersey. **2004.**
4. Hussain, A. I., Anwar, F., Chatha, S. A. S., Latif, S., Sherazi, S. T. H., Ahmad, A., Worthington, J., Sarker S.D. Chemical composition and bioactivity studies of essential oils from two *Thymus* species from the Pakistani flora. LWT – *Food Sci. Technol.*, **2013**, *50*, 185-192.
5. Jarić, S., Mitrović, M., Pavlović. P. Review of ethnobotanical, phytochemical, and pharmacological study of *Thymus serpyllum* L. *eCAM*, **2015**, *2015*, 1-10.
6. Jovanović, A., Vajić, J., Mijin, D., Zdunić, G., Šavikin, K., Branković, S., Kitić, D., Bugarski, B. Polyphenol extraction in microwave reactor using by-product of *Thymus serpyllum* L. and biological potential of the extract. *JARMAP*, **2022**, *31(10)*, 100417.
7. Brown da Rocha, C., Noreña, C. Microwave-assisted extraction and ultrasound-assisted extraction of bioactive compounds from grape pomace. *Int. J. Food Eng.*, **2020**, *16(1–2)*, 20190191.
8. Nastasi, J. R., Kontogiorgos, V., Daygon, V. D., Fitzgerald M. Pectin-based films and coatings with plant extracts as natural preservatives: A systematic review. *Trends Food Sci. Technol.*, **2022**, *120*, 193-211.

9. Panić, M., Radić Stojković, M., Kraljić, K., Škevin, D., Radojčić Redovniković, I., Gaurina Srček, V., Radošević K. Ready-to-use green polyphenolic extracts from food by-products. *Food Chem*., **2019**, *283*, 628-636.
10. Munin, A., Edwards-Lévy, F. Encapsulation of natural polyphenolic compounds: A review. *Pharmaceutics*, **2011**, *3*, 793–829.
11. Čančarević, A., Bugarski, B., Šavikin, K. & Zdunić, G. Biological activity and ethnomedicinal use of *Thymus vulgaris* and *Thymus serpyllum*. Lekovite Sirovine, **2013**, *33*, 3–17.
12. Jovanović, A., Djordjević, V., Petrović, P., Pljevljakušić, D., Zdunić, G., Šavikin K., Bugarski B. The influence of different extraction conditions on polyphenol content, antioxidant and antimicrobial activities of wild thyme. *JARMAP*, **2021**, *25*, 100328.
13. Zam, W., Bashour, G., Abdelwahed W., Khayata W. Effective extraction of polyphenols and proanthocyanidins from Pomegranate's peel. *Int J Pharm Pharm Sci.*, **2012**, *4*, 675-682.
14. Albu, S., Joyce, E., Paniwnyk, L., Lorimer, J.P., Mason, T.J. Potential for the use of ultrasound in the extraction of antioxidants from *Rosmarinus officinalis* for the food and pharmaceutical industry. *Ultrason. Sonochem.*, **2004**, *11*, 261-265.
15. Armendáriz-Barragán, B., Zafar, N., Badri, W., Galindo-Rodríguez, S. A., Kabbaj, D., Fessi, H., Elaissari, A. Plant extracts: from encapsulation to application. *Expert Opin. Drug Deliv.*, **2016**, *13*, 1165-1175.
16. Tavares, W. R., Barreto, M. D. C., Seca, A. M. Aqueous and ethanolic plant extracts as bio-insecticides-Establishing a bridge between raw scientific data and practical reality. *Plants*, **2021**, *10*, 920-950.
17. Fang, Z., Bhandari, B. Encapsulation of polyphenols—A review. *Trends Food Sci. Technol*., **2010**, *21*, 510–523.
18. Barros, L., Baptista, P., Ferreira, I. Effect of *Lactarius piperatus* fruiting body maturity stage on antioxidant activity measured by several biochemical assays. *FCT*, **2007**, *45*, 1731-1737.
19. Librán, C., Mayor, L., Garcia-Castello, E., Vidal-Brotons, D. Polyphenol extraction from grape wastes: Solvent and pH effect. *Agric. Sci*., **2013**, *4*(9B), 56-62.
20. Friedman, M., Jurgens, H.S. Effect of pH on the stability of plant phenolic compounds. *J. Agric. Food Chem.*, **2000**, *48*, 2101–2110.
21. Miraj, S., Kopae, M. R., Kiano, S. *Melissa officinalis* L: A review study with an antioxidant prospective. *eCAM*, **2016**, *22(3)*, 385-394.

22. Dastmalchi, K., Dorman, H. D., Oinonen, P. P., Darwis, Y., Laakso, I., Hitunen, R. Chemical composition and *in vitro* antioxidative activity of a lemon balm (*Melissa officinalis* L.) extract. LWT, *Food Sci. Technol*., **2008**, *41*, 391-400.
23. Triantaphyllou, K., Blekas, G., Boskou, D. Antioxidative properties of water extracts obtained from herbs of the species Lamiaceae. *Int J Food Sci Nutr*., **2001**, *52*, 313-317.
24. Skaf, D., Punzi, V., Rolle, J., Cullen, E. Impact of *Moringa oleifera* extraction conditions on zeta potential and coagulation effectiveness. *J. Environ. Chem. Eng.*, **2021**, *9(1)*, 104687.
25. Suliman, R. S., Asmani, F., Suliman, M. S., Hussain, M., Khan, J., Kaleemullah, M., Othman, N. B., Tofigh, A., Yusuf, E. A new approach for predicting antioxidant property of herbal extracts. *Int. J. Pharmacogn. Phytochem.*, **2015**, ***7****(1)*, 166-174.
26. Jurinjak Tušek, A., Benković, M., Valinger, D., Jurina, T., Belščak-Cvitanović, A., Gajdoš Kljusurić, J. Optimizing bioactive compounds extraction from different medicinal plants and prediction through nonlinear and linear models. *Ind Crops Prod.*, **2018**, *126*, 449-458.

OPTIMIZATION OF DIFFERENTIAL PULSE VOLTAMMETRIC METHOD FOR DETERMINATION OF TETRACYCLINE IN REAL SAMPLES WITH rGO-ZnO/GCE

Ana Đurović[1], Zorica, Stojanović[1], Zuzana Bytešniková[2], Snežana, Kravić[1], Lukáš Richtera[2,3], Martin Kormunda[4], Petr Bezdička[5]*

[1]*University of Novi Sad, Faculty of Technology Novi Sad, Bulevar cara Lazara 1, 21000 Novi Sad, Serbia*

[2]*Department of Chemistry and Biochemistry, Mendel University in Brno, Zemědělská 1, 613 00 Brno, Czech Republic*

[3]*Central European Institute of Technology, Brno University of Technology, Purkyňova 656/123, 612 00 Brno, Czech Republic*

[4]*Faculty of Science, J. E. Purkyne University, Pasteurova 1, 40096, Ústí nad Labem, Czech Republic*

[5]*Institute of Inorganic Chemistry of the Czech Academy of Sciences, Husinec-Řež 1001, 250 68 Husinec-Řež, Czech Republic*

*ana.djurovic@uns.ac.rs

Abstract

In this work, a differential pulse voltammetric methodology is optimized using a glassy carbon electrode modified with reduced graphene oxide – ZnO nanocomposite for the determination of tetracycline antibiotic. A Britton-Robinson buffer pH 8, which is used as a supporting electrolyte, provided one intense oxidation peak at +0.98 V *vs*. Ag/AgCl (3.5 mol/L, KCl). The analytical performance of the presented methodology under the optimized voltammetric parameters provides a linearity range of 4-400 μmol/L, detection and quantification limit of 0.632 μmol/L, and 1.915 μmol/L, respectively. Selectivity study showed that the developed methodology does not suffer from the influence of most investigated inorganic ions and organic molecules. In addition, high precision with values of RSD less than 2.5% (n=5 for intra- and inter-day) is achieved. A practical significance of the developed DPV protocol is demonstrated by direct quantitative analysis of the spiked water and human urine sample, with the obtained recovery values near 100%.

Key words: tetracycline, differential pulse voltammetry, modified glassy carbon electrode, water, urine

1. Introduction

Since its discovery in the 1950s, tetracyclines (TCs) as a group of antibiotics with more than twenty derivatives, have achieved a remarkable breakthrough in the therapy of various diseases. Characterized as broad-spectrum agents, TCs are efficient against gram-positive and gram-negative bacteria, as well as mycoplasma, chlamydia, rickettsiae and protozoan parasites (1,2). Besides, TCs also exhibit anti-inflammatory, anti-apoptotic, and antiprotease activities, and may be useful in the treatment of gingivitis, while recent studies have inquired about their potential in the treatment of COVID-19 due to their antiviral activity (1,3,4). Antibiotic activity is manifested as a consequence of binding to bacterial ribosomes, by inhibition of bacterial protein synthesis, resulting in bacteriostatic activity, rather than cell death (5). Apart from the wide human use, and low production cost, TCs are widely utilized in livestock feed as growth promoters with numerous beneficial aspects (6). Considering the fact that consumers do not fully absorb these antibiotics, they are mostly excreted into the environment, posing thus a severe threat to public health through bacterial drug resistance, carcinogenicity, hepatic and renal failure, which requires continuous monitoring in various samples (7).

High-performance liquid chromatography has already been established as a standard methodology for the determination of tetracycline (TC), a member of the TCs group. In contrivance of complicated chromatographic methods, with the use of easily accessible equipment that offers rapid *in-situ* analysis, without sample pre-treatment, voltammetric methods have also found their application in real sample analysis. Particularly dominant are methods based on the use of a glassy carbon electrode (GCE), and its different modifications (8–14). As the performance of the electroanalytical methodology largely depends on the type of the working electrode, herein reduced graphene oxide-ZnO nanocomposite (rGO-ZnO) is used as a GC modifier. The use of such a sensor for TC determination has already been reported by our research group with the use of square-wave voltammetry (SWV) (15). In order to expand the performance of such a sensor, differential pulse voltammetry (DPV), as a voltammetric method also characterized by high sensitivity, is applied in this paper. It has been proven that the application of such a modifier improves the performance of the GCE, by combining the advantages of these two interesting materials rGO and ZnO, and finds application for the determination of various analytes (16).

2. Experimental

DPV analyses are carried out in an electrochemical cell in a three-electrode system, using a potentiostat PalmSens 4 workstation (GA Houten, Netherlands), administered by PSTrace 5.8 software. The three-electrode system included rGO-ZnO modified GCE, Ag/AgCl (3.5 mol/L, KCl) and platinum wire as a working, reference and counter electrode, respectively. Before modification, the surface of the GCE is polished with alumina slurry on a special polishing cloth to a mirror-like surface. Afterwards, it is sonicated in a mix of ethanol and double distilled water (1/1, v/v), dried and used for modification.

Graphene oxide (GO) is prepared according to the simplified Hummer's method (17). 5 g of graphite flakes are oxidated in the mixture of concentrated H_2SO_4 and 30 g $KMnO_4$, with vigorously stirring. The oxidation is terminated after 10 days by the addition of 250 mL 30% wt H_2O_2 solution. GO is washed with 1 mol/L HCl (37% wt), and double distilled water (with a total volume of about 10 L) until a constant pH value (3-4) is achieved. 1 mL of GO (5 mg/mL) is added dropwise to the zinc solution $Zn(CH_3CO_2)x2H_2O$ (50 mL, 10 mmol/L) under stirring (400 rpm). Afterwards, a reducing agent (40 mg of $Na[BH_4]$) is slowly added to the mixture, and stirring is continued for the next 24 h to allow the reduction. The obtained nanocomposite is washed with double distilled water, and the final volume is adjusted to 10 mL. rGO-ZnO/GCE is prepared by dropping 10 μL of the suspension of the prepared nanocomposite on the surface of the GCE and allowed to dry for 15 min in the oven (50°C).

TC stock solution (2 mmol/L) is prepared by dissolving the solid substance (tetracycline hydrochloride 95%, Sigma Aldrich) in 0.01 mol/L HCl. As a water sample, tap water from the laboratory is used, while a human urine sample is obtained from a healthy adult and stored in the fridge. Before the analysis, the samples are diluted with the supporting electrolyte (0.1 mol/L Britton-Robinson (BR) buffer, pH 8) in the next ratio of 1/4 for water and 1/5 for a urine sample (v/v) and analyzed by the optimized DPV analysis using an rGO-ZnO/GCE as a sensing platform.

3. Results and discussion

An electroanalytical approach is proposed for the analytical determination of TC in different matrices by using rGO-ZnO decorated GCE as a sensing element, and DPV as a sensing technique. BR buffer pH 8 is selected as the optimal supporting electrolyte. By scanning the potential in the anodic range from +0.60 V to +1.30 V, one oxidation peak of TC is

discernible at the potential of +0.98 V. As demonstrated by preliminary experiments, rGO-ZnO is chosen as a modifier due to the remarkable increase in DPV response compared to the unmodified sensor. In fact, in DPV analyses, the anodic peak current in the case of the modified sensor increased almost 9 times in comparison to bare GCE (Figure 1). Such an appreciable increase in the signal is a consequence of the modifier presence, resulting thus in conductivity improvement and increasing in the active surface area of the modified sensor (15).

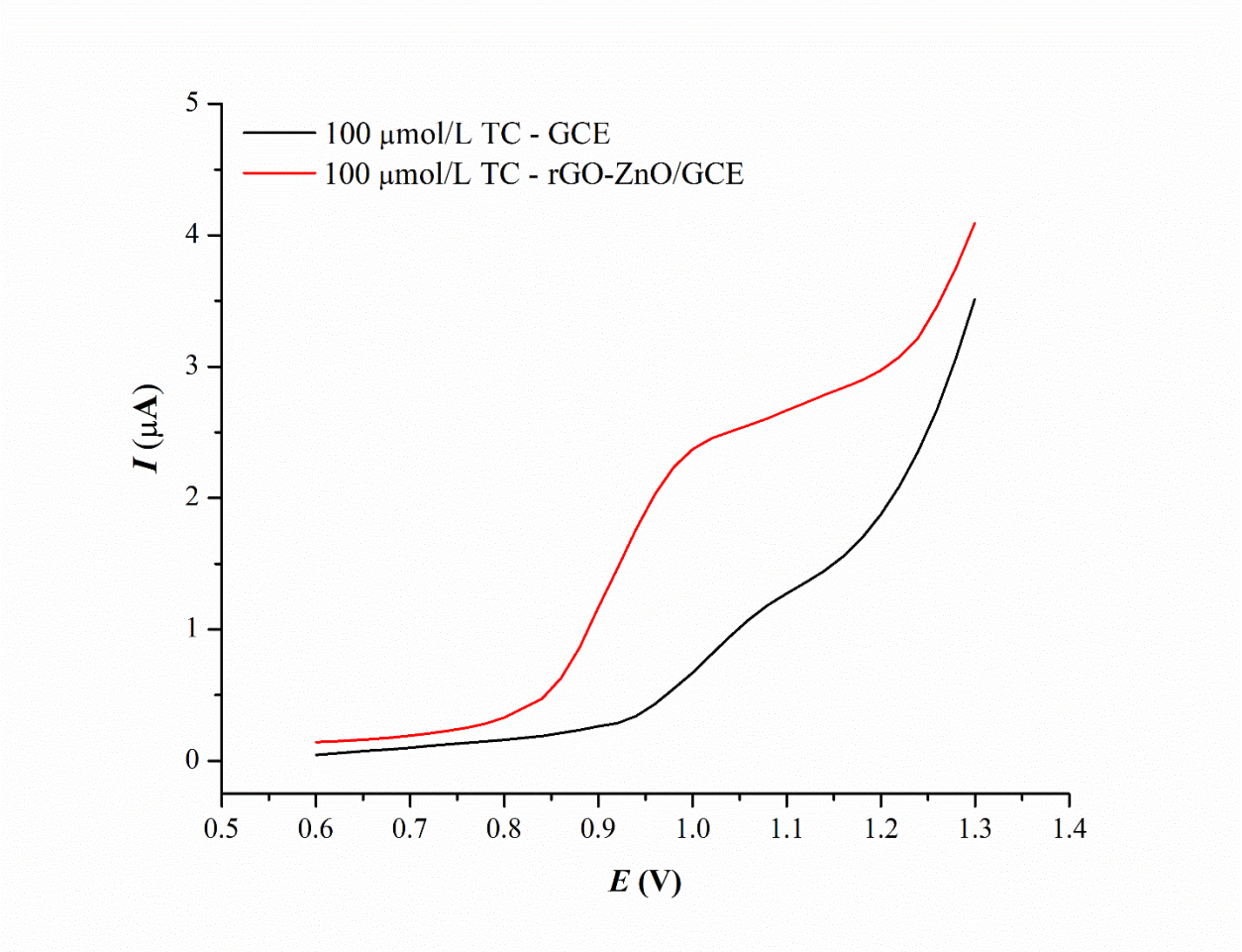

Figure 1. DPVs obtained by the preliminary experiments for GCE and rGO-ZnO/GCE (100 µmol/L TC) recorded in BR buffer pH 8

Achieving maximum sensitivity of the voltammetric analysis is performed by a detailed study whereby each parameter of the DPV study is carefully optimized. The effect of step potential (E_{step}), pulse amplitude (E_{pulse}), pulse time (t_{pulse}) and scan rate (v) on the oxidation peak current (50 µmol/L TC) is studied, and the obtained results are presented in Figure 2. The effect of the step potential is studied in the range of 5-50 mV. The obtained results demonstrated enhancement of sensitivity with increasing of a step potential up to 30 mV. A

decrease of sensitivity with values higher than 30 mV can be explained by too fast potential scanning, which is not appropriate for the oxidation of TC. Since the best peak shape is obtained with a step potential value of 20 mV, with a suitable current response, this value is adopted in further work.

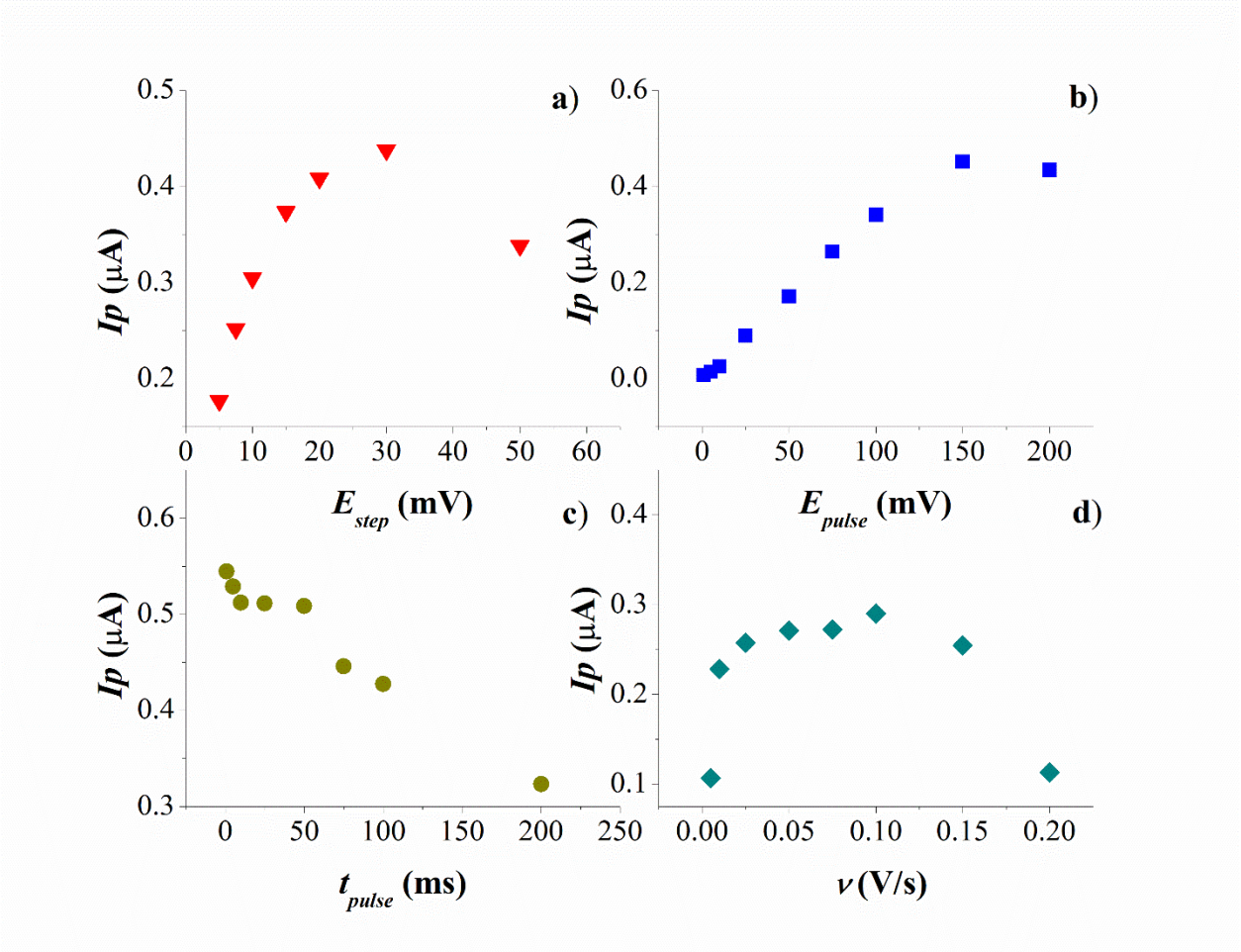

Figure 2. The effect of DPV parameters on peak height of TC (50 μmol/L) obtained on rGO-ZnO/GCE in BR buffer pH 8: a) step potential (E_{step}), b) pulse amplitude (E_{pulse}), c) pulse time (t_{pulse}) and d) scan rate (ν)

An increase of the pulse amplitude from 1 to 200 mV caused an increase of the signal intensity up to a pulse amplitude value of 150 mV, with a subsequent decrease. A value of 100 mV is accepted as optimal due to a peak broadening at higher amplitude values. Next, the impact of pulse time on TC oxidation peak current is investigated in the range from 1 to 200 ms. The experiments showed that slightly higher signal values are obtained for pulse time values from 1 to 50 ms, with a subsequent respectable decrease. The best appearance of the anodic peak is accomplished at a pulse time of 50 ms. The effect of the scan rate on the TC oxidation peak is studied in the 0.005-0.2 V/s. The value of peak current reaches its

maximum at 0.1 V/s and then begins to decrease, and this value is therefore chosen as optimal for performing the voltammetric analysis.

Further, analytical features of the voltammetric method regarding linearity, detection and quantification limit (LOD, LOQ), precision and selectivity are evaluated by following the optimal experimental and instrumental conditions previously established. A linear relationship between anodic peak current (*Ip*) and TC concentration (C_{TC}) is obtained for the eleven-point analytical curve in the concentration range from 4-400 µmol/L, with a correlation coefficient of $R^2 = 0.9959$ (Figure 3).

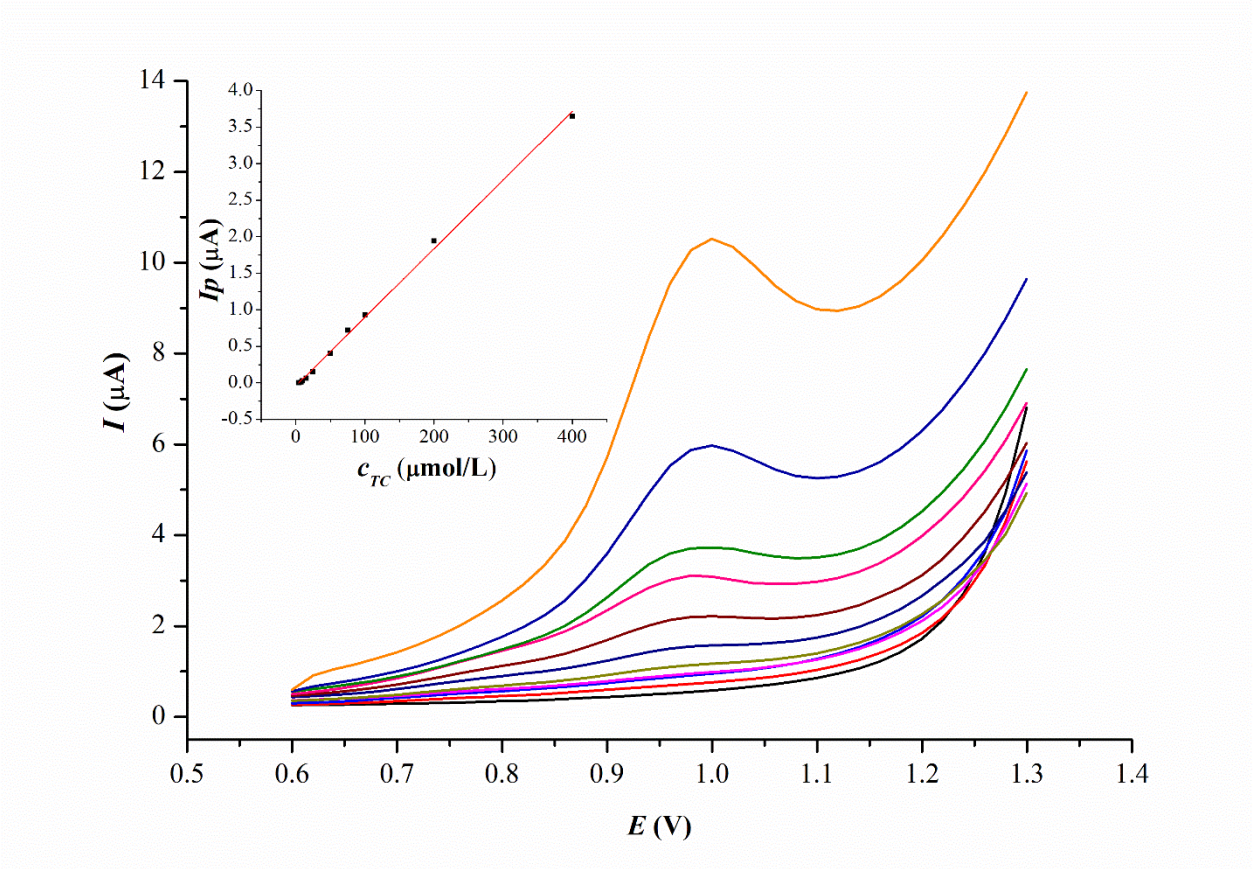

Figure 3. DPVs of TC recorded in BR buffer pH 8 with a blank at the bottom and increasing concentration of the analyte (4, 5, 7.5, 10, 15, 25, 50, 75, 100, 200 and 400 µmol/L TC) for rGO-ZnO/GCE. The inset shows the corresponding calibration curve.

The detection limit (0.632 µmol/L) and quantification limit (1.915 µmol/L) for TC are calculated from the calibration curve as follows: LOD = 3.3 SD/b and LOQ = 10 SD/b, where SD stands for a standard deviation of the intercept, and b is the slope of the calibration graph (18). The precision of the method (intra-day and inter-day) is estimated for two concentration levels (10 and 50 µmol/L), by performing scans for five probations prepared in an identical manner on the same day, and on five different days. The obtained RSD values for intra-day

and inter-day precision are less than 2.5%. The influence of some interfering agents such as inorganic ions and organic molecules, that can be often found in real samples is investigated. The experiments are performed in the fixed TC solution (20 μmol/L), with an increase in the concentration of each interference substance up to a 1000-excess value. $H_2PO_4^-$, SO_4^{2-} and urea completely did not affect, while 100-excess of Na^+, Cl^-, K^+ and NH_4^+ and 500-excess of Ca^{2+} depressed the TC analytical signal by less than 5%.

To test the utility of the developed methodology in real samples, it is applied for the analysis of TC in water and urine samples. The samples are analyzed after the simple dilution step, by following the optimized voltammetric parameters. Since the obtained voltammograms showed no detectable TC concentration, the samples are spiked with two different TC concentrations, while the standard addition method is used for quantitative purposes. The analysis of the samples is performed in triplicate (Table 1).

Table 1. The analysis of spiked water and urine sample using the proposed DPV method and rGO-ZnO/GCE.

Sample	Added (μmol/L)	Found[a] (μmol/L)	RSD (%)	Recovery (%)
Water	25	23.85	1.32	95.40
	50	51.18	2.51	102.37
Urine	50	49.91	2.20	99.82
	100	101.61	2.23	101.61

[a] n = 3.

The accuracy of the method has been evaluated throughout recovery values which are close to 100%. The obtained results indicate that the herein-developed methodology is useful for a simple and fast determination of TC antibiotic in samples of a complicated matrix, without any sample treatment.

4. Conclusion

In the present paper, the DPV technique is applied for the determination of the TC antibiotic using rGO-ZnO/GCE as a sensing platform. After a careful optimization study, the developed electroanalytical methodology provides an attractive alternative screening analysis with a detection limit of 0.632 μmol/L, a wide liner concentration range, high precision and rapid

response. Furthermore, rGO-ZnO/GCE in combination with DPV can be used as a useful tool for quantification of TC in complex real samples such as water and human urine, without complicated extraction procedures prior to the analysis.

5. Acknowledgment

The authors are grateful to the Ministry of Education, Science and Technological development of the Republic of Serbia for the financial support of this work (project number 451-03-68/2022-14/200134).

6. References

1. Grossman, T. H. Tetracycline Antibiotics and Resistance. *Cold Spring Harb Perspect. Med.* **2016**, *6(4)*, a025387.
2. Chopra, I., Roberts, M. Tetracycline Antibiotics: Mode of Action, Applications, Molecular Biology, and Epidemiology of Bacterial Resistance. *Microbiol. Mol. Biol. Rev.* **2001**, *65(2)*, 232–260.
3. Sodhi, M., Etminan, M. Therapeutic Potential for Tetracyclines in the Treatment of COVID-19. *Pharmacotherapy* **2020**, *40(5)*, 487–488.
4. Griffin, M. O., Fricovsky, E., Ceballos, G., Villarreal, F. Tetracyclines: A Pleitropic Family of Compounds with Promising Therapeutic Properties. Review of the Literature. *Am. J. Physiol. Cell Physiol.* **2010**, *299(3)*, C539–C548.
5. Thaker, M., Spanogiannopoulos, P., Wright, G. D. The Tetracycline Resistome. *Cell. Mol. Life Sci.* **2010**, *67(3)*, 419–431.
6. Granados-Chinchilla, F., Rodríguez, C. Tetracyclines in Food and Feedingstuffs: From Regulation to Analytical Methods, Bacterial Resistance, and Environmental and Health Implications. *J. Anal. Methods Chem.* **2017**, *2017*, 1–24.
7. di Cerbo, A., Pezzuto, F., Guidetti, G., Canello, S., Corsi, L. Tetracyclines: Insights and Updates of Their Use in Human and Animal Pathology and Their Potential Toxicity. *Open Biochem. J.* **2019**, *13(1)*, 1–12.
8. Turbale, M., Moges, A., Dawit, M., Amare, M. Adsorptive Stripping Voltammetric Determination of Tetracycline in Pharmaceutical Capsule Formulation Using Poly(Malachite Green) Modified Glassy Carbon Electrode. *Heliyon* **2020**, *6(12)*, e05782.

9. Palisoc, S., de Leon, P. G., Alzona, A., Racines, L., Natividad, M. Highly Sensitive Determination of Tetracycline in Chicken Meat and Eggs Using AuNP/ MWCNT-Modified Glassy Carbon Electrodes. *Heliyon* **2019**, *5(7)*, e02147.
10. Rajab Dizavandi, Z., Aliakbar, A., Sheykhan, M. A Novel Pb-Poly Aminophenol Glassy Carbon Electrode for Determination of Tetracycline by Adsorptive Differential Pulse Cathodic Stripping Voltammetry. *Electrochim. Acta* **2017**, *227*, 345–356.
11. Kesavan, S., Kumar, D. R., Lee, Y. R., Shim, J.-J. Determination of Tetracycline in the Presence of Major Interference in Human Urine Samples Using Polymelamine/Electrochemically Reduced Graphene Oxide Modified Electrode. *Sens. Actuators B Chem.* **2017**, *241*, 455–465.
12. Krepper, G., Pierini, G. D., Pistonesi, M. F., di Nezio, M. S. "In-Situ" Antimony Film Electrode for the Determination of Tetracyclines in Argentinean Honey Samples. *Sens. Actuators B Chem.* **2017**, *241*, 560–566.
13. Kushikawa, R. T., Silva, M. R., Angelo, A. C. D., Teixeira, M. F. S. Construction of an Electrochemical Sensing Platform Based on Platinum Nanoparticles Supported on Carbon for Tetracycline Determination. *Sens. Actuators B Chem.* **2016**, *228*, 207–213.
14. Vega, D., Agüí, L., González-Cortés, A., Yáñez-Sedeño, P., Pingarrón, J. M. Voltammetry and Amperometric Detection of Tetracyclines at Multi-Wall Carbon Nanotube Modified Electrodes. *Anal. Bioanal. Chem.* **2007**, *389(3)*, 951–958.
15. Đurović, A., Stojanović, Z., Bytešníková, Z., Kravić, S., Švec, P., Přibyl, J., Richtera, L. Reduced Graphene Oxide/ZnO Nanocomposite Modified Electrode for the Detection of Tetracycline. *J. Mater. Sci.* **2022**, *57(9)*, 5533–5551.
16. Manasa, G., Mascarenhas, R. J., Satpati, A. K., Basavaraja, B. M., Kumar, S. An Electrochemical Bisphenol F Sensor Based on ZnO/G Nano Composite and CTAB Surface Modified Carbon Paste Electrode Architecture. *Colloids Surf. B* **2018**, *170*, 144–151.
17. Hummers, W. S., Offeman, R. E. Preparation of Graphitic Oxide. *J. Am. Chem. Soc.* **1958**, *80(6)*, 1339–1339.
18. *ICH Topic Q 2 (R1) Validation of Analytical Procedures: Text and Methodology*. European Medicines Agency. https://www.ema.europa.eu/en/documents/scientific-guideline/ich-q-2-r1-validation-analytical-procedures-text-methodology-step-5_en.pdf (accessed 2022-06-06).

EFFECT OF DILUENTS ON PHARMACEUTICAL-TECHNOLOGICAL CHARACTERISTICS OF IMMMEDIATE RELEASE PARACETAMOL TABLETS

Jelena Čanji Panić[1], Nemanja Todorović[1], Milica Tubić[1], Ana Stjepanović[1], Nataša Milošević[1], Mladena Lalić-Popović[1*]

[1] University of Novi Sad, Faculty of Medicine Novi Sad, Department of Pharmacy, Hajduk Veljkova 3, 21137 Novi Sad, Serbia,

**mladena.lalic-popovic@mf.uns.ac.rs*

Abstract

Diluents are a very important group of excipients in tablets obtained by direct compression, as they make up the largest share of the mass of the tablet. In this study, the influence of the diluents on the properties of paracetamol tablets was examined. Four formulations of paracetamol tablets (F1, F2, F3 and F4) were made using a laboratory excenter machine. Lactose and microcrystalline cellulose were used as fillers which accounted for 88.5% of the tablet weight. The share of lactose in F1 was 0%, in F2 17.7%, in F3 70.8% and in F4 88.5%, while the remaining share of fillers was microcrystalline cellulose. Examination of dissolution profiles showed that all 4 formulations meet the requirements of the 10th European Pharmacopoeia for immediate release tablets. The difference in release rate was observed only in the first 5 min: F1 released the most (91.95%) and F4 the least (71.76%). These results were consistent with hardness and disintegration tests - formulations with a higher lactose content showed greater hardness and longer disintegration times. Mass variation testing showed that none of the four formulations met the requirements of the 10th European Pharmacopoeia, which is related to the poor flowability of the tested tableting masses. The optimal pharmaceutical-technological characteristics were obtained in formulation with a mixture of lactose and microcrystalline cellulose as diluents, where the share of lactose is higher (F3). In order to improve the flowability of the mixture, the tableting mass can be converted into granules, or a silica-type agent can be used.

Keywords: lactose, microcrystalline cellulose, dissolution profile, powder flowability, direct compression

1. Introduction

Tablets are the most commonly used oral solid dosage forms. One of the simplest methods of tablet formulation is direct powder compression. This process requires certain characteristics of mixture of excipients and active pharmaceutical ingredient (API), such as good compressibility and flow properties. Granulation is a method often used to improve powder properties, such as packing density and flowability, which leads to better compressibility (1).

Filling agents, also known as diluents, represent the most important group of excipients in tablets made by direct compression, because they make up the largest share of the tablet mass. Their main function is to achieve a practical size of a dosage form, be it powder, capsule filling or tablet. It often happens that the mass of the API in a single dose unit is small, therefore it is necessary to add an inert substance in order to produce a tablet of suitable size. These substances are expected to be physiologically and chemically indifferent, economically accessible, non-hygroscopic, biocompatible and to have an acceptable taste (2).

Microcrystalline cellulose (MCC) is one of the most important pharmaceutical fillers. Due to its excellent binding properties, good compressibility and good flow properties, it is suitable for direct compression method. It can also be used as a disintegrant, bonding agent, even as a lubricant (3). Lactose is a frequently used organic diluent. It is easily soluble in water, non-hygroscopic, cost-effective, easily available and compatible with most medicinal substances. It can be found in the following (pseudo)polymorphic forms: α-lactose monohydrate, anhydrous α-lactose, β-lactose and it can also be found in an amorphous form. Crystalline α-lactose monohydrate shows relatively weak binding properties and poorly flowability (4). Combining different diluents can lead to improvements in functionality of these excipients at subparticulate level, which results in better characteristics of their mixture compared to characteristics of each individual diluent (5).

Paracetamol is an API used to treat mild to moderate acute pain and elevated body temperature. It is usually formulated in the form of immediate release tablets (6). Paracetamol belongs to the III group of biopharmaceutical classification system, characterized by good solubility and poor permeability (7).

In this research, the influence of the choice and proportion of fillers (lactose and MCC) on the mechanical properties of paracetamol tablets made by the direct compression method was investigated. In addition, it was tested how and whether the release profile of the paracetamol changes depending on the composition of the tablet formulations.

2. Experimental

2.1. Chemicals

For the formulation of the tablets, paracetamol (Lachner, p.a., Czech Republic) was used as API, α-lactose monohydrate (Tablettose® Meggle, Hungary) and MCC (Vivapur® 101, Germany) were used as diluents, magnesium stearate (MgST) (Magnesium stearat®, Mosselman, Germany) as lubricant, and sodium starch glycolate (NaSG) (Primojel®, Alkaloid, North Macedonia) as super-disintegrant. Phosphate buffer (0.1 M, pH 6.8) was made using potassium dihydrogen phosphate (Lachner, p.a., Czech Republic) and sodium hydroxide (PanReac, p.a., Spain), in accordance with the United States Pharmacopoeia (8).

2.2. Tablet formulation

MCC and α-lactose monohydrate, as well as their mixtures, were used to evaluate the effect of the fillers. A full factorial design of 2^2 was applied and a total of four formulations were created. The composition of the tablets was formulated so that the proportion of all substances, except for fillers, was constant. Each formulation contained 7% paracetamol, 0.5% MgST and 4% NaSG. Lactose and MCC were used as fillers which accounted for 88.5% of the tablet weight. The share of lactose in F1 was 0%, in F2 17.7%, in F3 70.8% and in F4 88.5%, while the share of MCC was 88.5% in F1, 70.8% in F2, 17.7% in F3 and 0% in F4.

All the components were weighed and sieved through 355μm sieve. The powder mixture was then prepared in a mortar with a pestle, hand-mixed for approximately 30 min for each formulation. MgST was added 2 min before the end of mixing. Tableting was done using a laboratory excenter press. Die with a diameter of 12 mm was used. During tableting of different formulations, the position of the piston and the filling of the die were changed depending on the desired mass and mechanical properties of the tablets.

2.3. Flowability of powder mixture for tableting

The bulk and tapped density of samples of the powder mixture for tableting were tested in accordance with the 10th European Pharmacopoeia Method 1, in a graduated cylinder (9). The method was modified due to the limited amount of substances available for this research, and so a 100 ml graduated cylinder and 20 g of powder were used. Unsettled apparent volume V_0 and final tapped volume V_t were determined and bulk density (ρ_0) and tapped density (ρ_t) were calculated. Based on ρ_0 i ρ_t values, Hausner's ratio (HR) and Compressibility

Index (CI) were calculated and the obtained results were interpreted according to the guidelines of the 10th European Pharmacopoeia (9).

The angle of repose was also determined in accordance with the 10th European Pharmacopoeia (9). A funnel with a diameter of 20 mm was used, the wall of which is at an angle of 65° in the horizontal plane. The funnel was positioned at a height of 3 cm above the work surface.

2.4. Characterisation of tablets

The dissolution rate of paracetamol from the tested formulations was investigated using a paddle apparatus, according to the 10th European Pharmacopoeia (9). The release rate was measured using an Erweka device (model DT800, Germany). The speed of rotation of the paddles was 50 RPM, and the release of paracetamol was monitored for 60 min. Phosphate buffer pH 6.8 at a temperature of 37±0.5°C was used as a dissolution medium (900 ml). Phosphate buffer was chosen, because paracetamol dissolves best in this medium, and therefore solubility has no effect on the release profile of paracetamol, but only the pharmaceutical formulation of the tested tablets (10). Three samples of tablets from each prepared formulation were examined (12 tablets in total). Paracetamol concentrations were measured in samples after 5, 15, 25, 35, 45 and 60 minutes using a modified UV/Vis spectrophotometric method (11). The spectrum was recorded in the range from 200 to 400 nm. The samples were transferred to a quartz cuvette and the absorbance was measured at 243 nm. The blank used was the phosphate buffer (dissolution medium). Testing was performed on a UV/Vis spectrophotometer (Agilent Technologies, model 8453, USA). According to the requirements of 10th European Pharmacopoeia, the criteria for rapid release of the API are met if at least 80% of API is released within 45 minutes (9).

Testing of friability, disintegration, resistance to crushing, uniformity of mass and uniformity of content were also performed according to the regulations of the 10th European Pharmacopoeia (9). Friability was determined on a standard drum device (Erweka TA, Germany). The maximum permissible mass loss of the tested tablet samples is 1%, according to the Pharmacopoeia (9). Disintegration was measured using a standard device for determining disintegration (Erweka ZT54, Germany), with distilled water heated to a temperature of 37±0.5 °C as a medium. The Pharmacopoeial requirement for uncoated immediate release tablets states that the tablets should disintegrate within a maximum of 15 min (9). The resistance to crushing was measured with a Monsanto device. To determine the content of paracetamol, five tablets were crushed in a mortar with a pestle and dissolved in

phosphate buffer. The concentration of the obtained solutions was determined by the same spectrophotometric method used for the dissolution test (11). Tablets meet the test requirements of the Pharmacopoeia if each individual content is between 85% and 115% of the average content (9). The diameter and thickness of the tablet were measured using vernier caliper, and the measurement results were interpreted according to the regulations of the British Pharmacopoeia (12).

3. Results and discussion

The flowability of all four prepared mixtures for tableting was tested, using the methods of determining the bulk and tapped density, as well as by determining the angle of repose. The flowability of the tableting material is one of the critical factors during compression, because it greatly affects the accuracy of dosing and the uniformity of filling the tableting funnel. Also, flowability affects the mechanical characteristics of the manufactured tablets, which consequently affects the dissolution rate of the API.

It was determined that powder mixture for F1 has the lowest bulk and tapped density, followed by F2 and F3, and the highest bulk and tapped densities are observed for F4 powder mixture. Based on the values of CI and HR, it is concluded that all formulations have poor flowability, which can be seen in Table 1. The lower the values of HR and CI, the better the flowability of the powder mixture. We notice that F3 had the lowest values of HR and CI, thus the best flowability compared to the other prepared powder mixtures. It can be said that F3 powder mixture is even on the borderline between passable and poor flow properties according to the measured values of HR and CI.

Table 1. Evaluation of the flowability of powder mixture based on the bulk and tapped densities

Powder mixure	HR	CI [%]	Powder flow character
F1	1.41	29.17	Poor
F2	1.37	26.83	Poor
F3	1.35	26.17	Poor
F4	1.42	29.63	Poor

In addition to the assessment of the flow rate using the tapping method, the measurement of the angle of repose was also performed. The measured values are given in Table 2.

Table 2. Evaluation of the flowability of powder mixture based on the angle of repose

Powder mixture	Angle of repose [°]	Powder flow character
F1	41.15	passable
F2	38.78	fair
F3	31.74	good
F4	30.30	excellent/good

The formulation containing only lactose as a filler (F4) has the best flow properties based on the angle of repose. The difference in the results between the measurement of the angle of repose and the bulk and tapped density occurs because when evaluating flowability by bulk and tapped density, the propensity of the powder to distribute some particles between others is important, and the addition of MCC to lactose reduced the possibility of settling of lactose particles, which had the effect that F3 has the lowest CI and HR values. On the other hand, while the MCC particles are needle-shaped, the lactose particles are irregular in shape (13) and the MCC particles stack better onto each other and form a pile with a larger angle of repose.

The measured mean forces needed to crush a tablet are presented in Table 3. Formulation F1 showed the lowest resistance to crushing, while formulation F4 showed the highest values of mechanical hardness. Therefore, the formulation containing MCC as a filling agent produced a compact with the least strength, which is consistent with the fact that MCC is a ductile material. Lactose is a brittle material (13) and under similar pressure conditions, as was the case in this research, it makes harder tablets than MCC.

The measured values of friability test are shown in Table 3. Only F1 had a friability value of less than 1%, which is why it is the only tested formulation that complies with the requirements of 10th European Pharmacopoeia (9). Tablets with higher proportion of lactose, although harder, were more prone to chipping. The reason for this phenomenon is that lactose is plastic and MCC elastic material, thus tablets that contain predominantly lactose are more prone to chipping.

Results of disintegration test are shown in Table 3. It is possible that F1 and F2 showed the fastest disintegration due to the presence of a large proportion of MCC as a diluent, since MCC in contact with the aqueous medium swells and facilitates the release of the API (14). Also, the rate of disintegration is slower for tablets with a higher proportion of lactose, because they showed greater resistance to crushing.

Table 3 shows the results of measuring the paracetamol content in the tested tablets. The results are shown in percentages in relation to the possible content of paracetamol (the content of paracetamol is 7% of the weight of the tablet). All tested formulations correspond to the requirements of the 10th European Pharmacopoeia (9). The biggest deviation in relation to the average content is observed in F2, but it is still within the permissible limits of deviation prescribed by the Pharmacopoeia.

According to the requirements of the 10th European Pharmacopoeia, for tablets weighing more than 250 mg, the weights of 2 tablets are allowed to deviate by more than ±5% in relation to the average mass, and no mass may deviate by more than ±10% in relation to the average mass (9). The uniformity of mass test showed that none of the four prepared formulations met the requirements of 10th European Pharmacopoeia. Such a large mass variation is in accordance with the results of flowability testing, which indicated that none of the four tableting powder masses had satisfactory flowability. The mean values of the measured tablet masses are shown in Table 3.

Table 3. Results of pharmacopeial testing of the tablets

	F1	**F2**	**F3**	**F4**
Friability [%]	0.48	1.06	12.03	5.51
Disintegration [s]	7	4	37	55
Paracetamol content [%]*	110.45 ± 0.99	109.43 ± 11.56	102.64 ± 1.72	99.06 ± 7.31
Resistance to crushing [N]*	63.15 ±17.56	60.63 ± 15.64	86.23 ± 19.09	88.94 ± 10.7
Mass [g]*	0.42 ± 0.02	0.47 ± 0.03	0.71 ± 0.03	0.72 ± 0.03
Diameter [mm]*	12.02 ± 0.04	12.04 ±0.05	12.05 ± 0.05	12.01 ± 0.03
Thickness [mm]*	4.19 ± 0.04	4.42 ± 0.02	5.21 ± 0.05	5.09 ± 0.13

**mean value ± standard deviation*

The uniformity of diameter corresponded to the requirements of the British Pharmacopoeia (12), and so none of the tablets from all four formulations had a diameter variation greater than 5%. The same was the case with tablet thickness, where it was observed that none of the four tablet formulations varied in thickness by more than 5%. The mean tablet diameter and thickness are shown in Table 3.

Graph 1 shows the dissolution rate of paracetamol from the tested formulations. The percentage of paracetamol released was calculated in relation to the paracetamol content of

the manufactured tablets (each tablet contains paracetamol in the amount of 7% of its weight). All formulations met the pharmacopoeial requirements, that is, they released more than 80% of the paracetamol content in the first 45 minutes. Differences were observed only in the first five minutes, where F1 released 91.95% of its content, and the slowest release was shown by formulation 4, which released 76.71% of paracetamol. This indicates that tablets containing only lactose as a filler released paracetamol more slowly than those containing MCC. These results are consistent with the disintegration rate and resistance to crushing test results. Therefore, the formulation that disintegrated the slowest and had the highest resistance to crushing, which is formulation F4, also showed slowest paracetamol release rate.

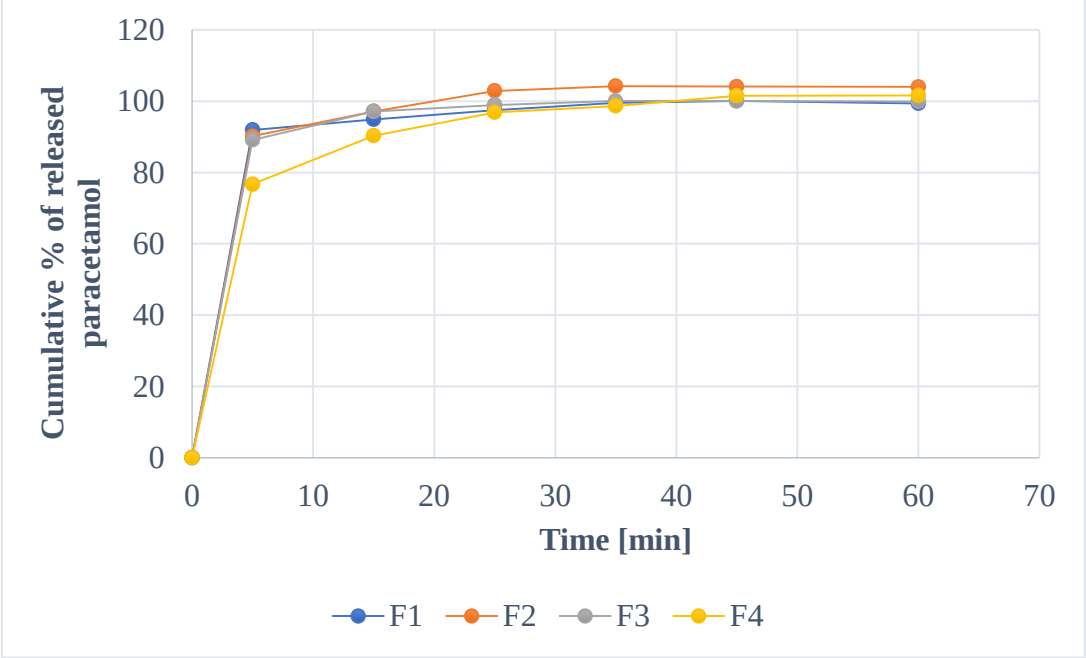

Graph 1. Dissolution profile of paracetamol from 4 tested formulations

4. Conclusion

This research showed that the filling agent has a great influence on the mechanical characteristics of the manufactured tablets as well as on the dissolution rate of paracetamol. The super-disintegrator NaSG was used in the preparation of the tablet formulations and immediate disintegration of all tablets was expected. However, it was observed that when lactose was used as a diluent, there was a slowdown in the disintegration and initial release of paracetamol. Tablets with higher amount of lactose had higher resistance to cruching, which

consequently had the effect of slowing down the disintegration of the tablets and the release of paracetamol.

Also, the flowability test indicated that another type of lubricating agent (for example silicon dioxide-type agent) should be added to the formulation to increase the flowability or the tableting mass should be converted into granulate. The best flowability was shown in formulation F3, which had a higher proportion of lactose and a lower proportion of MCC. This study suggests that when the disintegrant used in immediate release tablet formulation of paracetamol is NaSG, the diluent should be a mixture of MCC and lactose, where the proportion of lactose is greater than the proportion of MCC.

5. Acknowledgements

This study was supported by The Ministry of Education, Science and Technological Development, Republic of Serbia grant 451-03-68/2022-14/200114.

6. References

1. Tofiq, M., Nordström, J., Persson, A. S., Alderborn, G. Effect of excipient properties and blend ratio on the compression properties of dry granulated particles prepared from microcrystalline cellulose and lactose. *Powder Technol*. **2022**, *399*, 117207.
2. Alderborn, G., Frenning, G. Tablets and compaction. In *Aulton's Pharmaceutics: The Design and Manufacture of Medicines,* 5th edition; Aulton, E. M., Taylor, M. G. K., Eds.; Elsevier Ltd: London, **2018**; pp 517-563.
3. Hindi, S.S. Microcrystalline cellulose: the inexhaustible treasure for pharmaceutical industry. *Nanosci. Nanotechnol. Res*. **2017**, *4(1)*, 17-24.
4. Ilić, I., Kása Jr, P., Dreu, R., Pintye-Hódi, K., Srčič, S. The compressibility and compactibility of different types of lactose. *Drug Dev. Ind. Pharm.* **2009**, *35(10)*, 1271-80.
5. Akin-Ajani, O. D., Odeku, O. A., Olumakinde-Oni, O. Evaluation of the mechanical and release properties of lactose and microcrystalline cellulose and their binary mixtures as directly compressible excipients in paracetamol tablets. *J. Excip. Food Chem.* **2020**, *11(2)*, 42-52.
6. Fredholt, F., Di Meo, C., Sloth, S., Müllertz, A., Berthelsen, R. Direct visualizing of paracetamol immediate release tablet disintegration in vivo and in vitro. *Eur. J. Pharm. Biopharm*. **2022**, *180*, 63-70.

7. Kalantzi, L., Reppas, C., Dressman, J. B., Amidon, G. L., Junginger, H. E., Midha, K. K., Shah, V. P., Stavchansky, S. A., Barends, D. M. Biowaiver monographs for immediate release solid oral dosage forms: Acetaminophen (paracetamol). *J. Pharm. Sci.* **2006**, *95(1)*, 4-14.
8. The United States Pharmacopeia and National Formulary. USP 41–NF 36; The United States Pharmacopeial Convention, Inc.:Rockville, MD, **2018**.
9. European Pharmacopoeia, 10th ed.; European Directorate for the Quality of Medicines & Healthcare, Council of Europe: Strasbourg, France, **2019**.
10. Farheen, H., Mamatha, T., Yasmeen, Z., Sutradhar, S. Dissolution method development and validation of paracetamol–aceclofenac tablets. *Int. J. Pharm. Chem. Sci*. **2013**, 2(2), 902-908.
11. Ashraful Islam, S. M., Abuzar, S., Pijush Kumar, P. Validation of UV-Spectrophotometric and RP-HPLC methods for the simultaneous analysis of Paracetamol and Aceclofenac in marketed tablets. *Int. J. Pharm. Life Sci*. **2011**, *2(12)*, 1267-1275.
12. British pharmacopoeia; Medicines and Healthcare products Regulatory Agency; London, UK, **2017**.
13. Rowe, C.R.; Sheskey, J.P.; Quinn, E.M. *Handbook of Pharmaceutical Excipients*, 6th ed; Pharmaceutical Press: Grayslake, IL and American Pharmacists Association: Washington, DC, **2009**.
14. Yassin, S., Goodwin, D. J., Anderson, A., Sibik, J., Wilson, D. I., Gladden, L. F., Zeitler, J. A. The disintegration process in microcrystalline cellulose based tablets, Part 1: Influence of Temperature, Porosity and Superdisintegrants. *J. Pharm. Sci*. **2015**, *104(10)*, 3440-3450.

POTENTIALLY HARMFUL EXCIPIENTS IN PEDIATRIC ORAL COUGH MEDICINES AUTHORIZED IN SERBIA

Ana Stjepanović[1*], *Nemanja Todorović*[1], *Jelena Čanji Panić*[1], *Mladena Lalić-Popović*[1,2]

[1]*University of Novi Sad, Faculty of Medicine Novi Sad, Department of Pharmacy, Hajduk Veljkova 3, 21137 Novi Sad, Serbia*

[2]*University of Novi Sad, Faculty of Medicine Novi Sad, Centre for Medical and Pharmaceutical Investigations and Quality Control (CEMPhIC), Hajduk Veljkova 3, 21137 Novi Sad, Serbia*

*ana.stjepanovic@uns.ac.rs

Abstract

Some pharmaceutical excipients may cause adverse effects or excipient-related contraindications and interactions. The aim of this study was to identify all excipients with known effect (EKE) in pediatric oral cough medicines authorized in Serbia and evaluate EKE labeling in the corresponding Summaries of product characteristics (SmPCs) and Package leaflets (PLs). The study was designed as a post-authorization safety study and safety of excipients was considered in accordance with recommendations of the European Medicines Agency. Out of a total of 64 oral cough medicines authorized in Serbia, 58 (90.63%) of them were approved for pediatric use and all of these pediatric medicines contained one or more EKE. A total of 27 different EKE were identified, from 6 different functional categories (sweeteners, preservatives/antioxidants, electrolytes, solvents, solubilizing/emulsifying agents, and coloring agents) with most of them present in products approved for use across all ages of children and adolescents above the age of 2. A significant number of EKE labeling deficiencies were detected in product PLs and SmPCs, including complete omission of one or more EKE for 74.14% of products, as well as missing or incomplete EKE quantitative (44.83% of products) and/or safety information (44.83% of products). As negative effects of excipients may be more pronounced in the pediatric population compared to adults, it is especially important to consider EKE related safety issues when prescribing and dispensing medicines intended for children. Revision of the product PLs and SmPCs is recommended in order to eliminate deficiencies and improve EKE labeling.

Keywords: pediatrics, pharmaceutical adjuvants, pharmacovigilance, risk assessment

1. Introduction

Although the efficacy of several active ingredients in cough medicines has been brought into question in recent years (1), expectorants, mucolytics and antitussives are still widely used in Serbia. Based on a report for 2019, the annual sales of human and herbal cough and cold medicines (ATC group R05) in Serbia added up to approximately 7.6 million euros. Additionally, the same year, sales of traditional herbal cough medicines amounted to over 600,000 euros (2).

Cough is a very frequent symptom in children, as upper respiratory tract infections (URTI) are at least twice as common in the pediatric population compared to adults (up to 10 episodes a year) (1,3). The majority of cough medicines are liquid oral formulations which are particularly suitable for children due to the dosing flexibility and ease of swallowing (4,5). However, their formulation usually requires the use of excipients to improve the stability, palatability and taste of the preparation and some of these excipients can cause adverse effects, contraindications or interactions (4,6,7).

In the Annex to the European Commission guideline on 'Excipients in the labelling and package leaflet of medicines for human use', the European Medicines Agency (EMA) lists all the excipients with known action or effect (EKE) together with thresholds and additional safety information to appear in the corresponding product information (8). Appropriate EKE labeling is important for evaluation of possible excipient related adverse effects, especially for pediatric medicines as the negative effects of some excipients may be more pronounced in children compared to adults (9). Recognizing the unique vulnerability of the pediatric population, the European Paediatric Formulation Initiative (EuPFI) created the STEP (Safety and Toxicity of Excipients for Paediatrics) database to improve access to data on excipient safety in children (10).

Having in mind all the above, the aim of this study was to establish the number of oral cough medicines approved for pediatric use in Serbia as well as to detect all the EKE present in these products and determine EKE labeling deficiencies in the corresponding Summaries of product characteristics (SmPCs) and Package leaflets (PLs).

2. Experimental

The study was designed as a post-authorization safety study during March 2022. Data were collected from the Serbian national database of authorized human medicines and product SmPCs and PLs available online at the official website of the Medicines and Medical Devices

Agency of Serbia (11). SmPC sections 4.2. *Posology and method of administration* of all the oral cough medicines authorized in Serbia (ATC group *R05 - Cough and cold preparations* and traditional herbal medicines) were examined and preparations approved for use in the pediatric population were identified and further analyzed.

SmPCs of oral cough medicines authorized for pediatric use in Serbia were then scanned for qualitative and, if available, quantitative information on excipients and all EKE were identified. Excipients were classified as EKE if listed in EMA`s Annex (8) with the following routes of administration considered relevant: all, oral and local (e.g. possible effects on mucous membranes). The proportion of EKE containing pediatric oral cough medicines authorized in Serbia was determined as well as the prevalence of each identified EKE and, where available, the quantitative range at which these EKE were present in the products. EKE quantities were expressed per dose, taking into account all pediatric doses listed in the product SmPC and PL. For each EKE, the number of EKE containing preparations approved to treat cough depending on the pediatric age range was also determined.

The evaluation of EKE labeling in the PLs and SmPCs of analyzed pediatric oral cough medicines was done in accordance with the aforementioned Annex and the European Commission guideline on 'Summary of Product Characteristics' (8,12). If an excipient was not appropriately listed as EKE or appropriate quantitative and/or safety information was missing or incomplete in either the product SmPC or the PL, it was noted as a deficiency in EKE labeling.

3. Results and Discussion

Out of a total of 64 oral cough medicines authorized in Serbia, 58 (90.63%) of them were approved for use in the pediatric population. The number of different oral cough medicines approved for pediatric use in Serbia and the percentage of EKE containing products among them is shown in Table 1. All analyzed pediatric medicines contained at least one EKE (Table 1), which was unsurprising as most of them (43 preparations) were liquid oral dosage forms (syrups and oral solutions or powders and granules for oral solutions) that usually require the use of different excipients to ensure product stability and palatability, some of which are known to have negative physiological effects (4,6,7). Other pharmaceutical dosage forms included tablets and capsules (7 preparations), lozenges and pastilles (5 preparations) and effervescent tablets (3 preparations).

Table 1. Prevalence of EKE containing products among oral cough medicines (ATC R05 and traditional herbal medicines) approved for pediatric use in Serbia.

ATC classification			All medicines approved for pediatric use	EKE containing medicines approved for pediatric use (percentage [%])
R	R05	R05C	41	41 (100.00)
		R05D	6	6 (100.00)
		R05X	2	2 (100.00)
Traditional herbal cough medicines			9	9 (100.00)
		Total	**58**	**58 (100.00)**

R - Respiratory system, R05 - Cough and cold preparations, R05C - Expectorants, excluding combinations with cough suppressants, R05D - Cough suppressants, excluding combinations with expectorants, R05X - Other cough and cold preparations.

Table 2 shows the prevalence of each of the identified EKE, as well as, where possible, the quantitative range at which these EKE were present in pediatric oral cough medicines. A total of 27 different EKE were detected, from 6 different functional categories (sweeteners, preservatives and antioxidants, electrolytes, solvents, solubilizing/emulsifying agents, and coloring agents). Sorbitol and sodium were most frequently detected, with sorbitol being present in 41.38% and sodium in 36.21% of pediatric oral cough medicines authorized in Serbia (Table 2).

For each identified EKE, the number of medicines containing a particular excipient that are approved for use in children depending on age is shown in Figure 1. For most of the EKE, medicines containing them were approved for use across all age groups of children and adolescents above the age of 2 (Figure 1). None of the medicines were approved for children under 2, which was expected as cough and cold medicines are generally not recommended at this age due to the lack of clinical data and the possibility of adverse effects and dosing errors (13).

Table 2. Number of oral cough medicines approved for pediatric use in Serbia containing different EKE and the quantities at which the EKE were present in these preparations (where available).

EKE	EKE containing preparations (percentage of analyzed pediatric medicines [%])	EKE quantity	
		EKE quantity range in products [mg/dose]	Products with no information on EKE quantity (percentage of all products containing a specific EKE [%])
sweeteners			
sucrose	11 (18.97)	96,727-9.334,00	2 (18.18)
lactose	8 (13.79)	14,85-148,00	3 (37.50)
invert sugar	3 (5.17)	138,609-5.500,00	0 (0.00)
glucose	2 (3.45)	2,712-3.500,00	0 (0.00)
fructose	1 (1.72)	-	1 (100.00)
sorbitol (E420)	24 (41.38)	0,444-11.400,00	9 (37.50)
maltitol (E965)	10 (17.24)	530-6.021,705	6 (60.00)
isomalt (E953)	3 (5.17)	2.447,50	0 (0.00)
mannitol (E421)	2 (3.45)	-	2 (100.00)
xylitol (E967)	1 (1.72)	-	1 (100.00)
aspartame (E951)	2 (3.45)	-	2 (100.00)
preservatives and antioxidants			
(sodium)methyl paraben (E218, E219);	14 (24.14)	2,0-18,48	5 (35.71)
propyl paraben (E216)	6 (10.34)	0,6-2,00	2 (33.33)
sodium benzoate (E211)	7 (12.07)	-	7 (100.00)
benzoic acid (E 210)	6 (10.34)	-	6 (100.00)
butylated hydroxyanisole (E320)	4 (6.90)	0,0006	3 (25.00)
electrolytes			

sodium	21 (36.21)	5,8305-166,6	13 (61.90)
potassium	14 (24.14)	-	14 (100.00)
solvents			
ethanol	13 (22.41)	0,25-440,00	1 (7.69)
glycerol (E422)	11 (18.97)	-	11 (100.00)
propylene glycol (E1520)	10 (17.24)	350-700	9 (90.00)
solubilizing agents and emulsifiers			
macrogolglycerol hydroxystearat	2 (3.45)	-	2 (100.00)
hydroxypropyl betadex	2 (3.45)	-	2 (100.00)
coloring agents- Azo dyes			
Sunset yellow (E110)	3 (5.17)	-	3 (100.00)
Azorubin (E122)	2 (3.45)	-	2 (100.00)
Ponceau red (E124)	2 (3.45)	-	2 (100.00)
Brilliant black (E151)	2 (3.45)	-	2 (100.00)

Before therapeutic application of analyzed cough medicines, it is important to consider possible EKE related contraindications, such as those of certain sugars in adults and children with hereditary sugar intolerances or aspartame in patients with phenylketonuria (7,8). Additionally, possible gastrointestinal discomfort and diarrhea caused by sugar alcohols or glycerol and potential allergic reactions to parabens or azo-dyes (7,8) are only a few of the EKE related adverse effects to consider when these medicines are used to treat cough in adults and children. Excipient related interactions, such as those between ethanol and propylene glycol or other substances that inhibit or compete with the same metabolic pathways (e.g. disulfiram, metronidazole, some cephalosporin antibiotics, etc.) should also be taken into account (14). Serious adverse effects resulting from interactions between medicines containing ethanol and propylene glycol have been reported and are especially concerning in children (14, 15).

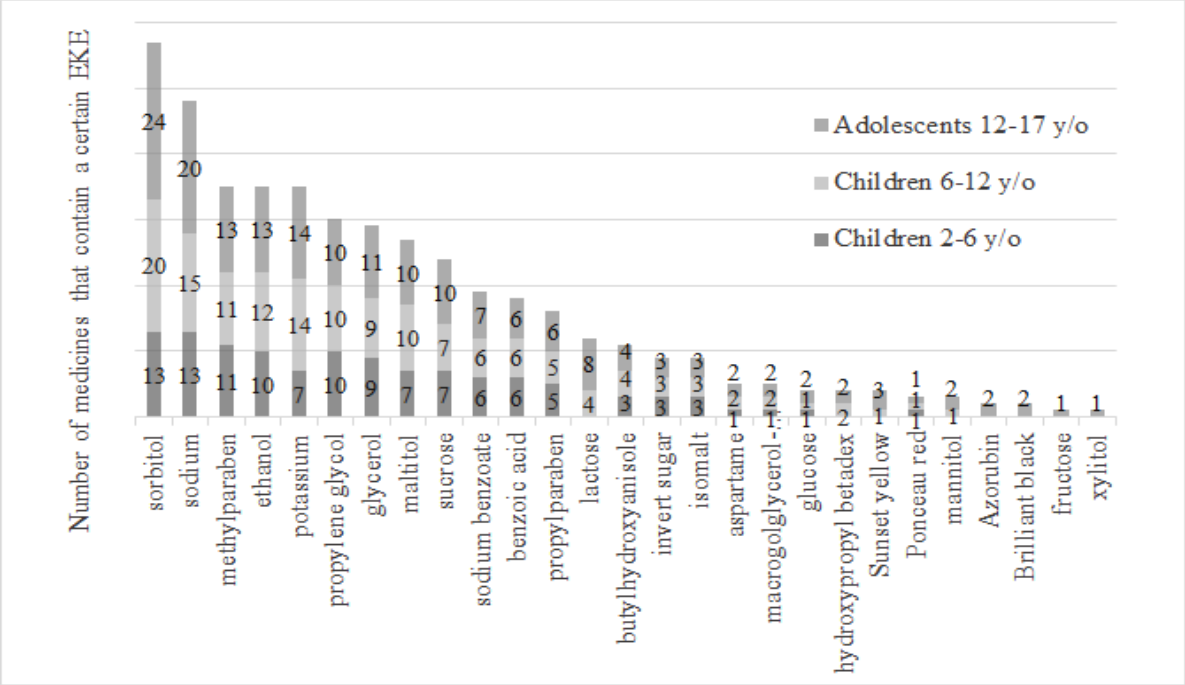

Figure 1. Number of EKE containing oral cough medicines on the market in Serbia approved for children depending on their age, in descending order of EKE frequency in the products.

An important factor to consider is the EKE quantity in the product. For example, if a product is used in accordance with patient instructions, exposure to ethanol at doses found in analyzed cough medicines (Table 2) would be less than 15 mg/kg/dose and would likely not have an effect on either adults or children (14). On the other hand, pediatric doses of some analyzed medicines contained up to 9.334 g of sugar per dose (Table 2), which, if taken three times a day, would result in a daily sugar intake equivalent to more than 50% of that recommended by the WHO for adults (16). Similarly, some of these pediatric medicines contained up to 166.6 mg of sodium per dose (Table 2), which would lead to a daily sodium intake equivalent to 25% of the daily limit for adults recommended by the WHO (17).

As EKE quantity was not included in the product information (SmPC and PL) for a number of analyzed pediatric cough medicines (Table 2), proper evaluation of potential risks of EKE related adverse effects or interactions is difficult. For example, propylene glycol content was not available for 90% of analyzed products (Table 2), but this information is important, especially when it comes to children below the age of 5 (Figure 1), who are susceptible to the toxicity of this excipient (15). Possible cumulative effect of propylene glycol and ethanol from multiple concomitantly administered medicines should also be taken into account (14,15,18).

Appropriate labeling of EKE quantity and additional safety information is an important prerequisite to prevent potential EKE related adverse drug reactions (ADRs) or investigate causes if an ADR already occurs. However, deficiencies in EKE labeling were discovered in a significant number of SmPCs and PLs of analyzed pediatric cough medicines (Table 3). Most notably, for 74.14% of these medicines, some of the EKE present in the products were completely omitted when labeling excipients with known effect in the corresponding SmPCs and PLs (Table 3). Additionally, missing or incomplete EKE quantitative and/or safety information was also very common among analyzed SmPCs and PLs (Table 3).

Table 3. Number of oral cough medicines approved for pediatric use in Serbia with EKE labeling deficiencies in their product information (SmPC and/or PL).

Products with one or more EKE not labelled as excipient with known effect in the SmPC and PL (percentage of all analyzed medicines [%])	**Products with missing/incomplete EKE information in SmPC and/or PL (percentage of all analyzed medicines [%])**	
	EKE quantitative information	**EKE safety information**
43 (74.14)	26 (44.83)	26 (44.83)

4. Conclusion

All of the pediatric oral cough medicines authorized in Serbia contained at least one excipient that may cause excipient related adverse effects, interactions and/or contraindications. Most of these EKE containing medicines were approved for use across all ages of children and adolescents above the age of 2. Due to the unique vulnerability of the pediatric population, safety issues of some excipients are more pronounced in children compared to adults, which should be taken into account when prescribing, recommending and dispensing these medicines. Cumulative intake of EKE from concomitant use of multiple medications as well as exposure from other sources (e.g. food) should also be considered. The numerous EKE labeling deficiencies in the SmPCs and PLs of pediatric oral cough medicines authorized in Serbia make the assessment of potential excipient related negative effects difficult for healthcare professionals and even more so for parents and patients. Revision of the product PLs and SmPCs is recommended in order to eliminate deficiencies and improve excipient labeling.

5. Acknowledgements

This study was supported by The Ministry of Education, Science and Technological Development, Republic of Serbia (project 451-03-68/2022-14/200114).

6. References

1. Morice, A., Kardos, P. Comprehensive evidence based review on European antitussives. *BMJ Open Resp. Res*. **2016**, *3(1)*, e000137.
2. Medicines and Medical Devices Agency of Serbia (ALIMS). Promet i potrošnja gotovih lekova za humanu upotrebu u Republici Srbiji u 2019. godini; P.Print: Belgrade, Serbia, 2020. https://www.alims.gov.rs/wp-content/uploads/2022/01/PPL_2019.pdf (accessed May 15, 2022).
3. Murgia, V., Manti S., Licari A., De Filippo M., Ciprandi G., Marseglia G. L. Upper Respiratory Tract Infection-Associated Acute Cough and the Urge to Cough: New Insights for Clinical Practice. Pediatr. *Allergy Immunol. Pulmonol*. **2020**, *33(1)*, 3-11.
4. Zupanets, K.O., Shebeko, S.K., Ratushna, K.L., Katilov, O.V. Cumulative Risks of Excipients in Pediatric Phytomucolytic Syrups: The Implications for Pharmacy Practice. *Sci. Pharm*. **2021**, *89*, 32.
5. Batchelor, H. K., Marriott, J. F. Formulations for children: problems and solutions. *Br. J. Clin. Pharmacol*. **2013**, *79(3)*, 405–418.
6. Council of Europe. European Pharmacopoeia, 10th ed.; EDQM: Strasbourg, **2019**.
7. Rowe, R. C., Sheskey, P. J., Owen, S. C. Handbook of Pharmaceutical Excipients, 5th ed.; Pharmaceutical Press: London, **2006**.
8. European Medicines Agency. Annex to the European Commission guideline on "Excipients in the labelling and package leaflet of medicinal products for human use" (SANTE-2017-11668), **2019.** https://www.ema.europa.eu/en/documents/scientific-guideline/annex-european-commission-guideline-excipients-labelling-package-leaflet-medicinal-products-human_en.pdf (accessed May 15, 2022).
9. Ivanovska, V., Rademaker, C. M., van Dijk, L., Mantel-Teeuwisse, A. K. Pediatric drug formulations: a review of challenges and progress. *Pediatrics.* **2014**, *134(2)*, 361-372.
10. EuPFI, European Paediatric Formulation Initiative. http://www.eupfi.org/ (accessed May 15, 2022).

11. Medicines and Medical Devices Agency of Serbia (ALIMS). https://www.alims.gov.rs/english/ (accessed May 15, 2022).
12. European Commission. Guideline on Summary of Product Characteristics, 2009. https://ec.europa.eu/health/system/files/2016-11/smpc_guideline_rev2_en_0.pdf (accessed May 15 2022).
13. Sen, E. F., Verhamme, K. M., Felisi, M., 't Jong, G. W., Giaquinto, C., Picelli, G., Ceci, A., Sturkenboom, M. C. Effects of safety warnings on prescription rates of cough and cold medicines in children below 2 years of age. *Br. J. Clin. Pharmacol*. **2011**, *71(6)*, 943–950.
14. European Medicines Agency. Information for the package leaflet regarding ethanol used as an excipient in medicinal products for human use, **2018**. https://www.ema.europa.eu/en/documents/scientific-guideline/information-package-leaflet-regarding-ethanol-used-excipient-medicinal-products-human-use_en.pdf (accessed May 15, 2022).
15. Yazbeck, N., Youssef, Y., Hanna-Wakim, R. A young child with HIV and unsteady gait: A case report. *IDCases*. **2020**, *19*, e00643.
16. World Health Organization. Guideline: sugars intake for adults and children, **2015**. https://www.who.int/publications/i/item/9789241549028 (accessed May 15, 2022).
17. World Health Organization. Guideline: sodium intake for adults and children, **2012**. https://www.who.int/publications/i/item/9789241504836 (accessed May 15, 2022)
18. European Medicines Agency. Propylene glycol used as an excipient, Report published in support of the ‘Questions and answers on propylene glycol used as an excipient in medicinal products for human use’ (EMA/CHMP/704195/2013), **2017**. https://www.ema.europa.eu/en/documents/report/propylene-glycol-used-excipient-report-published-support-questions-answers-propylene-glycol-used_en.pdf (accessed May 15, 2022).

Sustainable Development, Chemical and Environmental Engineering

APPLIED STATISTICS AS A TOOL IN QUALITY CONTROL ON ADVANCED PRODUCTION

Vesna Antoska Knights[1], Tatjana Kalevska[1]

[1] University "St Kliment Ohridski"- Bitola, Faculty or Technology and Technical Science -Veles, 7000, Bitola, Republic of North Macedonia

** vesna.knights@uklo.edu.mk*

Abstract

Nowadays, the application of statistical methods takes an increasingly important role in the management of companies, especially in the process of increasing quality, reducing costs, and increasing productivity. The purpose of this paper is to present Statistical Process Control (SPC) through a concrete example in production and processing and to find applications in other areas of technology such as advanced production and higher control. In the process of encouraging small and medium-sized companies in their development, it is necessary to implement computer technology in every segment of the processes. This paper will help to better understand this SPC through its statistical calculation, but also its implementation in companies by offering a suitable solution for its application through code. Applied statistics is a powerful tool in the area of SPC and it is very popular in the industry. The main objective of the control chart is to improve manufacturing processes by revealing the variability which is related to certain (specific) reasons. Once the underlying cause of variation is determined, managers take action to fix the process. Applications of statistical methods are in order to visualize, interpret and anticipate outcomes over collected data. It means to enable managers to make objective decisions based on analysis and experience and based on the analysis and processing of statistical data.

Keywords: applied statistics, statistical process control, SPC

1. Introduction

SPC refers to the use of statistical methods to maintain and improve the quality of products. In other words, it is a scientific, data-driven methodology for measuring and controlling quality during the manufacturing process. Quality data in the process measurements are obtained in real-

time during manufacturing. Statistical methods are then used to assess whether or not the process is in a state of control. This statistically-based process of information can provide a greater understanding of the process by providing a graphical interpretation of the variation in the process. Data is then plotted on a graph with predetermined control limits. Control limits are determined by the capability of the process, whereas specification limits are determined by the client's needs (1).

SPC as a control method monitors an industrial process through the use of a control chart. Much of its power lies in its ability to monitor both the processing center and its variation in that center. By collecting data from samples at various temporal and spatial points within the process, variations in the process that may affect the quality of the end product or service can be detected and corrected, thus reducing waste (2).

SPCs have a range of benefits: reduced wastage, maximized productivity in a manufacturing unit, increased operational efficiency, reduced need for manual inspections, enhanced customer satisfaction, controlled costs, and improved analytics and reporting. The bottom line is that SPC allows the people doing the work to know they are producing conforming products, and to take preventive actions as processes show signs of drifting out of control (3).

The concepts of SPC were initially developed by Dr. Walter Shewhart of Bell Laboratories in the 1920s, and were expanded by Dr. W. Edwards Deming (4), who introduced SPC to Japanese industry after WWII. After the early, successful adoption by Japanese firms, SPC has now been incorporated by organizations around the world as a primary tool to improve product quality by reducing process variation.

Variation is a natural and commonly occurring phenomenon but not all variation is created equal. A process may contain variation that is common or inherent to the process and, there may also exist variation that is not common or inherent to the process. Variation that is not common would be a result of a special cause outside of the normal process conditions.

In order to survive in a competitive market, improving quality and productivity of product or process is a must for any company. To make improvements in the company, strong commitment from the top management is required (5). Furthermore, the critical success factors are training and education, awareness of statistical methods, adequate measurement system etc. Cause and effect diagram is very helpful to the management. It is important to focus on the critical causes. However, other researchers found some issue with the control chart that cannot help to remove the assignable

causes of variation (6). The 7QC tools found are the base for implementation of the quality management system in industry. Also, for the data collection, analysis, measuring and decision making the tools found are very essential (7). Edgardo J. Escalante has given the relationship among variation, quality, and defects. He has identified the common and special causes of variation & defects and derived benefits from reducing variation & non-conformities (8). In six-sigma, for analyzing, measuring and controlling phases, SPC tools are very useful and play a vital role in finding causes (9).

2. Experimental

2.1. Method

Studying process variation can provide insight into the sources of variation and ways to minimize the variation in the manufacturing process. This knowledge can help lead to greater consistency in the final product and fewer deficiencies or defects. The use of statistics makes good sense in quality because even when all seems to be running well, there are many uncontrolled production factors that can affect product characteristics. The equation for sample variance is:

$$\sigma^2 = \frac{\sum_{i=1}^{n}(x_i - \mu)^2}{n-1}$$

Examples of quality control charts are Shewhart quality control charts, average value quality control charts and median quality control charts. For the definition of the interference and warning limits of quality rule maps, the following error bands are used:

α = 1% –> 99% error band –> control limit (UCL Upper Control Limit = μ +Lσ; LCL Lower Control Limit = μ –Lσ;)

α = 5% –> 95% error band –> warning limit (UWL Upper Warning Limit = μ +Lσ; LWL = Lower Warning Limit= μ –Lσ;

CL center line = μ,

where $CL = \mu = \bar{x} = \frac{\sum_{i=1}^{n} x_i}{n}$

L is the distance of the control limit from the center line, μ and σ are the mean and standard deviation of the sample statistic.

Fig. 1 shows graphical presentation of the Structure of a Quality Control Chart.

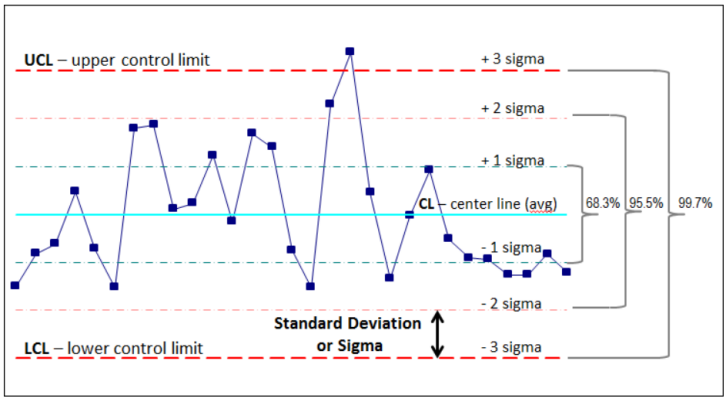

Figure 1. Graphical presentation of the Structure of a Quality Control Chart

The Upper Control Limit (UCL) and Lower Control Limit (LCL) are called action limits and generally at 3–sigma. Warning limits, often placed at 2–sigma, increase the sensitivity of the chart, but also increase the number of false alarms.

Conventional control charts in the SPC literature are developed under the routine assumptions that process observations are independent and identically distributed with a parametric in-control distribution (e.g., normal). These assumptions are rarely valid in practice. For instance, process observations collected at different time points could be serially correlated. Distributions of certain quality variables could be skewed and inappropriate to describe by a normal or another parametric distribution. In manufacturing industries, it might be reasonable to assume that the in-control distribution of process observations does not change over time (10*)*.

Using SPC methods and sample size and sampling frequency, usually, the changes in a process can be detected for:

(a) small sample size (n = 10), slow sampling frequency (every 1-2 hour)

(b) small sample size (n = 10), frequent sampling (every 1/2 -1 hour)

(c) large sample size (n = 25), slow sampling frequency (every 1-2 hour)

(d) large sample size (n = 25), frequent sampling (every 1/2 – 1 hour)

That means, if the values lie within the control and warning limits, the process can be continued without intervention. A violation of the warning limits leads to a monitoring of the process with increased attention. If the values fall outside the control borders, intervention must take place into the process, in order to guarantee quality of the product. In addition, the causes for the change of the process must be examined.

3. Results and discussion

In order to understand how control charts can be applied in production, it is considered the following example: In a “Choco Flips” production line, a manufacturer uses a machine to fill empty “Choco Flips” bags. The filling machine is set to fill each empty packet (pouch) with 80 grams of “Choco Flips”. As this is an electro-mechanical process, repeated over a long period of time, it is inevitable that there will be some degree of variation in the amount of “Choco Flips” filled into the bags.

The following table 1 shows the data obtained from 25 samples, each size n = 5 taken from a production line.

Table 1. The results of measurements of weight filled packages with Choco flips in a gram.

No.	**1st weighting**	**2nd weighting**	**3rd weighting**	**4th weighting**	**5th weighting**	**average**	**rank**
1	80.9	82.8	80.7	81.2	79.2	81.0	3.6
2.	79.8	83.5	79.3	82.5	81.2	81.3	4.2
3.	76.6	80.7	81.2	72.8	80.7	78.4	8.4
4.	80.3	83.8	77.9	79.9	81.8	80.7	5.9
5.	76.5	82.4	76.9	80.6	84.2	80.1	7.7
6.	79.8	78.5	81.2	75.8	75.4	78.1	5.8
7.	81.2	82.1	80.9	78.2	77.9	80.1	4.2
8.	83.2	83.9	78.6	80.5	79.9	81.2	5.3
9.	84.5	80.9	75.1	77.8	78.2	79.3	9.4
10.	78.5	77.9	76.8	82.2	76.5	78.4	5.7
11.	81.2	80.8	82.8	77.1	80.8	80.5	5.7
12.	84.2	76.7	75.9	81.4	81.5	79.9	8-3
13.	79.2	77.2	80.8	78.7	83.2	79.8	6.0
14.	81.5	79.4	77.7	80.5	84.5	80.7	6.8
15.	84.4	84.0	81.7	79.5	81.7	82.3	4.9
16.	77.3	82.8	78.6	77.8	76.7	78.6	6.1
17.	78.8	80.2	80.2	81.6	78.8	79.9	2.8
18.	76.8	76.7	82.5	82.2	79.4	79.5	5.8
19.	79.2	77.9	81.7	81.5	78.8	79.8	3.8
20.	79.1	80.9	80.4	80.9	76,5	79.6	4.4
21.	78.5	84.8	84.1	84.5	79.2	82.2	6.3
22.	82.2	77.2	76.8	78.4	81.3	79.2	5.4
23.	81.8	79.7	79.7	81.7	82.3	81.0	2.6
24.	78.4	84.7	81.9	83.1	80.8	81.8	6.3
25.	82.9	8.1	81.2	81.9	77.7	81.2	5.2

The mean value (average) and the range (rank) of each sample are calculated, as well as the upper and lower control limits. All necessary calculations are made in Microsoft Excel. In the production process, samples are taken at regular intervals, (for example) every 10 min, 15 min, 30 min, so here 25 samples are taken. After the constructed control chart, production engineers will be able to detect trends. That can be very important to manufacturing engineers who expect to take corrective action to prevent a manufacturing process from going out of control.

Using Microsoft Excel, the following results were obtained:

$$x = 80.2;\ R = 4.5;\ \sigma = 1{,}12$$

Using these values, the control limits (upper and lower) are defined as:

$$\text{UCL} = x+3\sigma = 80.2+3\cdot 1.12 = 83.13$$

$$\text{LCL} = x-3\sigma = 80.2-3\cdot 1.12 = 77.93$$

If the control limits are also checked using formula with coefficient (factor) for calculating the control limits, the same values for control limits are obtained:

$$\text{UCL} = x+A\cdot R = 80.2+4.5\cdot 0.577=83.13$$

$$\text{LCL}=x- A\cdot R=80.2-4.5\cdot 0.577=77.93$$

Where $A = 0.577$ is factors for calculating the control limits for sample size equal to 5.

Statistical methods are applied in order to visualize, interpret and anticipate outcomes over collected data, enabling the managers to make objective decisions based on analysis and experience, and based on the analysis and processing of statistical data. Figs. 2 and 3, present *x* control chart and *R* control chart, respectively.

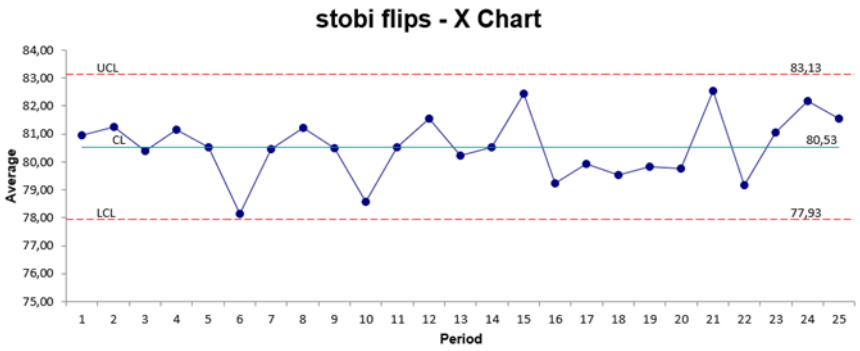

Figure 2. Quality Control of Packets of "Stobi Flips" using *x* Control Chart

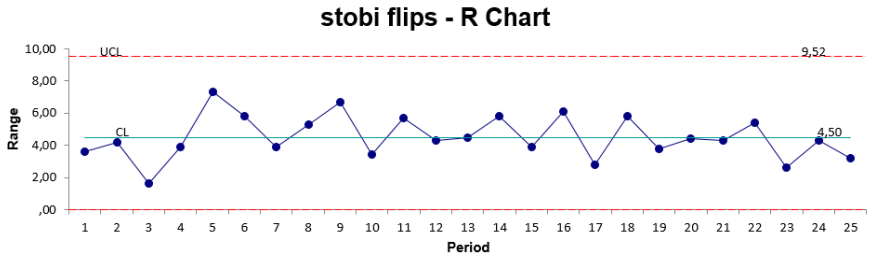

Figure 3. Quality Control of Packets of "Stobi Flips" using *R* Control Chart

Interpreting the control charts, according to (11), three of those displacements are:

1. Value outside the control limits (when a point is outside the control limit, that is, more than 3 sigma from the center line).

2. Trend in a sample statistic (six points in a row, all rising or falling). This type, known as a trend, indicates that the process is out of control and usually needs to be adjusted.

3. Many points are located on one side of the center line (nine points in a row are located on the lower or upper side (on the same side) of the center line). Such an arrangement in control charts is known as Run (flow or trend) and indicates that there are irregularities in the process that need to be corrected.

Described visual method allows production engineers more quickly and effectively perceive and respond to whether the variation is sufficient to result in significant emptying or overfilling of the packets. If there are any major variations that will result in major deviations in terms of more or less filling of packages, the process will be out of statistical control, requiring certain corrections to the operation of the machine.

Control limits calculated from our data also are presented in Figs. 2 and 3., showing that the operation of the "Choco Flips" charger is under statistical control. The *x* quality control chart presents upper and lower control limits with the calculated data. Also, the *R* quality control chart presents the rank of the variations, which, according to the obtained values of the examined parameters, meet the conditions prescribed in the quality regulations (12).

4. Conclusions

Studying process variation can provide insight into the sources of variation and ways to minimize the variation in the manufacturing process. This knowledge can help lead to a greater consistency in the final product and less deficiencies or defects. The use of statistics makes a good sense in quality, since even when all seems to be running well, there are many uncontrolled production

factors that can affect product characteristics. When manufacturing a product, most of the factors are unknown, can vary, and may not affect the process all of the time.

Under these circumstances, methods of probability and statistics are applied that predictions can be made, and those involved in the manufacturing of the product know what to expect. Controlling quality is a science, and the mathematics of quality is probability and statistics.

Control limits calculated from our data also are presented with formulas and the control charts. The *x* and *R* charts are made in Microsoft Excel, and they provided the capability for faster and not expensive way for process visualization. From the results of the control process for Stobi Flips chocolates, it can be seen that the process is within the limits of control.

In the process of encouraging small and medium-sized companies in their development, it is necessary to implement computer technology in every segment of the processes.

SPC is a continuous accompanying monitoring of the manufacturing processes by the collection of all characteristic numbers relevant for the product quality. SPC supplies the base data for the recognition of weak points, and, therefore, the condition for the constant improvement of the respective processes.

5. Acknowledgments

6. References

1. InfinityQS®: What is Statistical Process Control (SPC)?, available at: https://www.infinityqs.com/resources/what-is-spc
2. Zhang P. Advanced Industrial Control Technology. Elsevier Inc. **2010.**
3. Berk J, Berk S. Quality Management for the Technology Sector. Elsevier Inc. **2000.**
4. Deming E. Statistical Adjustment of Data. Dover Publications, New York. **1964.**
5. Rohani J. M., Konteg C. Improving quality with basic statistical process control tools: A case study. Jurnal Teknologi, **2002**, *35(A)*, 21-34.
6. Ribeiro L. M. M., Sarsfield Cabral J. A., The use and misuse of statistical tools. *J. Mater. Process. Technol.* **1999**, *92(93)*, 288-292.
7. Chandna P., Chandra A. Quality Tools to Reduce Crankshaft Forging Defects: An Industrial Case Study, *Int. J. Ind. Syst. Eng.* **2009**, *3(1)*, 27-37.

8. Escalante J. E. “Quality and productivity improvement: A study of variation and defects in manufacturing”. *Qual. Eng.* **1999**, *1(3)*, 427-442.
9. Shashank S., Ravindra M., Lokesh B., Katare S. K. Reduction of welding defects using six sigma techniques. *Int. J. Mech. Eng. & Rob. Res.* **2013**, 2(3), 404-412.
10. Qiu P. Some Recent Studies in Statistical Process Control. Chapter, **2004**, 1-18
11. Newbold P., Carlson W., Thorne B. Statistics for business and economics – 6th edition, New Jersey, **2007.**
12. Regulations on the method and procedure for performing metrological supervision and the requirements that the packaged products must meet in relation to the quantities, the way of marking the quantities and the permitted deviations from the indicated quantity and a list of the nominal quantities of the packaged products (Official Gazette of the RM, No. 83, **2009**).

IS THERE ALTERNATIVE TECHNOLOGY WHERE USE OF NaOCl IN WASTEWATER TREATMENT DOESN'T HAVE HARMFUL CONSEQUENCES?

***Ana Dajić*[1], *Marina Mihajlović*[1], *Milica Svetozarević*[1]**

[1]*Innovation Centre, Faculty of Technology and Metallurgy,* Karnegijeva 4, 11000 Belgrade, Serbia

aveljasevic@tmf.bg.ac.rs

Abstract

Almost all industrial wastewater must be treated before being discharged or reused. Widely used household bleach - sodium hypochlorite - is an excellent low-price disinfection agent and could be used in wastewater treatment processes. However, large amounts of residual sodium-hypochlorite at the end greatly increase chemical oxygen demand and additional processes should be applied to remove it for treated wastewater.

Treatment of textile industry wastewater with diluted sodium hypochlorite could be successfully done in microreactor systems. Microreactor systems are relatively new technological processes. One of the advantages of this technology is an improved diffusion process, thus smaller amounts of chemical agents are needed. As a result, outlet wastewater could be directly discharged into the recipient. In this paper, simulated wastewater from the textile industry was treated with diluted sodium hypochlorite in microreactor systems and experiments showed that highly contaminated textile wastewater could be purified to fulfill national laws requirements to be released into the environment. This paper shows how it could be done.

Keywords: Wastewater, microreactor system, NaOCl.

1. Introduction

Wastewater is an important problem nowadays. Before discharging, textile wastewater has to be treated to achieve the quality prescribed by national regulations. The discharge of textile wastewater into the environment can have indirect and direct effects. Direct effects can be the above-mentioned change of color, poor sunlight penetration damaging flora and fauna of the ecosystem, groundwater pollution (a consequence of contaminated water leaching through the

soil), and the suppression of the re-oxygenation capacity [1]. Colored wastewater released into the environment could cause acute toxic effects in exposed organisms, change in the coloration, and the reduction of photosynthesis since the dissolved colors absorb sunlight that enters the water [2,3]. In addition, the color influences the perception of water quality, as the presence of colors is esthetically unpleasant and is associated with contamination, as even low concentrations of the dye of 0.005 mg/dm^3 can be visible in river water [4]. Destruction of aquatic life (fish, plants, and mammals), toxicity and microtoxicity, eutrophication, and suppression of the immune system of human beings are considered indirect effects.

New treatment technologies are a topic that is constantly being researched from chemical technologies to chemical agents used in these processes. Chlorine is the most common disinfection reagent in wastewater treatment in developing countries although NaOCl has been classified as a hazardous substance. It is usually used as gas, sodium or calcium hypochlorite.

Microreactor systems are relatively new technological processes that have been used recently. Wastewater treatment using microreactor systems has been proven successful [5]. Thanks to their simplicity, microreactors have become good chemical technologies solutions for different problems. Because of the small volume, microreactors usually need to scale up. Scale up for these systems is simple and could be done by multiplying the number of microchannels. Benefits over traditional methods are minimal consumption of reactants, short reaction time, good temperature control, security in reactor control [6,7] but also efficiency over batch treatment [8]. The main problem of wastewater decolorization in microreactor systems is higher capital costs compared to decolorization in batch conditions. Additionally, microreactors have limiting conditions: materials and solvents that could be used. However, the use of simple microreactor systems connected to pumps could ensure relatively low material costs, and the aforementioned disadvantages would be negligible in relation to the success that could be achieved in this way.

The main advantage of the microreactor system is a significant reduction of sodium hypochlorite quantity, and therefore no residual sodium hypochlorite is discharged at the system inlet. Experiments were done with simulated textile industry wastewater contaminated with the dye Reactive orange 16. It belongs to the group of anionic dyes, with wide application in the textile and paper industry. Reactive dyes usually have azo compounds connected with different reactive groups. The reaction mixture was decolorized with NaOCl [9].

Conducted experiments aim to define optimal reaction parameters, with minimal effects on the environment.

2. Experimental

The microreactor set, shown in figures 1 and 2, was contracted of two pumps; T mixer and tube microreactor.

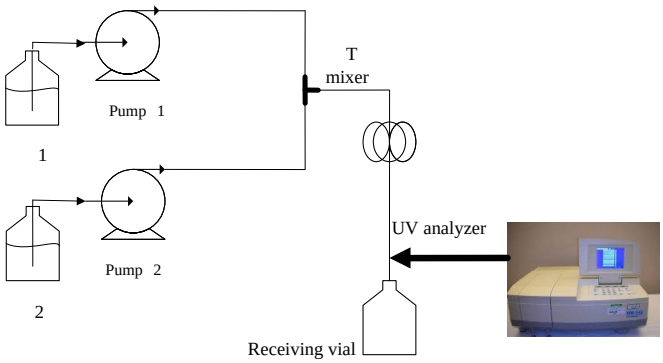

Figure 1. Sketch of experimental setup

Figure 2. Experimental set-up

Pumps, used in this experiment, are accurate, reliable pumps LC-20AD XR, Shimadzu Usa Manufacturing Inc. Outlet tubes were long 2 m, 4 m, 6 m and 9.8 m with inner diameter 0.5 mm and 0.25 mm. A T mixer was configured with inlets symmetrically with 180° and with asymmetrically 90° outlet.

VICI Jour was microreactors producer and it was made of chemically resistant high-performance polymer.

Simulated wastewater aims to mimic highly contaminated water with the dye Reactive Orange 16 as a pollutant. The solution was made by mixing demineralized water with RO-16 dye, and the final solution has a concentration of 80 mg/dm^3. The solution was mixed on a magnetic stirrer (C-MAG HS 7) for 15 min until complete dissolution. The decolonization agent was 1% w/w solution NaOCl (Alstman, Beograd). For these experiments, it was additionally diluted

and used for decolorization processes.

In the first set of experiments, microreactor length and velocity speed were varied. That resulted in a change in mixing intensity and reaction time. The next parameter was different concentrations NaOCl. The influence of reactor length and molar ratio on the decolorization was tested with flow velocity *f*(NaOCl):*f*(RO16) were 0.1:0.2 cm^3/min. Next set of experiments aimed to define the influence of residual time by varying flow velocity in a microreactor with different construction.

The samples of treated wastewater were collected in vials at the system outlet. The efficiency of the decolorization process was quantified using a UV vis spectrophotometer (Shimadzu UV-Vis 1700) at 489 nm. Experiments were done at room temperature, between 20 and 23 ºC, in triplicate.

COD of treated wastewater was analyzed by Lovibond MultiDirect multiparameter and Lovibond vario test tubes.

pH was measured on laboratory pH meter, InoLab 730, Germany.

The type of flow was defined by Reynolds number, obtained from mesured viscosity of reaction mixture. Viscosity was mesured with rotation viscosimeter (LE0089, EUInstruments).

3. Results and discussion

In the first set of experiments influence of reactor length and molar ratio were analyzed and obtained results are shown in Figure 3. Residual time was defined by flow velocity.

For each reaction mixture, molar ratios *n*(NaOCl)/*n*(RO16) were 3.35, 3.92 and 5.00. Residence time was set by setting velocity speed. Reaction with the shortest residence time and the shortest reactor length resulted with minimum 64% decolorization for any molar ratio. The best decolorization efficiency of 93% was achieved in case of the highest molar ratio and the longest residence time.

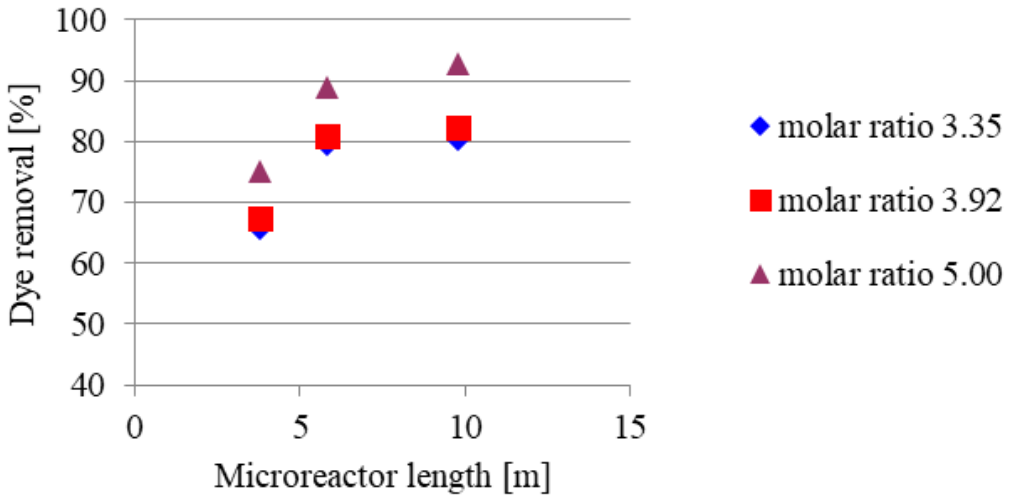

Figure 3. The influence of the reactor length and molar ratio on the decolorization for different molar ratios and relative flows (NaOCl/RO16) 0.1:0.2 cm^3/ min, with mixture molar ratios of 3.3, 3.9, and 5.0 at room temperature

The second set of experiments examined residual time effects on reaction efficiency. Microreactor system with 0.25 mm diameter and 3.8 m long was used and flow velocities were 70 µl/min and 105 µl/min. Obtained results are shown on Figure 4.

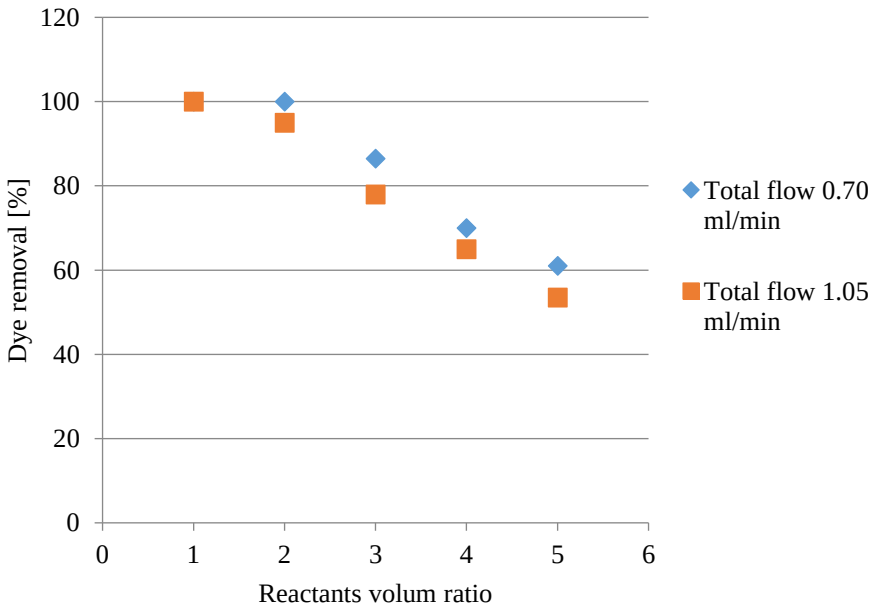

Figure 4. The influence of the f low velocity on dye removal

Figure 4 shows that decolorization is more successful at a total flow rate of 0.7 µl/min. Although the mixing is better at higher flow rates, in this case the efficiency of the

decolorization was more influenced by the time the mixture remains in the reactor, i.e. a longer reaction time.

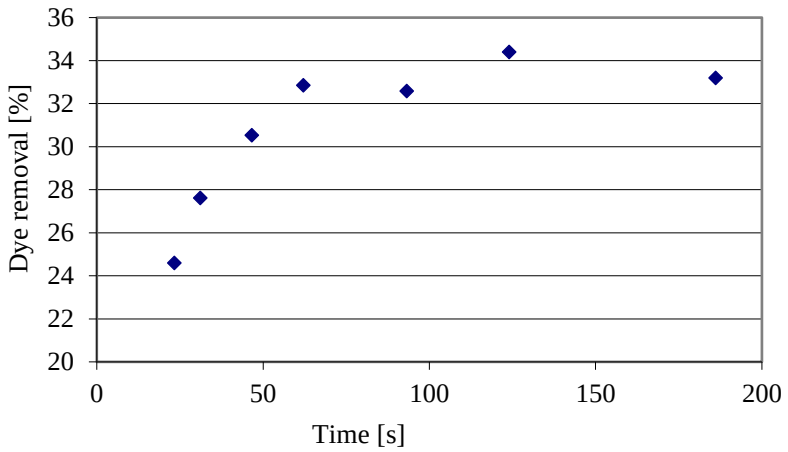

Figure 5. The influence of the concentration of NaOCl on wastewater decolorization

Figure 5 clearly shows that the success of removing the dye with a very dilute solution is only partially successful. It is necessary that the molar ratio is greater than 1. Up to the 50 s efficiency of decolorisation is influenced by residence time. After that time, residence time has no significant effect. Figure 6 shows the influence of microreactor construction on decolorization efficiency.

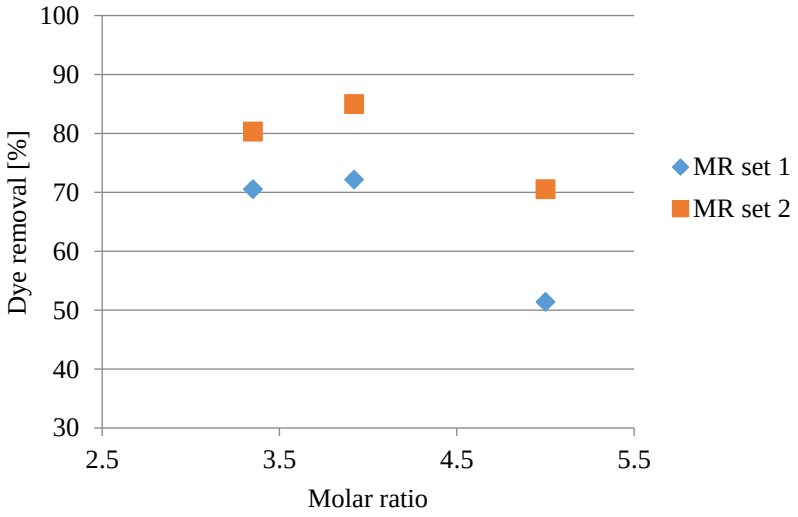

Figure 6 The influence of molar ratio on wastewater decolorization in different microreactor sets

Both microreactor sets have same tube length but of different diameters. System 1 is 6 m microreactor tube with diameter 0.5 mm, while system 2 consists of a 4 m long reactor with

0.25 mm diameter connected to a reactor 2 m long and 0.5 mm diameter. Based on the results shown in Figure 6, it can be concluded that decolorization in reactor unit 1 is more successful. More intense mixing in the first part of the reactor with a smaller diameter enables better mixing and better contact of the reactants, which results in more successful color removal.

pH values of reaction products were checked and their values were around 7 (6.694-6.880). pH value is one of the parameters important considering wastewater discharging.

The next important parameter is the COD value of wastewater. Obtained COD values are presented in Figure 7. Each of these products had COD value under 170 which means that the decomposition of organic molecules was successful and wastewater could be discharged into the water recipient.

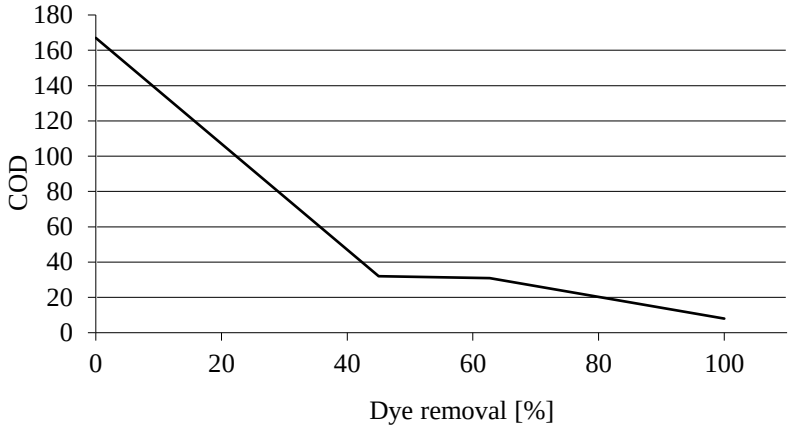

Figure 7. COD values depending of percentage of removed dye

The results, (Fig. 7) show that such a small amount of NaOCl in the reaction mixture removes the dye so well and that the reaction products do not disturb the COD value. Wastewater before treatment had a COD value of 167. COD values of treated wastewater were between 32 and 8.

4. Conclusion

This research was done with the aim to find is it possible to purify water with the minimum use of chemicals. The results show that a microreactor system constructed using medium length microreactor channels (5.8 m), low concentration of NaOCl (molar ratio of 3.35), small microreactor diameter (0.25 mm), low flow rate (0.2/0.1 ml/min), and medium residence times (around 300 s) leads to a decolorization of 80-90%, with minimal residual NaOCl.

This kind of treatment is modern and environmentally friendly with no toxic nus-product. Treated wastewater might be directly discharged into the water recipient. For all these reasons, treatment in microreactor systems should be considered for wide industrial applications.

5. Acknowledgments

The authors are grateful to the Ministry of Education, Science and Technological Development of the Republic of Serbia (Project No. 451-03-68/2022-14/200287 and 451-03-68/2022-14/200135) for its support.

6. References

1. Verma M, et al. Curcumin prevents formation of polyglutamine aggregates by inhibiting Vps36, a component of the ESCRT-II complex. *PLoS One,* **2012**, *7*(8), e42923.
2. Slokar, Y. M., Le Marechal, A. M. Methods of Decoloration of Textile Wastewaters, *Dyes Pigm.*, **1998**, *37*, 335-356.
3. Slokar, Y.M., Le Marechal, A. M. Methods of decoloration of textile wastewaters, *Dyes Pigm.*, **1998**, *37*, 335-356.
4. Banat, I. M., Datel Singh, P. N., Marchant, R. Microbial decolorization of textile-dyecontaining effluents: A review, *Bioresour. Technol.*,**1996**, *58*, 217-227.
5. Matsushita, B., Yang, W., Chen, J., Onda, Y., Qiu, G. Sensitivity of the Enhanced Vegetation Index (EVI) and Normalized Difference Vegetation Index (NDVI) to Topographic Effects: A Case Study in High-Density Cypress Forest. *Sensors*, **2007**, *7*, 2636-2651.
6. Jovanović, J., Rebrov, E.V., Nijhuis, T. A., Kreutzer, M. T., Hessel, V., Schouten, J.C. Liquid–Liquid Flow in a Capillary Microreactor: Hydrodynamic Flow Patterns and Extraction Performance. *Ind. Eng. Chem. Res.*, **2012,** *51* (2), 1015-1026.
7. Jovanovic J, Liquid-liquid Microreactors for Phase Transfer Catalysis, Doctoral thesis, **2011**.
8. Drhova, M., Hejda, S., Kristal, J., Kluson, P. Performance of continuous micro photo reactor - Comparison with batch process. *Procedia Eng.*, **2012**, *42*, 1365–1372.
9. Dajić, A. Development of final treatment processes for solid and liquid pollutants by cleaner production principles application, Doctoral thesis, **2019**.

PREPARATION AND DETERMINATION OF STABILITY AND PHYSICOCHEMICAL PROPERTIES OF TERPENE-BASED HYDROPHOBIC EUTECTIC SOLVENTS

***Edita Bjelić*[1*], *Mersiha Suljkanović*[2], *Jasmin Suljagić*[1], *Milan Vraneš*[3], *Miha Grilc*[4]**

[1]*Faculty of Technology, Urfeta Vejzagića br.8, 75000 Tuzla, Bosnia and Herzegovina*

[2]*Faculty of Natural Sciences and Mathematics, Urfeta Vejzagića br.4, 75000 Tuzla, Bosnia and Herzegovina*

[3]*Faculty of Sciences, University of Novi Sad, Trg Dositeja Obradovića 3, Novi Sad, Serbia*

[4]*National Institute of Chemistry, Hajdrihova 19,1000 Ljubljana, Slovenia*

edita.bjelic@untz.ba

Abstract

Terpene-based hydrophobic deep eutectic solvents are considered to be relatively non-toxic, less volatile, and environmentally friendly, which makes them promising alternatives to conventional solvents in liquid-liquid extraction of non-polar analytes from an aqueous environment. In this paper, series of different hydrophobic "deep" eutectic solvents based on L-menthol and Thymol (as H-bond acceptors) and a number of organic acids (as H-bond donors), with chain lengths from 8 to 18 C atoms, were prepared.The chemical stability of ten solvents was determined 24 hours after preparation and only four solvents formed a homogeneous transparent liquids and no crystallization at room temperature was observed. Considering that in the previous measurements of the extraction efficiency, the best results were obtained by the solvents with the composition: Men:DecA (1:1) and Men:OctA (1:1), the physicochemical properties (viscosity, density), electrical conductivity, thermal analysis (TG/DSC), water content and FTIR characterization for these solvents were carried out. FTIR spectra of prepared solvents compared to individual components, confirmed the formation of H bonds between donors and acceptors, in both cases.The results of Karl-Fischer titrations showed low water content (236 ppm for the Men:DecA (1:1) while for the Men:OctA (1:1), measured 258 ppm water), which confirms their hydrophobicity. Also, measured difference between solvent densities compared to water, enable macroscopic separation of phases during extraction. Furthermore, viscosities lower than 100 mPa·s, makes them acceptable solvents in industrial scale processes. Thermal stability of prepared solvents compared to starting materials, also contribute to their acceptability for investigated purposes.

Keywords: Hydrophobic deep eutectic solvents, menthol, thymol, decanoic acid, octanoic acid

1. Introduction

The term "deep eutectic solvent" (Deep Eutectic Solvent, DES) first appeared in 2001. when the group of scientists presented a highly promising category of designed solvents that could meet the principles of "green" chemistry, unlike the ionic liquids used at the time (1). Deep eutectic solvents are composed of two or three available and environmentally friendly components hydrogen bond acceptor (HBA) and hydrogen bond donor (HBD), that self-associate and form an eutectic mixture with a melting point lower than the melting point of the individual components of the mixture (2,3). The important properties of DESs include a lower melting point of prepared DESs than their individual components, low cost, low toxicity, renewability, sustainability, ease of preparation, and biodegradability (4,5). All of these benefits have reinforced the greenness of DESs, making them suitable alternatives to synthetic organic solvents. Hydrophobic DESs (HDESs) first time appeared in the literature in 2005 and their properties were less investigated compared to hydrophilic DESs, as well as their applications (6). By combining various starting components and various molar ratios, desirable features of DESs can be achieved. Following the pioneering research (7) DESs have found their applicability in a wide range of applications, including their use as solvents in extractions of metal cations, bioactive compounds for food and pharmaceutical applications (8,9,10). In this paper, hydrophobic deep eutectic solvents based on natural neutral ingredients were prepared. L-menthol was chosen as the H-bond acceptor, and a series of organic acids with different chain lengths as H-bond donors (3). After preparing a series of HDES solvents from different H-donors with different molar ratios of components, their stability to stay liquid at different temperatures was investigated. The most chemically stable deep eutectic solvents were selected for physico-chemical characterization.

2. Experimental

2.1 Materials

L(-)-menthol ($C_{10}H_{20}O$, 99,5%; Acros Organics), thymol ($C_{10}H_{14}O$,99%, Acros Organics) decanoic acid ($C_{10}H_{20}O_2$, 99%, Alfa Aesar), dodecanoic acid ($C_{12}H_{24}O_2$, 99%, Acros Organics), stearic acid ($CH_3(CH_2)_{16}COOH$, 95%, Acros Organics), and palmitic acid

($CH_3(CH_2)_{14}COOH$, 99% Sigma Aldrich).

2.2. Methods

2.2.1 DES preparation

The preparation of hydrophobic DESs, was done by mixing two solid components (L-menthol and thymol as HBA and different HBDs) in different molar ratios, e.g. 2:1, 1:1, and 1:2. The first component was weighed directly in the flask, and the second component was first weighed on a scale, after which the entire amount was transferred to the flask (11). After preparation and mixing, the flasks were heated and mixed at a temperature of approximately 40 °C until the melting of the solid components is achieved and stability of the resulting solvent (12). For mixtures that have not turned into a liquid state, the temperature is first increased to 60 °C, and if (according to the previously explained procedure) this is not enough, the mixture is further heated up to 80 °C (13).

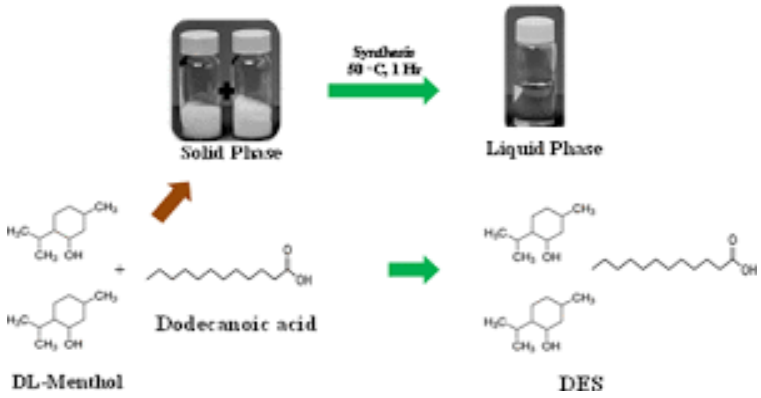

Figure 1. Preparation of HDESs

2.3. Instruments and procedures

2.3.1 Viscosity, density, electrical conductivity and water content measurements

An automatic densimeter Rudolph Research Analytical DDM 2911 was used to measure the density of the prepared HDESs (accuracy of ± 0.01% and temperature increments of 0.05 K). For viscosity measurements viscometer (Brookfield, DV-II+Pro) connected to PC (Pentium III) and thermostat (Lauda E 100, with the external flow and temperature regulation of ±0.1 K) were used. Conductivity meter (Jenco 3107), which measures conductivity with an accuracy of ±0.5%,was used for the experimental determination of electrical conductivity. Water content in HDES solvents was determined with the classic titration method with an automated 831 Karl Fischer Coulometer (Metrohm).

2.3.2 FTIR Analysis

FT-IR spectra of two prepared solvents and their corresponding HBDs and HBAs were recorded inthe range of 4000–600 cm^{-1}at room temperature (~ 298 K) using a Nicolet Model FTIR (Class 1 Laser Product Nicolet 6100, San Jose, CA) to assess the structure of the pure compounds as well as the prepared eutectic mixtures. FTIR absorption spectra are recorded with 4 cm^{-1}resolution and with 40 scans of the sample in the range of 4000 to 600 cm^{-1}.

2.3.3 TG and DSC Analysis

The thermal stability of the initial compounds and HDES systems was investigated with a TG/DSC thermal analyzer TA Instruments SDT Q600.

3. Results and discussion

In this work, hydrophobic deep eutectic solvents, based on L-menthol and thymol and a number of organic acids of different chain lengths were prepared (Table 1.). After preparation, chemical stability was determined as a property of HDES solvents that remains in the form of a homogeneous transparent liquid 24 hours after preparation. Considering that in the preliminary measurements of the extraction efficiency, the best results were shown by the solvents of the composition: Men:DecA (1:1) and Men:OctA (1:1), the physical-chemical properties (viscosity, density), electrical conductivity, thermal analysis (TG/DSC) and FTIR characterization were determined for the same mixtures. Given that the potential use of the prepared solvents is in liquid-liquid extraction, the water content in the HDES solvent after mixing with the aqueous solution was also determined.

3.1 Preparation and determination of stability of prepared solvents

Chemical stability of solvents was determined 24 hours after preparation. From ten prepared HDES, only four solvents formed a homogeneous transparent liquid and no crystallization at room temperature was observed (Table 1.)

Table 1.Determination of stability of prepared HDESs

DES No.	HBA	HBD	HBA/HBD	Formed on 80 °C	Liquid at 25 °C
DES 1	L-Menthol	Octanoic Acid	1:1	✓	✓
DES 2	L-Menthol	Decanoic Acid	1:1	✓	✓
DES 3	Thymol	Octanoic Acid	1:1	✓	✓
DES 4	Thymol	Decanoic Acid	1:1	✓	✓
DES 5	Thymol	Dodecanoic Acid	1:1	✓	x

DES 6	Thymol	Stearic Acid	1:1	✓	x
DES 7	Thymol	Stearic Acid	2:1	✓	x
DES 8	Thymol	Palmitic Acid	1:1	✓	x
DES 9	Thymol	Palmitic Acid	1:2	x	x
DES 10	Thymol	Palmitic Acid	2:1	x	x

3.2 Physico-chemical properties of prepared HDESs

3.2.1 Density

The hydrogen bonding between HBA and HBD is the main driving factor for DES formation. The increase in the number of −OH functional groups in HBD resulted in a higher number of hydrogen bonds. The higher number of hydrogen bonds reduces the free spaces available and consequently increases the density of DESs. It was reported that DESs obtained from benzyl trialkylammonium chloride saltsand ethylene glycol have lower densities than DESs obtained from diethylene glycol, triethylene glycol, and glycerol (14). Densities (d) were measured in the temperature range from 293.15 to 323.15 K at atmospheric pressure of 0.1 MPa. The obtained results are shown in Figure 2.

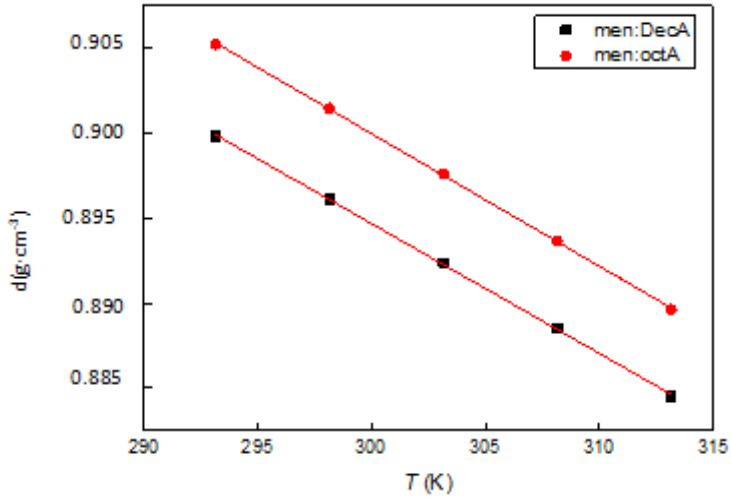

Figure 2. Density values at different temperatures

The results show that the densities of the investigated HDES solvents decrease with increasing temperature.The densities in the system with OctA have higher values compared to the DecA solvent. The smaller the difference in density between water and the hydrophobic solvent, the separation of phases after extraction is more difficult.

3.2.2 Viscosity

The most of the DESs possess a comparatively higher viscosity (>100 cP) at room temperature, which limits their extraction applications (15). The high viscosity reduces the mass transfer rate between the sample and extraction phase, owing to the formation of extensive hydrogen bond networks between the HBA and HBD components (16,17). The viscosities (η) were measured in the temperature range from 293.15 to 313.15 K. From the obtained results (Figure 3), it can be seen that viscosities decrease with increasing temperature. For a given temperature, the viscosities of the DESs were found to be in the following order: Men:DecA > Men:OctA. The higher viscosity values obtained for Men:DecA mean that a larger amount of energy needs to be supplied to initiate viscous flow in the mixture with DecA indicating stronger interactions between Men:DecA molecules than Men:OctA.

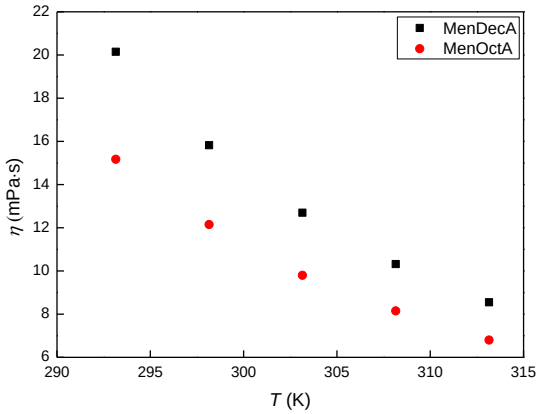

Figure 3. Viscosity values at different temperatures

3.2.3 Electrical conductivity measurements

The electrical conductivity of Men:OctA and Men:DecA was measured in the temperature range from 293.15 to 313.15 K. The measurement results are shown in Table 2.

Table 2. Values of electrical conductivity measurements at different temperatures

T (K)	κ (mS·cm^{-1})	
	Men:DecA	Men:OctA
293.15	0.00152	0.00151
298.15	0.00153	0.00153
303.15	0.00156	0.00157
308.15	0.00159	0.00159
313.15	0.00162	0.00163

3.2.4 Fourier-Transform Infrared Spectroscopy (FTIR) analysis

The selected HDES solvents (Men:DecA and Men:OctA) were analyzed by FTIR spectroscopy, in order to confirm the formation of H-bonds between H-donors and H-acceptors. Spectroscopic measurements were performed with a total of sixty scans at room temperature (298.15 K) and a spectral resolution of 2 cm^{-1}, in the wavenumber range of 640-4000 cm^{-1}. H-bonds are obviously formed by mixing L-menthol and decanoic acid in a molar ratio of 1:1, which is evident in the form of shifting of the characteristic bonds (O-H and C=O) on the FTIR spectrum HDES mixture (Figures 4. and 5.). The bands characteristic of CH-stretches, which expand in the region between 2650 cm^{-1} and 2950 cm^{-1}, show a typical structural rearrangement associated with the loss of the crystal structure of the molecule, due to the phase change that occurred when the two solid components were mixed. The stretching band of the C=O group is observed at the position of 1711 cm^{-1} (for both solvents) which represents a bathochromic shift compared to the same band of pure decanoic acid (1699 cm^{-1}) and also pure octanoic acid. It is possible that such changes originate from the influence of the nearby electron clouds of menthol, which are spatially nearby carbonyl groups of acids (18).

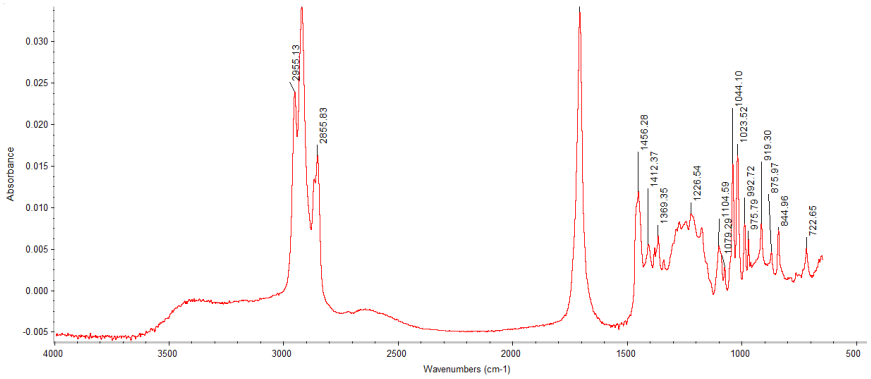

Figure 4. FTIR spectra of HDES solvent Men-DecA (1:1)

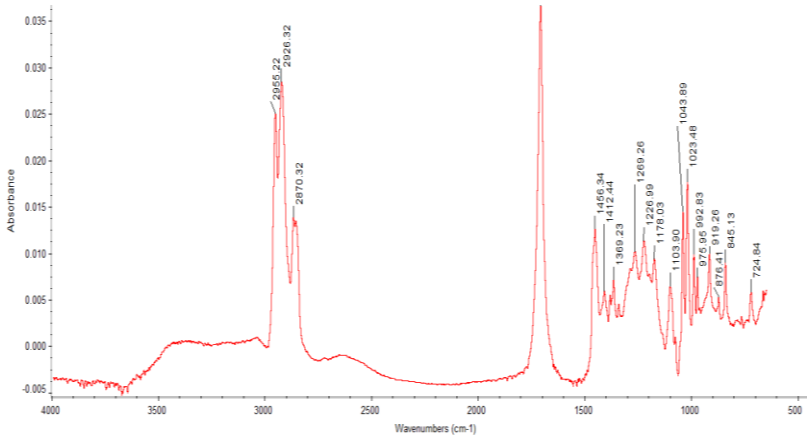

Figure 5. FTIR spectraof HDES solventMen:OctA (1:1)

3.2.5 Water content in HDES solvents

The results of Karl-Fischer titrations showed low water content 236 ppm for the Men:DecA (1:1) while for the Men:OctA (1:1), 258 ppm of water was measured, which confirms their hydrophobicity.

3.2.6 Thermal analysis

Thermal stability is one of the key parameters in considering the potential application of DESs,which limits the maximum operational temperature. In order to study the thermal stability of the tested compounds, a thermogravimetric analysis of individual components (octanoic, decanoic acid, menthol) and prepared HDES solvents: Men:DecA (1:1) and Men:OctA (1:1) was performed. The obtained thermo-analytical curves are presented in Figure 6. On all TG diagrams, mass loss due to decomposition occurs in one step, at temperatures above 100 °C. The difference in TG curves between the two HDES solvents is obvius. The thermogram for Men:DecA shows delayed decomposition compared to the thermogram for Men:OctA (1:1).

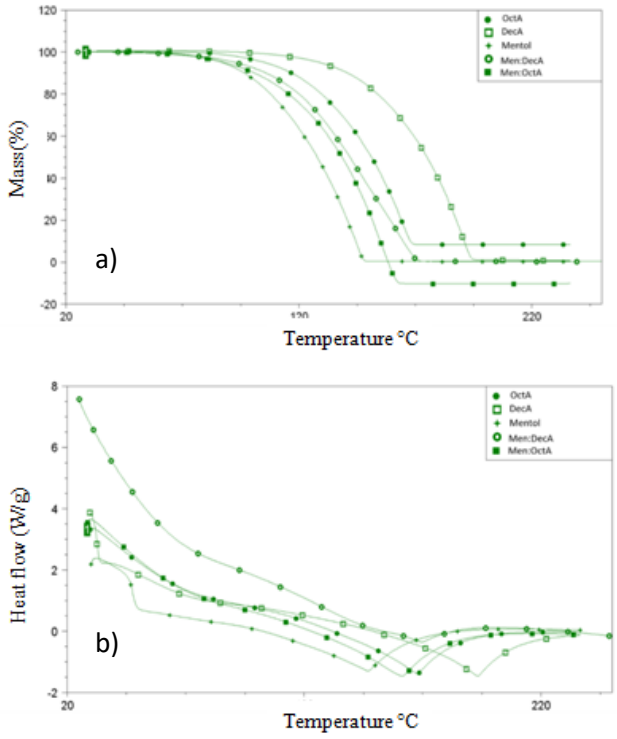

Figure 6. Thermograms for individual components and HDESs: (a)TG analysis, (b) DSC analysis

Table 3 shows results of TG and DSC measurements for individual components and prepared HDESs. Compared to previously published data for HDES solvents based on DecA and

quaternary ammonium salts, the degradation temperatures are much lower. In the obtained results, the addition of octanoic and decanoic acids significantly stabilizes the system. Menthol disrupts the interactions and structural organization of DecA, and disrupts DecA more drastically than OctA. The addition of menthol destabilizes the thermal system.In general, it can be assumed that lower temperatures do not represent degradation, but sublimation/evaporation of HDES solvent components.

Table 3. Values of TG and DSC measurements

DES	*T (°C)*	T_{onset}*(°C)*	$T_{5\%}$*(°C)*
Menthol	146.98	110.40	87.19
Men:OctA	161.27	123.15	88.13
Men:DecA	169.82	112.93	92.72
Octanoic acid	167.63	131.57	105.46
Decanoic acid	193.16	157.77	129.67

4. Conclusions

The suitable physico-chemical characteristics of HDES solvents enable their application in numerous analytical techniques. The water-immiscible nature of HDES solvents makes them promising in the liquid–liquid extraction of nonpolar analytes and transition metals from the aqueous phase. The low water content in hydrophobic DES solvents enables their use in LLE. Thermal analysis showed that the synthesized solvents are thermally more stable than their initial components. The electrical conductivities of the tested solvents do not change with increasing temperature.The viscosities of the tested liquids do not exceed 100 mPa·s, which makes them acceptable in industrial processes.

6. References

1. Anastas, P.; Eghbali, N. Green Chemistry: Principles and Practice.*Chem. Soc. Rev.* **2010**, *39*, 301–312.
2. Shishov, A.; Bulatov, A.; Locatelli M.; Carradori S.; Andruch V. Application of deep eutectic solvents in analytical chemistry. A review. *Microchem. J.* **2017**, *35*,33–38.
3. Ribeiro, B. D., Florindo, C., Iff, L. C., Coelho, M. A., Marrucho, I. M. Menthol-Based Eutectic Mixtures: Hydrophobic Low Viscosity Solvents. *ACS Sustainable Chem. Eng*. **2015**, *3*, 2469-2477.

4. Florindo, C.; Branco, L. C.; Marrucho, I. M. Quest for Green-Solvent Design: From Hydrophilic to Hydrophobic (Deep) Eutectic Solvents.*ChemSusChem* **2019**, *12*(8), 1549–1559.
5. Tuzen, M. Green and Deep Eutectic Solvent Microextraction Method for FAAS Determination of Trace Level Cadmium in Water Samples Using Multivariate Strategic Approach.*Atomic Spectroscopy* **2016**,*37*(6), 244–251.
6. van Osch, D.J.; Zubeir, L.F.; van den Bruinhorst, A.; Rocha, M.A.; Kroon, M.C. Hydrophobic deep eutecticsolvents as water-immiscible extractants. *Green Chemistry* **2015**, *17*, 4518–4521.
7. Abbott, A. P.; Boothby, D.; Capper, G.; Davies, D. L.; Rasheed, R. K. Deep Eutectic Solvents Formed between Choline Chloride and Carboxylic Acids:Versatile Alternatives to Ionic Liquids.*J. Am. Chem. Soc.* **2004**,*126*(29), 9142–9147.
8. Carriazo D.; Serrano M.C.; Gutierrez M.C.; Ferrer M.L.;Monte F. Deep-eutectic solvents playing multiple roles in the synthesis of polymers and related materials.*Chem. Soc. Rev.* **2012**, *41*, 4996–5014.
9. Pena-Pereira F., Namiesnik J. Ionic Liquids and Deep Eutectic Mixtures: Sustainable Solvents for Extraction Processes.*ChemSusChem.* **2015**, *7*,1–18.
10. Smith, E. L., Abbott, A. P., Ryder, K. S. Deep Eutectic Solvents (DESs) and Their Applications.*Chem. Rev*. **2014**, *114* (21), 11060–11082.
11. Rajabi, M., Ghassab, N., Hemmati, M., Asghari, A. Emulsification Microextraction of Amphetamine and Methamphetamine in Complex Matrices Using an Up-To-Date Generation of Eco-Friendly and Relatively Hydrophobic Deep Eutectic Solvent. *J.Chromatogr*. A **2018**, 1576, 1–9.
12. Cao, J., Yang, M., Cao, F., Wang, J., Su, E. Well-Designed Hydrophobic Deep Eutectic Solvents as Green and Efficient Media for the Extraction of Artemisinin from Artemisia Annua Leaves.*ACS Sustainable Chem. Eng.* **2017,** *5*, 3270-3278.
13. Phelps, T. E., Bhawawet, N., Jurisson, S. S., Baker, G. A. Efficient and Selective Extraction of 99mTcO4– from Aqueous Media Using Hydrophobic Deep Eutectic Solvents.*ACS Sustainable Chem. Eng.***2018**, *6* (11), 13656–13661.
14. Basaiahgari, A., Panda, S., Gardas, R. L. Effect of Ethylene, Diethylene, and Triethylene Glycols and Glycerol on the Physicochemical Properties and Phase Behavior of Benzyltrimethyl and Benzyltributylammonium Chloride Based Deep Eutectic Solvents at 283.15–343.15 K.*J. Chem. Eng. Data* **2018**, *63*(7), 2613–2627.

15. Dai, Y., van Spronsen, J., Witkamp, G.-J., Verpoorte, R., Choi, Y. H. Natural Deep Eutectic Solvents as New Potential Media for Green Technology.*Anal. Chim. Acta* **2013**, *766*, 61–68.
16. Vilková, M., Płotka-Wasylka, J., Andruch, V. The role of water in deep eutectic solvent-base extraction.*J. Mol. Liq.* **2020**, *304*, 112747.
17. Zhang, Q.; De Oliveira Vigier, K.; Royer, S.; Jérôme, F. Deep eutectic solvents: Syntheses, properties and applications.*Chem. Soc. Rev.* **2012**, *41*, 7108–7146
18. Ali, H. H., Ghareeb, M. M., Al-Remawi, M., Al-Akayleh, F. T. New Insight into Single Phase Formation of Capric Acid/Menthol Eutectic Mixtures by Fourier-Transform Infrared Spectroscopy and Differential Scanning Calorimetry.*Trop. J. Pharm.Res.* **2020**, *19*(2), 361–369.
19. van Osch, D. J. G. P.; Zubeir, L. F., van den Bruinhorst, A., Rocha, M. A., Kroon, M. C. Hydrophobic Deep Eutectic Solvents as Water-Immiscible Extractants. *Green Chem*. **2015**, *17*, 4518−4521.

HOW DOES USE OF PESTICIDES IN PROTECTION OF OILSEED RAPE PRODUCTION AFFECT BEE HEALTH AND SAFETY OF BEE PRODUCTS?

Brankica Kartalović[1*], Jelena Vranešević[1], Željko Milovac[2], Filip Franeta[2], Gorica Vuković[3]

[1] Scientific Veterinary Institute "Novi Sad", Rumenački put 20, 21000 Novi Sad, Serbia,

[2] Institute of Field and Vegetable Crops, Maksima Gorkog 30, 21000 Novi Sad, Serbia,

[3] Faculty of Agriculture, University of Belgrade, Nemanjina 6, 11080 Zemun, Serbia

*brankica@niv.ns.ac.rs

Abstract

For more than ten years, we have been witnessing a decrease in the number of honey bees and use of pesticides is recognised as one of the globally identified reasons. Our research aimed to test the presence of residues chlorpyrifos and two pyrethroids tau-fluvalinate and lambda-cyhalothrin samples collected on three apiaries (A, B and C). A modified QuEChERS (Quick Easy Cheap Effective Rugged Safe) approach was used for sample preparation, and the detection of the pesticides was done using GC-MS (Gas Chromatography-Mass Spectrometry). In apiary A, chlorpyrifos was detected in rapeseed flowers (1958.0 µg/kg), followed by pollen (334.5 µg/kg), dead bees (17.83 µg/kg) and honey (15.71 µg/kg), whilst lambda-cyhalothrin and tau-fluvalinate were not detected. Chlorpyriphos in pollen, perga and bees was also detected in apiary B, in average concentrations of 548.63 µg/kg, 46.83 µg/kg and 105.13 µg/kg, respectively. The presence of lambda-cyhalothrin in a concentration of 60.11 µg/kg of pollen was detected in this apiary, while the presence of tau-fluvalinate was not determined. In the samples from apiary C, chlorpyrifos was not detected, but in brood honeycombs, lambda cyhalothrin, tau-fluvalinate 1 and tau-fluvalinate 2 were found in the following concentrations: 69.90 µg/kg, 114.16 µg/kg and 105.36 µg/kg, respectively.

The obtained data indicate that it is necessary to establish constant monitoring of bee exposure to pesticides. This would ensure that the application of laws and regulations governing the use of pesticides in both Serbia and the EU ensures the successful protection of pollinators and enables their role in agroecosystems.

Keywords: Chlorpyrifos, pyrethroids, residues, bee products, bees

1. Introduction

Rapeseed, also known as oilseed rape or canola *(Brassica napus* subsp. *napus)*, is one of the salient industrial crops in the world and also in Serbia (1). It is possible to grow it in almost any agroecological area. Being rich in pollen and nectar, its flowers are a considerable bee pasture. However, the growth of rapeseed is accompanied by numerous insect pests of various importance, but also by useful insect species, especially pollinators, which is why the production of this crop has a considerable ecological impact. The use of pesticides is vital to assure higher oilseed rape yields, yet doing so degrades the environment and reduces the biodiversity of cultivated regions (2-4). The intensely yellow rapeseed blossom is particularly alluring to helpful insects, such as the honeybee (*Apis mellifera* L.), which raises the possibility of bee poisoning from pesticides. Bee exposure to pesticides through tainted flowers is frequently connected to cases of bee poisoning in canola-grazed areas (5).

A healthy and diverse floral environment is necessary for successful bee production. In the past, the only problems that could occur in apiaries were occasional infections with viruses, bacteria and parasites that could be fatal for bee colonies, as well as unpredictable weather events that could affect bees and their production (6). However, in the past decades, we have witnessed beekeepers facing a new threat-pesticides. In an effort to ensure the safe and healthy production of crops, fruits and other plants, there has been widespread use of pesticides, with the aim of controlling insects, pests, weeds and plant diseases. The uncontrolled use of insecticides poses a serious threat to people due to their sensitivity to the effects of these chemicals (6). In order to prevent this, developed countries took a serious approach to solve the problem by testing the toxicity before releasing such chemicals (7, 8), but also the fact that despite the regulations, the number of companies is decreasing, and one of the reasons is the uncontrolled use of pesticides.

As a result of all of this, agroecology rules have become more stringent, leading to the removal of an increasing number of active compounds and plant protection tools from the market. On the other hand, a minimal number of novel active compounds are registered due to the increasingly strict regulations for the registration of new plant protection products. According to tests, the indiscriminate use of pesticides is the main issue with agrochemical protection. The years-long, indiscriminate use of pesticides has brought about a return to the prophylactic use of pesticides, which has neglected the fundamental principle of integrated pest management, which is the use of pesticides only after all other options have been exhausted (9). This has once more led to the need for more pesticides. The repeated use of pesticides has

once more resulted in a new issue, which is the issue of insecticide resistance (10). The widespread use of pesticides has also been linked to a decline in plant blossoming, which directly impacts bees and their ability to produce, according to research (11, 12). It was discovered, as a result of the issues brought on by the use of pesticides, that the production of honey and other bee products, as well as the health of bees, depend not only on the availability of floral pasture but also on the quality of the food that bees collect. It is now understood that pesticide-contaminated flowers negatively impact bee colonies' health to the point that their productivity decreases (13). Stanimirović et al. (14) associated the occurrence of colony collapse disorder (CCD) not only with parasites and diseases but also with the use of pesticides (6, 15). In order to better manage this situation, we must first understand how bees are exposed to pesticides and what the consequences of such exposure are on the health of individual bees, their colonies and overall productivity. This, together with the declining availability of new active ingredients with pesticide activity due to declining discovery rates and stricter product approval legislation (16), represents a real threat to the effectiveness of pesticide use. Studies conducted around the world have shown that honeybees have problems with learning and memory after taking small doses of insecticides, potentially jeopardizing their success and survival.

Research has confirmed that the synergism of fungicides with pyrethroids and neonicotinoids results in much higher risks in spite of the low prevalence of their combined residues, due to the fact that specific combinations of residues may result in synergistic toxicity to bees (6).

The authors opted for the research into the - chlorpyrifos, tau-fluvalinate and lambda-cyhalothrin - on bees and bee products. These insecticides are often used for canola protection. Chlorpyrifos is an organophosphate compound used globally for plant protection against insects and mites. It is a broad-spectrum persistent insecticide, one of the last ones in the group of organophosphates. It has been allowed to be used in Serbia until the end of 2022. Despite detailed instructions on the use of chlorpyrifos, including the implementation of measures for the protection of beneficial insects, especially honeybees, from the dispersed chemicals, its residues have been detected in bees in numerous countries, which implies that it is still in use endangering the bees (17). Tau-fluvalinate, a member of the pyrethroid group, has been increasingly gaining interest as an eco-friendly insecticide, primarily when the influence on the honeybee (*Apis mellifera*) is taken into account. Lambda-cyhalothrin is a broad-spectrum insecticide widely used in agriculture production. Tau-fluvalinate and lambda-cyhalothrin belong to type II pyrethroids, which have been shown to be well tolerated by bees but still are not absolutely safe (18, 19).

Our study aimed to determine the presence of residues of chlorpyrifos, an organophosphate pesticide, and the two pyrethroids – tau-fluvalinate and lambda-cyhalothrin – in the samples of pollen, honey and perga and the bodies of dead bees.

2. Material and Methods

2.1. Pollen collecting for matrix match calibration

Solitary bee species from the genus *Osmia*, also known as mason bees, have been used in this trial. Solitary bees lack the complicated social structure present in social insects, such as honeybees. Instead, each female provides its offspring with a certain amount of pollen and nectar. They nest in natural cavities, in this case, reed stalks have been used as nests. The trial was set up at the Institute of Field and Vegetable crops in Novi Sad. Oilseed rape was used as a test plant. The plants were confined in isolation cages, netted with a fine mesh (1 mm) so that both pollen and insects could be kept from entering the cages. The pollen was extracted in September 2021, after the larval development was completed, from unused pollen in undeveloped cells and used in matrix-matched calibration.

2.2. Sample collection and handling

Samples of canola flower, pollen, honey, bee bread and dead bees were collected in May and June 2022 from three apiaries in Vojvodina: two of them in Srem District (A and B) and one in Bačka (C). The bee colonies were fed on canola pastures. The hives from which honey, bee bread and bees were sampled were randomly chosen. The apiaries were more than 20 km far from each other. All the hives were of the Langstroth type, with a pollen catcher inserted on the flight board, in front of the open hive entrance. Thus, the bees were compelled to go through the 5-mm openings of the mesh, while the pollen was taken from their hind legs and fell through the openings of the pollen catcher into the bowl intended for pollen collection. Honey and bee bread were sampled directly from the combs, and the dead bees were collected immediately in front of the hive entrance. All the samples were adequately packed and labelled.and with a request form transported to the laboratory of the Scientific Veterinary Institute "Novi Sad" within several hours.

2.3. Chemicals and materials

The reference standards of pesticides were purchased from AccuStandard (New Haven, USA) and Dr. Ehrenstorfer (Germany). HPLC-grade acetonitrile and methanol were obtained from Merck-Millipore (Darmstadt, Germany). Ultrapure deionized water was generated by a Millipore Milli-Q™ system Bundesil C18 and PSA were obtained from Agilent technologies

(USA). Anhydrous magnesium sulphate and sodium acetate were taken from Merck (Darmstadt, Germany).

2.4. Sample preparation

Sample preparation was based on a modified QuEChERS method (18). The sample (3 g) was measured and transferred into a polypropylene (PP) centrifuge tube (50 mL). The standard solutions were added at the appropriate spiking level for calibration and quality control samples. After the addition of acetonitrile (6 mL) the tubes were shaken vigorously by hand for 1 min. Then a salt mixture of 4 g of magnesium sulphate and 1 g of sodium acetate was added to the tubes, the tubes were closed and immediately shaken by hand for 1 min and centrifuged for 5 min at 4,500 rpm. An aliquot of 1 mL of supernatant was transferred into a 15 mL PP centrifuge tube with 150 mg anhydrous magnesium, 50 mg PSA and 150 mg C-18. After being shaken vigorously by a vortex, the tubes were centrifuged for 5 min at 4,500 rpm. Finally, the solution was purified and a clear extract was obtained and ready for GC-MS analysis. 1 mL of cleaned extract was transferred into an autosampler and injected in GC.

2.5. *GC-MS analysis*

The sample extracts in acetonitrile were analysed on an Agilent HP 7890B gas chromatograph coupled with an HP 5977A mass spectrometer (Agilent Technologies, CA, USA) operating in SIM mode (Table 1). The capillary column used was Agilent DB-5MS (30 m × 0.25 mm × 0.25 µm). Operating conditions: the carrier gas was helium at a constant flow rate of 1.2 mL/min injector temperature of 250°C and the interface temperature was 250°C. The initial oven temperature was 120°C (held for 1 min.), then increased to 280°C at a rate of 4°C/min (held for 4 min). The total analysis time was 45 min. The injection volume was 4 µL. The verification of the peaks was carried out, based on the retention times and target ions compared to those of external pesticides. Procedural blank and solvent blanks were analysed and quantified, but no target pesticides were found in these blanks. Determination was made in a splitless mode, the carrier gas was helium, the velocity 32.098 cm/s and the pressure was7.0 psi. Determination was made at constant flow.

2.6. Performance of analysis

The performance of the method was evaluated according to the EC guidance document SANTE 11312/2021 (20). Determination coefficients were higher than 0.999 for all compounds subjected to analysis. The mean variation of coefficients for repeatability of the method ranged from 4.0% to 13%, and the recovery ranged from 78% to 115%.

The limit of quantification (LOQ) for which the S/N ratio exceeds 10 was assumed at a concentration level of 0.0010 mg/kg for all pesticides LOQ was 0.0050 mg/kg.

Table 1. RT and Target and Qualified ions

No	Component name	RT	Target ion	Qualified ions		
1	Chlorpyriphos	19.84	314	197	199	-
2	Lambda-cyhalothrin	32.60	197	208	181	-
3	Tau-fluvalinate 1	31.03	502	250	252	281
4	Tau-fluvalinate 2	39.21	502	250	252	281

RT- retention time

3. Results and discussion

In this research, residues of chlorpyrifos, tau-fluvalinate and lambda-cyhalothrin were detected in rapeseed flowers, pollen, dead bees, bee bread and honey. In apiary A, chlorpyrifos was detected in rapeseed flowers (1958.0 µg/kg), followed by pollen (334.5 µg/kg), dead bees (17.83 µg/kg) and honey (15.71 µg/kg). Chlorpyriphos in pollen, perga and bees was also detected in apiary B, in average concentrations of 548.63 µg/kg, 46.83 µg/kg and 105.13 µg/kg, respectively. The presence of lambda-cyhalothrin was confirmed in the pollen collected from one apiary B (60.11 µg/kg), and in the brood combs in apiary C (69.90 µg/kg). Tau-fluvalinate, the substance approved for use in apiculture against the bee mite, Varroa destructor, was also detected in brood combs in the apiary C (114.16 µg/kg and 105.36 µg/kg).

This study is part of the project led by the Institute for field and vegetable crops. The project is aimed to investigate the influence of pesticides on the solitary bee species of the *Osmia genus* and their activities, in a controlled environment. Tau-fluvalinate, the substance approved for use in apiculture against the bee mite, *Varroa destructor*, was also detected in brood combs in the apiary C.

This study is part of the project led by the Institute for field and vegetable crops. The project is aimed to investigate the influence of pesticides on the solitary bee species of the *Osmia* genus and their activities, in a controlled environment.

Samples of dead bees collected from five hives in the three apiaries and analysed in this research were contaminated by chlorpyrifos in high concentrations (apiaries A and B), whilst in the bees from the apiary C chlorpyrifos was not detected. This pesticide has been widely used in agriculture, despite the recommendation that it should not be used in the flowering period. As reported by Lambert et al. (21), chlorpyrifos has been accused of bee poisoning across Europe. Mass poisoning occurred also outside Europe, in North America, which has been documented by numerous data (22). Owing to biotransformation and rapid excretion,

honeybees are insects that can lower the pesticide burden in their bodies but only if exposed to sublethal doses/concentrations, which mainly cause disorientation in bees (22). However, in two apiaries in the Srem District, the bees were exposed to lethal doses, which resulted in mortality. In the inspected dead bees tau-fluvalinate and lambda-cyhalothrin residues were not detected.

In honey samples originating from the inspected apiaries, collected in 2021 chlorpyrifos was detected in concentrations less than 15 µg/kg, which is below the maximum residue levels (MRL), (23), which is 50 µg/kg, whilst tau-fluvalinate and lambda-cyhalothrin were not detected.

In the current research samples of rapeseed flowers were collected from three fields and analysed. The average residues of chlorpyrifos reached 1,958.00 µg/kg on the fields visited by the bees from the apiaries A and B. Fresh pollen collected from three locations was also submitted to pesticide residue analysis. Chlorpyrifos residues averaged 334.5 µg/kg on apiary A and 548.63 µg/kg on apiary B, whilst on the C they were not detected. On collecting pollen from pesticide-contaminated pastures, honeybees inevitably import it into hives, which has been confirmed in a series of studies (24, 25). Research by Dolezal et al. (26) showed that high insecticide levels may lead to mortality in honeybees, but also some others confirmed that lower, sublethal doses may influence many aspects of bee physiology, including behaviour and learning. Contaminated pollen introduced into hives contaminates combs, bee bread and honey, however, it is also possible that combs are contaminated by pesticides used against varroa mites (22). In the comparison of these results with those reported by Calatayud-Vernich et al. (22), the confirmed chlorpyrifos concentrations were up to 40 times as previously reported, which is expected, given the bee mortality we witnessed. Calatayud-Vernich et al. (22) conducted their research on healthy bee colonies, whilst ours was done on apiaries where bee death was detected. Vernich et al. (22) found that 31% of the tested pollen samples were contaminated by chlorpyrifos (the mean concentration was 9.8 µg/kg).

Lambda-cyhalothrin was detected only in pollen sampled from apiary B, in the concentration of 60.11 µg/kg, whilst tau-fluvalinate was not detected in any of the pollen samples. Research made by Dolezal et al. (25) also confirmed the presence of lambda-cyhalothrin in concentrations below LD_{50}.

4. Conclusion

Although being below MRL, the obtained results pertaining the residue levels of pesticides show that the inadequate/uncontrolled use of pesticides may threaten the safety and tarnish the quality of the highly esteemed bee products. The presence of these pesticides in dead bees may suggest the possible cause of bee mortality. This will be further investigated within the research project led by the Institute for Field Crops, which deals with the topic.

The obtained data indicate that it is necessary to establish constant monitoring of bee exposure to pesticides. This would ensure that the application of laws and regulations governing the use of pesticides in both Serbia and the EU ensures the successful protection of pollinators and enables their role in agroecosystems. Only with adequate and prescribed application of pesticides is it possible to simultaneously provide protection for oilseed rape, a very important agricultural crop, and contribute to the reduction of mass bee deaths.

It is nessesery to control the use of pesticides, which are to be applied in proposed concentrations.

5. Acknowledgments

This study was funded by the Ministry of Education, Science and Technological Development of the Republic of Serbia by the Contract of implementation and funding of research work of NIV-NS in 2021, Contract No: 451-03-9/2021-14/200031 and was also supported by the Provincial Secretariat for Agriculture, Water Management and Forestry of Vojvodina, Contract No: 104-401-4672/2021/01.

6. References

1. Friedt, W., Tu, J., Fu, T. Academic and Economic Importance of *Brassica napus* Rapeseed. In: Liu, S., Snowdon, R., Chalhoub, B. (eds) The Brassica napus Genome. **2018,** 1-20.
2. Bianchi, F. J. J. A., Booij, C. J. H., Tscharntke, T. Sustainable pest regulation in agricultural landscapes: A review on landscape composition, biodiversity and natural pest control. *Proc. Royal Soc. B* **2006**, *273(1595)*, 1715-1727.
3. Robinson, R. A., Sutherland, W. J. Post-war changes in arable farming and biodiversity in Great Britain. *J. Appl. Ecol*. **2002**. *39(1)*, 157–176.

4. Schürch, R., Couvillon M. J, Ratnieks F. L.W. Determining the foraging potential of oilseed rape to honey bees using aerial surveys and simulations. *J. Apic. Res.* **2015**, *54(3)*, 238-245.
5. Stejskalová, M., Konradyová, V., Kazda, J. The influence of pesticides repellency used in oilseed rape (*Brassica napus* subsp. *napus*) on the preference by bees (*Apis mellifera* L.). *J. Apic. Res.* **2021,** *60(2)*, 270-276.
6. Sánchez-Bayo, F., Goka, K. Pesticide residues and bees - A risk assessment. *PLoS One*. **2014**, *9(4)*, e94482.
7. EFSA. Towards an integrated environmental risk assessment of multiple stressors on bees: review of research projects in Europe, knowledge gaps and recommendations. *EFSA J*. **2014,** *12(3)*, 3594.
8. OECD Test No. 213: Honeybees, Acute Oral Toxicity Test, OECD Guidelines for the Testing of Chemicals, Section 2, OECD Publishing, Paris, **1998**.
9. Lundin, O., Malsher, G., Högfeldt, C., Bommarco, R. Pest management and yield in spring oilseed rape without neonicotinoid seed treatments. *Crop Prot*. **2020,** *137*, 105261.
10. Skellern, M. P., Cook, S. M. The potential of crop management practices to reduce pollen beetle damage in oilseed rape. *Arthropod Plant Interact*. **2018,** *12*, 867–879.
11. Hald, A. B. Weed vegetation (wild flora) of long established organic versus conventional cereal fields in Denmark. *Ann Appl. Biol.* **1999,** *134(3)*, 307–314.
12. Hyvonen, T., Salonen, J. Weed species diversity and community composition in cropping practices at two intensity levels: a six-year experiment. *Plant Ecol.* **2002,** *159(1)*, 73–81.
13. Krupke, C.H., Long, E.Y. Intersections between neonicotinoid seed treatments and honey bees. *Curr. Opin. Ins. Sci*. **2015,** *10*, 8–13.
14. Stanimirović, Z., Glavinić, U., Ristanić, M., Aleksić, N., Jovanović, N., Vejnović, B., Stevanović, J. Looking for the causes of and solutions to the issue of honey bee colony losses. *Acta Vet.* **2019,** *69(1)*, 1-31.
15. Maini, S., Medrzycki, P., Porrini, C. The puzzle of honey bee losses: a brief review. *Bull. Insectol*. **2010,** *63(1)*, 153–60.
16. Poquet, Y., Vidau, C., Alaux, C. Modulation of pesticide response in honeybees. *Apidologie* **2016,** *47*, 412-426.
17. Urlacher, E., Monchanin, C., Rivière, C., Richard, F.-J., Lombardi, C., Michelsen-Heath, S., Hageman, K. J., Mercer, A. R. Measurements of Chlorpyrifos Levels in

Forager Bees and Comparison with Levels that Disrupt Honey Bee Odor-Mediated Learning Under Laboratory Conditions. *J. Chem. Ecol*. **2016**, *42(2),* 127–138.

18. Seidenglanz, M., Bajerová, R., Kolařík, P., Hrudová, E., Havel, J., Táncik, J., Ruseňáková, M., Bokor, P., Kocourek, F., Stará, J., VÍchová, L., Šafář, J. The correlation between the susceptibilities to lambda-cyhalothrin and tau-fluvalinate in Czech and Slovak pollen beetle populations. *Zemdirbyste-Agriculture* **2020**, *107(4),* 359-366.
19. Liao, C., He, X., Wang, Z., Barron, A. B., Zhang, B., Zeng, Z., Wu, X. Short-Term Exposure to Lambda-Cyhalothrin Negatively Affects the Survival and Memory-Related Characteristics of Worker Bees *Apis mellifera*. *Arch. Environ. Contam. Toxicol.* **2018**, *75(1),* 59-65.
20. European Commission. Analytical Quality Control and Method Validation Procedures for Pesticide Residues Analysis in Food and Feed. Doc. No. SANTE 11312/2021.
21. Lambert, O., Piroux, M., Puyo. S., Thorin, C., L'Hostis, M., Wiest, L., Buleté, A., Delbac, F., Pouliquen, H. Widespread Occurrence of Chemical Residues in Beehive Matrices from Apiaries Located in Different Landscapes of Western France. *PloS One* **2013,** *8(6),* e67007.
22. Calatayud-Vernich, P., Calatayud, F., Simo, E., Pico, Y. Pesticide residues in honey bees, pollen and beeswax: Assessing beehive exposure. *Environ. Pollut.* **2018,** *241*, 106-114.
23. European Union. Commission Regulation (EU) 2018/686 of 4 May 2018 amending Annexes II and III to Regulation (EC) No 396/2005 of the European Parliament and of the Council as regards maximum residue levels for chlorpyrifos, chlorpyrifos-methyl and triclopyr in or on certain products. **2018**, 30-62.
24. Krupke, C. H., Hunt, G. J., Eitzer, B. D., Andino, G., Given, K. Multiple Routes of Pesticide Exposure for Honey Bees Living Near Agricultural Fields. *PloS One* **2012,** *7(1),* e29268.
25. David, A., Botías, C., Abdul-Sada, A., Nicholls, E., Rotheray, E. L., Hill, E. M., Goulson, D. Widespread contamination of wildflower and bee-collected pollen with complex mixtures of neonicotinoids and fungicides commonly applied to crops. *Environ. Int*. **2016**, *88*, 169-178.

CIPROFLOXACIN REMOVAL USING SEPIOLITE-BASED ADSORBENTS

Vesna Marjanović[1*], Ivona Janković-Častvan[2], Slavica Lazarević[2], Željko Radovanović[3], Đorđe Janaćković[2], Rada Petrović[2]

[1] *Western Serbia Academy of Applied Studies, Trg Svetog Save 34, 31000 Užice, Serbia*

[2] *Faculty of Technology and Metallurgy, University of Belgrade, 11000 Belgrade, Serbia*

[3] *Innovation Center of Faculty of Technology and Metallurgy, Ltd, Belgrade, Serbia*

*vesnamarjanovic031@gmail.com

Abstract

Ciprofloxacin (CIP) as a broad-spectrum quinolone antibiotic is extensively used in daily life and can be detected in municipal and pharmaceutical wastewaters, as well as natural waters. In this study, natural mineral sepiolite (SEP), SEP modified with hexadecyltrimethylammonium-bromide (HDAB) and SEP composites with graphene oxide (GO) were used as adsorbents for the removal of CIP from aqueous solutions. The composites were prepared at a mass ratio SEP to GO of 2:1, using SEP and SEP modified by [3-(2-aminoethylamino)propyl]trimethoxy-silane (APT). Thermogravimetric analysis, X-ray diffraction and nitrogen adsorption-desorption were used to characterize the obtained adsorbents. The adsorption of CIP was investigated at a pH value close to the pH of natural waters. The concentration of CIP in an aqueous solution was determined by UV-Vis spectroscopy. GO showed the highest adsorption capacity (~ 150 mg/g). The capacity of SEP was about 60 mg/g, while the SEP modification with HDAB has led to a decrease in the adsorption capacity (~ 35 mg/g). The composite SEP/GO showed a higher adsorption capacity (~ 110 mg/g) than the composite SEP-APT/GO (~ 40 mg/g). The capacity of the composite SEP/GO was higher than that of the mixture of SEP and GO, which indicated a certain degree of GO exfoliation and intercalation of sepiolite particles, as was shown by X-ray diffraction. Equilibrium data for all adsorbents, except for HDAB modified sepiolite, fitted well to the Langmuir isotherm model.

Keywords: adsorption, ciprofloxacin, sepiolite, graphene oxide

1. Introduction

The widespread use of antibiotics has led to their increased content in wastewater from households, hospitals and the pharmaceutical industry. The continuous introduction of

antibiotics into the aquatic environment, even at low concentrations, can have a detrimental effect on ecosystems and represent a long-term potential risk for aquatic and terrestrial organisms (1). In general, antibiotics reach the aquatic environment in two ways: (i) about 30-90% of the used dose of antibiotics may remain undegraded in the body of humans or animals and be excreted as an active compound; (ii) direct release of antibiotics into the environment as waste materials of the chemical-pharmaceutical industry. Conventional wastewater treatment systems can remove approximately 85% of these pollutants, leading to an increase in their concentration in natural waters (2). Antibiotic contamination is one of the global environmental problems.

Ciprofloxacin (CIP) is a typical fluoroquinolone antibiotic that is widely used for the treatment of urinary and respiratory infections in humans, but in recent years it has also been widely used in veterinary medicine (3).

According to its chemical composition, ciprofloxacin is 1-cyclopropyl-6-fluoro-4-oxo-7-piperazine-1-yl-quinolone-3-carboxylic acid (Figure 1), which, in addition to the aromatic part, also contains functional groups suitable for hydrogen binding (4). Depending on the pH value of the medium, CIP molecules are found in different forms. At the pH values of natural waters (~ 7.5), ciprofloxacin is present as a neutral molecule or zwitter ion, which contains an ionized carboxyl ($–COO^-$) and a protonated amino ($–NH_2^+$) group.

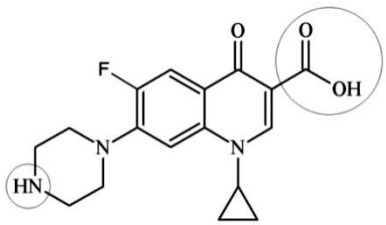

Figure 1. Structure of ciprofloxacin with characteristic groups marked (4)

For the treatment of effluents containing ciprofloxacin, electrochemical and chemical oxidation, photodegradation, catalytic decomposition, enzymatic decomposition and adsorption on selective adsorbents were used (5-8). Adsorption on suitable adsorbents has proven to be a practical, efficient and economically justified method for removing polluting substances from aqueous solutions and for separating adsorbed species for further analysis or regeneration. Properly designing and managing the adsorption process makes it possible to obtain high-quality purified water. The topic of research in a large number of papers (9-11) is the adsorption of ciprofloxacin from aqueous solutions using adsorbents based on activated carbon, graphene, graphene oxide and carbon nanotubes. Many materials have been shown to

have a significantly high adsorption capacity for ciprofloxacin, but for the practical application and economy of the procedure, the adsorbent must be also of low price.

Bearing in mind that the adsorption of ciprofloxacin on montmorillonite gave good results (12), *i.e.* that the adsorption capacity of montmorillonite (up to 330 mg/g) is higher than the capacity of some carbon materials (155 mg/g), we decided to use sepiolite as adsorbent, which proved to be a good adsorbent of cations. The subject of this work is the study of the adsorption of ciprofloxacin from aqueous solutions, at pH ~ 7.5, using natural sepiolite (SEP), sepiolite modified with hexadecyltrimethylammonium bromide (SEP-HDAB), graphene oxide (GO), a composite of natural sepiolite with graphene oxide (SEP/GO), and the composite of amino-silane ([3-(2-aminoethylamino)propyl]trimethoxysilane, APT) modified sepiolite with graphene oxide (SEP-APT/GO).

2. Experimental

Sepiolite from the Andrići deposit near Čačak was used as the starting raw material the experimental work, particle fraction <91μm. Previous research has shown that the impurity content is very low and the cation exchange capacity is 26mmol M^+/100g of sepiolite (13). Hexadecyltrimethylammonium bromide (HDAB) and [3-(2-aminoethylamino)propyl]trimethoxysilane (amino-silane, APT) of purity 99.99%, manufactured by Sigma Aldrich, were used for sepiolite modification.

2.1. Preparation of adsorbents

A suspension of 15 g of sepiolite and 50 cm^3 of water was treated with an ultrasonic (UV) probe, diameter 19 mm in the "+" mode, twice for 1 min, after which 5 g of sepiolite was added and treated with the probe for another 1 min, each time at an amplitude of 80%. Water was added to the suspension up to a volume of 1500 cm^3 and it was again treated with the probe twice for 5 min and once for 3 min, also at an amplitude of 80%. The sepiolite suspension was heated to 50°C and a modifier solution was added to it, which was obtained by dissolving 2.9 g of HDAB in 100 cm^3 of water, also heated to 50°C. The suspension with the added modifier was mixed for 24 hours, the first 3 hours of which were heated at 50°C. After mixing, the suspension was filtered twice on a Büchner funnel and dried at 60°C, after which the sample was dusted and additionally dried at 60°C. The modified sepiolite obtained in this way is designated as SEP - HDAB. Graphene oxide was synthesized based on a modified Hummers method (11) and designated as GO. The composite SEP/GO was prepared at the ratio SEP:GO= 2:1, by adding 3g of natural sepiolite and 1.5g of graphene oxide to

1000cm^3 of distilled water. The resulting suspension was treated with a UV probe for 5min (2+2+1). The suspension obtained in this way was filtered on a Büchner funnel, and the obtained solid phase was dried at 60°C, after which the obtained sample was powdered. The composite obtained in this way was designated as SEP/GO. The SEP-APT/GO composite was prepared in the same way as the SEP/GO composite, only instead of SEP, SEP-APT was used, prepared according to the previously given procedure given (14).

2.2. Characterization of samples

Thermogravimetric analysis of modified sepiolites, compared to unmodified ones, was performed on an SDT Q600 TGA/DSC (TA Instruments), at a heating rate of 20°C/min, with less than 10 mg of sample. Analyzes were performed in an air atmosphere, with a flow rate of 100 cm^3/min. The samples' specific surface area and volume and pore size distribution were determined based on nitrogen adsorption-desorption isotherms obtained using the Micromeritics ASAP 2020 device. The phase composition of the samples was determined by X-ray diffraction analysis (XDR) using an ITAL STRUCTURE APD 2000 diffractometer using CuKα radiation, in the 2θ range from 5° to 50°, with a step of 0.02.

2.3. Adsorption of ciprofloxacin

The basic solution of ciprofloxacin, with a concentration of 30mg/dm^3, was prepared by dissolving ciprofloxacin in deionized water at the pH value of natural waters (pH=7.5). All adsorption experiments were performed by equilibrating 200cm^3 of ciprofloxacin solution with 0.02 g of adsorbent in a thermostat with a shaker at a temperature of 298K for 24h. Ciprofloxacin concentration in starting solutions and solutions after adsorption was determined by UV-VIS spectrophotometry at a wavelength of 418nm. The amount of ciprofloxacin adsorbed per unit mass of adsorbent until reaching the equilibrium concentration of CIP on the adsorbent, q_e (mg/g), was determined using Eq. (1):

$$q_e = \frac{c_i - c_e}{m} V \quad (1)$$

where: c_i and c_e are the initial and equilibrium concentrations of CIP solution (mg/dm^3), V is the volume of CIP solution (dm^3) and m is the mass of adsorbent (g).

3. Results and discussion

The results of thermogravimetric (TG) analysis of unmodified and modified sepiolite are shown in Figure 2.

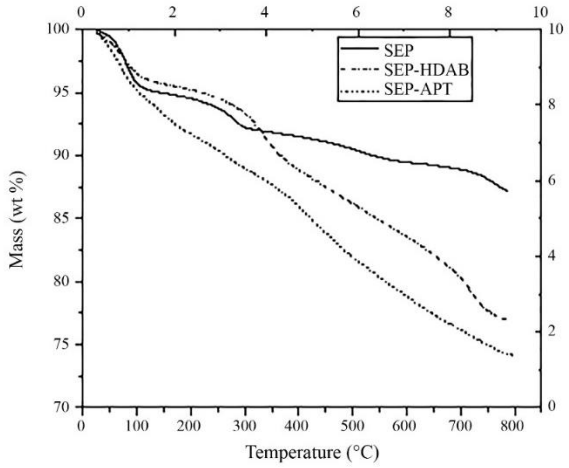

Figure 2. TG curves of SEP, SEP-HDAB and SEP-APT samples

The thermogravimetric curve of the SEP sample shows characteristic mass losses: up to approximately 120°C corresponding to the evaporation of hygroscopically bound water, and at temperatures of 340°C and 670°C due to the loss of bound water. In the case of SEP-HDAB, initially, up to approximately 300°C, a similar mass loss occurs as with the SEP sample, but after that, the mass loss is significantly higher. In the SEP-APT sample, the mass loss is higher than in the SEP already from the temperatures at which hygroscopic water is removed. Larger mass losses in the SEP-HDAB and SEP-APT samples are related to the presence of organic matter introduced by sepiolite modification, whose evaporation and combustion reduce the mass of the samples to a much greater extent than in the SEP sample. These results confirm that SEP-HDAB and SEP-APT samples contain organic modifiers, that is, that the modification procedures were successful. The textural parameters of the SEP, SEP-HDAB, GO, SEP/GO and SEP-APT/GO are shown in Table 1.

Table 1. Textural parameters of SEP, SEP - HDAB, GO, SEP - GO, APT SEP - GO samples

Sample	S_{BET} (m^2/g)	V_{total} (cm^3/g)	$V_{mesopore}$ (cm^3/g)	$V_{micropore}$ (cm^3/g)	D_{mean} (nm)	D_{max} (nm)
SEP	359.9	0.410	0.139	0.343	3.2	6.7
SEP-HDAB	105.5	0.387	0.368	0.031	14.1	3.6
GO	48.7	-	-	-	-	-
SEP-GO	209.2	0.337	0.318	0.083	7.5	4.3
APT SEP-GO	98.8	0.182	0.173	0.033	7.4	3.8

Sepiolite has the largest specific surface area (359.9 m^2/g) thanks, first of all, to a large proportion of structural micropores. Since the micropore volume decreases drastically during the modification of sepiolite with HDAB, while the mesopore volume increases, it is obvious that HDAB blocks the micropores. Graphene oxide has a significantly smaller surface area

because the structure is built from layers that are connected by weak bonds, that is, there are no well-defined micro- and mesopores. The specific surface area of the SEP/GO composite is following the surface areas of the components and their share in this composite. However, a significantly lower micropore content in the SEP/GO composite than in the SEP sample indicates the closure of the micropores during the synthesis of the composite. Reducing the content of micropores in SEP/GO may not affect the adsorption of ciprofloxacin, considering that the CIP molecule has large dimensions (3) and can hardly enter the micropores. The specific surface area of the SEP-APT/GO composite is smaller than that of SEP/GO, which is probably due to the smaller surface area of SEP-APT compared to the SEP sample, as shown in previous research (14).

The XRD results of graphene oxide and composites with graphene oxide are shown in Figure 3. The diffractogram of graphene oxide showed a peak at 2θ =13.2º, which corresponds to the distance between graphene oxide layers (d=0.67nm) and refers to the structure of graphene oxide, which correspond to literature (11). This peak was not visible on the diffractograms of the graphene oxide composite, only the peak characteristic of sepiolite was observed (Figure 3). It can be concluded that there was a separation of the graphene oxide layers during the formation of the composite and the sepiolite particles were incorporated between the layers, which was the goal of forming the composite.

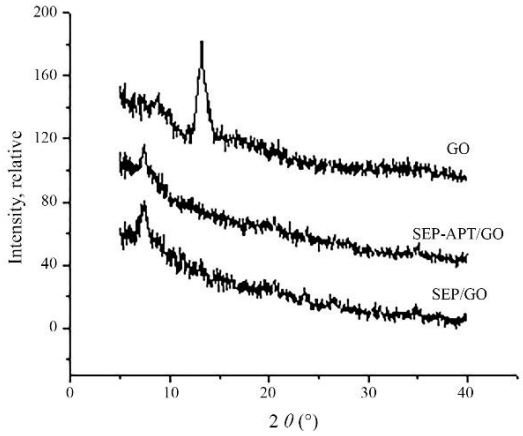

Figure 3. X-ray diffractograms of the GO and composites with GO

Figure 4 shows a comparison of isotherms for ciprofloxacin adsorption from solutions of different initial concentrations on SEP, SEP-HDAB, GO, SEP/GO and SEP-APT/GO samples.

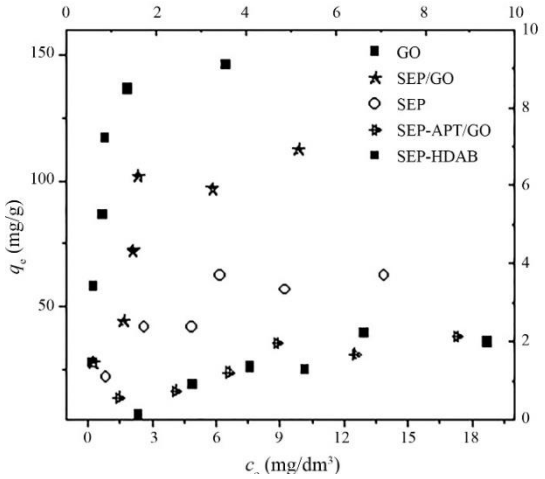

Figure 4. The adsorption isotherms of ciprofloxacin on GO, SEP/GO, SEP, SEP-APT/GO and SEP-HDAB adsorbents, at 298 K

The obtained isotherms showed an increase in the adsorbed amount of ciprofloxacin with an increase in initial concentrations, but they differed in the achieved maximum adsorption capacity of ciprofloxacin. The starting concentrations of the CIP solution in the adsorption experiments were less than 30 mg/dm^3, and isotherm determinations were performed at an initial pH of 7.5. Under these conditions, CIP occured predominantly in the form of a neutral molecule or as a zwitter ion. Graphene oxide had the highest adsorption capacity (~150mg/g). Adsorption of ciprofloxacin on graphene oxide can take place through electrostatic interactions between ionized carboxyl functional groups of graphene oxide and $–NH_2^+$ groups of zwitter ions of CIP, and π-π interactions of aromatic rings from the structure of CIP and graphene oxide. In the case of sepiolite, the adsorption capacity was lower (~ 60mg/g) than on graphene oxide, even though its specific surface area was much larger compared to graphene oxide (Table 1). The possible mechanism of ciprofloxacin adsorption, in this case, was electrostatic interactions between charged centers on sepiolite and ionized ($–COO^–$ and $–NH_2^+$) groups of CIP. The adsorption capacity of the SEP/GO composite was about 110mg/g, which was between the values of the adsorption capacity of the GO and the SEP. If the SEP/GO sample was a simple mixture of SEP and GO in a mass ratio of 2:1, the adsorption capacity would be about 90mg/g. The fact that the capacity of the SEP/GO sample was greater than in a simple mixture of SEP and GO, speaks in favour of the fact that the layers of graphene oxide were separated during the formation of the composite, between which sepiolite particles were inserted, which increased the surface area available for adsorption. On the other hand, the adsorption capacity of the SEP-APT/GO composite was significantly lower than both the adsorption capacity of GO and the capacity of unmodified sepiolite. SEP-

APT was used for the synthesis of this composite, to ensure better delamination of graphene oxide, thanks to the interactions of amino groups in SEP-APT and carboxyl groups on graphene oxide. However, there was a decrease in the number of groups available for CIP adsorption, so adsorption was significantly reduced. Also, the adsorption capacity of sepiolite after modification with HDAB was significantly reduced (Figure 4). Modification with HDAB is based on ion exchange of naturally occurring cations in the SEP structure with hexadecyltrimethylammonium ions, resulting in the dominantly hydrophilic surface of sepiolite becoming partially hydrophobic, and at the same time, there is a reduction of the specific surface area. Bearing in mind that the part of the CIP molecule that does not contain ionizable groups can be considered hydrophobic, partial hydrophobization of the sepiolite surface was expected to provide increased adsorption capacity. However, the significantly reduced adsorption capacity of CIP indicated that ciprofloxacin was adsorbed predominantly through ionized ($–COO^-$ and $–NH_2^+$) groups, that was, by electrostatic interactions.

The agreement of the obtained results with two models of adsorption isotherms, Langmuir's and Freundlich's, was examined. The parameters for the adsorption of ciprofloxacin from the aqueous solutions on the prepared adsorbents are given in Table 2 along with linearized forms of the Langmuir and Freundlich models.

Table 2. Parameters of Langmuir and Freundlich models for the adsorption of ciprofloxacin from the aqueous solutions on SEP, SEP-HDAB, GO, SEP/GO and SEP-APT/GO adsorbents

Adsorbents	Langmuir model $\frac{c_e}{q_e}=\frac{1}{K_L\cdot q_m}+\frac{c_e}{q_m}$			Freundlich model $\ln q_e=\ln K_f+\frac{1}{n}\ln c_e$		
	K_L	q_m	R^2	K_f	$1/n$	R^2
SEP	0.4736	71.07	0.96078	25.19	0.3804	0.85655
SEP-HDAB	0.0473	84.53	0.41977	4.071	0.8242	0.86107
GO	1.883	160.0	0.98771	89.72	0.6746	0.67460
SEP/GO	0.6260	128.2	0.92466	49.50	0.3972	0.78970
SEP-APT/GO	0.1732	49.02	0.86499	7.276	0.5499	0.89985

q_m (mg/g) - maximum adsorption capacity of the adsorbent, K_L (dm^3/mg) - Langmuir constant; K_f ((mg/g)(dm^3/mg)$^{1/n}$) - Freundlich's empirical constant, n - the Freundlich's intensity factor

The values of the correlation coefficient R^2 in Table 2 indicate that the adsorption results are better described by the Langmuir model, except when modified SEP-HDAB was used as an adsorbent, where a better correlation was shown with the Freundlich model, which is consistent with the results obtained in other works (10-12) where also this model better describes the process of adsorption of ciprofloxacin from the aqueous solutions.

4. Conclusion

The ciprofloxacin adsorption on the natural mineral sepiolite and the possibility of adsorption enchacement by modifying sepiolite were investigated. The results of the TG analysis showed that mass losses during heating of SEP-HDAB and SEP-APT were significantly higher than during heating of SEP, due to the removal of organic matter from SEP-HDAB and SEP-APT, indicating successful modification by HDAB and APT. All samples that were used as ciprofloxacin adsorbents are micro-mesoporous. SEP had the largest specific surface area. Modification SEP with HDAB drastically reduced the micropore content, whereby the mesopore volume increased, and the specific surface area decreased. Graphene oxide had a significantly smaller surface area than SEP. The specific surface area of the SEP/GO composite followed the component surface areas and their share in this composite, while the specific surface area of the SEP-APT/GO composite was smaller than that of SEP/GO. XRD analysis confirmed the structure of graphene oxide. It was found that individual layers of graphene oxide were represented in the composites, between which sepiolite particles were probably incorporated. GO has the highest adsorption capacity (~150mg/g) for CIP. The adsorption capacity of SEP was ~60mg/g, and the SEP/GO composite was ~110mg/g. The adsorption capacity of the composite SEP-APT/GO was lower than that of SEP/GO. Modification with HDAB led to a decrease in the adsorption capacity of sepiolite. The results showed that the natural unmodified mineral sepiolite, alone or in the form of a composite with graphene oxide, has great potential for removing ciprofloxacin from aqueous solutions.

5. Acknowledgements

The authors acknowledge funding from the Ministry of Education, Science and Technological Development of the Republic of Serbia through contracts No. 451-03-68/2022-14/200287, and 451-03-68/2022-14/200135.

6. References

1. Nasri A. *et al*, Restructuring of a meiobenthic assemblage after sediment contamination with an antibacterial compound: Case study of ciprofloxacin, *Ecotox Environ Safe*, **2020**, *205*, 111084.

2. Kovalakova P., Cizmas L., McDonald T. J., Marsalek B., Feng M., Sharma V. K., Occurrence and toxicity of antibiotics in the aquatic environment: A review, *Chemosphere*, **2020**, *251*, 126351.
3. Silva G. R., Farmacocinética e determinação de resíduos de enrofloxacina e seumetabólito em tecidos de frangos, Campinas, Thesis of PhD degree, Department of Analytical Chemistry, Institute of Chemistry, State University of Campinas, **2004**, 127.
4. Al-Omar A. M. Profiles of Drug Substances, Excipients and Related Methodology, *Ciprofloxacin: Analytical Profile*, **2005**, *31*, 179-207.
5. Chi Y. et al. Manganese oxides activated peroxymonosulfate for ciprofloxacin removal: Effect of oxygen vacancies and chemical states, *Chemosphere*, **2022**, *299*, 134437.
6. Kuila S. K., Gorai D. K., Gupta B., Gupta A. K., Tiwary C. S., Kundu T. K. Lanthanum ions decorated 2-dimensional g-C_3N_4 for ciprofloxacin photodegradation, *Chemosphere*, **2021**, *268*, 128780.
7. Cheng J. et al. Plasma-catalytic degradation of ciprofloxacin in aqueous solution over different MnO_2 nanocrystals in a dielectric barrier discharge system, *Chemosphere*, **2020**, *253*, 126595.
8. Wu M. et al. Competitive adsorption of antibiotic tetracycline and ciprofloxacin on montmorillonite, *Appl Clay Sci*, **2019**, *180*, 105175.
9. Darweesh T. M., Ahmed M. J. Adsorption of ciprofloxacin and norfloxacin from aqueous solution onto granular activated carbon in fixed bed column, *Ecotox Environ Safe* **2017**, *138*, 139-145.
10. Li H. et al. Removal of ciprofloxacin from aqueous solutions by ionic surfactant modified carbon nanotubes, *Environmental Pollution*, **2018**, *243*, 206-217.
11. Ge W. et al. Graphene oxide template-confined fabrication of hierarchical porous carbons derived from lignin for ultrahigh-efficiency and fast removal of ciprofloxacin, *J Ind Eng Chem*, **2018**, *66*, 456-467.
12. Jalil M. E. R., Baschini M., Sapag K., Influence of pH and antibiotic solubility on the removal of ciprofloxacin from aqueous media using montmorillonite, *Appl Clay Sci*, **2015**, *114*, 69-76.
13. Lazarević S. Proučavanje sorcionih svojstava sepiolita, Magistarska teza, Tehnološko-metalurški fakultet Univerziteta u Beogradu, Beograd, **2007.**

14. Marjanović V. Proučavanje sorpcije hroma(VI) iz vodenih rastvora na funkcionalizovanim sepiolitima, Doktorska disertacija, Tehnološko-metalurški fakultet Univerziteta u Beogradu, Beograd, **2013.**

BIO-OIL MODEL SYSTEM SEPARATION BY VACUUM DISTILLATION: OPTIMIZATION WITH ASPEN PLUS

Jelena Kovač[1], Branislava Nikolovski[1]*, Jelena Bajac[1]

[1] University of Novi Sad, Faculty of Technology Novi Sad, Bulevar cara Lazara 1, 21000 Novi Sad, Serbia

**barjakb@uns.ac.rs*

Abstract

The current and future sustainable development of humanity seems to be dependent on finding alternative sources of energy. Biomass, a renewable source of energy, is transformed into bio-oil, a complex mixture of various chemicals, through the pyrolysis process. Bio-oil can be used as a substitute for liquid fossil fuels for obtaining heat and steam, or as a source of fine chemicals, and hydrogen production resources. However, the components need to be separated and purified using technologies such as catalytic cracking, hydrodeoxygenation, extraction, catalytic esterification, column chromatography, and vacuum distillation, the latter proving to be the best because it is simple, efficient, and allows for easy large-scale application. The vacuum distillation process should be optimized due to competing cost effects that appear as the process pressure is lowered. Namely, lower operational costs for energy are accompanied by greater capital costs for sizable columns and condensers.

Aspen Plus is a powerful tool for simulation, design, and optimization, and it was used in this work to optimize the vacuum pressure of the process. Due to the complexity and varying composition of bio-oils, as well as to verify the experimental results of vacuum distillation, a model system of bio-oil can be used instead of the oil itself. A bio-oil model was composed of seven of the main characteristic components of bio-oil: distilled water, ethanol, acetic acid, furfural, phenol, guaiacol, and 3-methyl-1, 2-cyclopentadione. The system was used to check the results of simulations obtained in this work by previously published experimental results obtained from literature.

Keywords: Bio-oil model system, vacuum distillation, rectification, Aspen Plus, optimization

1. Introduction

Issues concerning the limited resources of fossil fuels and their impact on the environment, in the form of an increase in the greenhouse effect, have led in recent decades to increased efforts to develop more efficient systems and greater use of alternative energy sources. Sustainability and greenhouse gas saving criteria are set out in many documents (1-3). The global increase in energy prices, and the fact that Europe is facing the highest energy prices in the world at the moment, impose the need to urgently find a way to reduce the consumption of fossil fuels. One of the good alternatives, the use of which will be much more pronounced in the future, is biomass (1-4). Bio-oil, a complex mixture of various oxygenated chemical compounds, can be obtained from biomass through either pyrolysis or hydrothermal liquefaction process (4).

Pyrolysis bio-oils contain more than 400 compounds (organic acids, esters, alcohols, aldehydes, ketones, furans, phenols, and dehydrated carbohydrates); with a composition depending on the biomass feed composition and conditions of the pyrolysis process (5-8). Therefore, a number of fine chemicals can be extracted from bio-oils, as well as components that can be used as a source for obtaining hydrogen (4, 5). Although bio-oil can be used as a substitute for liquid fossil fuels for obtaining heat and steam, usually it can't be used as a fuel directly (5).

For bio-oils purification and separation of compounds and fine chemicals originating in bio-oils, technologies such as catalytic cracking, hydrodeoxygenation, extraction, catalytic esterification, column chromatography, and vacuum distillation are used, the latter proving to be the best because it is relatively simple, efficient, and allows for easy large-scale application (6). However, the separation of bio-oil components according to their different boiling points is by no means easy. In the case of such a multicomponent raw material, the number of variables available for optimization in a batch distillation process can be very large and designing is an iterative process (9).

Since the composition of bio-oil is very complex, it is difficult to carry out distillation and separation directly in a small or pilot plant, and the characteristics of bio-oil distillation itself are not clear (6). In the available literature, it is possible to find results of separation experiments of a model system, composed of the main characteristic components of bio-oil ("bio-oil models"), investigating the effect of different degrees of vacuum on the distillation characteristics of known bio-oil components and analyzing the distillate rate of each component under different degrees of vacuum (6). These experiments are conducted on a

small-scale distillation apparatus (6). Unfortunately, some details that could be vital for the mathematical modeling of that batch process were not given in the paper, such as the retention of liquid in the stages and in the reflux drum.

Modeling of discontinuous distillation of multicomponent systems is a great challenge, primarily due to the very nature of the batch operation, and the possibility to approach it in several ways in order to achieve the necessary separation of all components (10, 11). This paper provides results of mathematical modeling of the continuous and discontinuous distillation process of the bio-oil model system under atmospheric pressure (100 kPa) and different values of vacuum (97 kPa, 95 kPa, 93.5 kPa, 92 kPa, 40 kPa and 70 kPa) in order to examine the distribution of product components under different conditions. Simulation and optimization were done with the Aspen^{TM} software package.

2. Experimental

Bio-oil is represented by a model system consisting of distilled water, ethanol, acetic acid, furfural, phenol, guaiacol and 3-methyl-1,2-cyclopentadione (methylcyclopentenolone) (CAS number 765-70-8). The above components were entered into the Aspen Plus V12.1 software package. The system was chosen because experimental data could be found for it in the literature (6). The seven listed substances were mixed in a mass ratio of 5:4:4:2:2:2:1, and the initial mixture was mixed for 24 h in order to achieve complete mixing (6). To verify the simulation results obtained in this work, the experimental results of the vacuum distillation process of the selected model of the bio-oil system performed on a discontinuous distillation column of small dimensions that exist in the literature (6) were used. For each experiment, 2000 g of bio-oil model compounds were used both in the experiments and in the simulations. Experiments were performed under pressures of 100 kPa (atmospheric pressure), 97 kPa, 95 kPa, 93.5 kPa and 92 kPa (6), while simulations were also performed at lower pressures of 70 and 40 kPa.

3. Mathematical modeling in Aspen Plus

Continuous distillation of the studied bio-oil system model was firstly modeled by simplified methods, i.e. shortcut methods/ blocks: DSTWU (Winn-Underwood-Gilliland method) (10) and Distl (Edmister method) (10). Thereafter, the RadFrac model (10), which includes rigorous calculation methods for a continuous separation process, was applied. Finally, the

discontinuous distillation process was modeled by the BatchSep block, a rigorous model for simulating multistage batch distillation columns.

The results obtained by shortcut methods are used as baseline estimates for rigorous methods (10, 11). DSTWU and Distl models/blocks are very useful for obtaining first approximations for column parameters (11). These models are based on the assumptions of constant relative volatility and constant molar flow of phases within each of the column sections and therefore their results are not very accurate. In order to obtain more accurate results in the next step, rigorous separation models (RadFrac or BatchSep) are applied using individual column parameters obtained by shortcut methods.

The thermodynamic method used for calculations is NRTL (Non-random two-liquid model). The NRTL term is based on Wilson's theory that the local concentration surrounding the molecule differs from the total concentration (9). The original plan was to use the NRTL-HOC model due to the presence of acetic acid in the system, which uses a modification of the equation of state (Renon) proposed by Hayden-o'Connell (Hayden-o'Connell equation of state) in combination with Henry's law for equilibrium gas-liquid. However, the lack of appropriate parameters relevant to the application of this model, related to the presence of the 3-methyl-1,2-cyclopentadione component in the system, prevented the use of this model.

BatchSep is a unit operating model for batch distillation. The BatchSep model uses a robust and efficient algorithm to solve the unsteady heat and material balance equations that describe the behavior of the batch distillation process. Rigorous heat and material balances, as well as phase equilibrium relations, are applied in each phase (10).

Multicomponent distillation can be modified by changing the reflux ratio, introducing additional heating in the boiler, or changing the operating pressure (9). The retention of liquids in the column on individual stages (holdup) determines the level of volatile impurities remaining in the product extracted from the distillate. Similarly, retention in the reflux drum will exceed the purity of the distillate, especially if the volatile product is a negligible component of the feedstock (9). Only a simulation model can accurately predict these impacts (9).

To achieve proper purity criteria at the start of the system start-up, batch distillation columns are often operated at total reflux for a period of time before the feed mixture is introduced into the system. The time required for column equilibration can represent a significant portion of the total cycle time, which is typically one to three hours. Very often, time will be provided based on previous column experience or operational capabilities (where the operator has other duties) (9).

When simulating the separation of a model bio-oil system in a discontinuous distillation column using the BatchSep model, simulations that start with the equilibrium state in the column (total reflux ratio) and those that start from the point of introduction of the feed mixture into the column were tested. When starting from introducing the feed mixture into the column, the program requires the introduction of air (or some other gas) as a component, in order to start the calculation.

4. Results and Discussion

Aspen Plus™ V12.1 reports that in this bio-oil model system there are three azeotropes at 101.325 kPa: water-ethanol (mole ratios 0.105:0.895, at temperature 78.151°C); water-furfural (0.908:0.092, 97.781°C); water-phenol (0.983:0.017, 99.954°C). The first azeotrope is homogeneous and was classified as an unstable nod, and the second and third are classified as saddle, but the second being heterogeneous, and the third being homogeneous. The influence of the pressure change on the position of the azeotropic point is shown in Table 1. An increase in vacuum degree, increases the content of water only for the azeotrope water-phenol. For the other two azeotropes, the concentration of water in azeotropic mixtures decreases with distillation pressure decrease.

Table 1. Influence of the pressure change on the position of the azeotropic point

Azeotropes	**Pressure, kPa**						
	40	70	92	93.5	95	97	100
Water mass frac.	0.0384	0.0414	0.0435	0.0437	0.0438	0.0440	0.0443
Ethanol mass frac.	0.9616	0.9586	0.9565	0.9563	0.9562	0.9560	0.9557
Temperature, °C	56.59	69.18	75.78	76.18	76.57	77.09	77.86
Water mass frac.	0.6463	0.6475	0.6495	0.6497	0.6498	0.6501	0.6504
Furfural mass frac.	0.3537	0.3525	0.3505	0.3503	0.3502	0.3499	0.3496
temperature, °C	73.93	87.74	95.12	95.56	96.00	96.57	97.42
Water mass frac.	0.9193	0.8617	0.8363	0.8348	0.8333	0.8314	0.8286
Phenol mass frac.	0.0869	0.1383	0.1637	0.1652	0.1667	0.1686	0.1714
Temperature, °C	75.81	89.77	97.06	97.50	97.93	98.50	99.34

The values of boiling temperatures at different pressures for the first five components are given in Table 2. The boiling points of the components were calculated using the Aspen Hysys V12.1 software package. The boiling points increase with increasing pressure as expected. Changes in the boiling temperature of the water and acetic acid with decreasing pressure are similar, while relative to the value of the boiling temperature at atmospheric

pressure, the boiling temperature of phenol decreases the least with decreasing pressure in the system.

Table 2. Effect of pressure on boiling temperatures: water, ethanol, acetic acid, furfural, phenol and the bio-oil model system (bio-oil)

Boiling point, °C	**Pressure, kPa**						
Component	40	70	92	93.5	95	97	100
Water	75.87	89.95	97.31	97.76	98.20	98.78	99.63
Ethanol	56.42	69.11	75.75	76.15	76.55	77.07	77.84
Acetic acid	90.2	106.2	114.7	115.2	115.7	116.4	117.4
Furfural	130.4	148.4	157.9	158.5	159.0	159.8	160.9
Phenol	150.8	168.7	178.2	178.7	179.3	180.0	181.1
Bio-oil	68.53	82.10	89.20	89.66	90.05	90.43	91.43

Shortcut methods were used for the design of continuous distillation, where the DSTWU model gave results with errors, while simulations with Distill block (Edmister method, Table 3) gave results that could be used to set parameters for a rigorous calculation method (RadFrac block).

Table 3. Results of simulations with Edmister model (Distil block) at pressure 90 kPa

Recovery of Light key component in distillate Acetic acid 0.9999	**Recovery of Heavy key component in distillate Phenol 0.0001**	**Acetic acid in distillate, mass fraction**	**Acetic acid in bottom, mass fraction**	***N***	***N*$_F$**	***R***	***T*$_D$, °C**	***T*$_B$, °C**	***D*/*F***
		0.254	$1.08 \cdot 10^{-6}$	24	12	0.18	85.45	183.57	0.92

N - Number of stages, N_F – feed stage, *R*- reflux ratio, T_D – distillate temperature, T_B – bottom's product temperature, D/F distillate to feed mass flows ratio.

Simulations (rigorous calculation) of bio-oil separation in a continuous rectification column were performed with a given ethanol recovery in the distillate of 100% at all tested pressures. In addition to ethanol, the distillate contains all water, acetic acid and 3-methyl-1,2-cyclopentadione (methylcyclopentenolone), and 80% of furfural, while the rest contains phenol and guaiacol.

Table 4. Results of simulations with the Radfrac model at different pressures

Pressure, kPa	40	70	90	92	93.5	95	97	100
Q_{REB}, kW	83.157	71.903	76.304	54.094	113.953	100.313	93.455	79.840
Q_{CON}, kW	-83.913	-71.544	-75.395	-53.334	-113.156	-99.480	-92.575	-78.890
T_R, °C	156.4	174.7	183.6	184.4	185.0	185.6	186.4	187.5
T_C, °C	65.3	78.661	85.1	85.6	86.0	86.5	87.0	87.8
RR	2.304	1.860	2.036	1.1490	3.562	3.012	2.736	2.187

Table 4 shows the change of the following parameters: the amount of heat in the reboiler (Q_{REB}), the amount of heat in the condenser (Q_{CON}), the temperature of the reboiler (T_R), the temperature of the condenser (T_C) and the reflux ratio (RR) obtained by Radfrac block simulations at different pressures. At a pressure of 0.92 bar, it is necessary to introduce the smallest amount of heat into the system, due to the lowest value of the reflux ratio. The highest reflux ratio is at a pressure of 0.935 bar, when the amount of heat in the reboiler, and the condenser, is the highest.

The effects of the amount of liquid retained in the reflux vessel (0.05, 0.01 and 0.025 kg); the amount of liquid retained on the floors (0.01 and 0.05 kg); the pot heat duty (1, 3 and 5 kW) and the influence of pressure (40, 70 and 100 kPa) on batch separation of the bio-oil model system were investigated. The results for the components ethanol and furfural were chosen to depict the characteristics of the discontinuous distillation process under all tested conditions.

The graphs given in Fig. 1 show the total yields of ethanol and furfural in the distillate expressed relative to the content of the component in the feed mixture. Separation was done for 1 h at a pressure of 100 kPa, the reflux ratio was five, and the pot heat duty was 3 kW. Reflux drum liquid holdup values were 0.05, 0.1 and 0.25 kg, while the stage holdups were 0.05 kg.

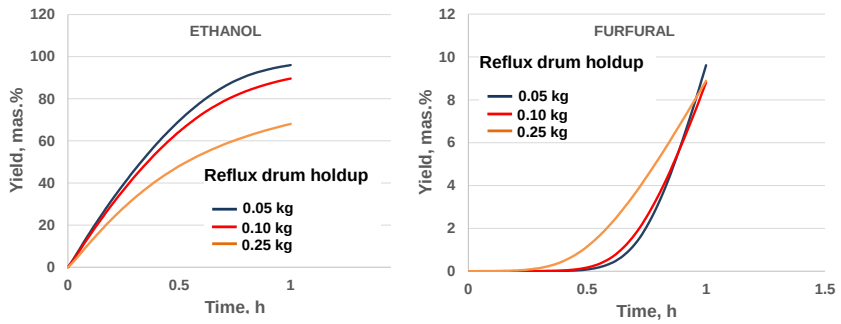

Figure 1. Influence of the reflux drum holdup on ethanol and furfural distillate yields

The ethanol content in the distillate increases inversely proportional to the amount of liquid in the reflux vessel, i.e. the less liquid retained in the reflux vessel, the more ethanol in the distillate. The simulation model predicted that the effect of an increase in reflux drum liquid holdup was the opposite for furfural compared to ethanol. When the value of the liquid in the

reflux vessel is 0.25 kg, the separation of furfural in the distillate is more intense, while for the cases of 0.05 and 0.1 kg of liquid in the reflux vessel, separation is negligible before 0.6 h, and after that time furfural appears in the distillate. For a period of 1 h, the proportion of furfural in the distillate, regardless of the amount of holdup, will not exceed 10 wt. %.

Fig. 2 shows the yields of ethanol and furfural in the distillate expressed relative to the content of the component in the feed mixture for a time period of 1 h depending on the retained amount of liquid on the stages (the stage holdup). The amounts of liquid in the stages that were selected for the experiments are: 0.01 and 0.05 kg. As in the previous case, the pressure is 1 bar, the amount of heat in the reboiler is 3 kW, the reflux ratio is 5, and the amount of liquid in the reflux vessel is 0.05 kg. All the ethanol turns into distillate (100% for a time period of 0.77 h) in the case where the amount of liquid in each stage is 0.01 kg. The separated amount of furfural in the distillate after one hour is 60 wt.% of the initial amount, when 0.01 kg of liquid is on the floors in the column, while for a smaller value of 0.05 kg of liquid on the floors, the part of predistilled furfural does not exceed 10 wt.%. It can be seen that the less holdup liquid on the floors, the greater the distilled amount of components.

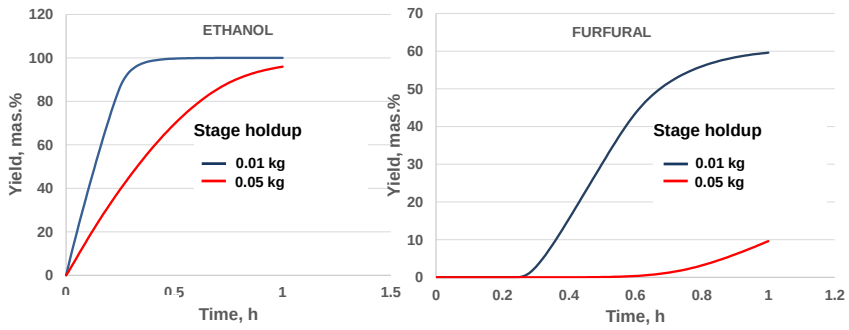

Figure 2. Influence of the stage holdup on ethanol and furfural distillate yields

The graphs in Fig. 3 show the influence of the amount of heat supplied to the pot on the amount of distilled components (the graphs show the cases for ethanol and furfural). The applied amounts of heat for heating the pot in the simulations were 1, 3 and 5 kW, at atmospheric pressure and at a reflux ratio of 5.

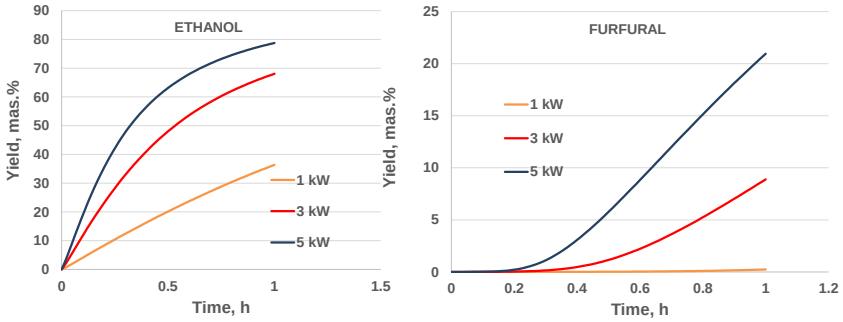

Figure 3. Influence of the pot heat duty on ethanol and furfural distillate yields

Distilled amount of a component was the largest when the amount of supplied heat was also the largest, in this case when it was 5 kW. The distilled amount of ethanol in relation to the initial content of the compound in the initial mixture, when the amount of heat was 1 kW, was the smallest. The more heat we bring to the distillation system, the more components will pass into the distillate. Furfural will not distill for a value of 1kW of the pot heat duty.

Fig. 4 shows the influence of pressure of 40, 70 and 100 kPa on the amount of distilled components (the graphs show the cases for ethanol and furfural) for a time period of one hour. The pot heat duty was 3 kW, the reflux ratio was 5, and the reflux drum holdup was 0.05 kg, and the stage holdups were 0.05 kg. The change in ethanol yield in the distillate with the change in pressure is negligible. For a period of one hour, the amount of distilled ethanol is about 68 wt.%. With furfural at all three pressures, the amount of furfural in the distillate is small, but it is still noticeably higher when the pressure in the system is 1 bar.

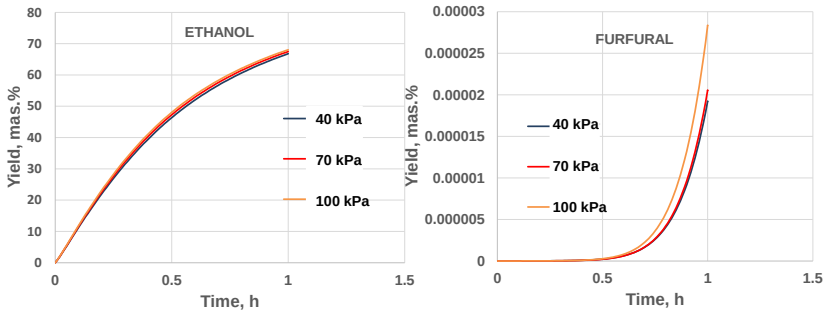

Figure 4. Influence of the pressure on ethanol and furfural distillate yields

In a complex system, such as bio-oil, the Aspen software package could play a key role in the design, simulation and optimization of a batch process, as the results of this work show. The vacuum distillation process should be optimized due to competing cost effects that appear as the pressure of the process is lowered. Namely, lower operational costs for energy are accompanied by greater capital costs for sizable columns and condensers. This would be the subject of some further investigations.

5. Conclusions

Based on the presented results, it can be concluded that with the appropriate choice of the amount of heat supplied to the pot, the amount of reflux liquid retained in the reflux vessel and the reflux ratio, a set of time cycles could be created in which products could be obtained sequentially. For example, it is possible to extract ethanol and water first, and then gradually other components. Results of this word are in good agreement with previously published experimental results (6). The main difficulty in the design of discontinuous processes is the consideration of the time-varying nature of the process, which means that dynamic process models and more sophisticated simulation and optimization techniques are required. Aspen software package can play a key role in the design, simulation and optimization of such a batch process.

6. Acknowledgments

This research study was supported by the Ministry of Education, Science and Technological Development of the Republic of Serbia (Project No. 451-03-68/2022-14/200134).

7. References

1. European Community. Directive 2009/28/EC of the European Parliament and of the Council of 23 April 2009 on the promotion of the use of energy from renewable sources and amending and subsequently repealing Directives 2001/77/EC and 2003/30/EC. **2009**, 16-62.
2. European Union. Directive (EU) 2015/1513 of the European Parliament and of the Council of 9 September 2015 amending Directive 98/70/EC relating to the quality of petrol and diesel fuels and amending Directive 2009/28/EC on the promotion of the use of energy from renewable sources. **2015**, 1-29.
3. European Union. Directive (EU) 2018/2001 of the European Parliament and of the Council of 11 December 2018 on the promotion of the use of energy from renewable sources. **2018**, 82-209.
4. Đurišić-Mladenović, N., Predojević, Z. Alternativna goriva, Tehnološki fakultet Novi Sad, Univerzitet u Novom Sadu, **2021**.

5. Lyu, G., Zhang, H. Estimation and comparison of bio-oil components from different pyrolysis conditions. *Front. Energy Res*. **2015**, *3(article 28)*, 1-11.
6. Ma, Y.-K., Yuan, X.-H., Luo, Z.-J., Zhu, X.-F. Influence of vacuum degrees in rectification system on distillation characteristics of bio-oil model compounds. *J. Fuel Chem. Technol*. **2022**, *50(2)*, 160-165
7. Yaman, S. Pyrolysis of biomass to produce fuels and chemical feedstocks. *Energy Convers. Manag.* **2004**, *45(5), 651–671*.
8. Demirbas, A. Biorefineries: current activities and future developments. *Energy Convers. Manag*. **2009**, *50(11)*, 2782–2801.
9. Hawkins, G. *Process Engineering Guide: Batch Distillation,* **2013.**
10. Aspen Plus; *Aspen Plus User Guide*, Version 10.2, **2000.**
11. Luyben, W. *Distillation Design and Control Using Aspen*^{TM} *Simulation*, Lehigh University, John Wiley & Sons, Inc., **2006.**

REVIEW OF SIMULATION TOOL PACKAGES FOR LIQUID – SOLID TWO PHASE FLOW

Goran Pajić[1]*, Lato Pezo[2], Predrag Kojić[1], Jelena Lubura[1], Rahmi Uyar[3], Ozan Karatas[4], Ferruh Erdogdu[4]

[1]University of Novi Sad, Faculty of Technology, Bulevar cara Lazara 1, 21000 Novi Sad, Serbia

[2]Institute of General and Physical Chemistry, P.O. Box 45, 11158 Belgrade 118, Serbia

[3] Department of Food Engineering, Aksaray University, 68100 Aksaray, Turkey

[4]Department of Food Engineering, Ankara University Golbasi, Ankara 06830, Turkey

**pajic.175.15.h@uns.ac.rs*

Abstract

Mixtures containing liquid and solid phase are still a challenge for numerical simulation and numerous software packages are used for these purposes. The solution is a combination of the Discrete Element Method (DEM) and Computational Fluid Dynamics (CFD). Therefore, in this paper, the approach of numerical simulation instead of conventional experimental determination of particle velocity in two-phase flow will be analyzed. Available scientific literature and software packages will be examined and commented. Governing equations of continuity and momentum will be introduced and their accuracy of estimation will be analyzed comparing with experimental results. This way, the main goal will be the possibility of using numerical simulation for problems that are difficult or impossible to determine experimentally. The Euler – Lagrange approach is reviewed, as it treats particles as discrete elements, which calculates interactions between the solid and fluid phase and collisions among particles, for each particle independently. Discrete phase model in ANSYS Fluent gave a demonstration of relatively good prediction of critical velocities in two – phase flows. For modeling macroscopic particles, that requires special treatments as taking into account effects like fluid volume blockage, the proper evaluation of drag forces, collision effects and friction dynamics, Macroscopic Particle Model is evaluated and discussed. Coupling methods, between DEM and CFD is innovative, promising approach to model two phase flows. Two different coupling methods are reviewed, coupling between ANSYS Fluent and ROCKY DEM – simulation of fluidized bed, and coupling between ANSYS Fluent and EDEM – simulation of abrasion effects on process equipment. Simulations generated realistic solid phase trajectories, relatively

good values of velocities and pressure drops that showed good accordance to literature correlation.

Keywords: numerical simulation, liquid – solid flow, CFD, DEM

1. Introduction

This paper primarily considers transport modeling in pipes and focuses on the turbulent flow of a two-phase solid-liquid mixture, where the particles are large enough to affect the flow structure, causing a non-uniform distribution of velocity, as well as a non-uniform distribution of particles across the pipe cross-section. The possibilities of modeling solid phase in liquid are presented, where it is possible to present solid phase in two ways: continuous and discrete phase. The main equations for the liquid phase are presented: the equation of continuity and equation of fluid motion, as well as equations for the solid state, using Newton's second law and certain contact models. As simulation possibilities, three models are presented, combining two numerical methods: discrete element method - DEM and computational fluid dynamics - CFD. Discrete phase modeling, macroscopic particle modeling and the combination method of software packages such as Rocky and EDEM are presented as models.

Particle and fluid flow is complex and its behavior depends on a large number of different factors, leading to a large number of different flow regimes. Some of the factors are flow rate, pipe diameter and its orientation, physical and rheological properties of the fluid, particle size, density and concentration. Categorization of solid-fluid mixtures according to their behavior is divided into two groups: mixtures that don’t settle and mixtures that settle. Mixtures that settle are mixtures containing large particles (homogenous), while others are suspensions of fine particles (heterogeneous) (1).

For large particles, the heterogeneous model can be significantly more developed, with the accumulation of particles at the bottom of the horizontal tube, where such particles move by a sliding mechanism – sliding bed (2).

Current research on two-phase fluid-particle systems is based on laboratory investigations and macroscopic numerical models. These methods don’t provide sufficient understanding of the microscopic information involved in particle motion, which is crucial for developing a general approach for scaling up processes and modeling fluid-particle systems (3).

2. Computational fluid dynamics

Various multiphase systems, such as solid-liquid mixtures, are successfully modeled, although there are certain limitations. Multiphase CFD allow a better understanding of the complex interactions between different phases and provide detailed three-dimensional information that experiments are unable to provide. The application of these models, among others, indicates the potential of computational fluid dynamics in the simulation of complicated fluid flows and their application in various industrial processes (4).

The ANSYS Fluent software package has the ability to model a large number of different incompressible and compressible, laminar and turbulent fluid flows. An additional, very significant group of models that Fluent contains are models for multiphase modeling, which can be used for modeling and analysis of solid – liquid flows (5).

To mathematically describe physics of fluid flow, two basic equations are used, continuity equation and momentum equation, known as Navier – Stokes equation:

$$\frac{\partial \rho}{\partial t} + \nabla \cdot (\rho \boldsymbol{v}) = 0$$

$$\frac{\partial \rho \boldsymbol{v}}{\partial t} + \nabla \cdot (\rho \boldsymbol{v}\boldsymbol{v}) = -\nabla p + \nabla \cdot \tau + \rho \boldsymbol{g} + \boldsymbol{F}$$

Here p is the static pressure, τ is the stress tensor, ρ is the density, v is the velocity vector, t is time, ρg is gravitational force and F is external body force.

Increasing the complexity of the process being modelled, the mathematical model complicates and energy, reaction, diffusion or turbulence equations are added, in order to adequately describe the model. The two basic approaches to multiphase flow modeling are the Euler-Euler (E-E) approach and the Euler-Lagrange (E-L) approach. In the E-E model, both phases are considered as continuous, and for this reason it is suitable for modeling multi-fluid systems. It can also be used for modeling dispersed flows, where total movement of particles is more important than movement of individual particles. As models suitable for modeling larger particles, which use the Euler-Lagrange approach and follow each particle and track its movement, the Fluent software package has three options: Discrete phase modeling - DPM, macroscopic particle modeling - MPM, as well as the possibility of coupling, combining, with other programs specialized for modeling the solid phase and its interactions, in which two computer methods CFD-DEM are combined (5).

3. Discrete phase modeling – DPM

If the interactions between particles can be ignored, this method can be simplified, which is possible in the case where volume fraction of the particles is very small. If the fraction of particles cannot be ignored, interactions between particles can be included using the discrete element method – DEM (5).

The mathematical formulation consists of two sets of equations, the continuous phase equation and the discrete phase equation. The equations for the continuous phase are the equations of mass conservation and the equations of fluid motion. Using Newton's second law, the ordinary differential equations that describe the motion of a particle are:

$$m_p \frac{d\boldsymbol{v_p}}{dt} = F_d + F_{gb} + F_{vm} + F_{is} + F_{DEM}$$

$$\frac{dx_p}{dt} = \boldsymbol{v_p}$$

Here x_p and v_p are the position and velocity of the particle, m_p is the mass of the particle, F_d is the frictional force, F_{gb} is the resultant of gravity and thrust, F_{pg} is the pressure gradient force, F_{is} is the Saffman buoyancy force, F_{vm} is the virtual mass, and F_{DEM} is the force associated with the interaction between individual particles (5), (6).

By comparing the DPM model and the Euler model, by simulating the transport of sand particles through a horizontal pipe, limitations of Euler model are observed. With the DPM model, it is possible to predict and determine the limiting speed due to the accumulation of sand particles at the bottom of the pipe (Figure 1). Also, the Euler model does not change its results with changing grid cell size. The DPM model gives different results, better results with larger cells, which is not the typical case for CFD simulations. The results obtained with larger grid cells cannot be said to be incorrect, given that the visual representation of the simulation agrees quite well with the experiment. The DEM method of particle-particle interactions was not included in the simulation, which could contribute to the accuracy of the simulation, as it is manifested by an underestimated limiting transport velocity. The DPM model shows the reasonable possibilities of modeling the two-phase flow and the accumulation of sand particles in the pipe at low fluid velocities, which gives the possibility of determining the limiting fluid velocity that prevents accumulation.

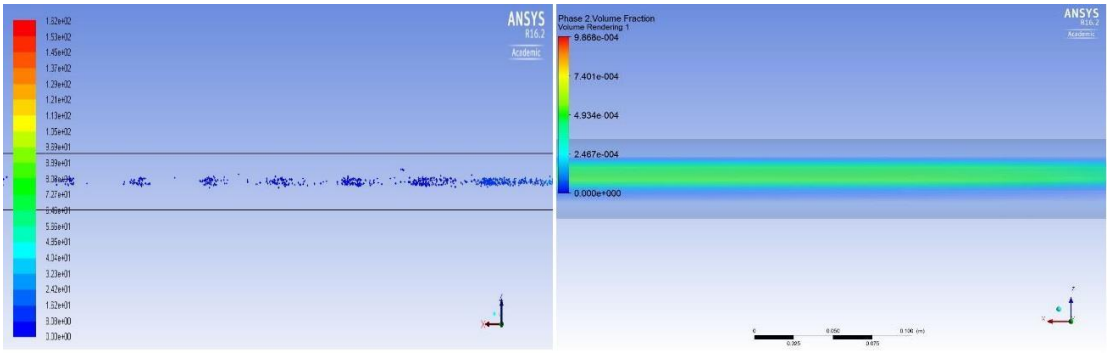

Figure 1. DPM (left) and Euler (right) model

Varying the velocities, key moments and behavior of the particle flow can be seen. The top view is a better view for low speeds and visualization of sand accumulations, and the side view for higher speeds and suspended particles in the flow (Figure 2). The limit speed ranges from 0.2 to 0.3 m/s, depending on the sand granulation (80-350 μm) (7).

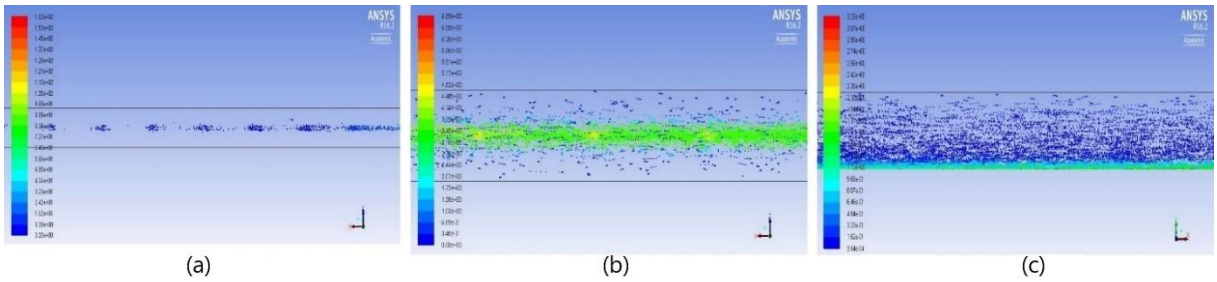

Figure 2. a) 0.1 [m/s] top view, b) 0.3 [m/s] top view, c) 1 [m/s] side view

4. Macroscopic particle modeling – MPM

In some cases, it is very important to take into account the total volume of particles because it can have a significant impact on the fluid flow, and particles are significantly larger than the grid cells. For these specific simulations, MPM model, is an innovative additional model, which provides the ability to predict the behavior of particles and their interaction with the fluid, interaction with walls and mutual interaction. It is part of the software package as a User Defined Function (UDF), written in the "C" programming language, which is imported into the ANSYS Fluent software package (8).

Each particle touches a certain number of cells, and is represented by a spherical shape with six degrees of freedom (6dof) to account for translational and rotational motion of the particles in all directions. The movement of each particle is calculated by transport equations that are solved by Lagrange's approach (9).

One of the tests is filtration simulation, filtration two types of particles through the filtration medium (Figure 3), where larger particles are retained on the filter, and smaller ones pass through the filter. Which is an effective way of modeling particle separation. As an additional effect, gravity force was included, what manifested as accumulation of particles on the lower part of the pipe (9).

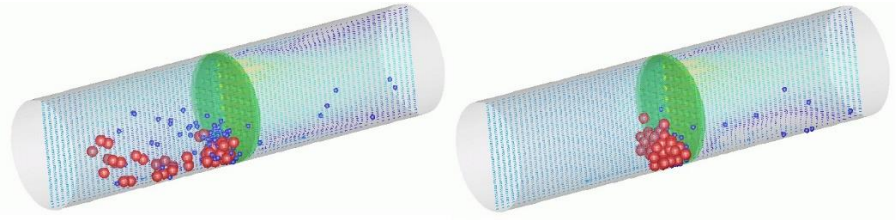

Figure 3. Filtration simulation

5. CFD-DEM coupling

Interactions between software packages that use the DEM and CFD is an innovative approach to fluid-particle system modeling. Particles within the computational domain are tracked using the Lagrange method, explicitly solving Newton's second law, which solves the translational and rotational motion of the particle. While, the fluid phase is solved by the Navier-Stokes fluid motion equations and the continuity equation (10).

This paper describes the combination of the methods of the software packages Rocky - ANSYS Fluent (10), and EDEM - ANSYS Fluent (11). In the Rocky - ANSYS Fluent simulation, the fluidized state of particles was modeled and analyzed, and the pressure drop through the fluidization column was determined. The effect of particle abrasion on the obstacle in the pipeline was modeled by the simulation performed using the EDEM - ANSYS Fluent interaction.

5.1 EDEM – ANSYS FLUENT

To analyze the results of the simulation, which was performed using the combination of ANSYS Fluent and EDEM software, to determine the influence of particles on the flow and interactions of particles in the pipe, a non-invasive optical experiment was conducted using the Laser Doppler Anemometry LDA method, which obtains profiles of liquid and solid phase velocity (11). A closed loop was formed to conduct the experiment on a standardized model, using a centrifugal slurry pump to push a mixture of water and sand particles. In order for the flow to develop fully, a cylindrical obstacle is placed at a distance from the entrance to the pipe at twenty times larger than the diameter of the pipe. A heat exchanger was built in to the

experimental plant to maintain the temperature of the mixture at 20°C. Due to the necessary homogeneous mixture of sand and water at the suction flow of the pump, the output flow from the pump is divided into two parts, where one flow returns to the tank as recirculation to mix the mixture, and the other is led to the model on which the experiment is performed. Using the DEM method, the trajectory of each particle was calculated in order to simulate the behavior of all particles, that is, the two-phase flow. With each time branch, the forces acting on the particle are calculated, and the new positions of the particles and their velocities are determined. Forces acting on particles include particle interaction forces. The motion and properties of the liquid phase are obtained by solving the equations of fluid motion and the continuity equation. The computer simulation was performed only by modeling a standardized element with a cylinder as an obstacle. As the input flow to the model, a fully developed turbulent flow is defined through the UDF function, which represents the fitted results of the input flow obtained by the experimental LDA method. The profile is described by the kinetics of the Michaelis – Menten reaction (11).

The simulation was performed through the interaction between ANSYS Fluent and EDEM software. At each time step, the results obtained in EDEM were transferred to Fluent where the effects of particles on fluid flow were considered, after which the results of fluid flow were transferred to EDEM with the next time step, in order to determine the effect of fluid flow on solid particles. The resulting simulation is shown in Figure 4, in which about 1.5 million particles were included and it took 3 weeks to complete the calculation (11).

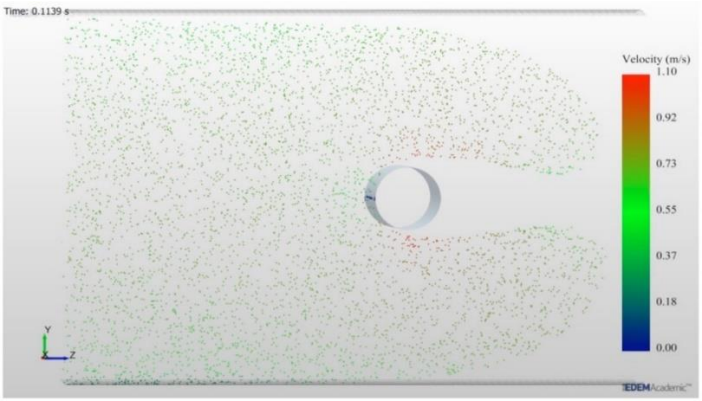

Figure 4. ANSYS Fluent and EDEM simulation

Particle velocity profiles determined by the LDA method, at a position of 34 mm before the obstacle in the form of a cylinder, for five different flow rates ranging from 3000 to 5000 l/h, are shown in Figure 5 (a). Comparison of the obtained simulation and experiment results at a flow rate of 4000 l/h are shown in Figure 5 (b), where the simulation was done in two ways:

ANSYS Fluent-EDEM and ANSYS CFX. The results obtained by the Fluent - EDEM simulation match better with the results from experimental method, except in the upper zone. By changing the volume flow, the mean speed of the particles increases linearly, and it can also be affirmed that the speed from the center up is higher than from the center down. Speed was also determined at a position of 16 mm after the obstacle, where it can be seen that the CFX results agree better with the experimental in the zone of the center, zone of Karman vortices, which are a consequence of the obstacle in the form of a cylinder. Whereas, the DEM results agree better with the experimental values in the upper and lower zones of tube (11).

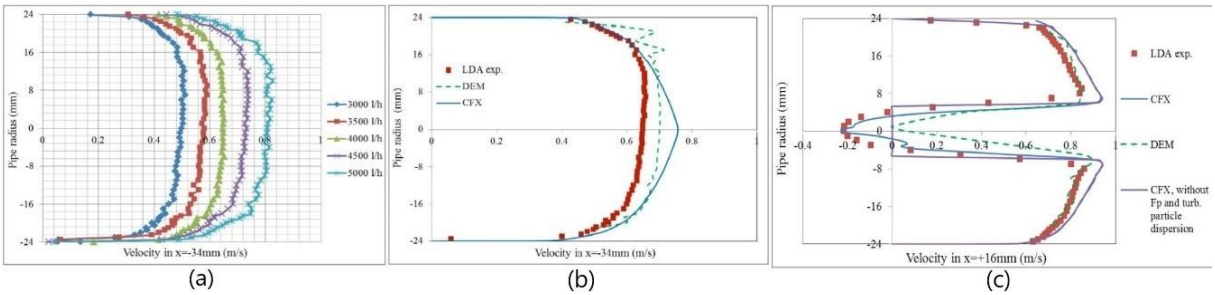

Figure 5.(a) Five different flow rates ranging from 3000 to 5000 l/h, (b) Comparison of simulation and experiment results at a flow rate of 4000 l/h, (c) Speed at a position of 16 mm after the obstacle

5.2 ROCKY – ANSYS FLUENT

Whit respect to high concentration of the solid phase, it is necessary to consider the model of two-way interaction, where fluid and particles mutually influence each other. The gas phase enters the bottom of domain at a uniform rate, leaving at the top of the column under atmospheric conditions. In order to analyze the beginning of fluidization, air speed at the beginning of the simulation is 0 m/s, and reaches the maximum value at which the simulation takes place for t=2s. This approach to simulation also increases numerical stability. The predicted pressure drop determined by Ergun's equation was calculated for three different volume fractions of the liquid phase. The obtained curves are valid only until the moment when fluidization start. The pressure drop between inlet and outlet, determined by simulation, is represented by the orange continuous line in Figure 6 (a). The pressure drop obtained from the simulation and the Ergun equation match quite well up to the point of fluidization onset. A comparison of the simulation and the mean pressure drop obtained by experimental measurement is shown in Figure 6 (b). where the speed of fluidization that was determined experimentally agree relatively well with the moment in the simulation at point where is a shift with a linear change of the pressure drop to its constant valuen (10).

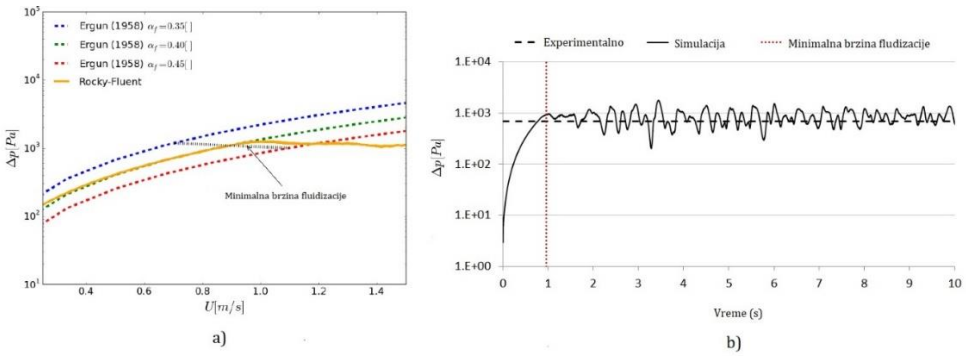

Figure 6. a) Predicted pressure drop, b) Comparison of the simulation and the mean pressure drop measured in experiment

6. Conclusion

CFD, along with DEM method, has great potential for solid-liquid flow simulation. The simulations show realistic visual movement of particles in the flow, relatively good results of velocities and pressure drop, parameters that are important for designing process plants. The accuracy of the obtained results depends as much on human influence as on the capabilities of the computer hardware used. It is very important to eliminate the influence of the human factor on unreliability of the results and carefully select the models, modeling parameters and define the calculation domain. When the influence of human error is eliminated, modeling capabilities are limited by computer hardware, and the time required to complete a simulation. Particles range from very small, which are relatively easy to model due to their small influence on the flow and the importance of the movement of the overall flow, to very large ones, which become more difficult to model as they increase in size. Further research should be devoted to the modeling of large solid particles - elements, as well as the modeling of the non-uniform shape of the particles and the determination of their influence on the fluid flow, with the benefit of the rapid development of computer hardware.

7. Acknowledgements

The authors would like to acknowledge to the Bilateral project between Republic of Serbia (Ministry of Education, Science and Technological Development) - Project No. 451-03-812/2021-14/8 and Republic of Turkey (TUBITAK) – Project No. 220N413 for the financial support

8. References

1. Puderbach, V., Schmidt, K., Antonyuk, S. A coupled cfd-dem model for resolved simulation of filter cake formation during solid-liquid separation. *Processes* **2021**, *9*, 826.
2. Messa, G.cV., Yang, Q., Adedeji, O. E., Chára, Z., Duarte, C. A. R., Matoušek, V., Rasteiro, M. G., Sanders, R. S., Silva, R. C., de Souza, F. J. Computational Fluid Dynamics Modelling of Liquid–Solid Slurry Flows in Pipelines: State-of-the-Art and Future Perspectives. *Processes* **2021**, *9*, 1566.
3. Haotong, Z., Guihe, W., Cangqin J., Cheng, L. A Novel, Coupled CFD-DEM Model for the Flow Characteristics of Particles Inside a Pipe, *Water,* **2019**.
4. Muhammad, E. CFD studies of complex fluid flows in pippes, Birmingham: The University of Birmingham, **2009**.
5. ANSYS Fluent Theory Guide, Canonsburg: ANSYS, Inc., **2021**.
6. Marcos, V. B., Fernando, D. L. C., Admilson T. F., Silvio, L. M. J. Eulerian-lagrangian approach applied to particulate flow using dense discrete phase model," *Journeys in Multiphase Flows,* **2015**.
7. Timur, B., CFD Simulations of Multiphase Flows with Particles, Norwegian University of Science and Technology, **2016**.
8. Andrea, R., Sahan, T. W. K., Mohammad S. I., Suvash, C. S. A macroscopic particle modelling approach for non-isothermal solid-gas and solid-liquid 1 flows through porous media, *Applied Thermal Engineering,* **2019**.
9. Madhusuden, A., André, B. Michael, T. P. Macroscopic Particle Model - Tracking Big Particles in CFD, u *AIChE 2004 Annual Meeting*, Austin, **2004**.
10. Clarissa, B. F., João, A. A. O. J., Lucilla, C. d. A. DEM-CFD coupling: mathematical modelling and case studies using rocky-dem® and ansys fluent®," u *Eleventh International Conference on CFD in the Minerals and Process Industries*, Melbourne, **2015**.
11. A. M, L. M i J. B. H, „Investigation of Particulate Flow in a Channel by Application of CFD,DEM and LDA/PDA," *The Open Chemical Engineering Journal,* t. 8, pp. 1-11, **2014**.

PROCEEDINGS of the 2nd International Conference on Advanced Production and Processing, May, 2023.

International Conference
on Advanced Production and Processing

Министарство просвете,
науке и технолошког
развоја

University of Novi Sad
Dr Zorana Đinđića 1,
21000 Novi Sad, Serbia

Faculty of Technology Novi Sad
Bulevar cara Lazara 1,
21000 Novi Sad, Serbia